DEPARTMENT OF TRANSPORT AND REGIONAL SERVICES

Gutteridge Haskins and Davey Pty Ltd

Cocos (Keeling) Islands Storm Surge Study

August 2001

Systems Engineering Australia Pty Ltd

Numerical Modelling and Risk Assessment

J0005-PR001C

Department of Transport and Regional Services

Gutteridge Haskins and Davey Pty Ltd

Cocos (Keeling) Islands Storm Surge Study

August 2001

ACN 073 544 439

Systems Engineering Australia Pty Ltd
7 Mercury Court
Bridgeman Downs QLD 4035
Australia

J0005-PR001C

Table of Contents

List of Figures

List of Tables

1 Executive Summary

This report describes a technical study to update existing probabilistic estimates of extreme water levels due to the effects of tropical cyclones both within the lagoon of Cocos (South Keeling) Island and also on the exposed ocean reef flats. The work was commissioned by Gutteridge Haskins and Davey Pty Ltd, Perth W.A. on behalf of the Commonwealth Department of Transport and Regional Services. The Scope of Work is given as Appendix A for reference.

The study has undertaken the following tasks:

1. An analysis of historical tropical cyclone activity in the region within a 500 km radius of the atoll leading to a series of statistical relationships for intensity, frequency and track;
2. Verification of a numerical wind and pressure model of tropical cyclones against airport weather station records for a "top 10" selection of historical cyclones;
3. Numerical modelling of resultant storm surge, wave and wave setup phenomena for each of the "top 10" cyclones;
4. Verification of the storm surge model against recorded storm surge values at Home Island jetty tide gauge;
5. Construction of a statistical simulation model capable of integrating the various components of storm tide level (astronomical tide, inverted barometer effect, surface wind stress and breaking wave setup);
6. Verification of the statistical model against long-term wind speeds from the airport weather station and against long-term tide levels;
7. Probabilistic analysis of combined storm surge, tide and wave setup levels at inshore (lagoon) and offshore (reef flat) sites;
8. Estimates of wind speed (mean and gust) and wave height as a function of return period;
9. Predicted levels of total storm tide (and its components) for 10, 50, 100, 500 and 1000 year ARI (Average Recurrence Interval or Return Period) and the assessment of inundation levels at nominated island locations.

It is concluded that the Cocos (South Keeling) Island atoll is a very complex hydrodynamic environment requiring a significant level of numerical analysis in order to estimate the potential for significant storm tide events. This has been achieved by the combined use of 2D and 1D hydrodynamic models, 2D spectral wave models, wave setup models and statistical simulation models. The study shows that the local ocean response to tropical cyclone forcing on the outer atoll is likely to be dominated by the effects of breaking wave setup but, for sites on the lagoon, by locally generated wind stress. Overall, breaking wave setup dominates total water levels.

The various numerical models used and the assumptions made have been tested as much as possible against measured data but it should be noted that there is a significant absence of recorded wave height and period information and very limited water level information for the site (other than the long term tide gauge on Home Island). The longest period of measurement of any data is that for wind speed and direction at the Airport on West Island. In addition, information on reef flat characteristics (widths, levels, and slopes) which are potentially important controlling parameters for breaking wave setup, is relatively sparse. In order to account for some of these latter deficiencies, sensitivity tests to some important parameters have been included.

The critical outcomes from the study are as follows:

- the maximum possible tropical cyclone intensity in the region is assumed to be 880 hPa, with an estimated return period of between 200 and 500 years depending on track class;
- the average peak error in modelling the mean wind speed for the "top 10" cyclones was 6.7%;

- the predicted 1000 year return period values for wind speed are approximately 37 ms^{-1} (10 minute mean) and 59 ms^{-1} (3 second gust);
- 2D surge modelling of the "top 10" cyclones was typically within 0.1 m of the measured surge;
- 2D surge modelling indicates total surge offshore of "ocean" sites being within ± 0.01 m of the Inverted Barometer Effect alone; and
- although no recorded wave data is available, it is concluded that the 2D spectral model estimates of wave height are within 10% of actual values.

Table 1.1 summarises the estimated storm tide threat for the base case of the *1%* (or upper envelope) breaking wave setup component. The report also details a number of sensitivity tests which may produce slightly higher water levels than these depending on the exact choice of parameters. The 50 y and 1000 y ARI values are indicated for a number of critical locations in terms of the absolute water level relative to MSL and also the water level relative to a nominal local ground level. The ***greyed*** cells highlight situations where the local ground level is expected to be exceeded. The encounter probability is also indicated on the basis of a 50 y risk horizon, which shows the chance of equalling or exceeding the indicated levels at least once during any 50 y period. No allowance for possible Greenhouse-induced sea level rise is included in these values.

Table 1.1 Predicted base case 1% setup storm tide levels for selected atoll locations.

	ARI	**50 y**		**1000 y**	
	% Chance in 50 y	**64%**		**5%**	
	Typical Local Groundlevel MSL	**Relative to MSL**	***Relative to Ground Level***	**Relative to MSL**	***Relative to Ground Level***
Location	**m**	**m**	***m***	**m**	***m***
Whole of Atoll		2.7		3.5	
Trannies Beach	2.0	1.7	*-0.3*	2.2	***0.2***
West Is Jetty	1.5	0.9	*-0.6*	1.2	*-0.3*
Rumah Baru	1.1	0.9	*-0.2*	1.3	***0.2***
Airport North	2.5	1.0	*-1.5*	1.5	*-1.1*
North Park	3.5	1.7	*-1.8*	2.1	*-1.4*
Airport Settlement*	4.0	1.7	*-2.3*	2.2	*-1.8*
Airport South	2.8	1.6	*-1.2*	2.1	*-0.7*
Home Is (SE)	3.0	2.6	*-0.4*	3.5	***0.5***
Home Is (South)	1.0	0.9	*-0.1*	1.2	***0.2***
Home Is (Jetty)*	1.5	0.9	*-0.6*	1.1	*-0.4*
Home Is (North)	3.0	2.4	*-0.6*	3.1	***0.1***

* location of cyclone shelters

The first entry in the table is for the whole-of-island case, which accumulates the probability of exceedance from all of the other sites considered (refer Table 5.1 and Figure 5.1 for details). In this context, there is no local ground level reference. Importantly, the localised risk of inundation is predicted to vary at individual sites around the island, mainly as a function of their relative exposure to extreme wave conditions. The highest storm tide level in these examples is indicated on the outer side of Home Island and the lowest storm tide level is at Home Island jetty. The most vulnerable site (i.e. greatest over-ground depth) is the outer SE corner of Home Island. Table 6.2 summarises similar information for other island sites and for other ARI values. Overall, the most vulnerable sites to storm tide inundation from tropical cyclones are near the lagoon Southern Entrance, South Island and Horsburgh Island.

Based on the experience in conducting this study, it is also considered possible that non-cyclonic wave setup events (e.g. SW swell) may also be capable of producing storm tide levels similar to these at some island sites. While such non-cyclonic episodes may not be capable of attaining the peak levels estimated for cyclones, it is likely that the frequency of occurrence of lower levels will be higher than that for cyclones. Anecdotal evidence suggests that the non-cyclonic inundation episodes are reasonably common.

The present study has combined a number of sophisticated modelling approaches in order to represent the physical processes at work that lead to storm tide events during tropical cyclones. However, with the exception of wind and tide data, there is a significant lack of any long-term measured data against which to adequately verify the operation of the models in this remote and isolated region. Also, information on reef-top levels and widths is also reasonably scant and certain assumptions have been made to suit the requirements of the analyses. The model assumptions in regard to the physics of reef-top wave setup are also largely laboratory-based and depend on calibration information from other regions. Until such verification can take place, the predictions in this report should be viewed with caution and a conservative approach should be followed in regard to the location of storm tide shelters.

It is recommended that a number of data collection studies be undertaken to assist in verifying future technical assessments of this type. The principal and minimum needs are detailed below:

1. A long-term regional measurement program (more than 5 years) for waves using a directional waverider buoy or equivalent, probably moored north-west of Horsburgh Island where ocean depths are more manageable;
2. A progressive program of surveying of the reef-top levels, extending to the reef-face where possible;
3. A limited deployment of water level and current recorders at various island locations so as to be able to better relate atoll MSL variations to the tide gauge on Home Island;
4. A facility to measure reef-top wave setup phenomena so as to verify the assumptions in the wave setup model. This might consist of a number of water level recorders installed across a nominated reef flat with at least one instrument sensitive enough to be able to resolve local wave height, with offshore wave data being provided by the waverider buoy facility.
5. A program of detailed documentation of any inundation events around the island to include observor, dates, times, places, damage, photographs and elevations or limit of incursion. This should be backdated as far as local knowledge permits to provide a baseline reference of frequency and intensity against which to verify the model probabilistic performance. A detailed island map template could be used to accurately locate the position of each event.

All of the above measurements will not only underpin future technical studies of extreme events but will be essential for the long-term coastal management of the atoll system. This will be critical in the context of potential rises in sea level due to enhanced Greenhouse effects.

With increased information from the above instrumentation, combined with island wind and tide data, it would also be possible to provide a simple early-warning system for the local population. With the support of some additional numerical modelling, such a system should be able to provide a 6 to 12 h warning of conditions likely to cause inundation episodes at certain locations around the island.

2 Introduction

This section provides an introduction to a number of salient features of the island environment which are relevant to consideration of the potential impact of tropical cyclones. The following geomorphological overview was compiled by Dr Michael Gourlay based on published material for the region (see Section 8 for specific references).

2.1 Formation of Atoll and Islands

The Cocos (Keeling) Islands are an isolated group of islands in the eastern Indian Ocean (Figure 2.1). The major (southern) group form a typical small to medium sized coral atoll system in which a large lagoon is surrounded by an enclosing intertidal reef on which the various islands are located (Figure 2.2). A single northern island, North Keeling, is located 26 km north of the main group on the same underwater geological structure (refer Figure 5.4 later for detail).

Figure 2.1 Location map.

The Cocos (Keeling) atoll is of considerable significance for scientific research on the geology and geomorphology of coral atolls. It was the only atoll which Charles Darwin actually visited and he sought evidence there for his theory that coral atolls were derived from the original fringing reefs formed around a volcanic island which had subsequently gradually subsided below sea level. It has only been during the latter half of the twentieth century that sufficient scientific evidence has been obtained to verify this theory. Considerable research concerning the geology and geomorphology of Cocos (Keeling) Atoll has been published during the last decade.

Briefly, the late Quaternary development of the Cocos (Keeling) Islands involves a combination of subsidence, solution and sedimentation processes as sea level has fallen and risen during the last 120 000 years. Darwin's subsidence theory provides an understanding as to how the structure of the atoll originally developed over a much longer time period. During the last interglacial period the atoll existed in much the same general form as today. As sea level fell the atoll become a limestone island which was subjected to subaerial weathering with solution of the exposed limestone surface (Figure 2.3). This process, together with the continuing much slower subsidence of the original volcanic structure (ca 2mm/century), resulted in the level of the Pleistocene surface of the atoll

platform being generally 12 to 15 m below the present mean sea level at the peak of the last ice age twenty thousand years ago. At that time sea level was more than 100 m below its present level.

As sea level rose rapidly following the ice age the weathered limestone island was submerged about eight thousand years ago and the present Holocene reefs began to grow. Subsequently lagoonal sedimentation also occurred. The formation of the present reef islands involved three phases (Figure 2.4) -

Catch up reef growth	7 to 5 ka BP
Reef flat consolidation	4.5 to 2.5 ka
Reef island formation	2.5 to O ka

During the period of reef flat consolidation sea level attained an elevation approximately one metre higher than it is now. Most of the reef islands have formed on a conglomerate platform, derived from the reef flat during this higher sea level period but now emergent above the present reef flat.

Hence, whereas the geological structure of the atoll is primarily the result of subsidence of an original volcanic island, the present geomorphology of the atoll is a consequence of the more recent sea level history, controlling the accompanying solution weathering (karst processes), reef growth and sedimentation processes.

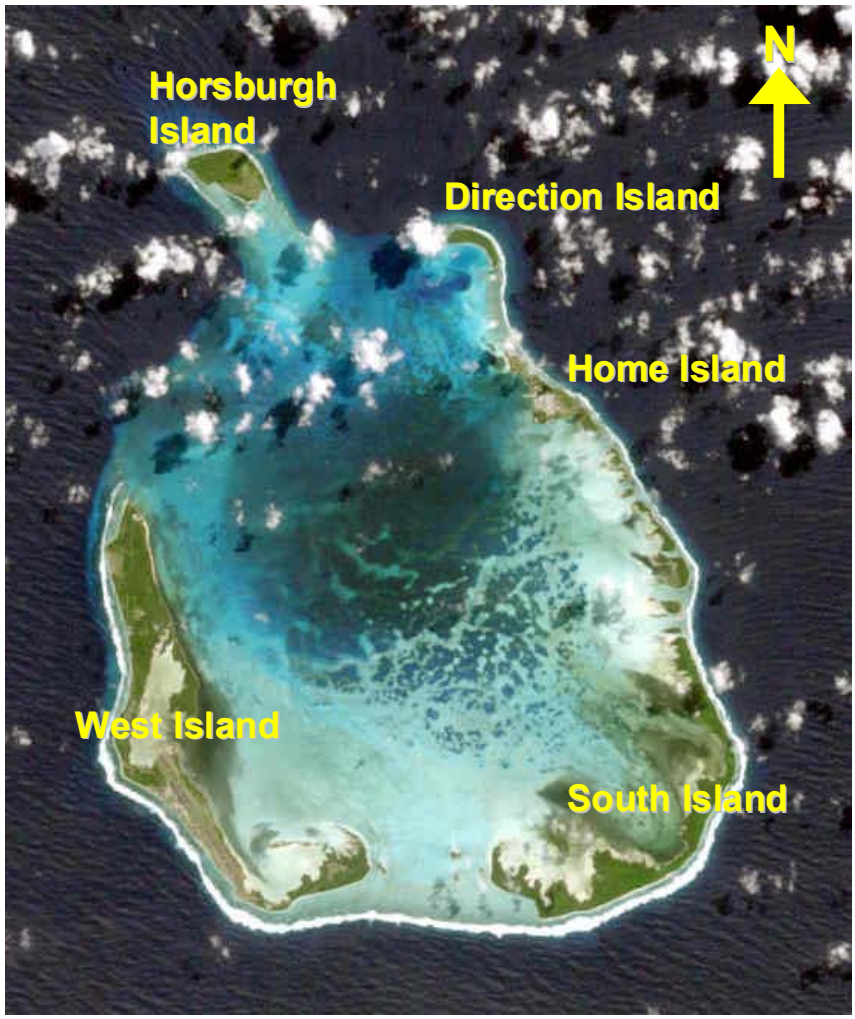

Figure 2.2 Cocos (South Keeling) Island -12.1°S 96.8°E

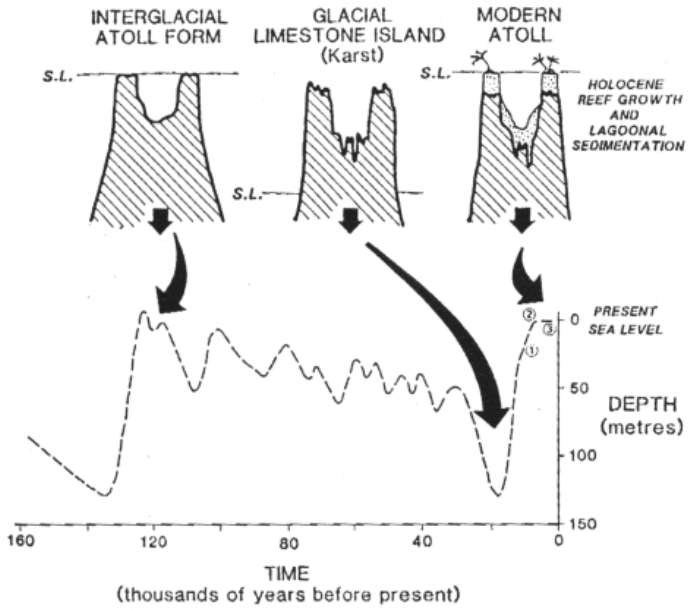

Figure 2.3 A model of the late quaternary development of the Cocos (Keeling) Islands (after Woodroffe *et al.* 1994)

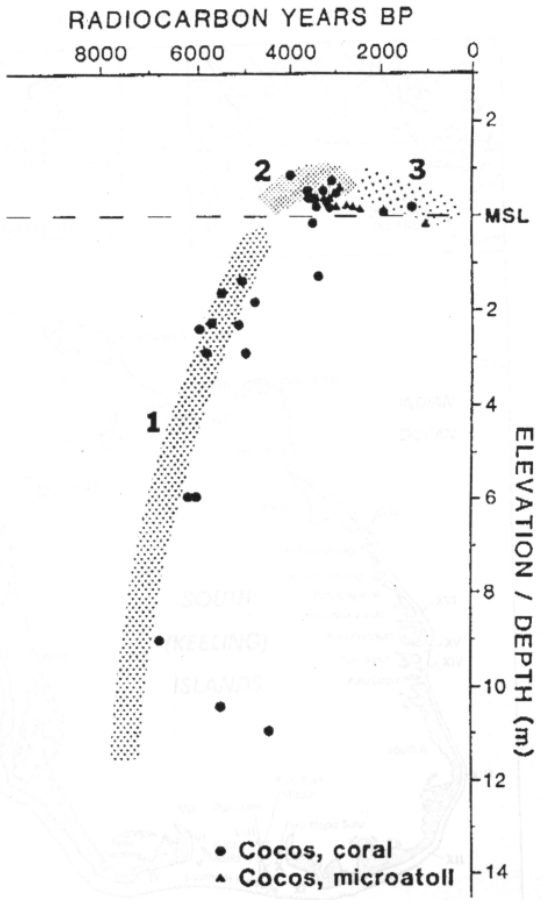

Figure 2.4 Age-depth plot of radiocarbon dates from Cocos (Keeling) Islands (after Woodroffe *et al.* 1994)

2.2 Description of Atoll and Islands

The reef is horseshoe shaped, open to the north and northwest with two passages 12 to 14 m deep (Figure 2.2). The atoll is about 12 km in the east to west direction and 15 km north to south and has an area of about 190 km^2. In general the reef on the oceanward side of the atoll has three zones -

- a generally horizontal intertidal reef flat with a surface elevation less than one metre below mean sea level;
- a gently sloping submerged reef extending to a depth of 10 to 20 m;
- a steeply sloping reef face extending down to depths of the order of 4 km;

The reef flat varies in width. It is less than 50 m on the northern side of Direction Island on the north-eastern side of the atoll, about 70 m along Home Island, and then increases to 170 m on the southeastern side of South Island. It is over 800 m in front of the islets in the southern passage between South and West Islands. On the southern side of West Island it decreases from over 500 m width to under 300 m, while along most of the western side of West Island it is about 200 m wide, reducing to about 70 m at the two narrowest locations and increasing to 280 m at the northern end of West Island. At the southern end of the atoll the reef crest consists of a broad algal pavement strewn with coral boulders up to 1 m in diameter. The reef flat is variable in depth. In some places it is at or above mean sea level; in many places it is less than 0.5 m below mean sea level; in other places it is as much as 1 m below mean sea level. Generally the reef flat elevation is somewhat higher along the southern side of the atoll in front of the passages between South and West Islands than it is in front of Home Island or the northern end of West Island.

The submerged reef varies in width from less than 200 m in front of Home Island to more than 300 m in front of the northern part of West Island but this information is not very reliable particularly for the eastern and southern sides of the atoll. The general slope of the submerged reef is of the order of 1 in 20 to 1 in 25 along the western sides of West Island and Horsburgh Island. The edge of the submerged reef lies at 10 to 20 m depth and probably represents the seaward edge of the underlying Pleistocene reef structure. No information is available concerning the slope and form of the reef face on the eastern and southern sides of the atoll but on its western side the reef face slope varies between 1 in 1 and 1 in 2 down to a depth of about 100 m, below which it steepens down to 200 m (a selection of reef profiles is provided in Section 5.2).

Twenty six islands or islets are located around the rim of the atoll. The largest, West Island, on which the airfield and government offices are situated, has an area of 6.23 km^2 and there are only three other islands with areas of the order of 1 km^2 or more - South (3.63 km^2), Horsburgh (1.04 km^2) and Home (0.95km^2). Most of the permanent residents live on Home Island, the area of which has been increased by reclamation works. A platform of cemented coral conglomerate underlies much of the sediment deposits forming the atoll's islands. It is generally exposed along the seaward side of the northern and eastern islands where the reef flat is narrow. It is not so evident along the southern portion of South Island or along West Island (except but not always where the reef flat is narrower than its general width). The higher portions of the conglomerate are about 0.5 m to 1 m above mean sea level and hence subject to wave action at the higher high tides. The islands generally are composed of sand and shingle or sometimes coral rubble. They are highest on their ocean shores; generally there is a ridge 3 to 4 m above mean sea level but this is occasionally higher in places. The highest point reaches 11 m on the southern shore of South Island where a distinct wind-blown sand dune has formed. Dunes are also found on the ocean shore of two of the larger islands, Home and West. The elevation of the islands tends to fall towards the lagoon with much of the land being only 1 to 1.5 m above mean sea level. In many cases there is low ridge on the lagoonward side of the island.

The small elongated reef islands tend to be crescentic or horseshoe shaped with accretionary sand spits formed at either end of their lagoonward sides, whereas the smaller "circular" islets tend to have a single sand deposit on their lagoonward sides. The formation of these spits is associated with the dominant wave-induced flow through the several generally narrow, shallow passages between the individual small islands along the eastern and southern sides of the atoll. In due course, the two crescentic spits join together on the lagoonward side of the island enclosing a small lagoon or swamp which eventually infills to form a larger, wider island.

The longer elongated South and West Islands each appear to have once been composed of three or four separate islands, the original gaps between them now being closed by narrow shingle-dominated ridges. However, dating of one of these ridges on West Island indicates that it is in reality older than other portions of the island. On the lagoonward sides of these ridges there are large shallow muddy embayments, which are dry or almost dry at low tide.

While the more exposed eastern and southern island shores are generally formed of, and protected by, shingle and rubble storm berms overlying the conglomerate platform, the more sheltered seaward shore of West Island has prograded about 500 m seaward since the original island(s) were formed three or four thousand years ago. Lesser lagoonward accretion also has occurred on the northern and southern portions of West Island. As the seaward shore of West Island has moved closer to the reef edge, the height of its beach ridge has increased in response to the increasing size of the waves reaching the shore over the decreasing width of reef-flat.

Both the western end of South Island and the eastern end of West Island show the successive development of recurved spits directed into the lagoon. Those on West Island have been dated as forming sequentially during the last 1500 years. Their formation must be associated with the net lagoonward flow through the shallow southern reef entrances, together with wave-generated alongshore transport. It is likely that this process is localised to the portions of the reef-flat and shoreline adjacent to the entrance (1 km on the South Island and 1.7 km on West Island) where the reef-flat is wider and the shoreline further from the reef edge compared with the shorelines further to the west and to the east respectively. However, the exact transport mechanisms and sequences of sand movement require further investigation, particularly on the western end of South Island where it is possible that, rather than the development of recurved spits by alongshore transport, two or three islets may have been joined to the main island. Whatever the physical mechanisms for sediment accretion, it is important to recognise that biological production of skeletal material on the reef flat is a continuing process contributing to the sediment supply.

At the northern end of West Island there has been significant shoreline accretion (ca 150 m) on the lagoonward side in the vicinity of the jetty since 1952. Refraction analysis (DHC 1986) has shown that this is consistent with the penetration of waves into the northwestern lagoon entrance and consequent local southward alongshore transport on the lagoonward side of the island. These waves could either be infrequent ones coming from the west or southwest or refracted/diffracted swells originating from the dominant southeasterly weather conditions. As at the southern entrance, the source of this sand may be the adjoining reef-flat fronting the indented 750 m long portion of the shoreline immediately south of the northern tip of the island and north of the conglomerate outcrop close to the reef crest.

Apart from the localised sites adjacent to the lagoon entrances there is very little evidence of alongshore sediment transport along the island shorelines. Most of the land surface of the islands was cleared and planted with coconuts during the nineteenth century. Hence it is not possible to find much evidence of past accretion from vegetation zonation or topographical features recorded on recent aerial photographs.

Pleistocene limestones underlie the reef islands at depths of 8 to 13 m below mean sea level with the shallowest strata lying at 6.7 and 6.8 m under West Island. At the centre of the lagoon these depths are significantly greater reaching 22 to 24 m. Fresh water lenses occur under the wider parts of West, South and Home Islands. However, the presence of the more permeable Pleistocene limestones, generally limits the depth of these lenses to the less permeable Holocene sediments overlying the older strata. Climatic variability affects recharge of the fresh water and causes the extent and depth of the lenses to fluctuate.

2.3 Physical Processes in the Atoll

Wave-action dominates the exposed reef flats on the seaward sides of the islands but tidal action dominates the sheltered lagoon enclosed by the reef and islands. Twelve shallow interisland passages connect the reef flat and shallow lagoon on the eastern and southern rim of the atoll. The depths in these passages are less than 1.5 m below mean sea level. Exchange of water between ocean and lagoon occurs along their total width of 4 km, as well as through the two deeper channels on the northern and northwestern sides of the atoll. On the lagoonward side of the passages there are large sand deposits up to 1500 m length, formed where the lagoonward transporting energy of the waves is dissipated and/or counteracted by the tide within the lagoon. The southern and eastern two thirds of the lagoon are shallow, 0 to 3 m below mean sea level. In some places there are mud flats; in others sea grass beds; and there is a variable cover of coral, sand and algae. The northern one third of the lagoon is deeper, 10 to 20 m below mean sea level, and the bottom is covered generally with sand, dead coral, etc. The southsoutheasterly trade wind-driven swell breaks around the exposed reef rim with breakers of the order of 2 m height. This swell is diffracted and refracted around the atoll and enters the deeper northern passages with much reduced were heights although these may be enhanced locally by refraction, e.g. in the vicinity of the jetty at the northern end of West Island.

Tides are mixed microtidal but mainly semi diurnal ($F = (K_1+O_1)/(M_2+S_2) = 0.57$). Tidal ranges generally vary between 1.1 m and 0.5 m with a maximum range of 1.3 m. There is a permanent tide gauge at Home Island jetty. During a period of 18 days (Dec-Jan 1993) a second gauge was installed at the southern end of the lagoon. The tidal datums of both gauges were related to mean sea level by survey. It was found that tides in the south are 35 to 80 minutes later than in the north and that tide levels are generally greater in the south than in the north. This increase in tide levels is most likely the result of wave set-up (ca 0.15 to 0.2 m) generated by waves breaking on the reef crest opposite the passages between South and West Islands but may also be due to tidal interaction in the shallow lagoon.Current measurements showed that there is unidirectional flow through the interisland passages from the ocean side reef flat into the lagoon during neap tides. In the eastern passages this flow reverses direction and flows seaward during low spring tides but this reversal does not occur in the southern passages where the reef flat is generally 0.1 m higher than the eastern reef flat. Gravity wave energy dominates current spectra in the eastern reef passages, whereas infragravity wave energy dominates in the southern reef passages because of both the higher reef crest and wider reef flat in the south.

Overtopping of the seaward beach ridge by waves at high tide occurs from time to time. The most recent event was recorded on 5 August 1999 in the vicinity of the sea wall protecting houses on West Island. Such overtopping is known to have occurred at least three times during the last 20 years. Significant overtopping and damage to the sea wall occurred in August 1980 during a period of low winds and extraordinary high tides. Cyclone *Doreen* (970 hPa) passed over the atoll on 21 January 1968 without causing any recorded storm tide damage. However, West Island was inundated four times by king tides and heavy swells during the previous six months. Significant movement of coral boulders, overwash of island foreshores and damage to houses and roads occurred during these last events.

3 Methodology Overview

3.1 Overall Philosophy

The study site is essentially an open ocean location in deep water within a tropical cyclone environment. The meteorological and oceanographic impacts can be summarised as:

- Low tidal environment
- Exposed wind environment
- Exposed wave environment on the outer reef
- Protected wave environment within the lagoon but directionally sensitive

It can therefore be expected that the principal threat of inundation due to extreme water levels on the outer reefs will be due to the combined effects of (i) the pressure deficit component of a storm surge acting coincidently with (ii) a high tidal level and (iii) high wave setup, caused by wave breaking on the outer reefs and reef entrances (refer Figure 3.1). Wave setup is likely to be the dominant water level controller, with pressure deficit (or inverted barometer effect - IBE) being a secondary component. The maximum potential inverted barometer effect is of the order of 1 m and would only be realised during a very close approach of a very intense storm (e.g. 900 hPa). Wave setup plus tide is therefore expected to largely control the statistics of open ocean water levels. It is expected that wind-stress induced storm surge setup will be generally small because of the surrounding deep ocean environment but may be more significant in some parts of the shallow lagoon (refer Figure 3.2).

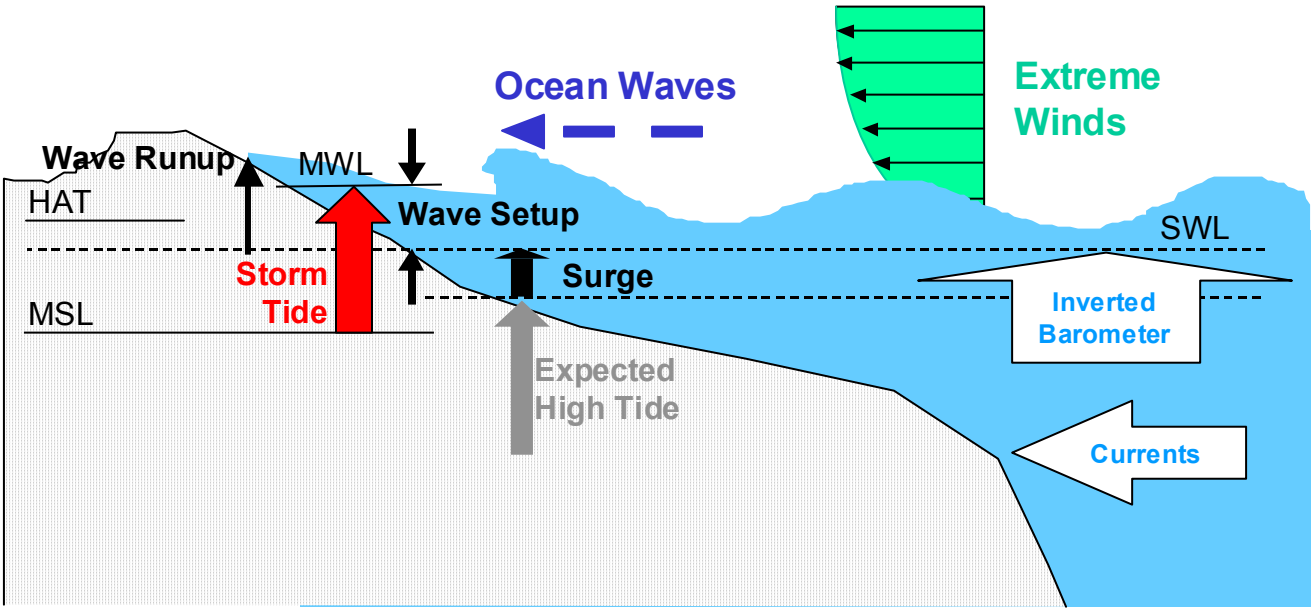

Figure 3.1 Factors influencing extreme water levels on the outer atoll.

Because of the potentially complex interactions of storm surge, tide and breaking wave setup, a statistical simulation methodology has been adopted. This firstly comprises a statistical analysis of the storm climatology to provide a complete range of potential storm parameters. These are then used to control a Monte Carlo simulation which invokes deterministic (parametric) models of each phenomena (surge, waves, setup) and assembles a synthetic time history of extreme water levels from which return periods of water levels may then be derived.

This technique allows a fully objective assessment which accounts for the joint probability of all the necessary parameters. A complete return period estimation of water levels is obtained to any desired ARI which does not directly rely on data fitting assumptions. The simulation can be easily altered to test the sensitivity to the controlling assumptions taken from the storm climatology and to any other assumptions such as reef wave setup response. This technique however relies on establishing parametric models of the various factors.

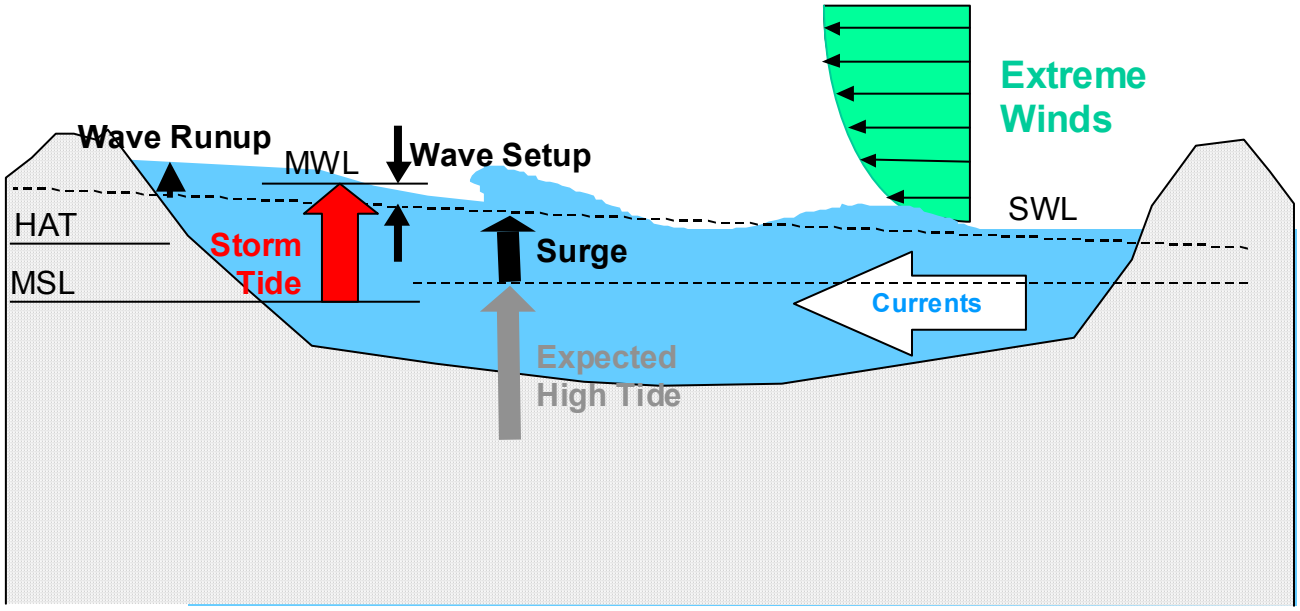

Figure 3.2 Factors influencing extreme water levels on the inner lagoon.

3.2 Detailed Methodology

Details of the various numerical modelling systems used are provided in Appendices, namely:

1. Tropical cyclone wind and pressure model (Appendix B);
2. 2D numerical hydrodynamic model SURGE (Appendix C);
3. 2D spectral wave model ADFA1 (Appendix D);
4. SATSIM parametric storm tide model (Appendix E);
5. Analytical breaking wave reef setup (Appendix F).

3.2.1 Assessment of Recorded Data

Principal recorded data sources for the study have included National Tidal Facility (NTF) hourly water level data from 1986 to 1999 and long-term Bureau of Meteorology wind and pressure records for the airport site on West Island.

3.2.2 Deterministic Model Checks

A series of deterministic model checks were then undertaken to:

(a) examine the characteristics of water level response from selected storms of record, and
(b) prove the accuracy of parametric models of surge, wave height and setup to be applied during the simulation phase

This involved:

- Establishing nested numerical model domains for the 2D ADFA1 spectral wave model and a grid for the 2-D SURGE hydrodynamic model to allow coverage of the open ocean area of influence and to also resolve details within the lagoon and its entrances
- Assembling historical track details for the selected storms (e.g. *Doreen* Jan 1968; 971 hPa, Dec 1992; 990 hPa)
- Running the models with applicable tidal levels to estimate the various water level components during those events
- Comparing the model results with any available measured data (wind, pressure, wave height and period, water level)
- Comparing the numerical model performance with the embedded parametric models to be used in the SATSIM simulations

3.2.3 Simulation Production Modelling

The SATSIM simulation model (BPA 1985, Harper *et al.* 1989, Harper 1999) has been established with the statistical tropical cyclone parameters for the region and the local tidal constituents. To this was added the inner and outer reef parameters required for the Gourlay (1997) methodology for wave setup at the selected atoll locations. The pressure deficit model was specifically augmented to include local wind setup as a result of deterministic model checks which indicated such enhancement was necessary.

SATSIM embodies a full analytical model of tropical cyclone wind and pressure fields (Harper and Holland 1999) which permits direct calculation of the local hydrostatic pressure deficit (storm surge in an open ocean environment). The model has been successfully validated against long-term wind records at Port Hedland, Onslow and many east coast sites. The parametric wave model is derived from a multi-dimensional interpolation of many hundreds of detailed ADFA1 model simulations for an open ocean site. The wave setup method of Gourlay (1997) will be added to the parametric wave model allowing wave setup estimates to be calculated at any exposed atoll site.

The embedded parametric wind, surge, wave and setup models in SATSIM then generate synthetic time-aligned histories of the following parameters:

- Mean and gust wind speed
- MSL atmospheric pressure
- Storm surge pressure deficit
- Open coast wave height and period and wave setup
- Lagoon wave height

for many thousands of regional storm scenarios. The statistics of exceedance of the water level components are then accumulated for direct analysis of the return periods of interest. The model also automatically generates joint probability statistics of storm parameters such as intensity, proximity, speed etc. The period of model simulation can be varied and is typically 10,000 years, thus providing 10 estimates of the 1000 year return period event. The highest simulated level also provides an estimate of the probable maximum water level under present climate.

4 Regional Tropical Cyclone Climatology

The Bureau of Meteorology, through the Western Australian Regional Office (Perth), has WMO operational jurisdiction for issuing tropical cyclone warnings in the Cocos Islands region, at least south of 10°S and west to 90°E. While this just manages to include the Cocos Islands, the subsequent database maintained by the National Climate Centre contains essentially the complete estimated track and intensity information even if the tropical cyclone moves outside this jurisdictional region. The latest dataset (current to 1999/2000 season) was obtained for the present analysis. This dataset is believed superior to the US Navy (1994) data for the same area.

4.1 Statistical Assessment of the Cyclone Hazard

For the purpose of statistical analysis, a specific subset of the available tropical cyclone dataset is selected. Firstly, the data is limited to the period 1959 onwards as recommended by Holland (1981). This is a nominal start date which recognises that prior to this time many tropical cyclones, especially in the open ocean, where not always detected. The advent of satellite photography during the early 1960s quickly ensured that all potential cyclones were at least detected and could be tracked. Secondly, objective intensity estimation methods also followed the availability of satellite photography and these were only fully established by the 1970s. Reducing the available dataset to post-1959 does not especially detract from the utility of the data in this case since the earliest storms recorded are in 1950 and only eight storms are recorded prior to 1959. A total of 41 seasons of data are therefore available for analysis.

Secondly, a statistical "control volume" is selected, taken as a 500 km radius of South Cocos Island. This radius ensures that all cyclones which could have influenced the atoll within a travel period of approximately 24 h are considered in the analysis. Clearly, if too small a radius is selected, the resulting storm sample size is also very small and the estimated point statistical properties are much less certain. If too large a radius is taken then the climatology may not be stationary. The 500 km radius has been found to be adequate for these purposes in a number of previous analyses.

On the basis of considering data only since 1959 and within 500 km of South Cocos Island, Figure 4.1 presents a summary of the annual frequency of occurrence in histogram format. The greatest number in any season was a total of six in 1974/75, although five occurrences in a single season have been recorded on several occasions. The 5 year average frequency of occurrence is also shown in order to reduce the annual variability. This indicates that prior to the 1970s the annual average was about 1.5 storms. This rose to almost three per year up until the mid-1980s and then reduced to around two per year until about 1995 when numbers again increased slightly. Also shown on Figure 4.1 is the annual and five year averaged Southern Oscillation Index (SOI), which is known to be an indicator of monsoonal intensity in Northern Australia and India. Whilst not overly compelling in regard to the occurrence of tropical cyclones at the Cocos Islands, certainly the increased activity during the 1970s is consistent with the rest of Australia and the heightened value of the SOI. It might be inferred from the SOI record though, that the decreased frequency of occurrence during the 1960s may not be overly biased by a lack of observational systems and accordingly the full post-1959 period is retained for further analysis. This results in a total of 95 storms over the 41 season period, or an average of 2.32 storms per season, within a 500 km radius.

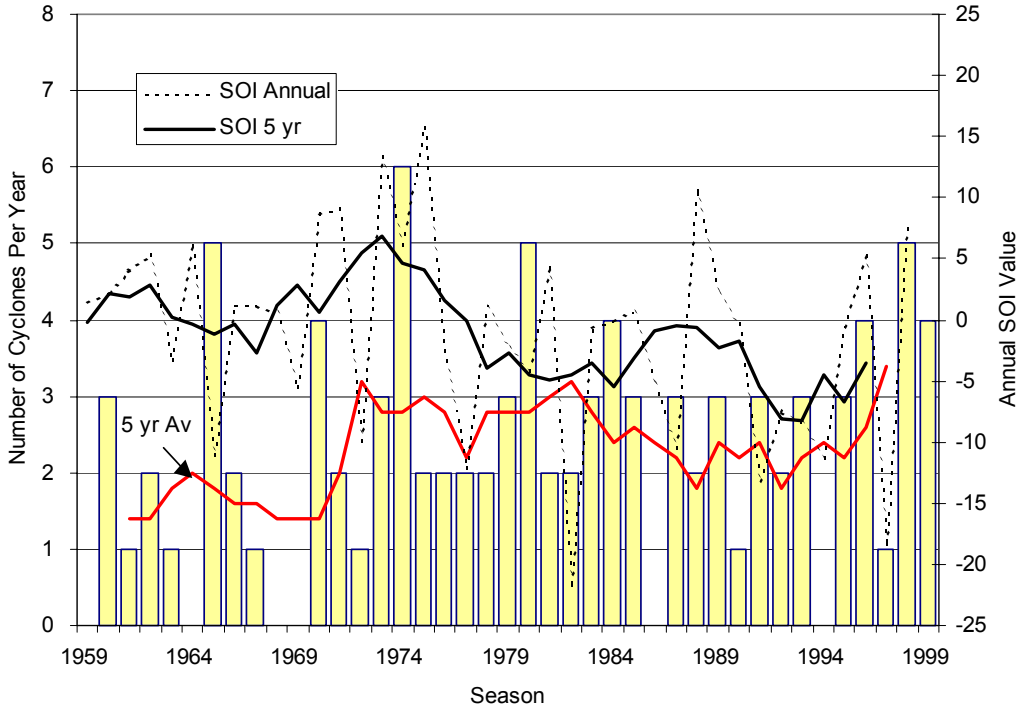

Figure 4.1 Frequency of occurrence of tropical cyclones within 500 km of the Cocos Islands.

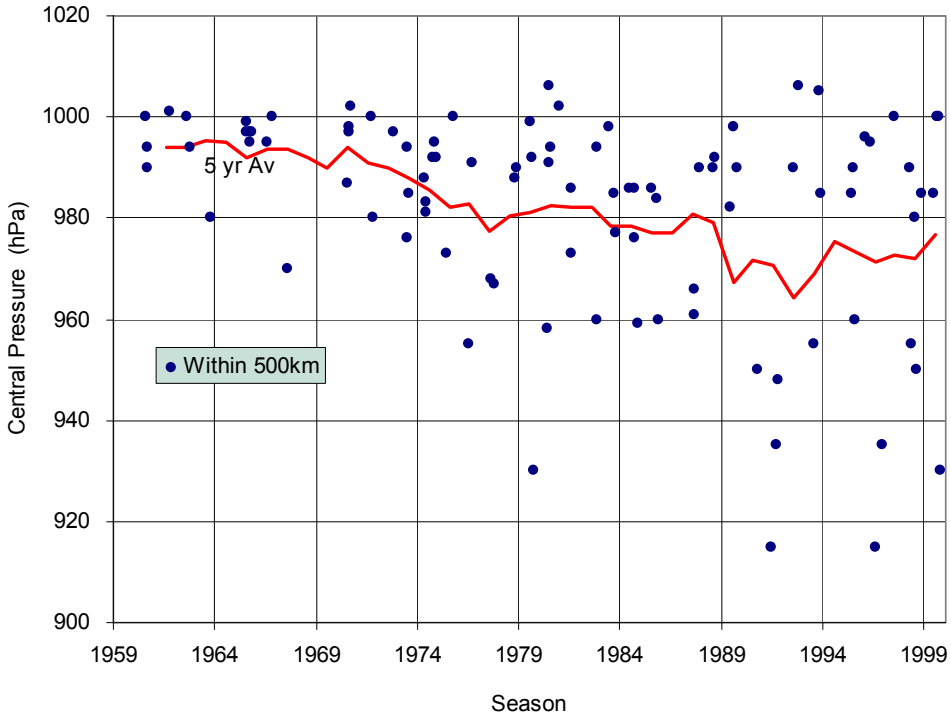

Figure 4.2 Intensity of tropical cyclones within 500 km of the Cocos Islands.

Figure 4.2 presents the corresponding time history of maximum intensity estimates (central pressures) of tropical cyclones within the adopted 500 km radius. This also suggests a possible trend towards increasing estimated intensities over time, probably due to the gradual adoption of the objective satellite techniques. However, this possible bias is perhaps limited to a period up until the early-1970s and after that time it is likely that the variability is natural.

Figure 4.3 presents the seasonal distribution by month, showing December has the highest incidence at 20% of the total, followed closely by January at 18% and a further smaller peak of 16% in March. This shows a bias towards the start of the season but with a consistent occurrence rate across to April before rapidly decreasing in the winter months. The duration within radius distribution is given in Figure 4.4, showing a reasonably even spread over one to three days but with some particularly long-lived events. Figure 4.5 indicates how close these storms have come to the Cocos Islands in the past 41 years as a histogram of the closest approach distances. In this case the straightness of the cumulative distribution line shows this to be a reasonably even distribution of tracks, which is what could be expected in the open ocean environment free from the influences of continental landmasses.

Figure 4.6 presents the histogram of forward speeds of the storms at their point of closest approach. This shows a bias towards slower storms in the 2 to 4 ms^{-1} band but still results in an average speed of about 4.5 ms^{-1} (16.2 km h^{-1}). Occasionally, some storms exhibit extremely fast movement but these are normally tending extra-tropical and weakening. The next figure (Figure 4.7) shows the corresponding distribution of track bearings at time of closest approach, which highlights a significant bi-modality. Peak bearing (distance towards) occurrence can be seen to be grouped around the south-east and the south-west even though the bottom Figure 4.8 suggests reasonably chaotic track behaviour. The Cocos Islands are located near the centre of this figure, which covers the 500 km radius statistical control volume.

Appendix G provides a summary of all tropical cyclones within the 500 km radius based on the official Bureau of Meteorology track dataset. This base information needs to be further enhanced for modelling purposes, as discussed in the next section.

4.2 Parameterisation for Modelling Purposes

The adopted climatology model has the ability to describe the regional behaviour of tropical cyclones in terms of a mixture of different storm "populations". This allows for potential differences in the intensity, track and speed of tropical cyclones from different sources or under different broadscale climate influences. The initial climatology analysis points to the fact that there are essentially two storm population sources in the region - the north-west source with storms moving typically south-east and the north-east source typically moving south-west. The data set was then stratified so as to allocate each storm in the dataset to one of these two broad populations and the statistics were re-worked to determine if any significant differences could be found.

Firstly, Figure 4.9 presents the separated track plots for each case. Many individual storms have erratic paths and may form loops with extensive north-south or even east-west excursions but generally each of the storms can reasonably be allocated to one of these track origins. What appears immediately obvious from this separation is that the density of tracks is greatest for the north-east origin class.

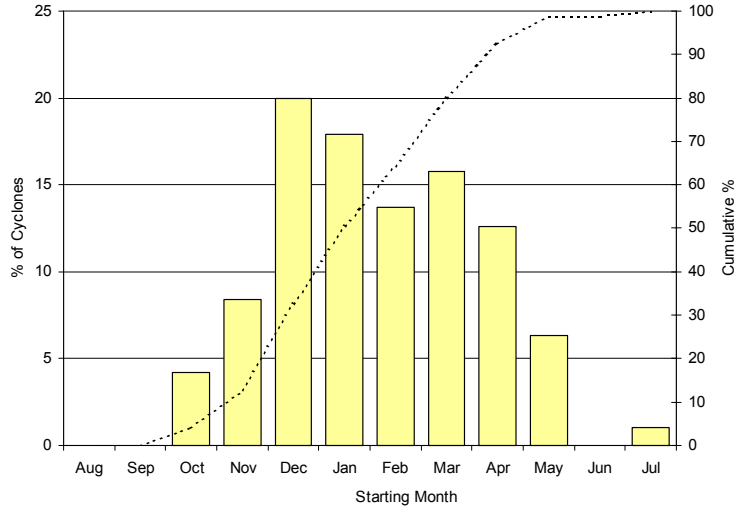

Figure 4.3 Seasonal distribution of cyclone occurrence.

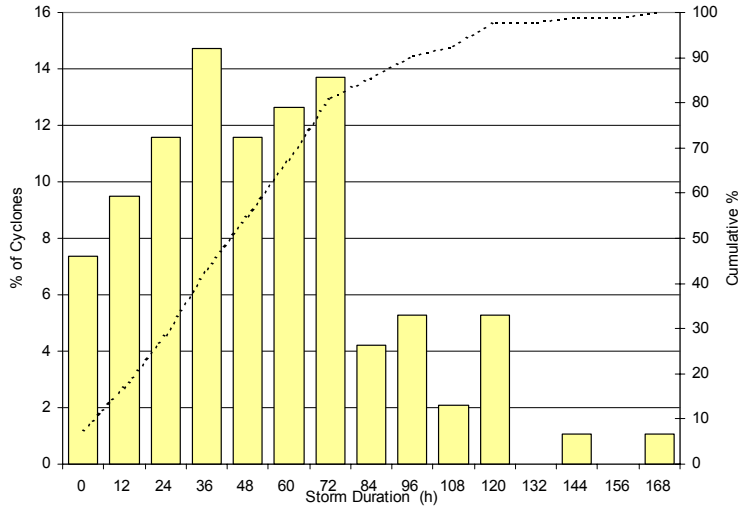

Figure 4.4 Duration distribution within radius.

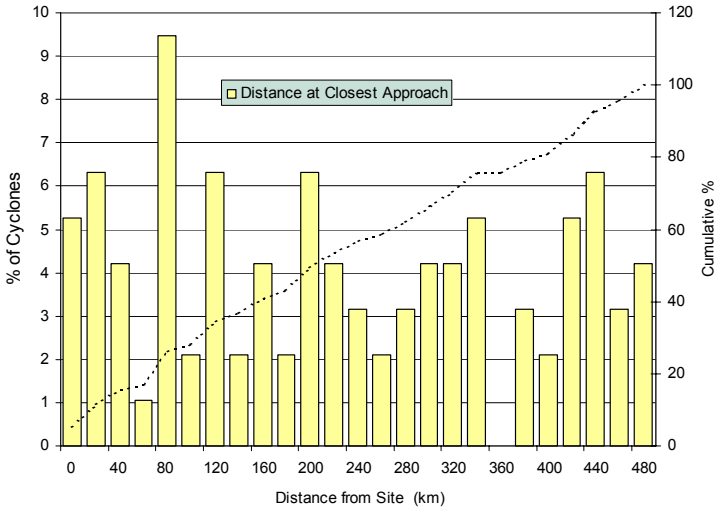

Figure 4.5 Distance of approach distribution.

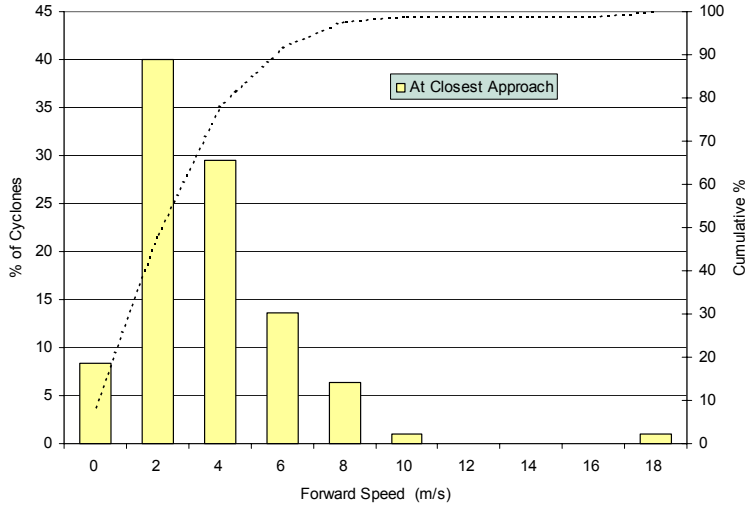

Figure 4.6 Forward speed distribution.

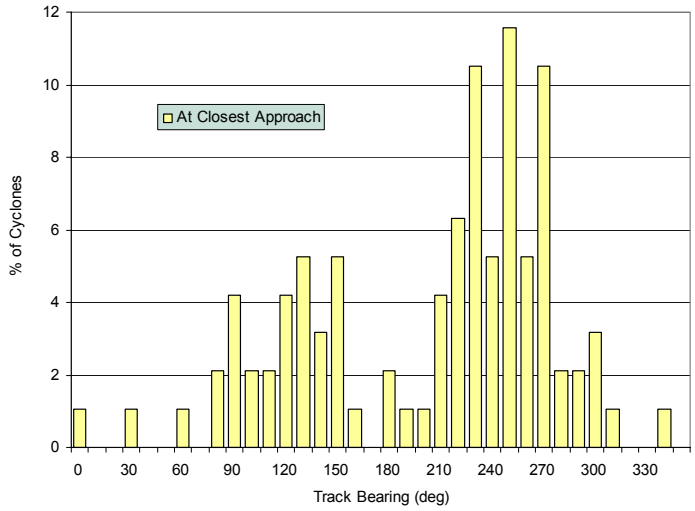

Figure 4.7 Track bearing distribution.

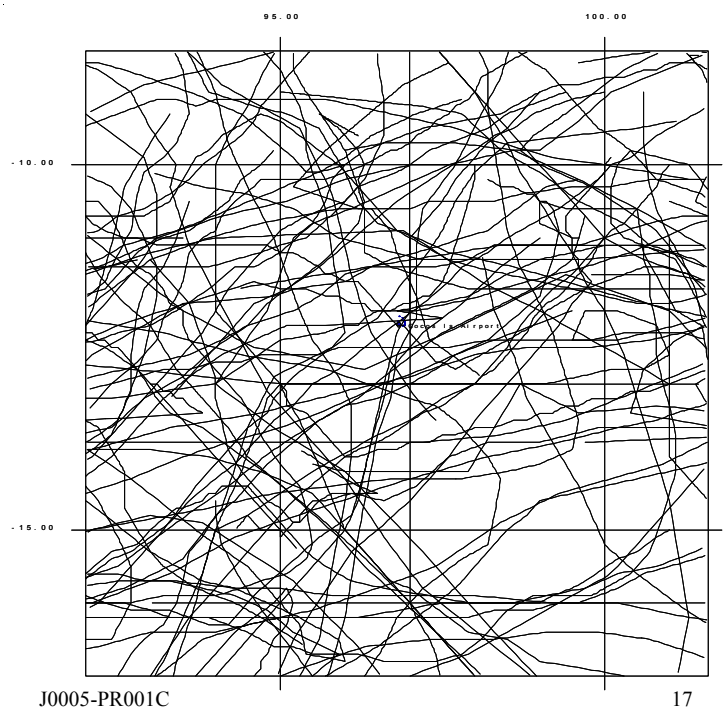

Figure 4.8 Combined tracks since 1959.

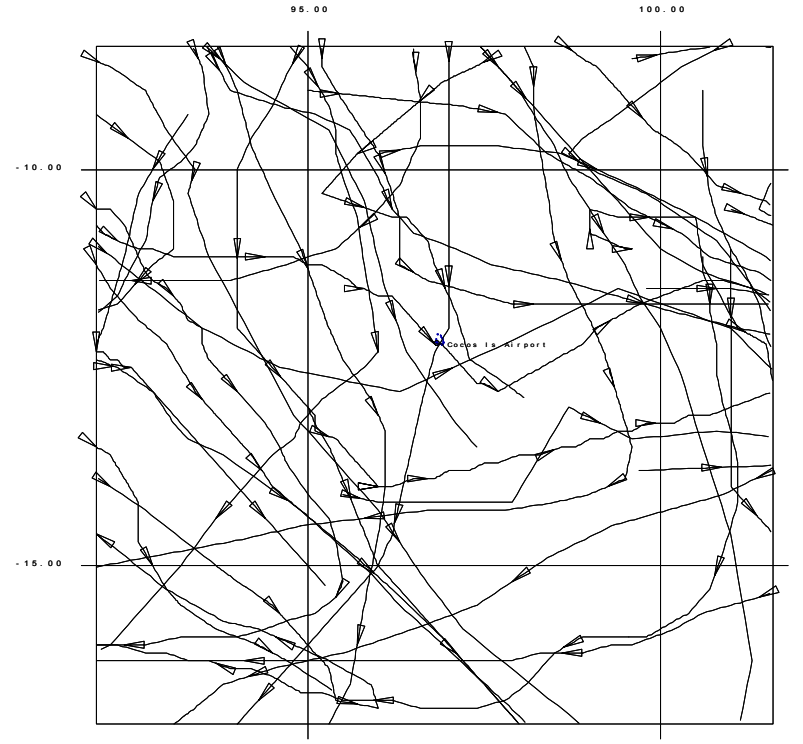

(a) North-West track origin class

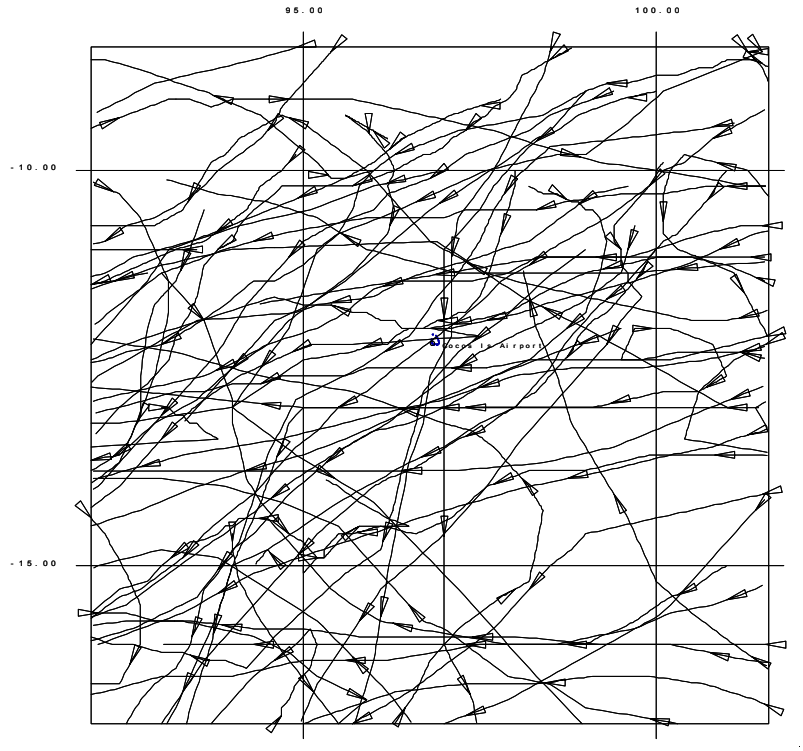

(a) North-East track origin class

Figure 4.9 Tropical cyclone tracks separated by origin class.

Following separation of the tracks, extreme value statistical analysis is carried out on the estimated central pressure data. Figure 4.10 presents these results in terms of the best fit line for each origin class (NW and NE), the combined classes line and the combined dataset. These curves were obtained following the method of Petrauskas and Aagaard (1971) and are specified as Extreme Value Type I (Gumbel) curves, the parameters for which are summarised in Table 4.1. The analysis shows that the NE origin class is the more intense storm population. In each case the continuous distributions are truncated at a nominal *Maximum Potential Intensity* (MPI) following the work of Holland (1997), which considers the theoretical thermodynamic limits as a function of regional climate and ocean indices. No specific assessment of the MPI for this region is available but a value consistent with the North West Shelf region of Western Australia has been adopted and is considered reasonable. This limits the maximum possible intensity in the region to 880 hPa which, based on Figure 4.10, has an estimated return period of about 200 years for the NE origin class and about 500 years for the NW origin class.

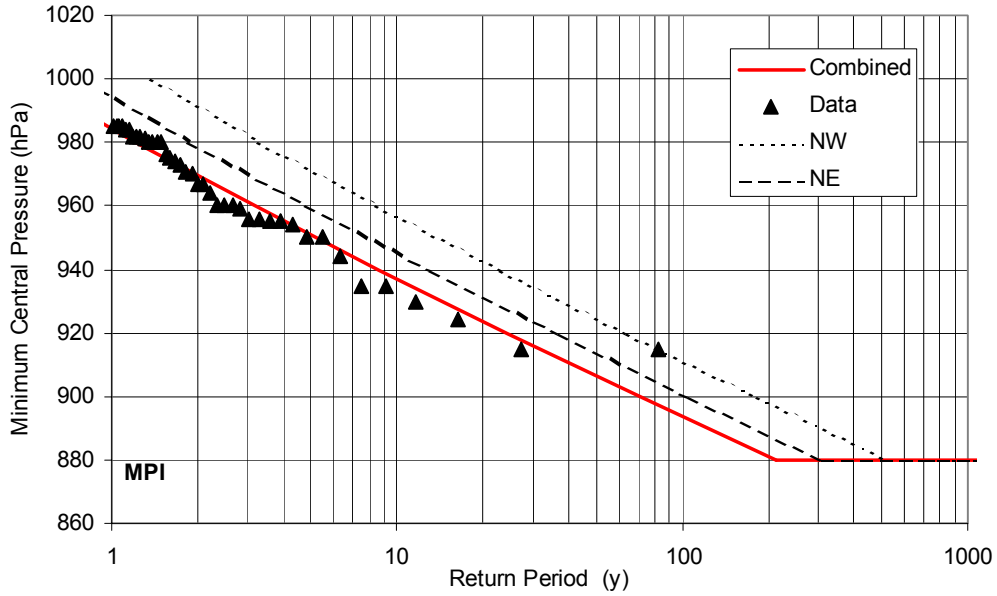

Figure 4.10 Extreme value analysis of central pressure estimates.

It remains to specify a number of other parameters to describe the regional tropical cyclone climate for each of the separated origin classes, i.e.

- distance of closest approach to target X_{prox}
- track bearing variability θ_{fm}
- forward speed variability V_{fm}

These are histogrammed similarly to the combined dataset and provided to the model as a series of smoothed data cumulative distribution functions (CDFs) as shown in Figure 4.11. Also, the Bureau of Meteorology track dataset does not provide information on the variability of the important storm spatial parameters:

- radius to maximum winds parameter R_c
- Holland wind field peakedness B_0

Distributions for the above parameters are therefore estimated based on experience in fitting the wind field model to various Australian storms.

Table 4.1 Statistical parameters adopted for climate modelling.

Track Population	Model Parameters			Cocos Region
	Name	Variable	Units	
	Ambient Pressure	p_n	hPa	1009
NW Origin	% This Track			38.9
	Av. No. Per Year			0.902
	Gumbel Intensity Parameters	U	hPa	997.63
		α		0.0524
	Max Potential Intensity	MPI	hPa	880
NE Origin	% This Track			61.1
	Av. No. Per Year			1.415
	Gumbel Intensity Parameters	U	hPa	994.76
		α		0.0529
	Max Potential Intensity	MPI	hPa	880

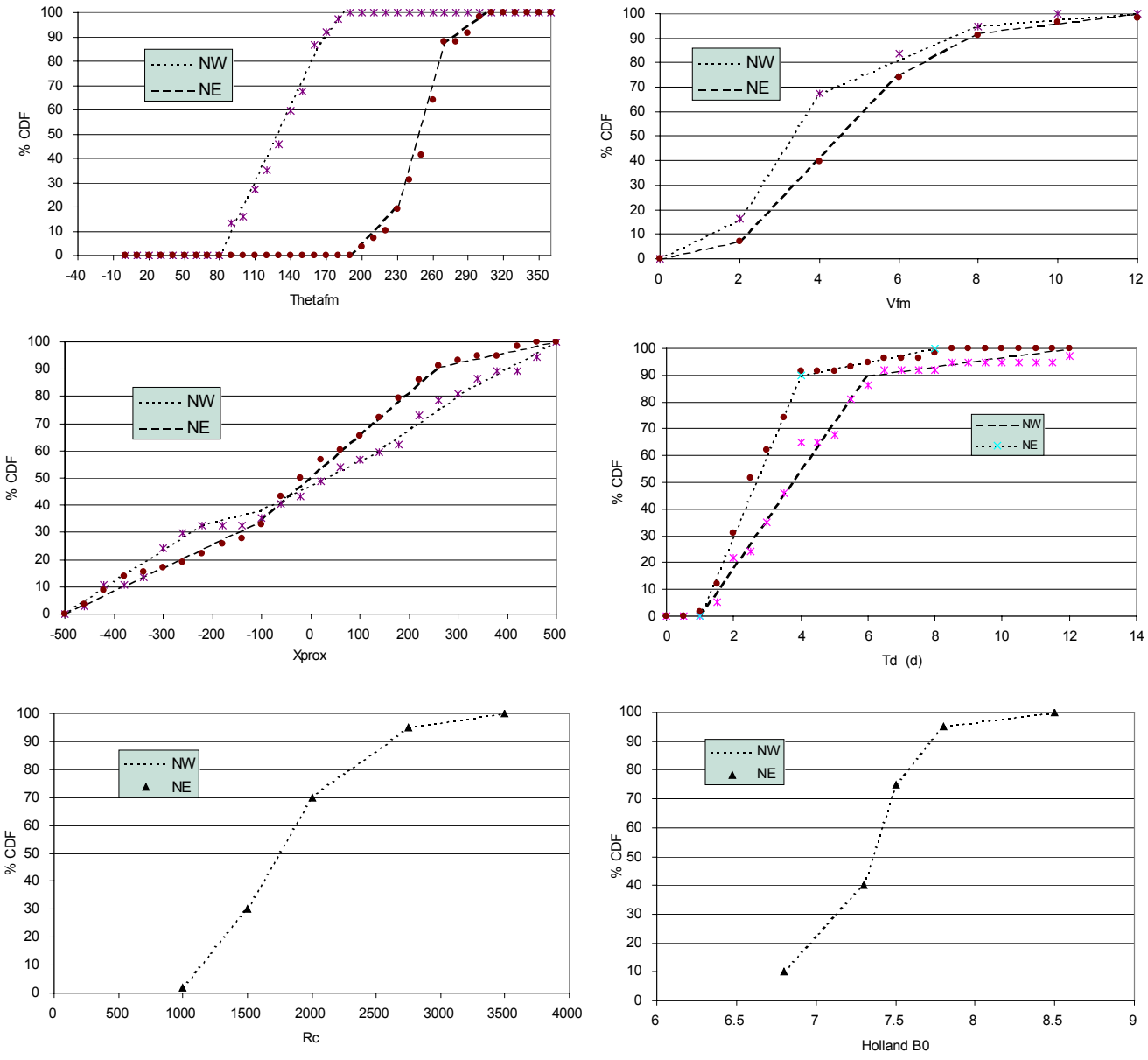

Figure 4.11 Smoothed storm parameter distributions provided to the model.

4.3 Regional Wind Speed and Pressure Data

The Bureau of Meteorology operates a standard weather station at the Cocos Islands airport and all available data from that station was obtained for analysis to determine the long term wind speed return period relationship and to provide calibration data for a selection of historical cyclones. Table 4.2 summarises the data sources and associated parameters of interest, where V_m is the 10 minute mean wind, θ_m the associated direction, V_3 is the 3-second peak gust speed and p is the MSL pressure.

Table 4.2 Cocos Islands wind records.

Type	Parameters	Start	End	No. Years	% avail
3 Hourly	V_m θ_m p	14-Feb-1952	16-Aug-2000	48.537	76
Daily	V_3	18-Jun-1952	24-Jan-1981	28.6219	98.5
METAR (10min WST)	V_m V_3 p	19-Nov-1995	16-Aug-2000	4.5	100

The 3 hourly and daily wind data sets were analysed to check the consistency of the data and provide some indication of regional variability. The mean summer MSL pressure of 1009 hPa was selected as the ambient pressure for modelling purposes. The wind data was then processed using a data window of 7 days to ensure independent events were obtained. Figure 4.12 presents the resulting mean wind speed and direction distribution in histogram format, consisting of data for all months overlaid with the January data. This shows the dominance of the E - SE direction sector which shifts more southerly during January under tropical cyclone influence. Also, the January wind speeds are generally lower than the full year distribution but have a longer high speed tail. Figure 4.13 presents the corresponding speed distribution for wind gusts, although the record is considerably shorter and no directions are available. This shows a bi-modal quality where the "storm" population can be seen to be separated from the background speeds above about 13 ms^{-1}. The extended upper tail during January is again evident.

Each of the data sets was then merged to form a composite set for extreme value analysis of both mean and gust wind speeds. In this case only the peak winds recorded during the period of activity of each recorded tropical cyclone were retained for analysis. For example, the peak winds of record are during cyclone *Doreen* in January 1968, being V_m of 39 ms^{-1} and V_3 of 51 ms^{-1}. In this case the analysis has been based on the method of maximum likelihood (Benjamin and Cornell 1970) again using Extreme Value Type I (Gumbel) guidance. The results are presented in Figure 4.14 for mean winds and Figure 4.15 for wind gusts, with predicted 1000 year return period values (the middle lines) of approximately 37 ms^{-1} and 59 ms^{-1} respectively. In each case the only significant outliers beyond the 90% confidence limit of the analysis (the upper and lower lines) are cyclones *Doreen*, *Annie* and *Harriet.* These results are compared with the SATSIM model predictions in Section 5.

4.4 Selection of Hindcast Storms

As part of the overall model validation process, a "top 10" storm set has been assembled for consideration. This is based on those storms which passed within 150 km of the Cocos Islands with central pressure below 990 hPa. Table 4.3 summarises their parameters at closest approach while Figure 4.15 shows their combined tracks. Wind speed and pressure data for each event was extracted from the data record for use in Section 4.

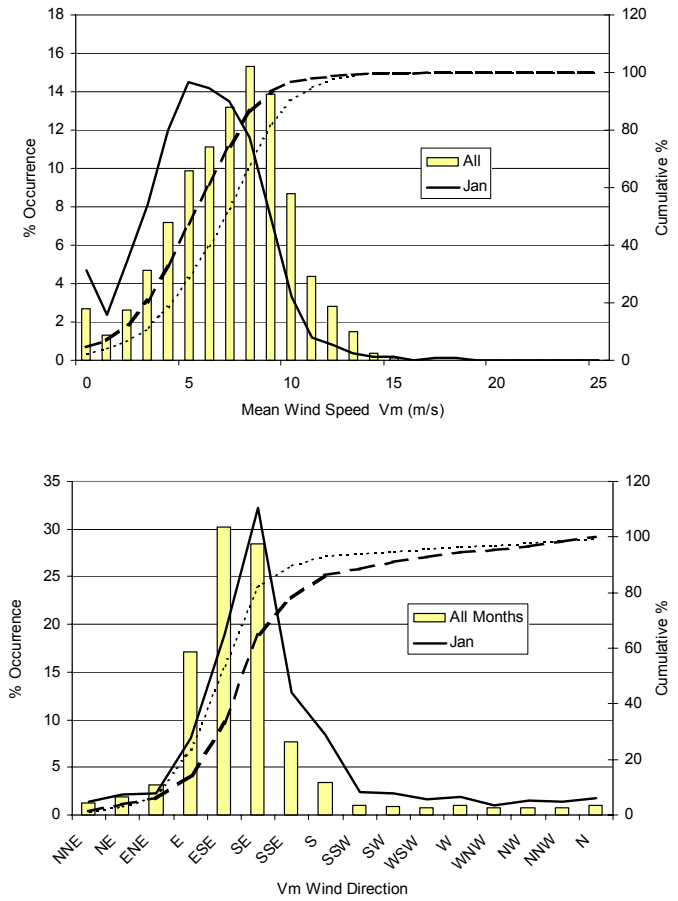

Figure 4.12 Mean wind speed and direction distributions.

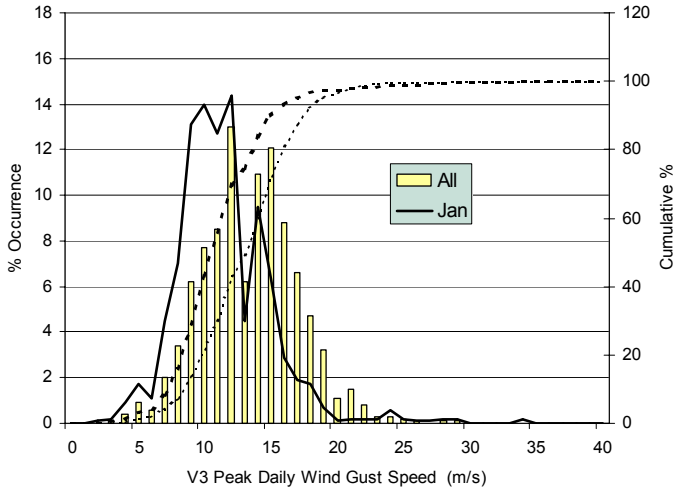

Figure 4.13 Peak daily wind gust speed distribution.

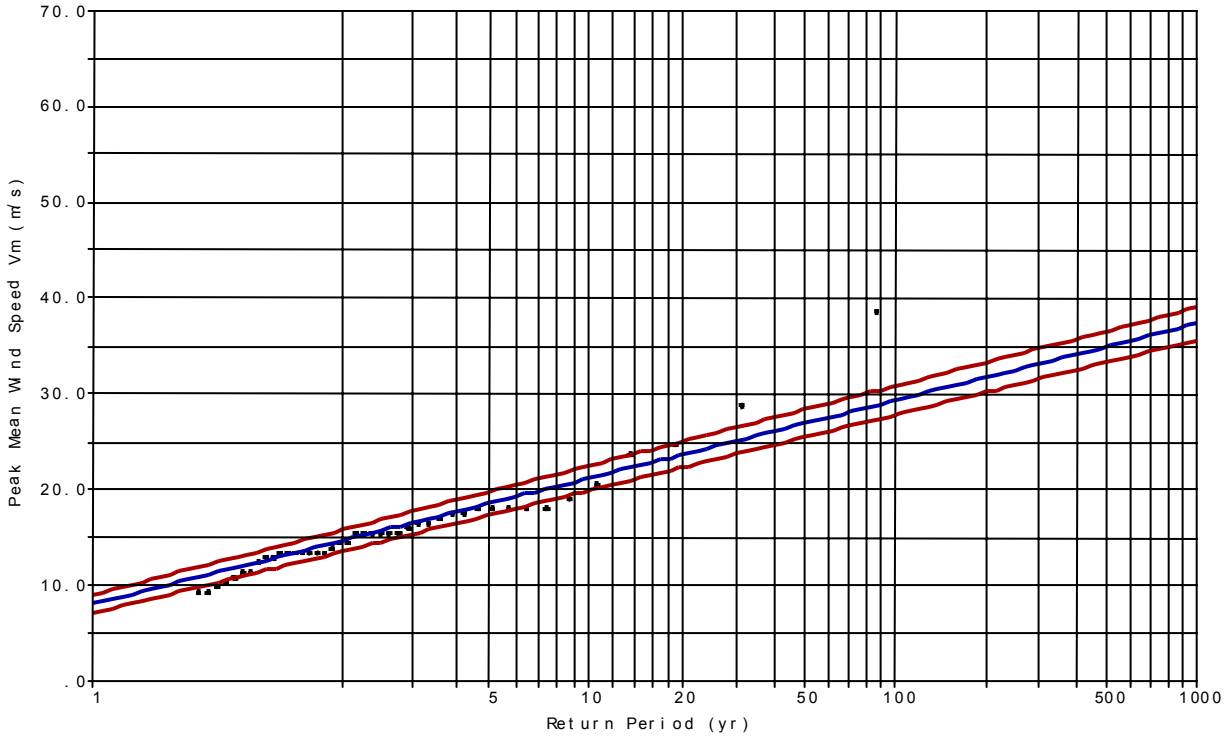

Figure 4.14 Extreme value analysis of mean wind speed during tropical cyclones.

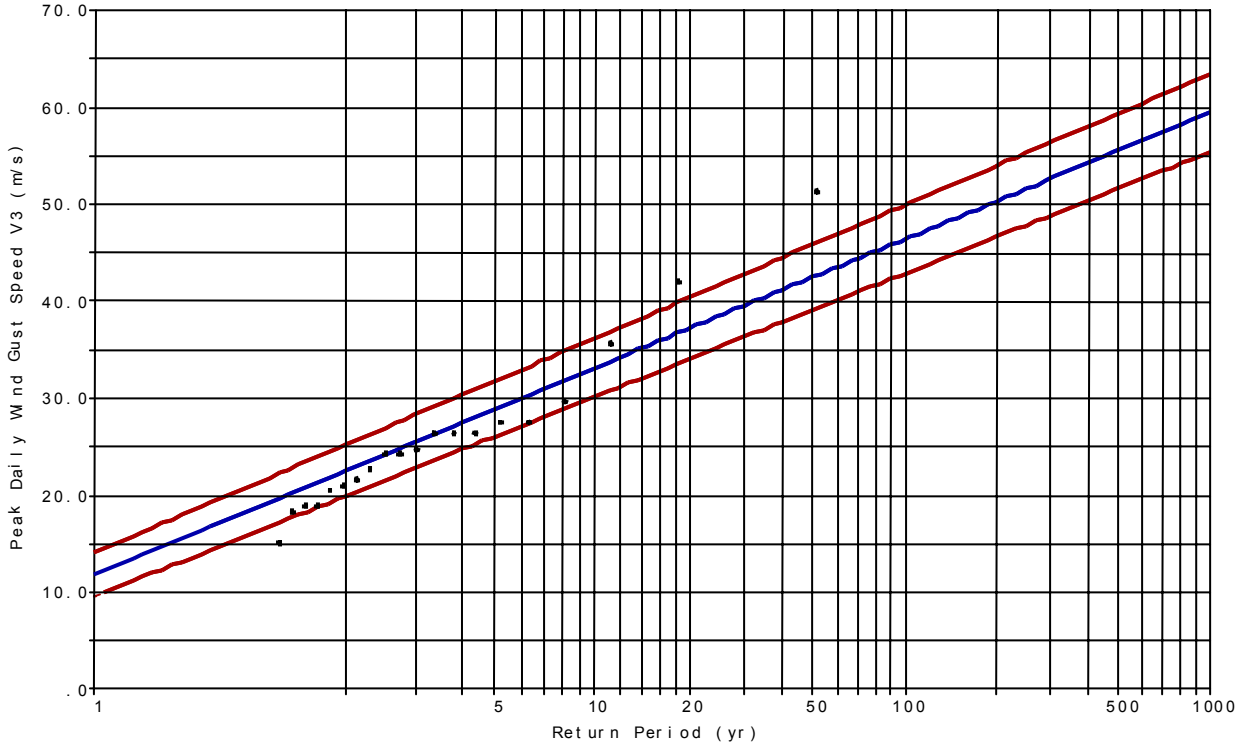

Figure 4.15 Extreme value analysis of wind gusts during tropical cyclones.

Table 4.3 "Top 10" hindcast storms.

		At Closest Approach to Site						
Sequence	Name	p_0	Date	Time	Dist	Bear	V_{fm}	θ_{fm}
No.		hPa		hhmm	km	°	m/s	°
196308	*Hazel*	988	09-Mar-1964	1000	89	182	4.0	270
196708	*Doreen*	970	21-Jan-1968	900	4	107	3.7	213
198319	*Daryl*	984	11-Mar-1984	1130	80	160	5.3	252
198502	*Ophelia*	989	11-Jan-1986	830	41	68	3.2	161
198702	*Frederic*	989	30-Jan-1988	1600	20	115	5.9	210
198901	*Pedro*	982	10-Nov-1989	1200	128	232	2.3	153
199101	*Graham*	926	05-Dec-1991	2200	132	20	5.5	112
199105	*Harriet*	973	27-Feb-1992	800	9	50	9.1	266
199506	*Hubert*	977	07-Jan-1996	2330	97	341	3.2	251
199802	*Alison*	967	08-Nov-1998	2030	88	153	4.5	242

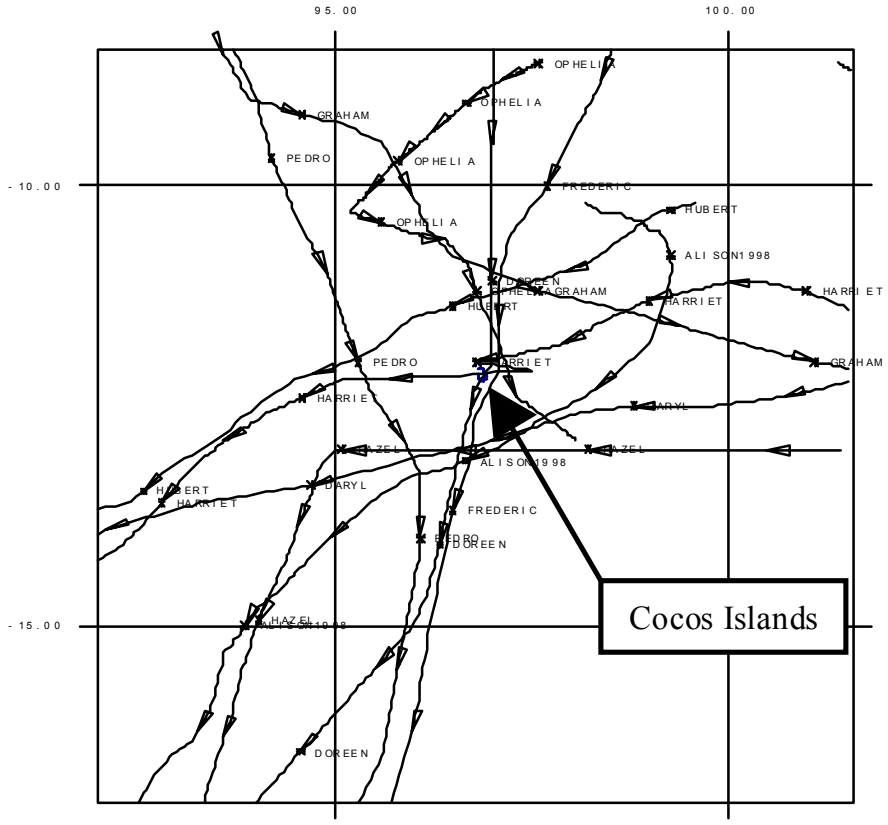

Figure 4.16 Tracks of the "top 10" storms.

5 Numerical Model Development and Testing

This section outlines the development of the various numerical modelling systems (winds, waves and surge) and the extent to which comparisons have been able to be made with measured data to provide model verification.

The "top 10" tropical cyclones as determined from Section 4 form the basis for *deterministic* comparison and testing. Long-term measured wind data and tidal planes form the basis of verification for *probabilistic* aspects.

5.1 Model Site Selection

A total of 20 atoll sites were specified by GHD for the purpose of deriving site-specific model output. These are shown in Figure 5.1 and their nominal positional details are tabulated in Table 5.1. These site numbers and/or names are referred to throughout the report.

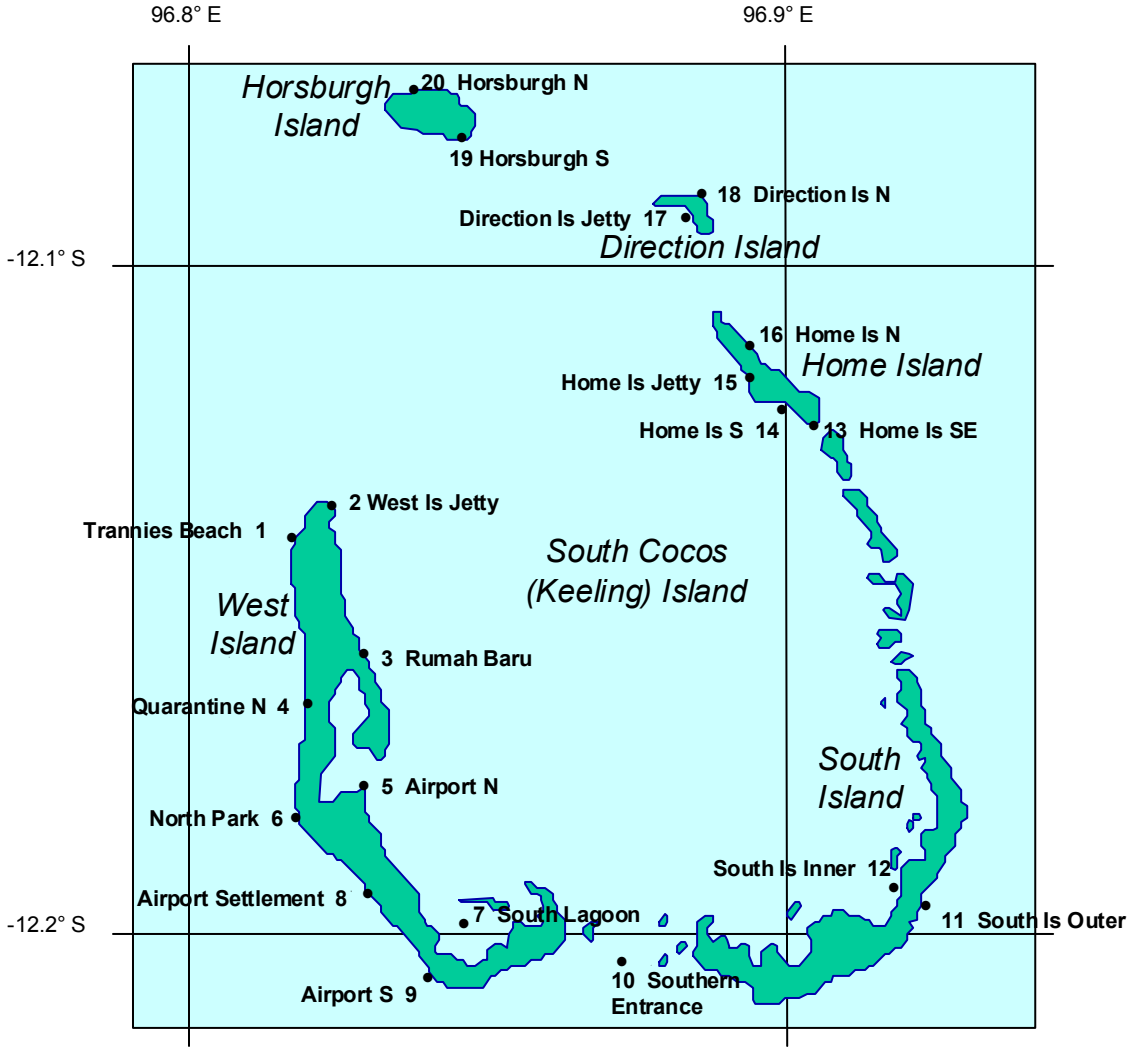

Figure 5.1 Specified atoll sites for model predictions.

Table 5.1 Specified atoll sites for model predictions.

Site_No	Site_Name	Lat °	Long °
1	Trannies_Beach	-12.1407	96.8177
2	West_Is_Jetty	-12.1360	96.8240
3	Rumah_Baru	-12.1585	96.8292
4	Quarantine_N	-12.1658	96.8207
5	Airport_N	-12.1781	96.8295
6	North_Park	-12.1818	96.8192
7	South_Lagoon	-12.1985	96.8466
8	Airport_Settlement	-12.1935	96.8297
9	Airport_S	-12.2062	96.8403
10	Southern_Entrance	-12.2038	96.8724
11	South_Is_Outer	-12.1954	96.9235
12	South_Is_Inner	-12.1928	96.9190
13	Home_Is_SE	-12.1231	96.9055
14	Home_Is_S	-12.1212	96.8990
15	Home_Is_Jetty	-12.1166	96.8909
16	Home_Is_N	-12.1130	96.8956
17	Direction_Is_Jetty	-12.0945	96.8849
18	Direction_Is_N	-12.0903	96.8864
19	Horsburgh_S	-12.0814	96.8470
20	Horsburgh_N	-12.0738	96.8357

5.2 Model Domain Selection

5.2.1 Spectral Wave Modelling

The grid system used for the spectral wave modelling consists of a set of four nested grids of increasing resolution and decreasing size, to maintain a balance between accuracy and computational efficiency. The largest grid CA (Figure5.2) was sized to accommodate the storm tracks of the top 10 data set and to ensure full fetch and duration effects were retained. A spatial resolution of 60 km was chosen with consideration for computational time and the required sub-grid resolution in the Cocos Islands area. The nested grids CB, CC and CD use resolutions of 20 km, 4 km, and 200 m respectively and are shown in Figure 5.3, 5.4 and 5.5. The grids are shown in their nested grid locations on the figure of the next largest grid. Underlying the basic wave calculation grids the sea bed bathymetry has been resolved at 60 km, 20 km, 1 km and 100 m for the CA, CB, CC, and CD grids respectively. The bathymetry is resolved at a finer resolution on the grids with shallow water to achieve a more accurate representation of the wave refraction effects. The spectral wave model grid details are given in Table 5.2.

Table 5.2 Spectral wave model grid domain details.

Grid Name	Grid Origin Latitude	Grid Origin Longitude	Size (nx,ny)	Wave Grid Resolution	Bathymetry Resolution	Source of Bathymetry
	°	°		m	m	
CA	-21.25000	87.33333	36,36	60,000	60,000	AUS Chart 4070
CB	-13.50000	95.50000	16,19	20,000	20,000	AUS Charts 4070 & 606
CC	-12.40667	96.13333	16,21	4,000	1,000	AUS Chart 606
CD	-12.22639	96.79861	81,101	200	100	GHD 80m grid + Aus Chart 607

The CA and CB grids are deepwater grids where the water depths are such that they have no effect on the wave predictions and are used only to ensure that the wave energy generated remotely from the site is correctly generated and used to provide realistic boundary conditions for the finer grids. At the resolution of the CC grid the physical features of the Cocos Islands are recognisable and the CD grid provides sufficient resolution to model all but the very fine detail of the atoll group. A computational resolution of 200 m and a bathymetry resolution of 100 m was required to reliably calculate the wave heights at the study sites which are close to shore.

The bathymetry information is based on the available chart information supplemented with information supplied by GHD, which has been used in many areas particularly around the outer reef shelf of the atoll and the southern half of the central lagoon which are marked as unsurveyed on the Charts. For the extent of this uncharted area refer to AUS chart 607. Efforts to use satellite imagery to supplement this information were unsuccessful.

The spectral wave model has a directional resolution of 22.5º and utilises 15 frequency bands (0.030, 0.043, 0.058, 0.074, 0.081, 0.097, 0.113, 0.129, 0.144, 0.160, 0.190, 0.230, 0.265, 0.300, 0.433 Hz)

5.2.2 2D Surge Modelling

The spectral wave model fine scale grid (CD), with a resolution of 200 m, was used for the 2D numerical hydrodynamic modelling.

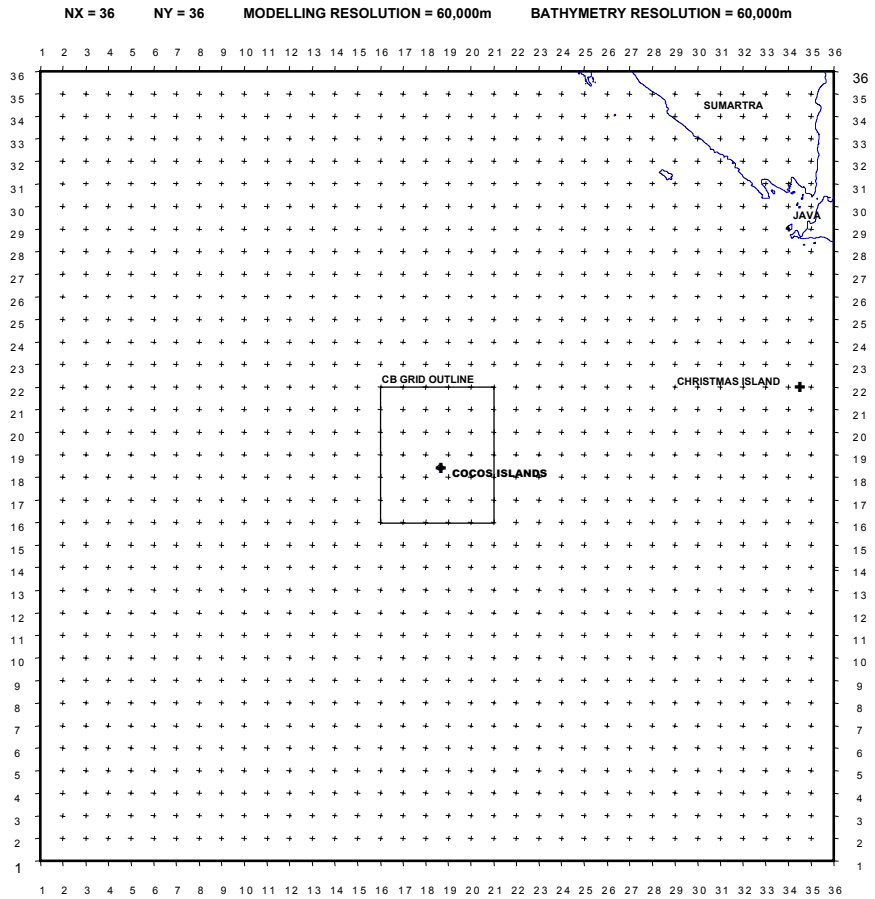

Figure 5.2 "A" grid spectral wave model domain.

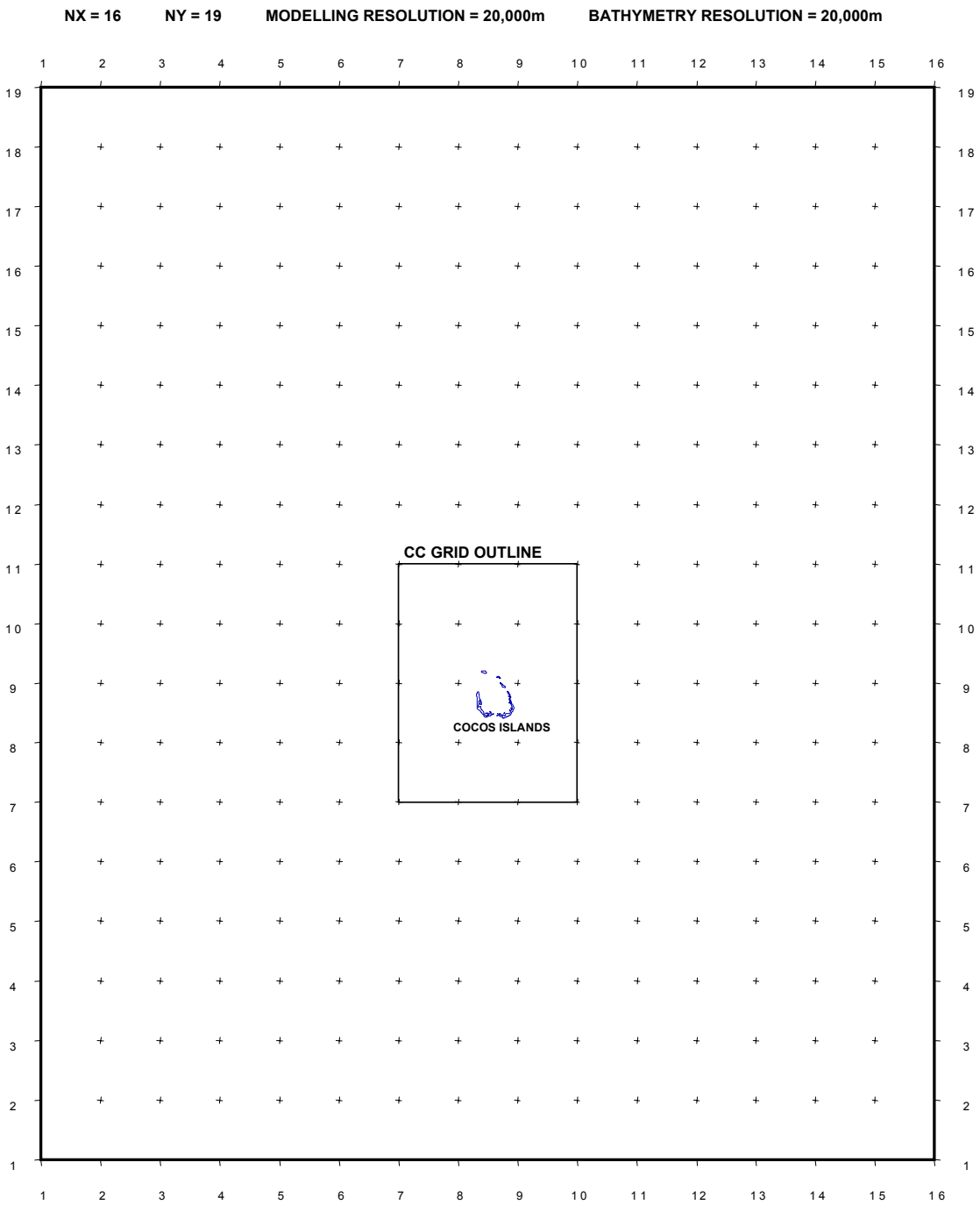

Figure 5.3 "B" grid spectral wave model domain.

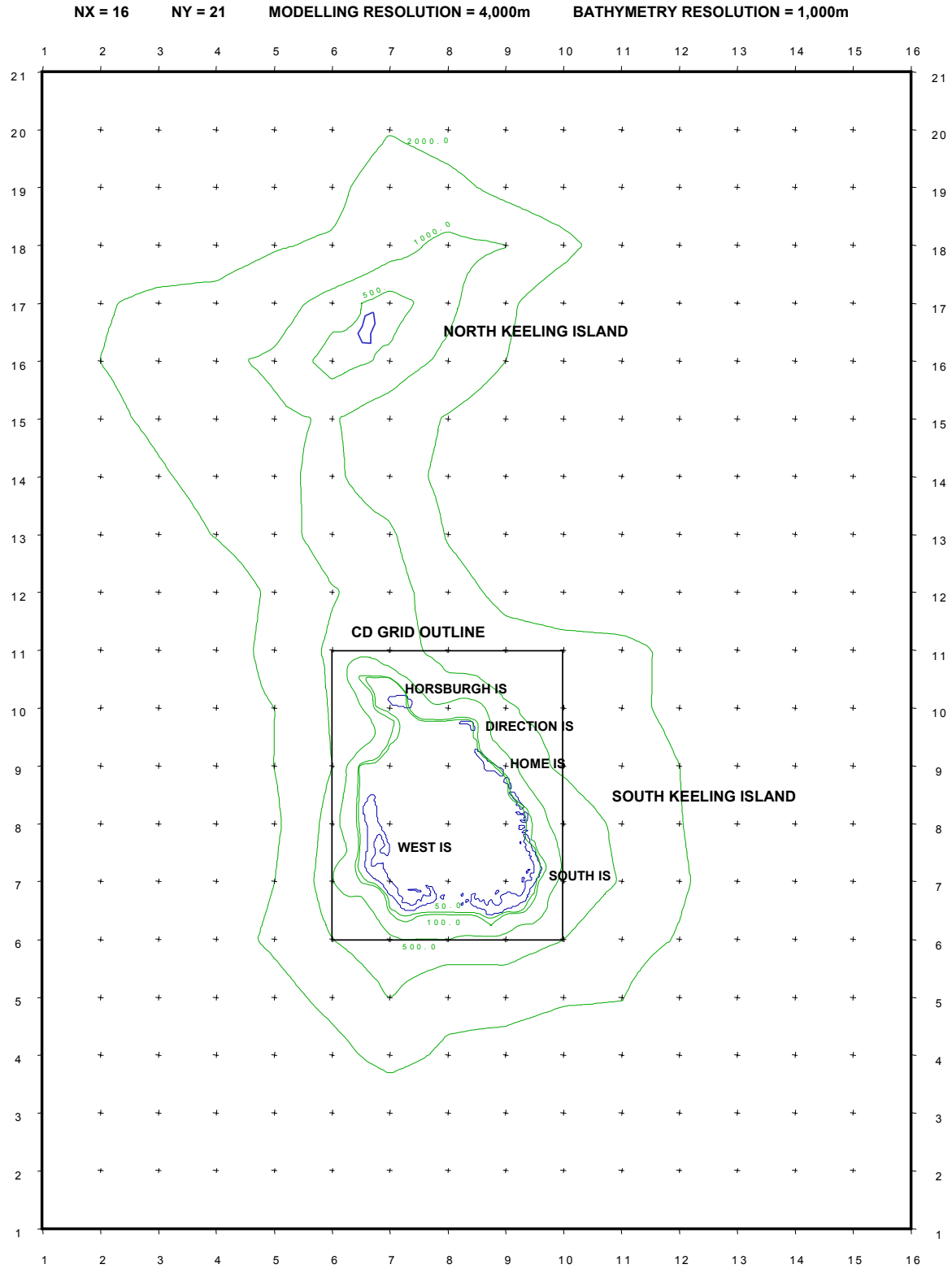

Figure 5.4 "C" grid spectral wave model domain.

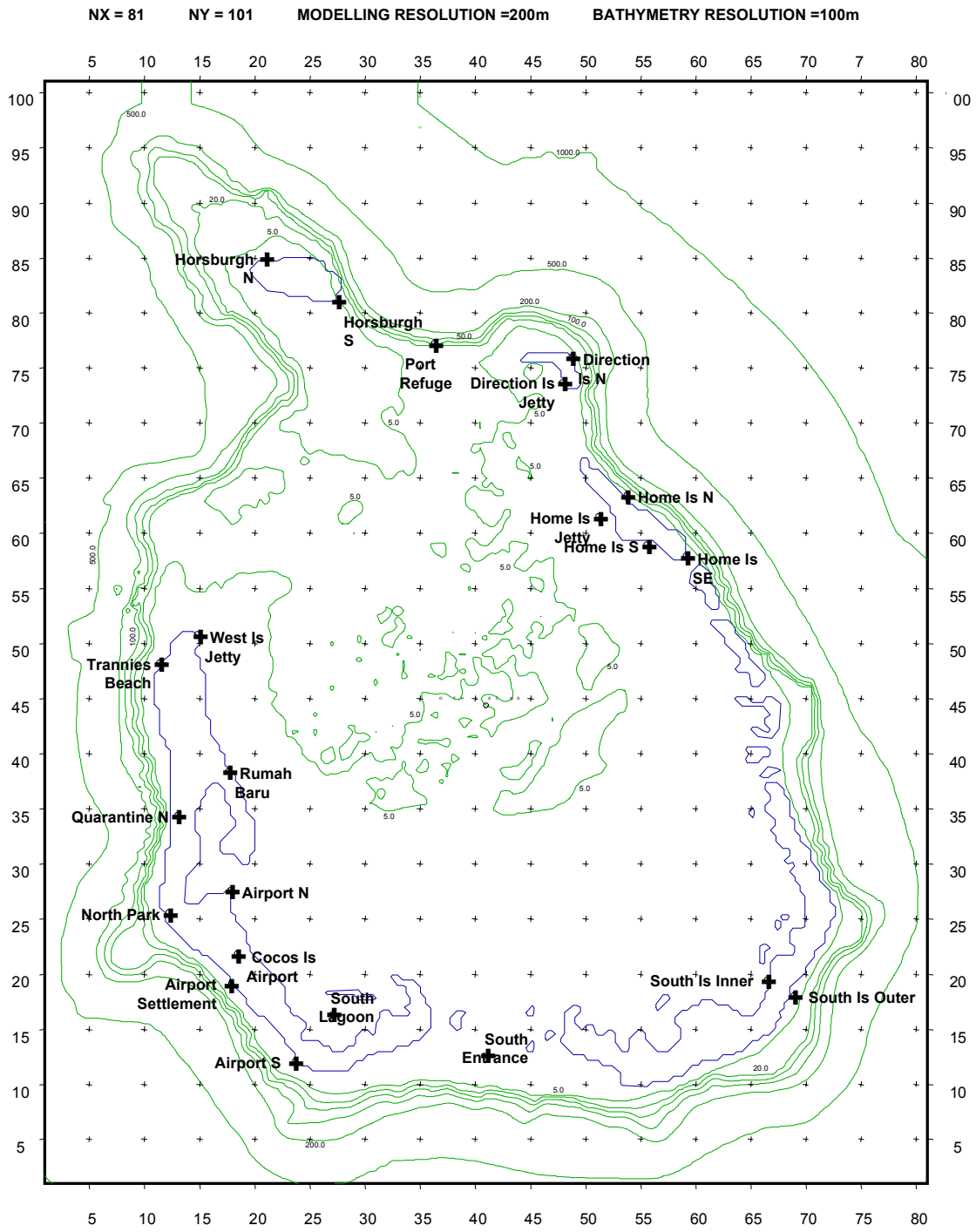

Figure 5.5 "D" grid spectral wave model domain.

5.2.3 1D Bathystrophic Storm Tide Modelling

This also utilised the CD grid but the gridded dataset was used only to extract a series of 1D depth profiles for each site at a directional resolution of 10°.

5.3 Reef Parameterisation

As discussed in Appendix F, wave-induced setup is known to be very sensitive to the relationship between water level, reef crest height and the slope of the reef-rim and reef-face. Accordingly, it is important to have reasonably accurate descriptions of the fringing reef structures. Unfortunately, no specific or detailed set of survey data presently exist and the study has had to rely on a variety of information from a number of different sources. These sources are summarised below and their approximate spatial distribution is indicated on Figure 5.6.

5.3.1 Data Sources

An attempt was made early in the investigation to utilise remote sensing techniques as an aid to determining the distribution of water depths throughout the atoll and islands. A LANDSAT™ image was located (refer Figure 2.2) and subsequently analysed by GEOIMAGE Pty Ltd but due to the highly variable lagoon substrates, wave contamination over the fringing reefs and an overall lack of groundtruth, the derived depths could not be calibrated successfully. Accordingly, more conventional data sources were relied upon.

(a) HMAS Moresby Survey (Sites 1, 19, 20)

This naval hydrographic survey (RAN 1983) was limited to the north-western portion of the atoll and concentrated on establishing depths for shipping activities through Port Refuge (between Horsburgh Is. and Direction Is.) and the Western Entrance (between Horsburgh Is. and West Is.). The survey data is in the form of Fair Charts but provides some indication of nearshore fringing reef profiles near the northern tip of West Island and around Horsburgh Island. Adjustment to MSL and interpretation of these profiles was undertaken by Dr M. Gourlay.

(b) GHD 80m Gridded Depths (General Use Only)

This is the same gridded data set (GHD 2000b) used as a basis for the 200 m resolution wave and surge modelling. GHD advise that coordinates are AGD84 from Chart AUS 607 and the grid was created for wave penetration studies into the lagoon so external reef areas were not critically reviewed. Manual changes to the base admiralty chart data were effected by GHD (C.Jones *pers comm.*) such that deep areas were all set at -1000 m and depths between the reef edge (taken nominally as -10 m and inferred from GHD satellite photograph) and -200 m were estimated only. Reef heights in the south channel were inferred from the satellite image and site visits, together with channel depths north of Home Island. Depths inside the lagoon are from surveys and charts with the bluehole area in SE of the lagoon inferred from satellite image and weed growth areas. Depths were adjusted from chart datum to MSL. This data set has been used only for general guidance in the absence of any other information.

(c) CSIRO Outfall Survey (Site 4)

This dataset was provided by GHD (GHD 2000c) and consists of a series of three east-west offshore echo sounder profiles near Site 4 Quarantine North undertaken by CSIRO. The three profiles are within a 150 m stretch of the foreshore and commence below 4 m depth. They offer no reef flat

information but provide a good indication of the slope of the submerged reef face. The exact vertical datum is apparently uncertain but unimportant for the purposes here. The principal profile from this dataset was used as a proxy for all locations in the absence of any other information.

(d) GHD Nearshore Survey (Site 8)

A contour map of reef flat levels adjacent to the seawall at Site 8 was provided by GHD (GHD 2000a) and interpreted by Dr M. Gourlay. The survey extends along some 700 m of shoreline and shows a highly variable reef surface. This is the only area encountered where available data indicates reef flat levels at or above MSL across the reef flat. An average of six sections was taken as being representative of the site.

(e) Aerial Photography (All Sites)

Aerial photography (ASO 1987) from August 1987 was provided by GHD and interpreted by Dr M. Gourlay to provide estimates of reef flat and submerged reef widths at all sites, in conjunction with any other site specific information. The tide level and wave conditions were generally suitable for determining the nominal width of the reef flat and the width of the submerged reef rim.

(f) Geomorphological Studies (Sites 1, 4, 6, 9, 10, 11, 13, 16)

Dr M. Gourlay researched a number of geomorphological studies undertaken at the atoll over the past 10 years which provided transects relative to MSL datum, many of which extended across the reef flats to the crest region in a variety of areas. Based on discussions with one of the principal authors (C. Woodroffe *pers comm.*) Dr Gourlay believes that the survey techniques applied are reasonably accurate. Profiles were taken from a variety of sources and enlarged to facilitate extraction of reef top data to perhaps an accuracy of about 0.1 m. The sources used were Woodroffe et al. (1990), Woodroffe et al. (1991), Woodroffe et al. (1994) and Smithers and Woodroffe (2000).

(g) Dr Paul Kench (*personal communication*)

Paul Kench is a Research Fellow in the International Global Change Institute (IGCI) at the University of Waikato who conducted an extensive data collection program at the Cocos Islands during late 1991 and 1992. Findings based on his research relating to the hydrodynamics of the lagoon system have been variously published (Kench 1994; 1998ab) but without specific details of the reef flat profiles. Dr Kench kindly agreed to provide some of his as yet unpublished surveyed profiles for the purpose of this investigation. These consist of reef crest to lagoon longitudinal profiles through each of the 7 passages south from Home Island to the Southern Entrance (where 3 profiles are available). Each survey was tied to semi-permanent marker pegs installed on the conglomerate platform around the atoll. These pegs were all surveyed and closed off to the permanent survey markers on Home Island and South Island (Scout Park). In the case of the eastern passage profiles there may be some effects of scouring although the predominant flow is lagoonward.

5.3.2 Methodology and Adopted Profile Parameters

All data relevant to each site was considered in the assessment and profiles were overplotted to facilitate analysis. Typically this involved selection of the closest reef flat profile (where available) and merging it with the most appropriate submerged reef profile available (e.g. Moresby or CSIRO etc). Small adjustments were needed to suit reef flat width information from the aerial photography, especially if the closest reef flat profiles were at wider or narrower sections. Emphasis was placed on determining the reef crest height (most often taken from the geomorphology sections), the reef

rim slope merged with the crest height and then the reef face slope. The reef flat width was principally from the geomorphological sections or aerial photography. The reef rim slope is controlled in the majority of cases by the submerged width from the aerial photography and the assumption of a nominal -10 m at the outer limit, derived by comparison with the CSIRO profile. Least information is available in regard to the reef face (i.e. -10 m and deeper) and the CSIRO profile remains the main reference, except for Site 20 where the chart indicates an undersea ridge. The final profiles are essentially deliberately schematised to suit the reef setup method of Gourlay (refer Appendix F).

Figure 5.7 presents a graphical summary of all profiles devised for the fringing reef situations and Table 5.3 provides an indication as to the exact data sets used in each situation. Numbers in parenthesis indicate the specific survey section applied. At Site 19 there are two potential exposures and a compromise profile biased towards the (deemed more conservative) NE exposure is adopted; Sites 18, 19 and 20 have no objective reef crest heights and -0.5 m is assumed as a nominal value.

5.3.3 Reef Parameter Variability

Based on the present analysis, reef top parameters may vary considerably around the atoll and, as determined by the available data, the assumptions summarised in Table 5.3 are consistent with the observations by Kench (1998, 2000) - namely that the reefs on the eastern side are narrower than the south and the west and that the reef crest height rises towards the south. This latter feature is apparently controlled by the predominant SE and SW swell conditions providing a background wave setup, at which the reef growth has reached equilibrium, but also by the tidal plane amplification in the southern part of the lagoon (refer Section 5.5.3).

Some variability can also be quite localised, as shown where more than one section was available at a single site (e.g. GHD 2000a,c) and some geomorphology studies). In an attempt to provide a range of parameters to the statistical water level simulation an analysis of this variability was attempted. For example, Figure 5.8 summarises the variability at Site 8 based on six sections only 100 m apart where the standard deviation can be high as 0.3 m across the flat but reduces to about 0.1 m near the crest. In the absence of any more definitive information 0.1 m could be taken as representative of localised crest height variability. No other site provides similarly detailed information although the series of Kench (2000) profiles across the Southern Entrance suggest the variability in that region is much less. His profiles have an erratic horizontal interval (between 1 and 50 m typically) but when smoothed and interpolated to a common base of 5 m over the first 100 m shoreward from near the crest show a standard deviation on common chainage of less than 0.1 m. Taking the "near crest height" as the main controller of reef top setup, a nominal standard deviation of 0.1 m is therefore adopted for sensitivity testing in Section 6.

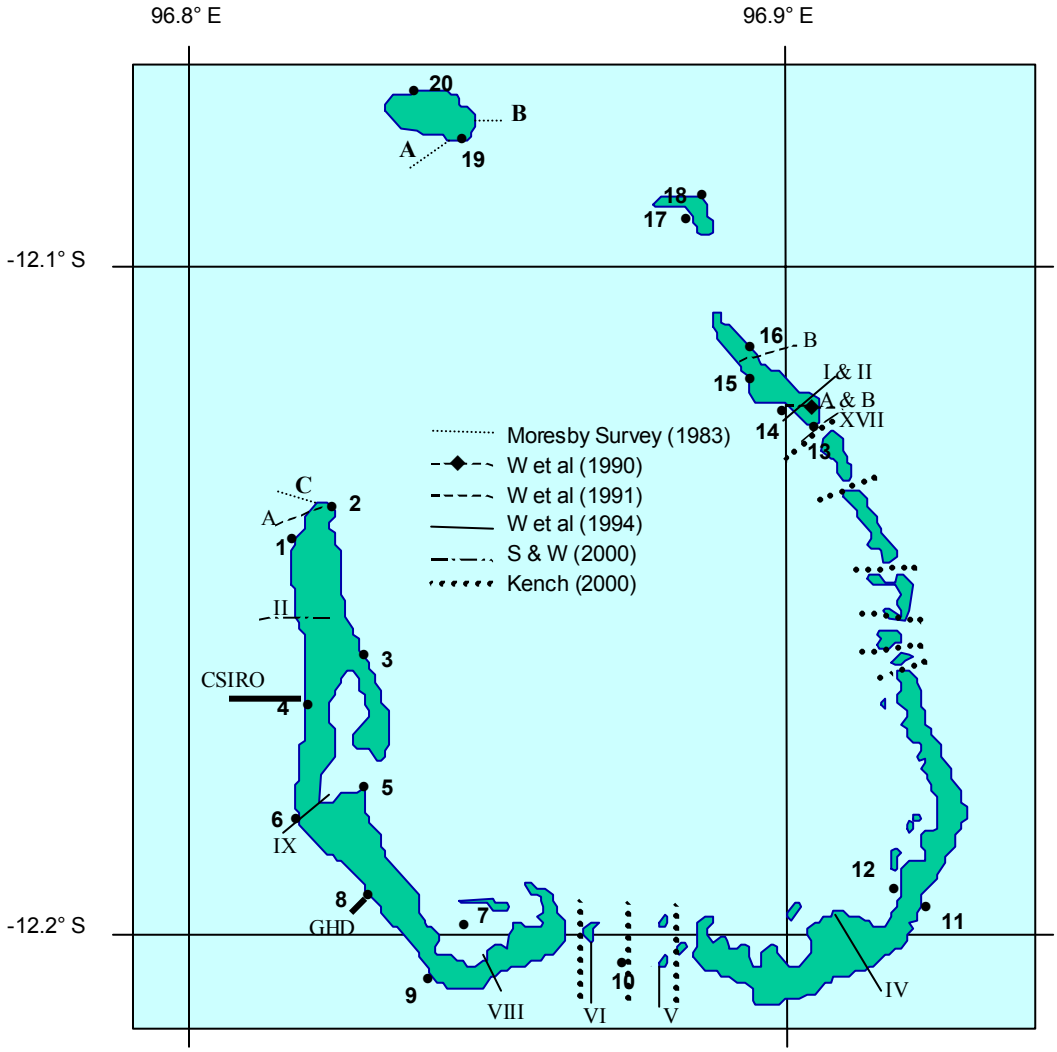

Figure 5.6 Location of various data sources used for establishing reef parameters.

Table 5.3 Summary of Reef Parameter Data Assessment

Site	Name	Reef Crest	Reef Flat	Reef Edge	Sub Reef	Rim Slope	Face Slope	Data Sources Used and General Order of Precedence									
		m MSL	m	m MSL	m	tan α	tan α	Kench (2000)	Moresby Survey*	S&W (2000)	W et al. (1990)	W et al. (1991)	W et al. (1994)	CSIRO Outfall	GHD 80m	GHD Survey	Aerial Photos*
1	Trannies Beach	-0.60	250	-14.0	380	0.04	0.36		2			1 (A)					3
4	Quarantine N	-0.80	200	-10.0	280	0.04	0.36			1 (II)				2			3
6	North Park	-0.50	200	-10.0	280	0.03	0.36						1 (IX)	2			3
8	Airport Settlement	-0.10	200	-10.0	280	0.04	0.36							2		1	3
9	Airport S	-0.30	200	-10.0	280	0.03	0.36						1 (VIII)	2			3
10	Southern Entrance	-0.35	200	-10.0	250	0.04	0.36	1					3 (V & VI)	2			4
11	South is Outer	-0.35	180	-10.0	250	0.04	0.36	2					1 (IV)	3			4
13	Home Is SE	-0.50	100	-10.0	180	0.05	0.36	1		2 (XVII)	2 (A & B)		2 (II)	2	4		3
16	Home Is N	-0.50	150	-10.0	200	0.04	0.36	2				1 (B)	2 (I & II)	2	4		3
18	Direction Is N	-0.50	50	-10.0	280	0.03	0.36								2		1
19	Horsburgh Is S	-0.50	100	-10.0	180	0.05	0.36		1								2
20	Horsburgh Is N	-0.50	100	-10.0	180	0.06	0.01		1						2		3

* Analyses by M. Gourlay

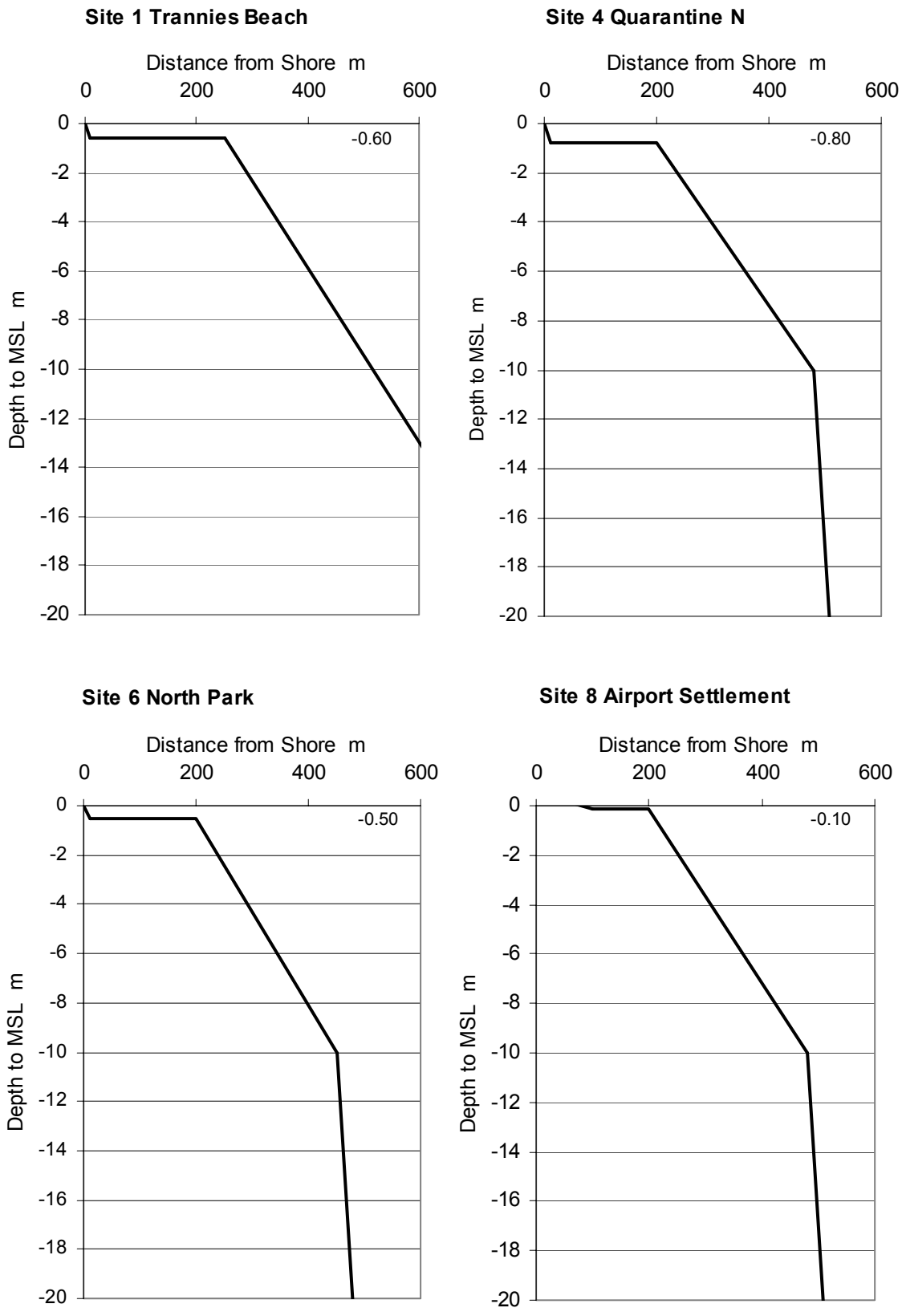

Figure 5.7 Schematised Reef Profiles

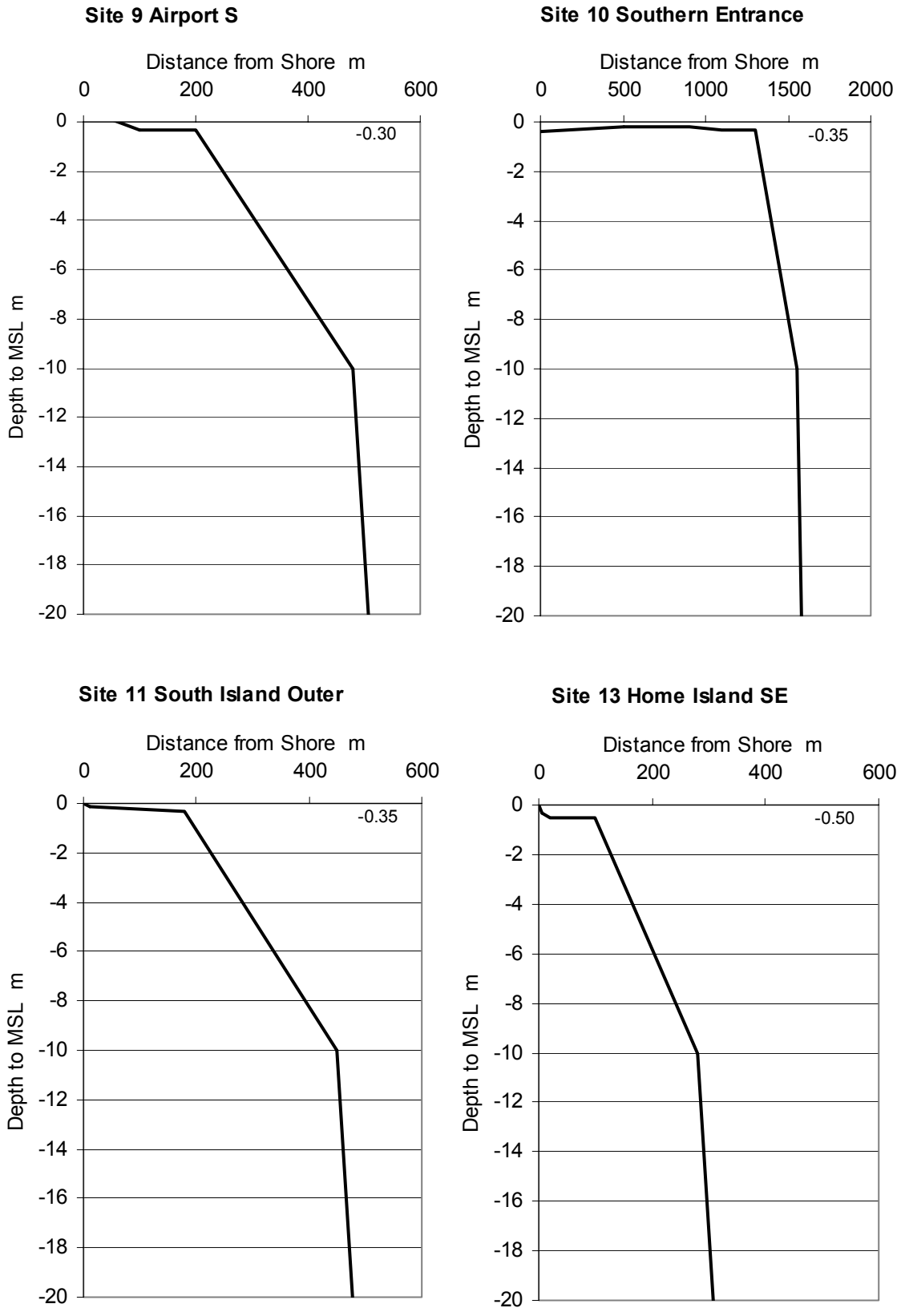

Figure 5.7 (cont) Schematised Reef Profiles

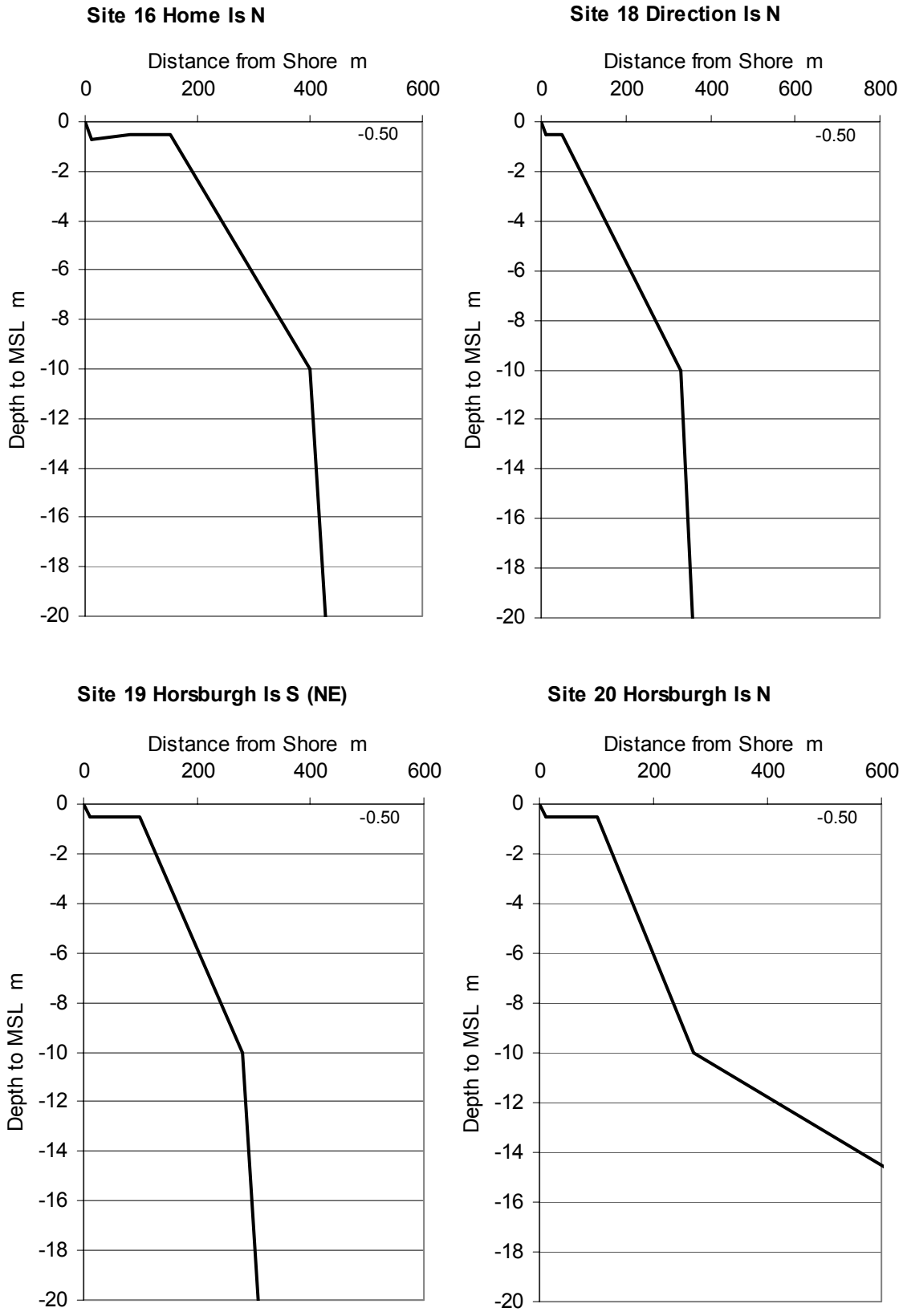

Figure 5.7 (cont) Schematised Reef Profiles

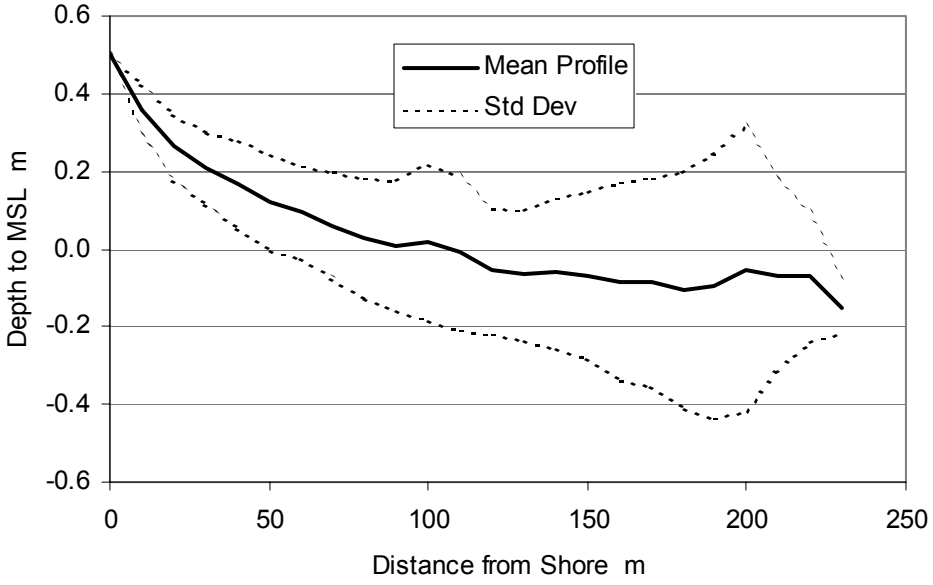

Figure 5.8 Variability in six reef flat profiles at Site 8 (after GHD 2000a).

5.4 Wind and Pressure Field Modelling

In order to model the generation of waves, wave setup and storm surge it is first necessary to ensure that the wind and pressure forcing applied to the models is representative of each cyclone event. As mentioned previously, the Bureau of Meteorology track database does not provide estimates of all the parameters required to enable reconstruction of the wind and pressure fields. Specifically, B_0 and R_c remain essentially as calibration parameters in this context.

Each of the "top 10" storm events was subjected to a process of model calibration whereby the historical track and intensity information was combined with a range of possible B_0 and R_c values. The resulting time history of predicted wind and pressure at Cocos Islands Airport was then compared with the available measured data. In this way a set of optimum parameters could be constructed using the error between the peak predicted and peak measured values as the primary reference. Also, to ensure the phasing of the modelled and measured time histories was reasonable, the bias error over a finite period of time was also used. An example of the calibration process is provided here for cyclone *Alison* in 1998 and Appendix H details the individual calibration results for the remaining storms in the "top 10".

Cyclone *Alison* was the most recent cyclone to have significantly affected the Cocos Islands and has the benefit of hourly and sometimes 10 minute measured winds and pressures at the airport. Earlier storms prior to the introduction of the Automatic Weather Station (AWS) only have 3 hourly winds and pressures available. Figure 5.9 summarises the full set of storm parameters developed for cyclone *Alison* as a time history of central pressure p_0 (peaking at 955 hPa 200 km after passing the atoll), radius to maximum winds (derived from R_c), forward speed V_{fm} and bearing θ_{fm} and finally distance from the atoll. At its closest approach to the atoll, 88km to the SE, the central pressure was 967 hPa, radius to maximum winds about 30 km, and it was travelling at 4.5 ms^{-1} towards the SW. At this time, the estimated wind (asymmetric contours at 5 ms^{-1} intervals and vectors) and pressure fields (concentric 5 hPa contours) are shown in Figure 5.10, whereby predominantly westerly winds were being experienced at the atoll. This placed the atoll on the "weak" side of the storm, the strongest winds being located forward and to the left-hand side of the track of the storm.

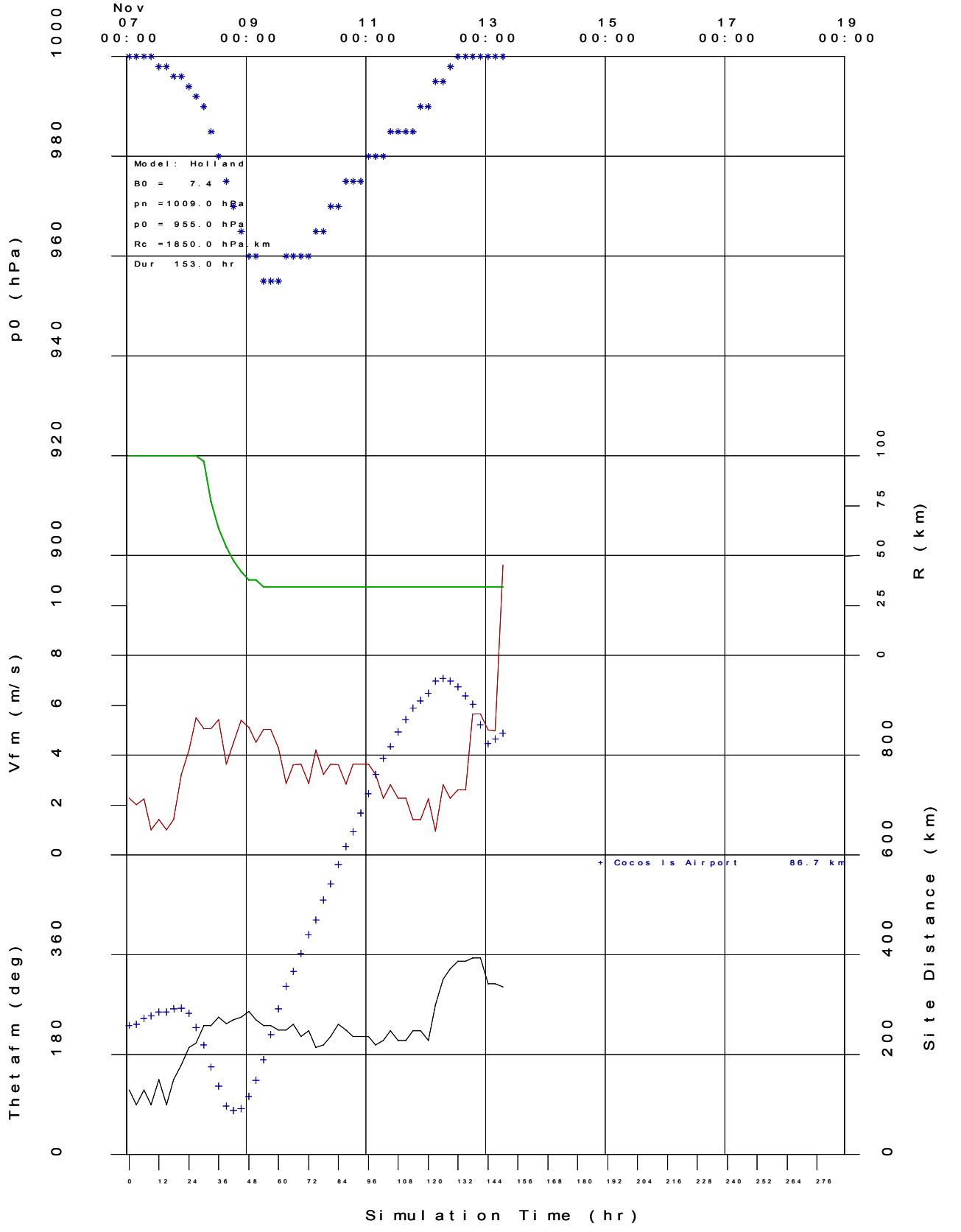

Figure 5.9 Modelled track parameter time history for *Alison*.

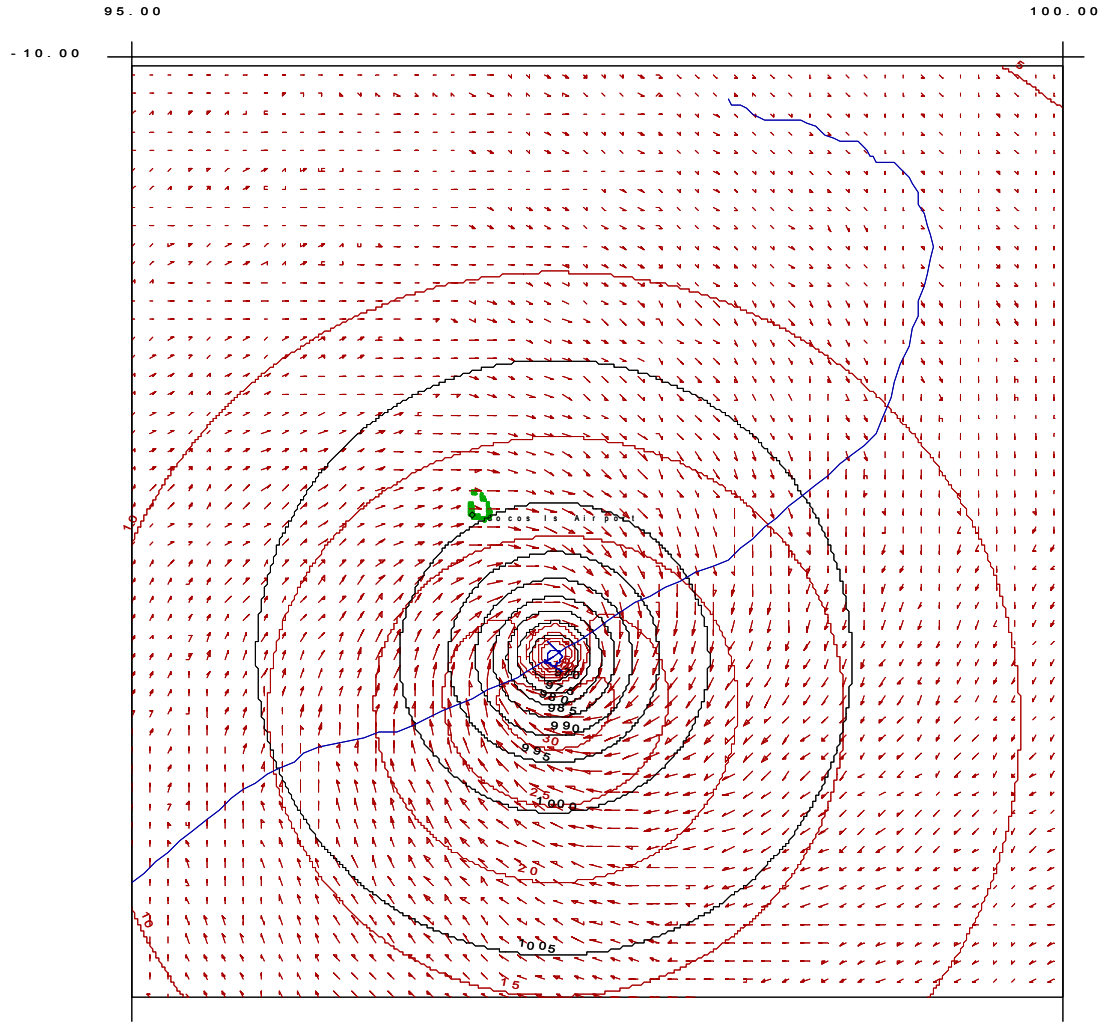

Figure 5.10 Modelled wind and pressure fields for *Alison* at time of closest approach.

Figure 5.11 presents the comparison between the modelled and measured winds and pressures at the airport location. The top curve indicates the 10 minute mean wind comparison (V_m), the second showing the 3 second peak gust comparison (V_3) and the third showing the wind direction comparison (θ_m). Finally, the comparison of MSL pressures is shown. In all cases quite a reasonable agreement is obtained, the mean wind peak error (Ep) being within 5% and with a bias error (Eb) of only 6%, the pressure being within 3%. The wind gusts are overpredicted in this case by about 10%, indicating a lower level of turbulence than currently assumed by the windfield model.

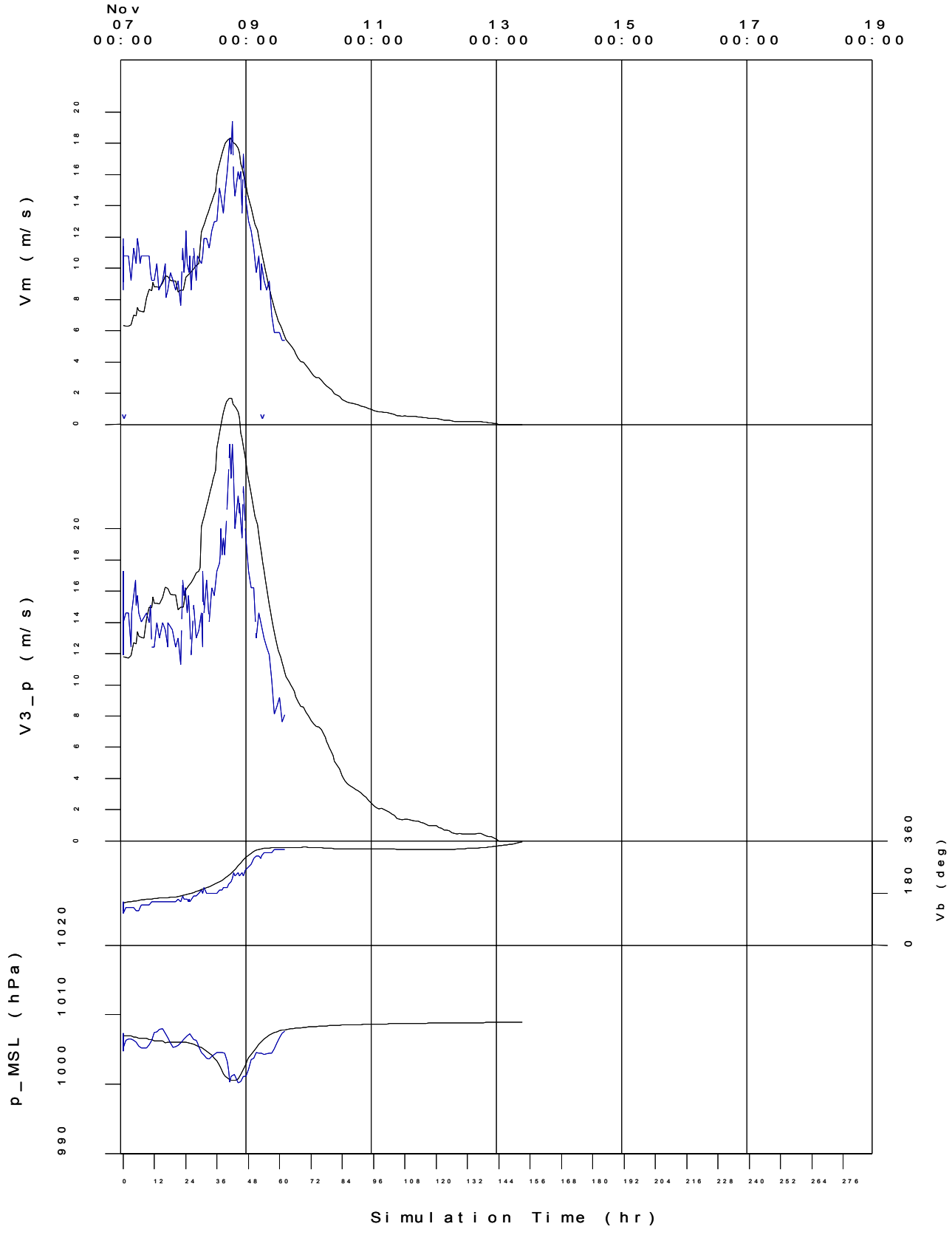

Figure 5.11 Comparison of modelled and measured wind and pressure for *Alison*.

The remaining "top 10" storms were similarly calibrated and their wind and pressure verification graphs are presented in Appendix H. Table 5.4 summarises the results of the calibration in terms of the adopted parameters and wind and pressure error values. And a short commentary on each storm follows, in chronological order:

Hazel (March 1964)

This storm passed E-W approximately 90 to the south of the atoll and proved the most difficult to calibrate. After much analysis it was determined that the estimated central pressure of 988 hPa at closest approach was approximately 10 hPa too high and was not capable of generating the winds measured at the atoll. Accordingly, this was the only storm where a change to the "official" Bureau intensity values was found necessary. Interestingly, it occurred during the period when the objective intensity estimation techniques were still developing. After the intensity adjustment, peak winds were overpredicted but the bias was essentially zero.

Doreen (Jan 1968)

This is the "storm of record" for the Cocos Islands, passing directly over the atoll with a central pressure reading of 970 hPa on the 21st January 1968. The eye of the storm is depicted in the wind and pressure records, although the 3 hourly interval lacks considerable detail compared with the modelled result and causes some apparent phasing errors because of the long data interval which are then reflected in the bias error. However, the modelled wind peak is within 3% of the only measured value and the pressure is quite reasonable.

Daryl (March 1984)

This storm followed a similar westerly track to *Hazel*, approximately 80 km south of the atoll. The initial winds leading the storm are not so well represented by the model but the peak error is reasonable, again allowing for the 3 hourly sampling, and the pressure match is good.

Ophelia (January 1986)

This storm followed a meandering path, first SW to the north of the atoll and then veering SE to pass east of the atoll during the final stages of its life. The winds are quite well represented by the model but the pressure drop is overestimated. It is likely that the decay of the central core had commenced and the winds were commencing to spin-down.

Frederic (January 1988)

This storm followed a very similar path to *Doreen* although its eye may have just veered to the east of the atoll since it is not visible on the measured winds. The modelled winds show a small impact of the eye, which could have occurred within the 3 hourly measurements. Overall, the modelled results are quite good.

Pedro (November 1989)

This storm passed approximately 130 km to the west of the atoll on a SE track. The winds and pressures are well matched, although the measured winds show a fast drop-off after the storm passes which may be due to structural changes.

Graham (December 1991)

This is the most intense storm (926 hPa) to affect the atoll, although its track 130 km north of the atoll and heading ESE placed the atoll on its weaker side. The measured and predicted winds and pressures are in good agreement.

Harriet (February 1992)

This was another storm which passed over the atoll with similar intensity to *Doreen*. In this case the storm actually circled around the atoll for a period of over 12 h, before continuing towards the SW. The winds were less than those during *Doreen*, explained by the model choosing a lower wind peakedness factor. The modelled and measured results are very good although the actual "looping" of the storm could not be detailed due to a lack of track information[1].

Hubert (January 1996)

This storm passed 100 km north of the atoll on a SW track, placing the atoll on the strong side but outside the radius to maximum winds. The modelled phasing of the mean winds is somewhat at variance with the measured values but the peak is similar. Pressures are reasonable.

Table 5.4 Summary wind and pressure calibration results.

							Recorded Wind	Wind and Pressure Calibration			
Storm Name	p_0	Date	Dist	p_n	B_0	R_c	V_m	V_m		p	
	hPa	UTC	km	hPa		hPa.km	ms^{-1}	Ep	Eb	Ep	Eb
								%	%	%	%
Hazel	978	09-Mar-64	89	1009	7.1	2250	18.0	10.2	-0.3	-13.5	
Doreen	970	21-Jan-68	4	1009	8.5	1600	38.6	-3.1	-14.5	13.2	16.4
Daryl	984	11-Mar-84	80	1009	7.6	1000	15.4	6.6	-37.6	-1.4	
Ophelia	989	11-Jan-86	41	1012	7.2	1000	18.0	8.1	5.6	59.0	34.0
Frederic	989	30-Jan-88	20	1009	7.2	900	16.0	6.9	-13.5	38.5	
Pedro	982	10-Nov-89	128	1009	7.5	1600	23.7	-5.3	-4.1	10.8	
Graham	926	05-Dec-91	132	1014	7.0	2000	17.0	8.7	-11.3	-0.5	
Harriet	973	27-Feb-92	9	1012	7.1	1000	28.8	4.8	-2.2	26.1	-3.0
Hubert	977	07-Jan-96	97	1010	8.3	1200	20.5	5.6	25.6	-28.8	30.1
Alison	967	08-Nov-98	88	1009	7.4	1200	19.4	-5.3	-6.3	-2.9	-3.3

It is concluded that the adopted wind and pressure model of tropical cyclones is suitable for application to the Cocos Islands and the calibrated storm details may be used for prediction of storm surge and wave effects.

[1] The Perth Regional Office was contacted to determine if any more accurate track information was available.

5.5 Storm Surge Modelling

This was undertaken in two stages; the first to explore the overall hydrodynamic response of the atoll to a tropical cyclone; and the second to parameterise that response for application in the statistical model of storm tide. For the first stage, the fully two-dimensional (2D) numerical hydrodynamic model SURGE (Harper 1978) was used. For the second stage, coupled Inverse Barometer Effect (IBE) and Bathystrophic Storm Tide (BST) models were incorporated into the SATSIM model. Calibration and verification of the models is based on the comparison with measured water elevations at the Home Island Jetty.

5.5.1 Measured Storm Surge at the Cocos Islands

The present investigation limits the assessment of measured storm surge at the Cocos Islands to the selected "top 10" tropical cyclone events and does not consider an analysis of the full measured record. It is possible that other periods have experienced similar surge magnitudes under the influence of strong monsoonal or other effects.

Tide data used has been sourced from the National Tidal Facility (NTF) ; measured data from 1986 to 1999 provided through GH&D; measured data for 2000 and predicted data from 1986 onwards obtained directly from the NTF. The NTF advised subtracting 0.771 m from the supplied observations and predictions to reduce the levels to Mean Sea Level (MSL). Tidal planes at the Cocos Islands are therefore as given in Table 5.5, relative to MSL.

Table 5.5 Tidal planes to MSL.

Plane	m
HAT	0.89
MHHW	0.55
MLHW	0.07
MSL	0.00
MHLW	-0.07
MLLW	-0.55
LAT	-0.64

A 36 h data period has been selected around the time of closest approach of each of the "top 10" storms and the residual water level (measured - predicted) is plotted for each storm in Figure 5.12. Note that measured data in digital form is only available from 1986 onwards, thus excluding *Hazel*, *Doreen*, and *Daryl* from this present assessment.

The peak water levels are summarised in Table 5.6 for each event, firstly as the surge magnitude (measured-predicted) and secondly as the total water level relative to MSL. It can be seen that the highest surges were experienced during *Frederic* (0.27m) and *Pedro* (0.25m), followed by *Alison* (0.21m). In each of these cases the total water level attained was about 0.1 m below HAT. Also, the total water level difference between predicted and measured levels during each of these 36 h periods only exceeded 0.1 m in the single case of *Pedro*, where the difference was only 0.2 m. It can be noted that the relatively low surge recorded during *Harriet* appears as a possible anomaly compared with the other results. As was expected though, it can be concluded that the atoll morphology effectively works to prevent the generation of extreme storm surge, at least at the Home Island Jetty location. The 2D SURGE model is next used to explore the possible surge response at other atoll locations.

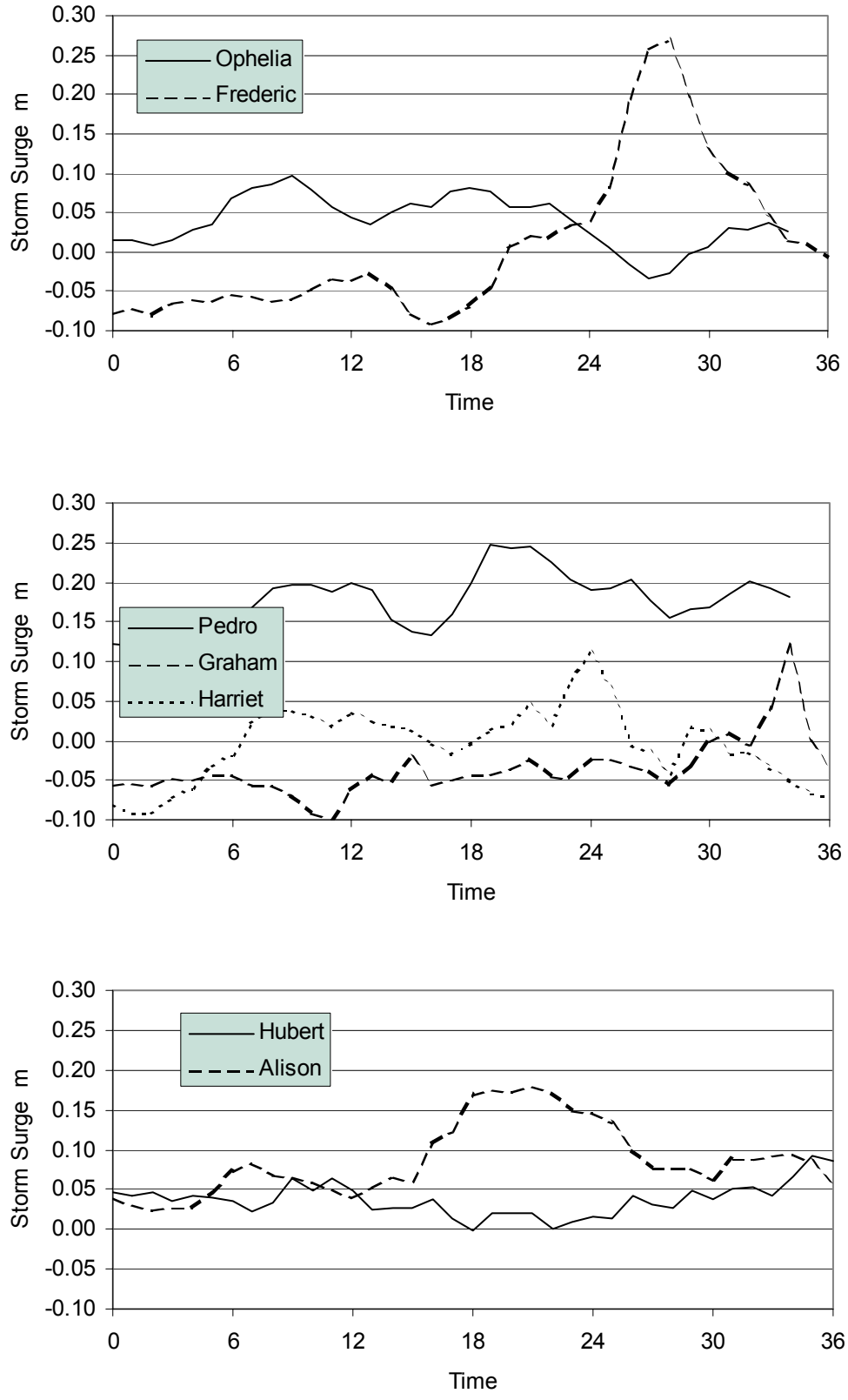

Figure 5.12 Storm surge magnitudes recorded during the "top 10" storms at Home Island Jetty tide gauge.

Table 5.6 Summary of peak surge magnitudes at the Home Island Jetty.

Storm	p_0	Date	Dist	V_m	θ_m	Recorded Surge η	Peak Water Level
Name	hPa	UTC	km	ms^{-1}	°	m	m (MSL)
Ophelia	989	11-Jan-86	41	18.0	140	0.10	0.78
Frederic	989	30-Jan-88	20	16.0	135	0.27	0.43
Pedro	982	10-Nov-89	128	23.7	0	0.25	0.77
Graham	926	05-Dec-91	132	17.0	135	0.12	0.75
Harriet	973	27-Feb-92	9	28.8	180	0.11	0.23
Hubert	977	07-Jan-96	97	20.5	125	0.09	0.62
Alison	967	08-Nov-98	88	19.4	275	0.21	0.79

5.5.2 2D SURGE Modelling

The 2D depth-integrated numerical model SURGE has been used to investigate the possible storm surge response in and around the atoll. The model domain is based on the "D" grid as discussed earlier, being a 200 m resolution extending over the whole of the atoll. The model open sea boundaries were set to the local IBE condition for MSL cases and to the IBE plus predicted tide level in the case of tidally-forced boundaries. The model timestep was chosen as 5 s based on an applied depth cut-off of 80 m. The sensitivity to this assumption, designed to increase the model timestep, was tested with a 160 m depth cut-off and found to be satisfactory. The model required a small modification due to the very shallow water depths in some parts of the lagoon (70% less than 0.2 m relative to MSL) to prevent drying under some circumstances. This modification ensured the minimum depth at any location would be preserved as 0.1 m.

A large number of tests were undertaken to ensure the model was operating in a reasonable manner, although it must be stressed that a detailed calibration of a tidal model for such a complex region would require a considerable amount of field data (levels and currents). The types of tests performed (using *Alison* as the test case) included:

(i) Depth cut-off assumption (as mentioned previously)
(ii) With tide / without tide
(iii) With reef / without reef
(iv) Reef crests set at 0, -0.5, -1 m MSL

Reef boundaries were added to the "D" grid along the reef crest around the atoll to determine if this would have any dramatic impact on the tide and/or surge response. The reef boundary is implemented in SURGE as a submerged broadcrested weir with a specified crest height. Even with a 200 m grid resolution, this was not easily achieved in the fringing reef zones. However, the variety of tests showed that the reef parameterisation had little impact on predicted surge levels either inside or outside of the lagoon. In the case of tide and surge modelling, the presence of the reef assisted slightly by providing some additional dampening. In general, the very shallow depths combined with the fine scale resolution in this case probably negates the need for a broadcrested weir control.

Each of the "top 10" storms was modelled for a period of 36 h, taking in the period of closest approach to the atoll. *Alison* is selected again for a detailed assessment because of its superior wind calibration, while results for the other storms are presented in summary only.

5.5.2.1 2D Tidal Modelling

The NTF-supplied tidal constituents were used to provide open boundary forcing to the model and the resulting water level variation at the Home Island Jetty was compared with the predicted levels during cyclone *Alison*. This was done for the purpose of providing a tidally modulated water level for subsequent surge modelling to ascertain the extent of non-linear surge-tide interaction, rather than to develop a proper tidal model of the atoll. Accordingly, no sensitivity to the constituent selection was undertaken, although some obvious shallow water terms were omitted. Based on the constituents provided, there does not appear to be much shallow water effect at the tide gauge site, which is adjacent the deeper part of the lagoon (10 to 12 m) and only a few kilometres from the open ocean.

The result for *Alison* is shown in Figure 5.13, comparing the predicted tide level at the Home Island Jetty with the modelled tide height at the same point. The tidal boundary is ramped over a period of 6 h to intersect the predicted level at that time, so as to reduce initial transient effects. This has been achieved to some extent but the first high tide is overpredicted by the model. After that time the agreement is quite good and suitable for the present purposes. Results for the other storms (shown later) are of similar accuracy.

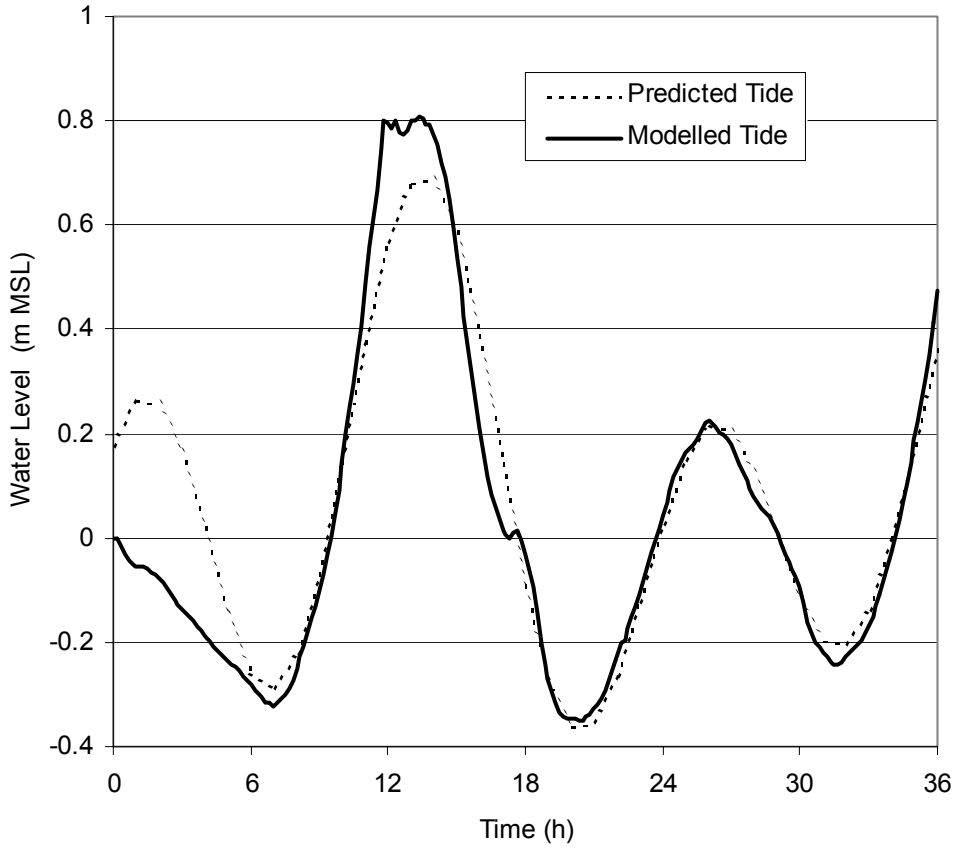

Figure 5.13 Predicted and 2D modelled tide during *Alison*.

Although the hydrodynamic model has not been specifically calibrated, it is interesting to note that it qualitatively reproduces the observations by Kench (1998b), namely an amplification of the tidal response in the southern part of the lagoon. This is due to the dominant northern passages in admitting the tide on the one hand and the very shallow southern lagoon which impedes the tide, especially during the low water cycle. The end result can be seen in Figure 5.14 which first compares the modelled tidal trace during the latter part of the *Alison* period at Site 15 (Home Island Jetty) with those at the southern lagoon locations. Next is the difference in water levels between Site 15 and those other sites. The amplification at high water and the retardation at low water are clearly reproduced by the model. Kench reports a difference in absolute water levels between north and south of 0.1 m, which may also include some wave setup contribution through the southern entrance. These results are not inconsistent with his observations.

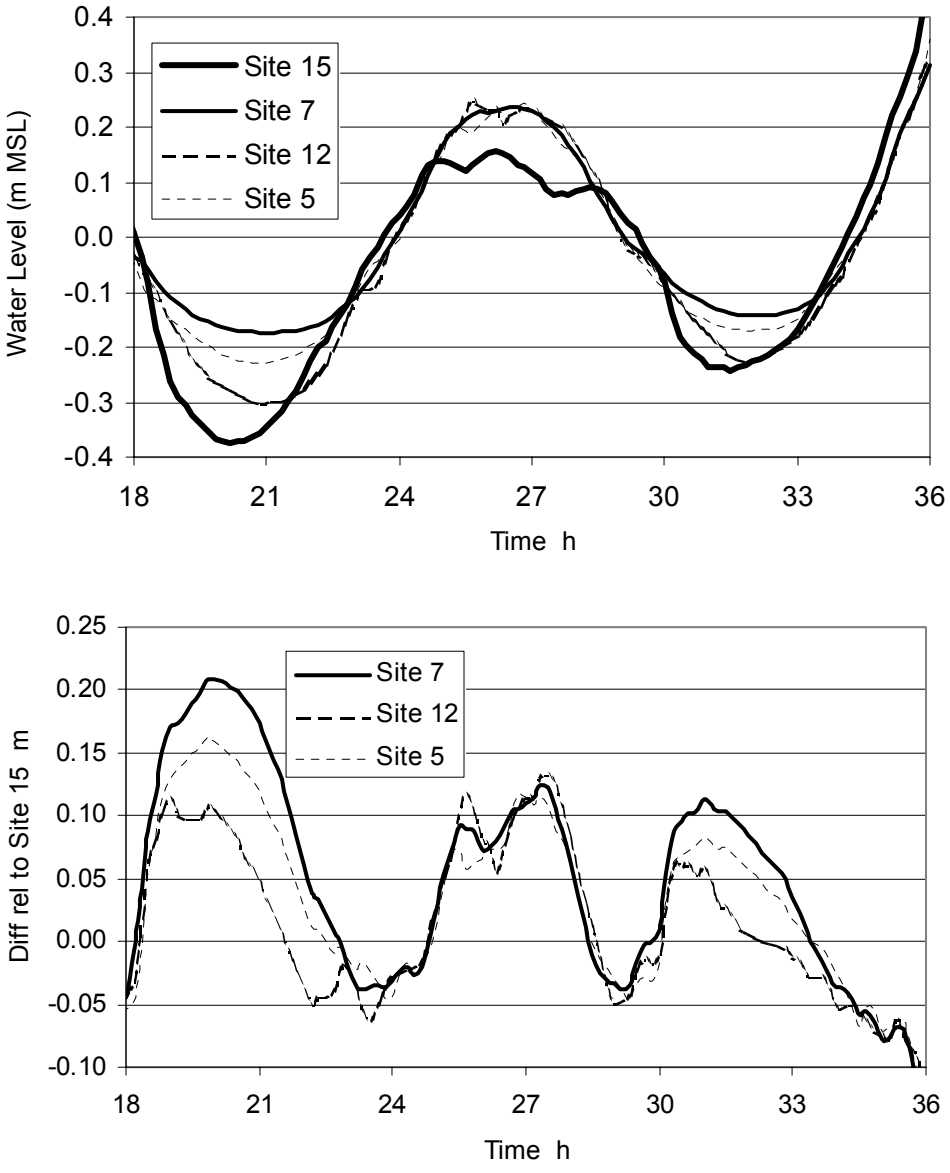

Figure 5.14 Modelled tidal amplification in the southern lagoon.

5.5.2.2 2D Surge plus Tide Modelling

Having established a reasonable basis for modulating the local water levels by the tidal constituent boundaries, the surface wind and pressure forcing was applied to enable generation of a storm surge. The result for *Alison* is shown in Figure 5.15.

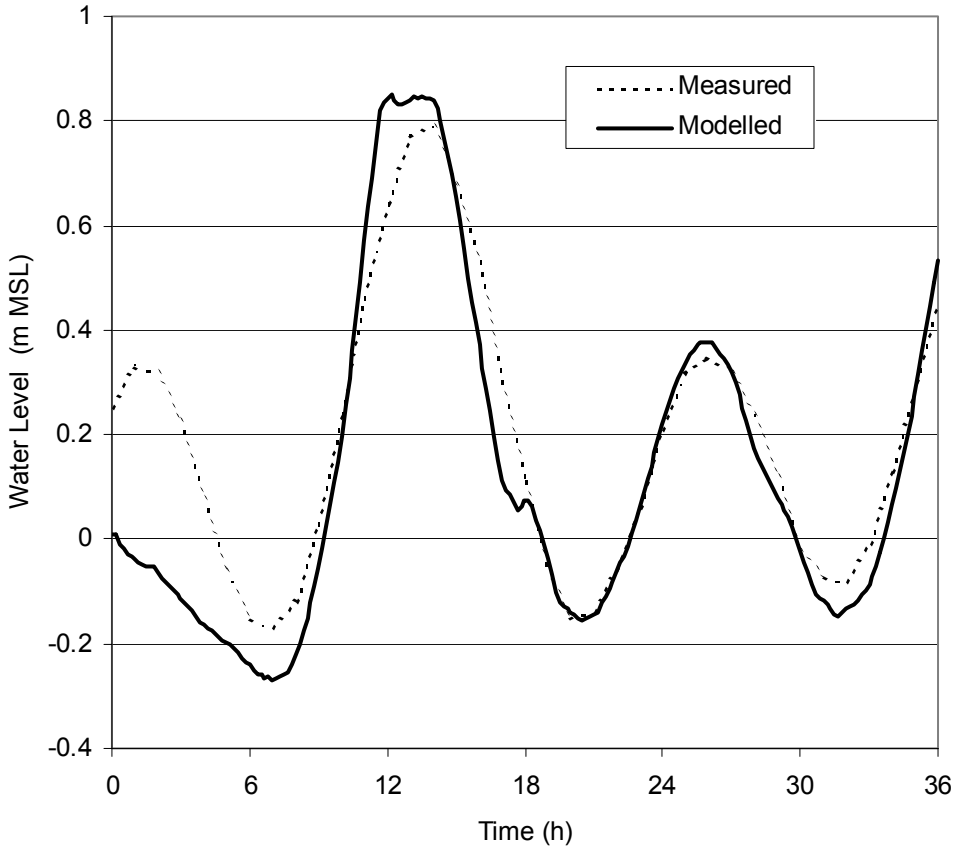

Figure 5.15 Measured and 2D modelled total water level during *Alison*.

This appears similar to the previous graph because the tidal amplitude is much greater than the surge, but essentially the curves are now higher by approximately 0.2 m at around time 20 h. The modelled "notch" around time 18 h is a little more pronounced than before, and it is thought to be due to the initial transients interacting with the shallow water. It becomes accentuated in the following graph, Figure 5.16, which compares the water level residuals (measured-predicted) and (modelled tide - modelled total level) during *Alison.*

In this case the "notch" appears exaggerated due to the change of scale and its separation from the modulated tide level but this does not overly interfere with the model's ability to represent the measured residual (or storm surge). It should be noted that the surge magnitude of order 0.2 m is a relatively small quantity and that the atoll morphology is complex. Accordingly, this is regarded as a good result for the model, considering the absence of a detailed calibration against field data.

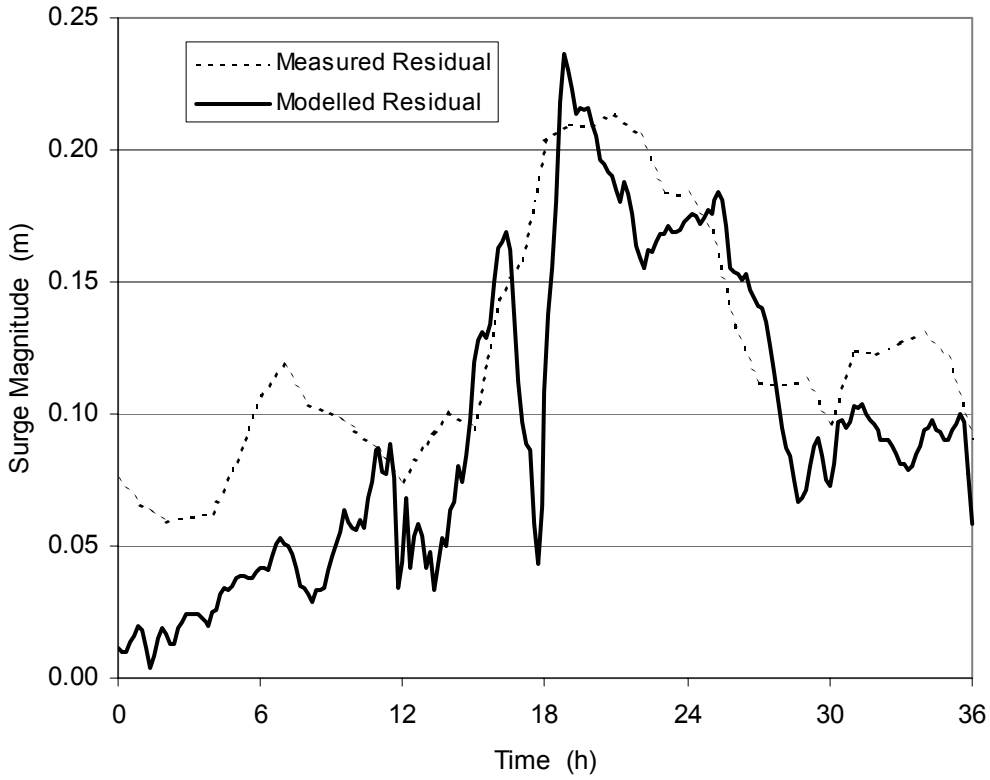

Figure 5.16 Comparison of 2D tidal residual water levels during *Alison.*

5.5.2.3 2D Surge Modelling Without Tide

The previous section demonstrates the ability of the 2D model to match the total water level. It remains instructive though to consider the case without the tidal modulation present since the spatially varying response around the atoll can then be more easily assessed. Also, some indication of the non-linear surge and tide interaction can be determined. For this test the water level is initially set at MSL and then only modulated by the wind and pressure forcing from *Alison*.

Figure 5.17 shows the equivalent comparison to the previous figure, which again shows the same measured residual (measured-predicted tide) but with the surge generated from a MSL base level, which is now free of the transient "notch" caused by the tidal boundary. This result changes from the previous slight overprediction of the peak measured level by 0.03 m with tide modulation, to a similar underprediction without tide modulation. Again it should be remembered that ±0.03 m is a very small error in either case, but some non-linear surge-tide interaction is indicated. This will be due to the tidally modulated water levels being slightly below MSL during the critical time of maximum winds, thus adding to the storm surge generation potential.

These results have shown that the 2D SURGE model appears capable of quite accurately predicting the recorded surge levels at Home Island Jetty during *Alison.* It is instructive therefore to look at what the modelled surge response is for other atoll locations. Firstly, the overall atoll response can be viewed in Figure 5.18.

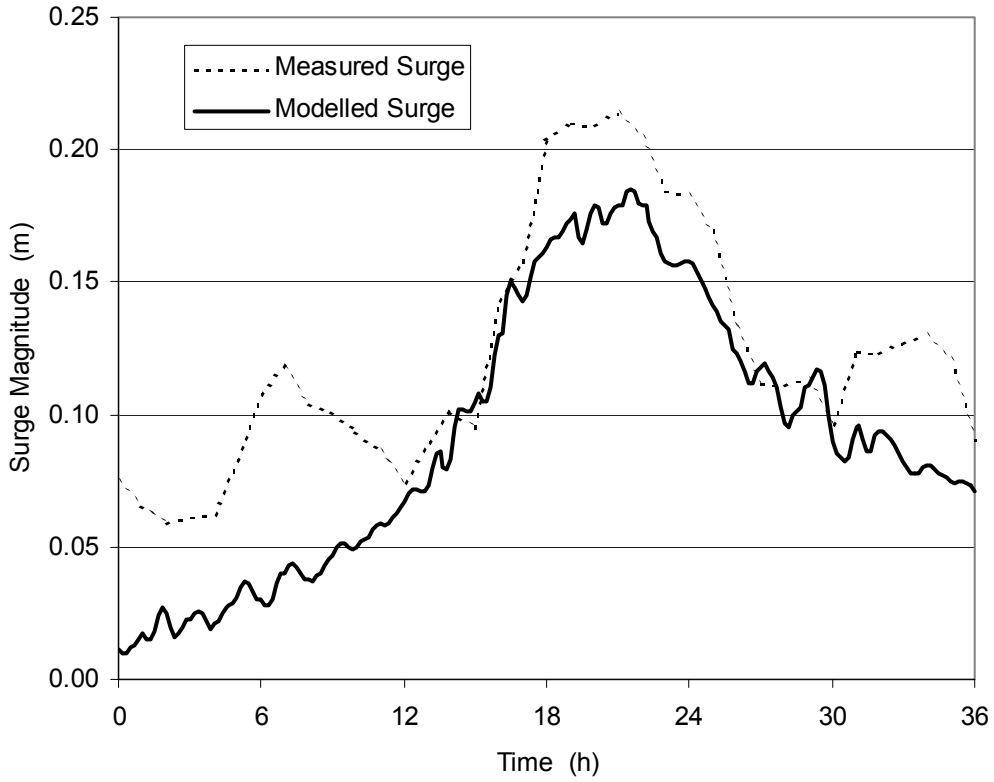

Figure 5.17 Modelled 2D surge-only and measured storm surge during *Alison.*

The development of the surge during *Alison* is presented as a series of three time intervals, each 4 h apart, commencing close to the time of peak surge level at Home Island Jetty. The left hand panels show the vector mean wind field, whose values are advised in the captions. The middle panel shows the pattern of flow velocities throughout the model domain. The right hand panel shows contours of water level relative to MSL; the interval is 0.1 m.

Figure 5.18 therefore shows at time 20 h the winds were well established from the west at 17.8 ms^{-1}. The flow pattern shows water entering the western channel area, exiting through the various northern passages between Horsburgh Island, Direction Island and Home Island, but also forcing a circulation within the southern lagoon. There is little flow exiting through the southern entrance at this stage. The water level contours show a classic wind stress setup on the eastern side of the lagoon essentially normal to the applied wind stress, the 0.2 m water level contour located just to the south of Home Island Jetty at this time.

At 00 h, the wind has slightly decreased and veered to the NW, flow is now exiting the southern entrance, and the region of setup has rotated towards the SE and increased in magnitude with some southern lagoon sites now experiencing in excess of 0.4 m. At 04 h the wind has veered further south and reduced in intensity; flow through the southern entrance is well established and water levels are slightly lower in the lagoon and again rotated further south. Note that during this episode, ocean levels were generally below 0.1 m, the contribution from the IBE alone.

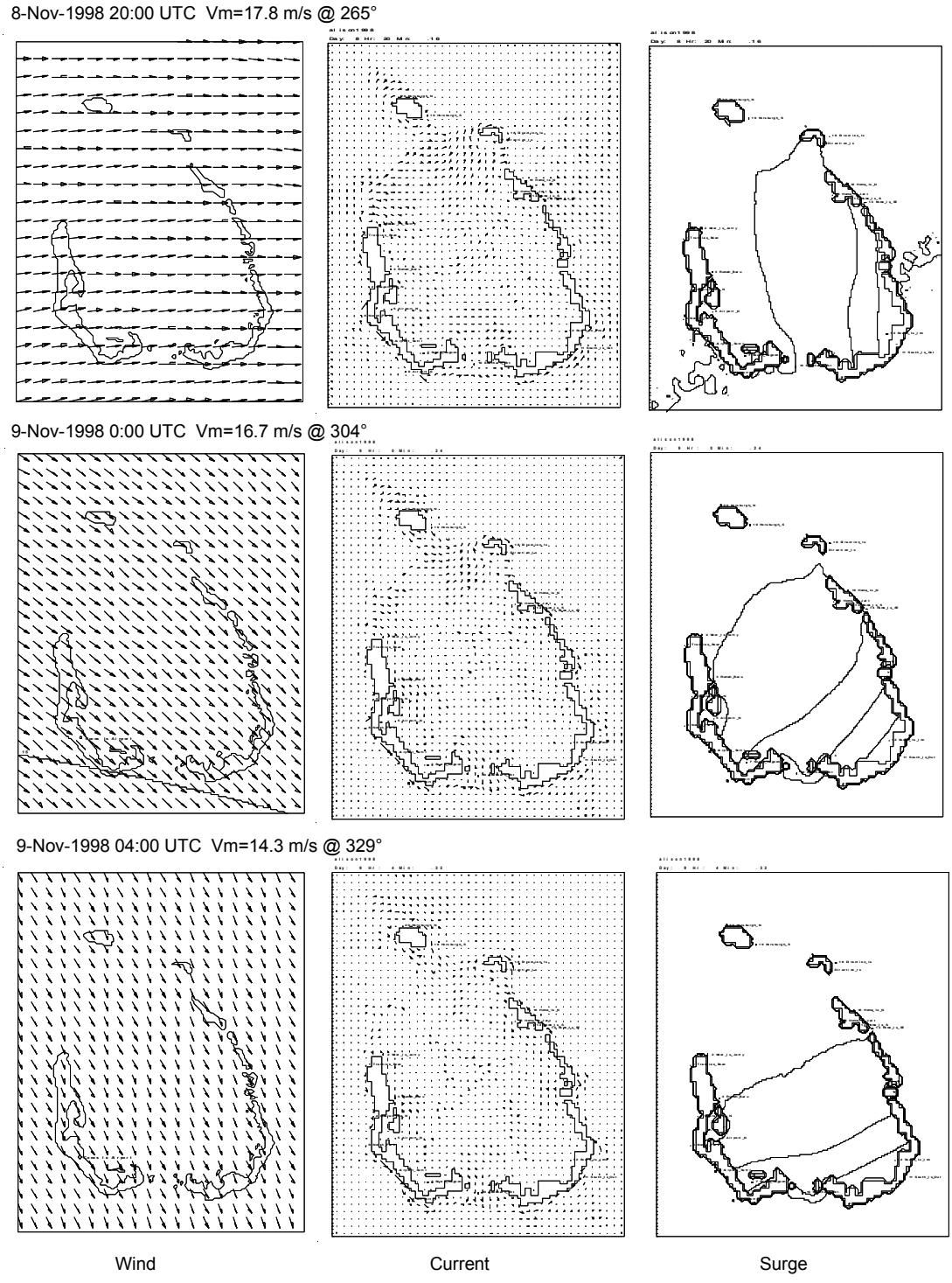

Figure 5.18 Development of the storm surge during *Alison.*

The individual time history of surge response at each of the nominated study sites can now be examined, as shown in Figure 5.19, where the sites have simply been grouped into "ocean" influenced and "inner lagoon" influenced sites to assist readability; the "ocean" group having a plotted surge scale twice as large as the "inner lagoon" to accentuate the site differences. In both cases the IBE curve has been added as a reference line.

Considering the "ocean" sites first, almost all are within ± 0.01 m of the inverted barometer effect. Site 17 (Horsburgh Inner) is slightly higher since it experiences some wind stress setup across the northern part of the lagoon. Site 2 (West Island Jetty) lags the IBE due to the drawdown effect caused by the wind setup but eventually comes close and also shows some oscillations due to the later relaxation of the wind setup.

The "inner lagoon" sites by comparison have much greater wind stress influence and Site 10 (Southern Entrance) is included here because its levels are influenced in this case more by the lagoon setup than the site's immediate ocean connection. Site 12 (South Island Inner) clearly has the highest response, followed by Site 7 (South Lagoon). These two sites are located closest to the region of maximum setup as seen in the previous development, Site 7 lagging Site 12 as the wind setup maxima rotated from E through to S. Sites 14 and 15 on Home Island can be seen to lead the southern sites response. The more western sites (3,5,7,10) also initially show a drawdown and only recover positive levels following the relaxation of the setup on the eastern side.

It can be concluded that any ocean site will essentially be governed by the inverted barometer effect (IBE) but that lagoon sites are highly sensitive to wind stress induced setup across the lagoon, which is directed by the local strength and direction of the wind. Some seiching is also evident following the relaxation of the wind stress but the peak levels at most sites are due to either the IBE or the direct effect of wind stress.

5.5.3 1D Parametric Modelling

In regard to storm surge only (neglecting wave setup for the moment), the SATSIM parametric model incorporates the following major deterministic elements:

(i) Point wind and pressure values from the 2D tropical cyclone model
(ii) Point inverted barometer effect (IBE)
(iii) Point bathystrophic storm tide estimate (BST) based on local wind speed and direction fetch
(iv) Generated point astronomical tide

Because the SATSIM parametric model does not consider inertia or other 2D effects and the major interest in this context is on the lagoon BST response, it is referred to here as a "1D" parametric model.

The results for *Alison* are shown in Figure 5.20, comparing the measured and modelled total water level and residuals at the Home Island Jetty location. In this case the tide level is generated directly by SATSIM and so does not experience the numerical transients seen in the 2D SURGE model result. The modelled and measured residuals (storm surge components) are seen to be similar, although the modelled result is 0.08 m lower than measured. Considering the model prediction at the other sites, all "ocean" sites are assigned IBE only, but Figure 5.21 presents the predicted residuals at the "inner lagoon" sites.

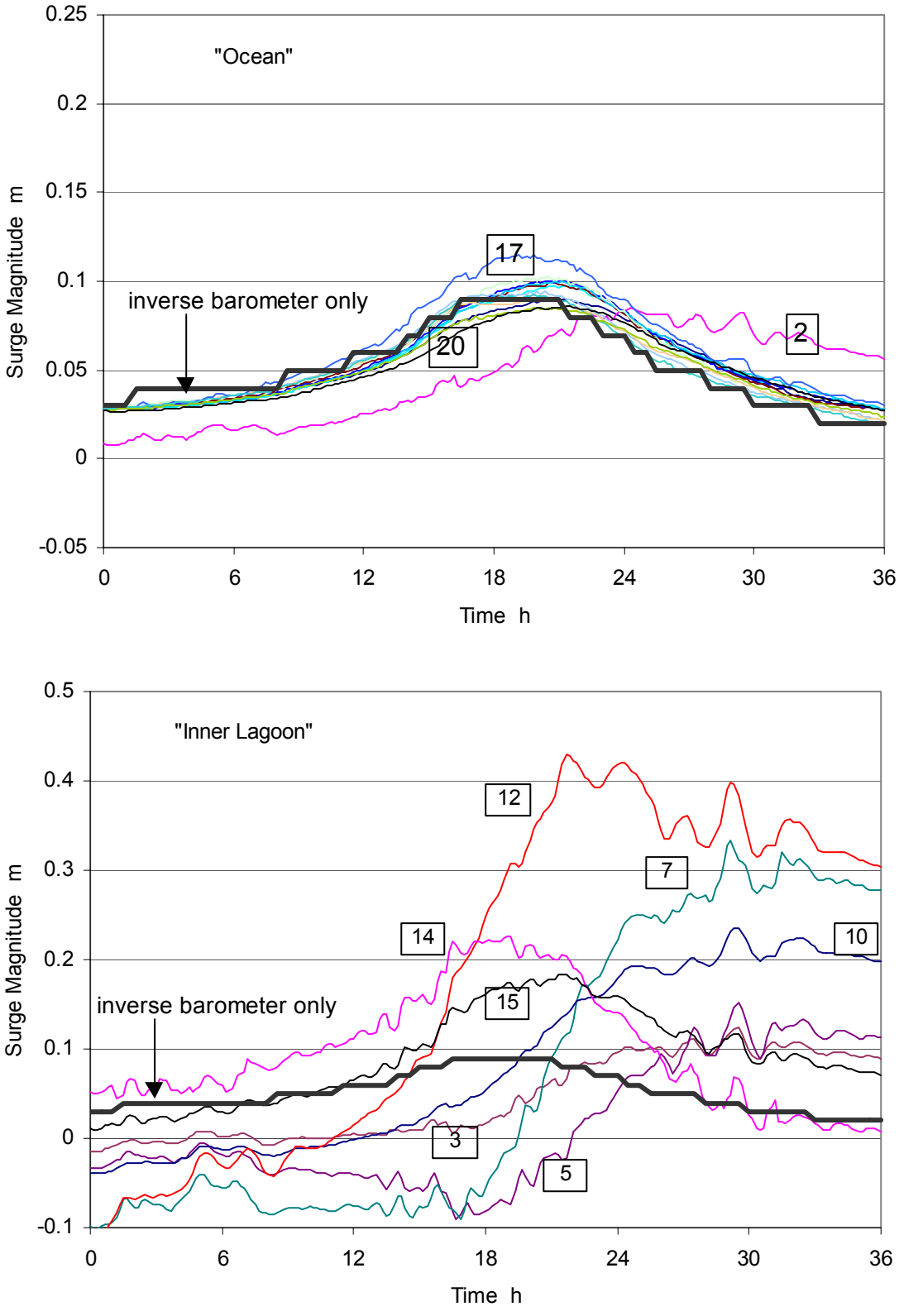

Figure 5.19 Predicted site specific 2D surge response during *Alison*.

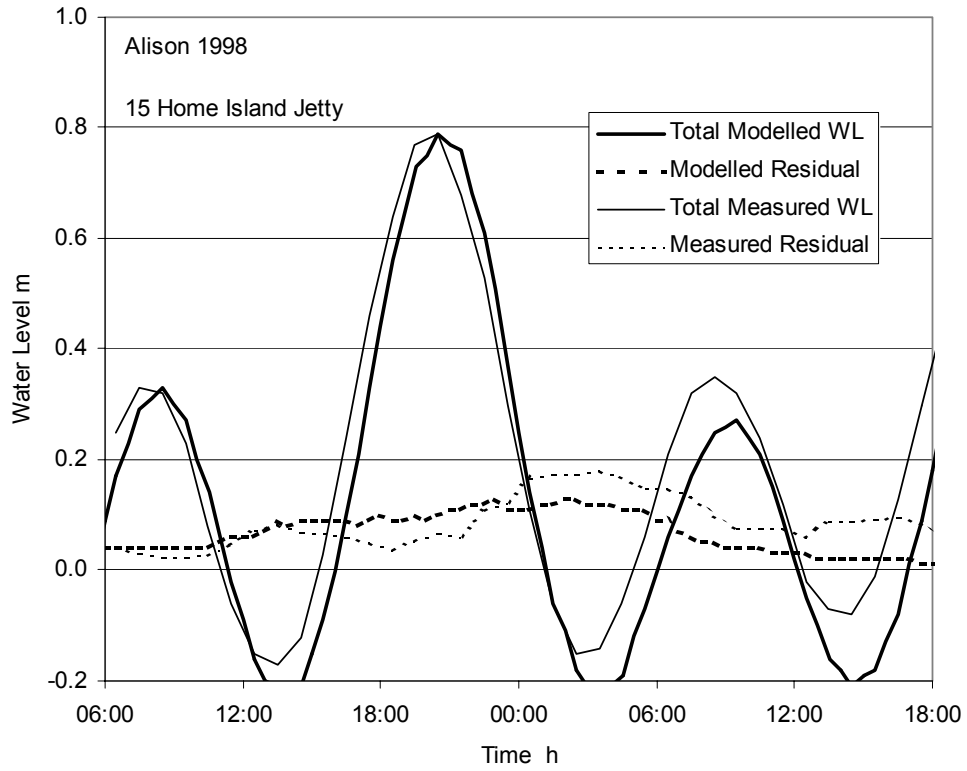

Figure 5.20 Measured and modelled 1D surge response during *Alison*.

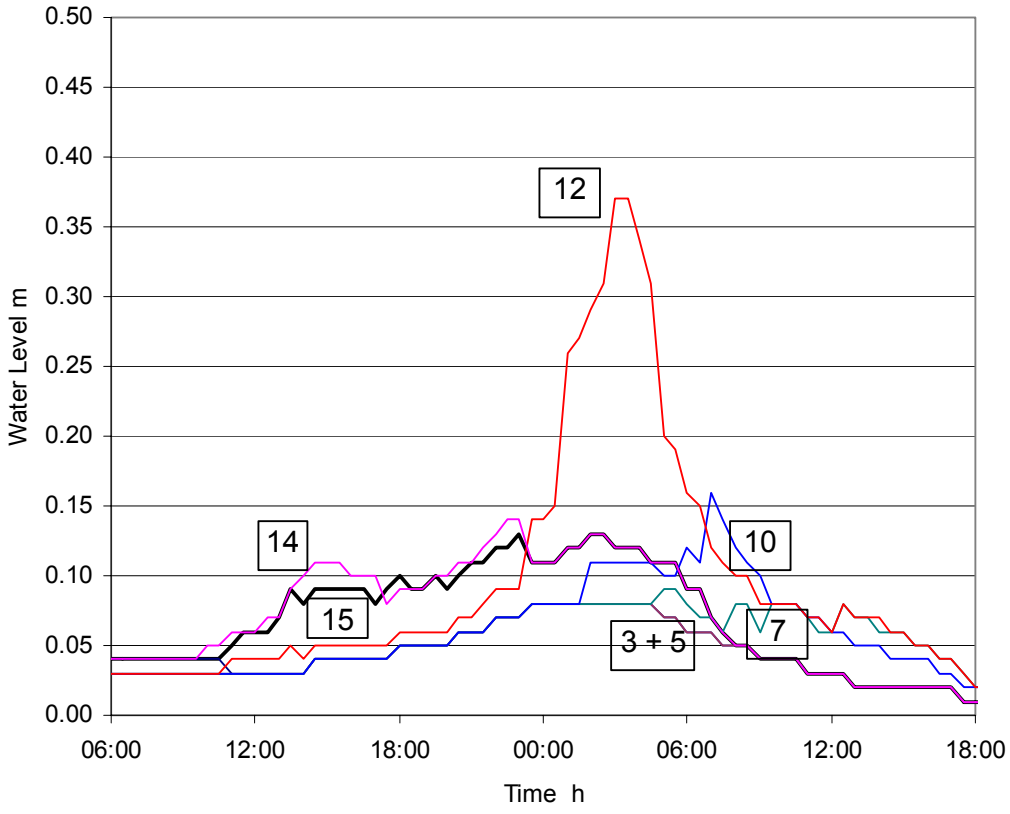

Figure 5.21 Modelled 1D inner lagoon surge response during *Alison*.

Figure 5.21 shows Site 12 with clearly the greatest response, with a significant BST component. Sites 14 and 15 are similar throughout with some BST impact. The model treats Sites 3, 5, 7 and 10 identically during the initial stages, but later Site 10 emerges with a BST component and Site 7 with a lesser effect. Sites 3 and 5 are essentially IBE only. In comparing the Figure 5.21 1D results with those from Figure 5.19 for the 2D surge model, it can be seen that the magnitude agreement is quite reasonable, although the 1D results are slightly lower.

It can be concluded that the 1D parametric surge model in SATSIM is capable of reproducing the qualitative variation in site specific response predicted by the 2D SURGE model and is also quantitatively quite accurate (within 0.05 m) for the sites most affected.

5.5.4 Overall Comparison of Measured, 2D and 1D Modelled Surge Results

Appendix I presents summary plots for the seven available measured storms from the "top 10" set which compare the measured, 2D and 1D modelled surge responses at the Home Island Jetty tide gauge (Site 15). These results are summarised in Table 5.7 below and the peak prediction error (Ep) is indicated.

The summary shows that the 2D model is typically within 0.1 m or better of the measured peak, except for *Graham* (0.14 m) and *Harriet* (0.4 m), which it overpredicts in both cases. Likewise, the 1D model is typically within 0.15 m, does better than the 2D model for *Graham* but also overpredicts *Harriet* by the same amount. Ignoring the *Harriet* result for the moment, both models show an averaged Ep across the other six storms of less than 0.1 m. In terms of a % error this might be regarded as still being relatively high but significantly more sophisticated models, together with more detailed bathymetry and field measurements, would be required to improve this result. Given the relatively low surge magnitudes (compared with, for example, the expected wave setup) this is considered a low priority. Accordingly it is concluded that the simplified 1D model is suitable for the intended purpose of predicting the storm surge component of storm tide at the Cocos Islands.

Some special note is relevant in the case of cyclone *Harriet*, which is apparently overpredicted by both models. This is the storm which apparently circled around the atoll and, although the wind speed comparison in Appendix H can be seen to be quite good, there is a significant difference in direction at the time of the peak wind between the modelled and measured values. The model produces a southerly wind which forces a wind setup towards the tide gauge site whereas the measured direction is closer to an easterly. This example shows the sensitivity which can occur for close approach storms and the need for a statistical approach to the problem.

Also, an examination of the error values for both surge models will show that, ignoring *Harriet*, the greatest overprediction occurs for situations where the winds are typically from the SE. This could mean that the models are slightly overpredicting the wind speeds incident on the lagoon surface and is consistent with a comment by researcher Paul Kench (Kench 1998b) who found the south-east corner of the lagoon unusually sheltered by the fringing palm forest. The very shallow waters and weed banks may also be generating greater frictional resistance than can be represented by the present 2D model. In any case, this results in a potential slight over-conservativeness in the present context.

Appendix I also presents the modelled 1D and 2D results for the remaining "top 10" storms for which there is no verification data. The 2D model is higher by about 0.15 m for *Hazel* but the two models are almost exact for *Daryl*. During *Doreen*, the 2D model predicts a 0.3 m higher surge than the 1D model. However, it is believed that the 2D model may be overestimating the surge due to

initial drying of the southern lagoon. Again, a more detailed model could provide better detail. Neither result appears inconsistent with the lack of reports of inundation at this point (Ryan 1968) since both are at or below HAT.

Table 5.7 Comparison of 2D and 1D surge model results.

						Recorded	Modelled Magnitude		Peak Error Ep	
Storm	p_0	Date	Dist	V_m	θ_m	Surge η	SURGE	SATSIM	SURGE	SATSIM
Name	hPa	UTC	km	ms^{-1}	°	m	m	m	m	m
Ophelia	989	11-Jan-86	41	18.0	140	0.10	0.19	0.25	0.09	0.15
Frederic	989	30-Jan-88	20	16.0	135	0.27	0.26	0.21	-0.01	-0.06
Pedro	982	10-Nov-89	128	23.7	0	0.25	0.19	0.10	-0.06	-0.15
Graham	926	05-Dec-91	132	17.0	135	0.12	0.26	0.17	0.14	0.05
Harriet	973	27-Feb-92	9	28.8	180	0.11	0.51	0.54	0.40	0.43
Hubert	977	07-Jan-96	97	20.5	125	0.09	0.00	0.12	-0.09	0.03
Alison	967	08-Nov-98	88	19.4	275	0.21	0.18	0.13	-0.03	-0.08

5.6 Wave Modelling

5.6.1 Measured Waves at the Cocos Islands

There is no recorded wave data which can be used for the purpose of verifying either the ADFA1 numerical spectral model or the SATSIM parametric wave model for tropical cyclone waves in the Cocos Islands context. Accordingly, a summary of the results obtained by hindcasting the "top 10" storms using the 2D spectral wave model is presented for guidance.

5.6.2 2D Spectral Wave Modelling

Again, cyclone *Alison* is used to illustrate the modelling approach. Firstly, Figure 5.22 shows the computed wave field for the "A" grid domain at time 19:45 UTC when the storm centre is to the SE of the atoll. The contours indicate significant wave height (H_s) at 0.5 m intervals while the vectors indicate mean wave direction and their lengths indicate peak spectral period (T_p). On this basis the wave energy can be seen to be propagating out from the storm centre, with the region of maximum waves (peaking at 7 m) being to the left (south) of the track in the region of the maximum winds.

As mentioned earlier, the "A" grid model domain provides boundary data for the finer scale "B" grid domain surrounding the atoll. The results at time 20:15 are shown in Figure 5.23, indicating some differences in detail over the "A" grid result, essentially due to a more accurate representation of the surface windfield structure. In this case an 8 m H_s is indicated south of the storm track, with the 3.5 m contour passing through the atoll.

A sequence of "C" grid domain results is shown in Figure 5.24, now clearly showing the shielding being generated by the atoll and the effect of the changing wind direction over the period of time shown. Some large changes in mean wave direction are seen in the atoll wake as the model "looses" energy from some directions. Finally, Figure 5.25 shows the "D" grid domain at time 20:00 UTC which illustrates the complex shielding patterns and the low penetration of wave energy into the lagoon in this situation.

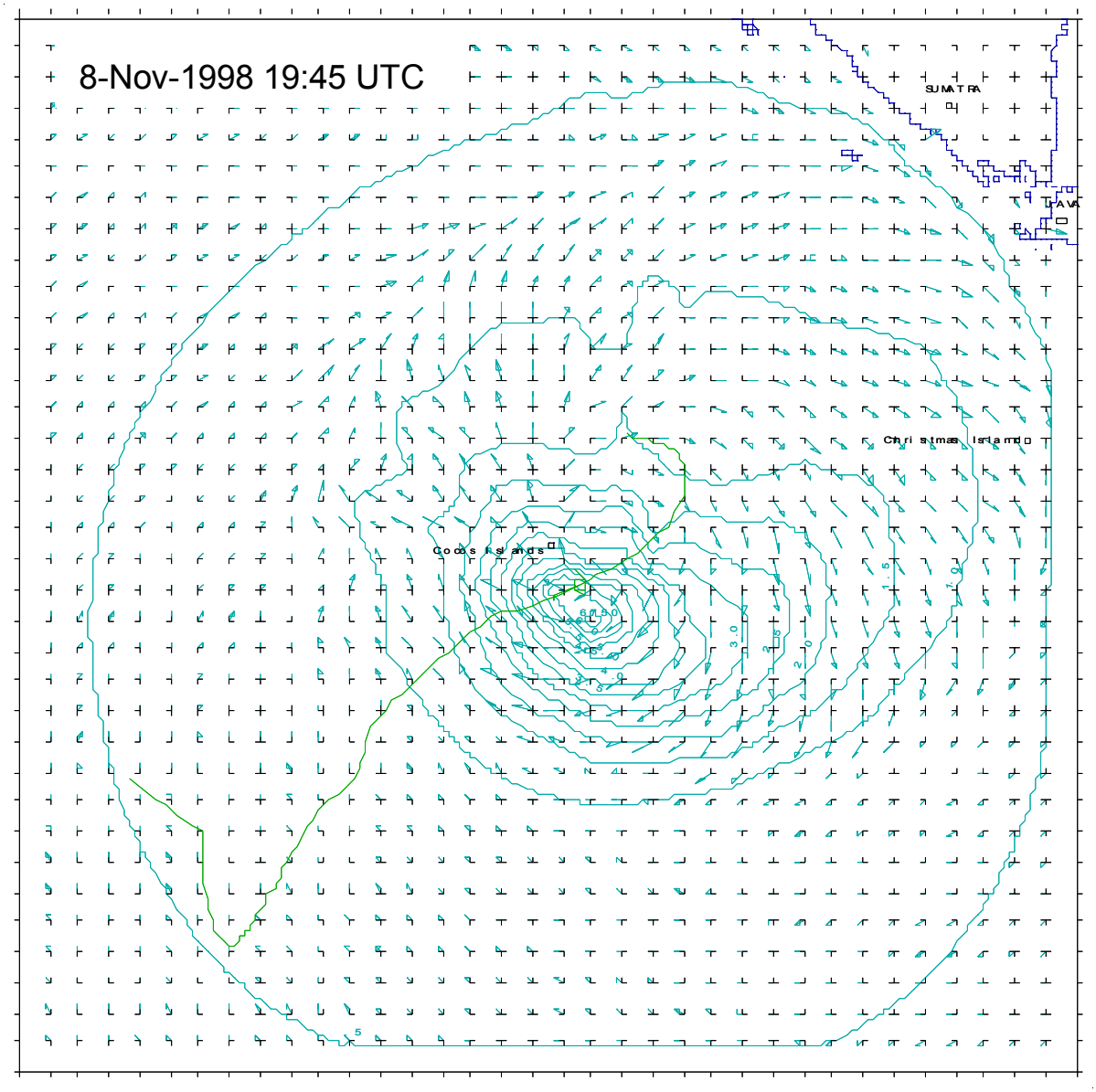

Figure 5.22 "A" grid spectral wave model domain during *Alison*.

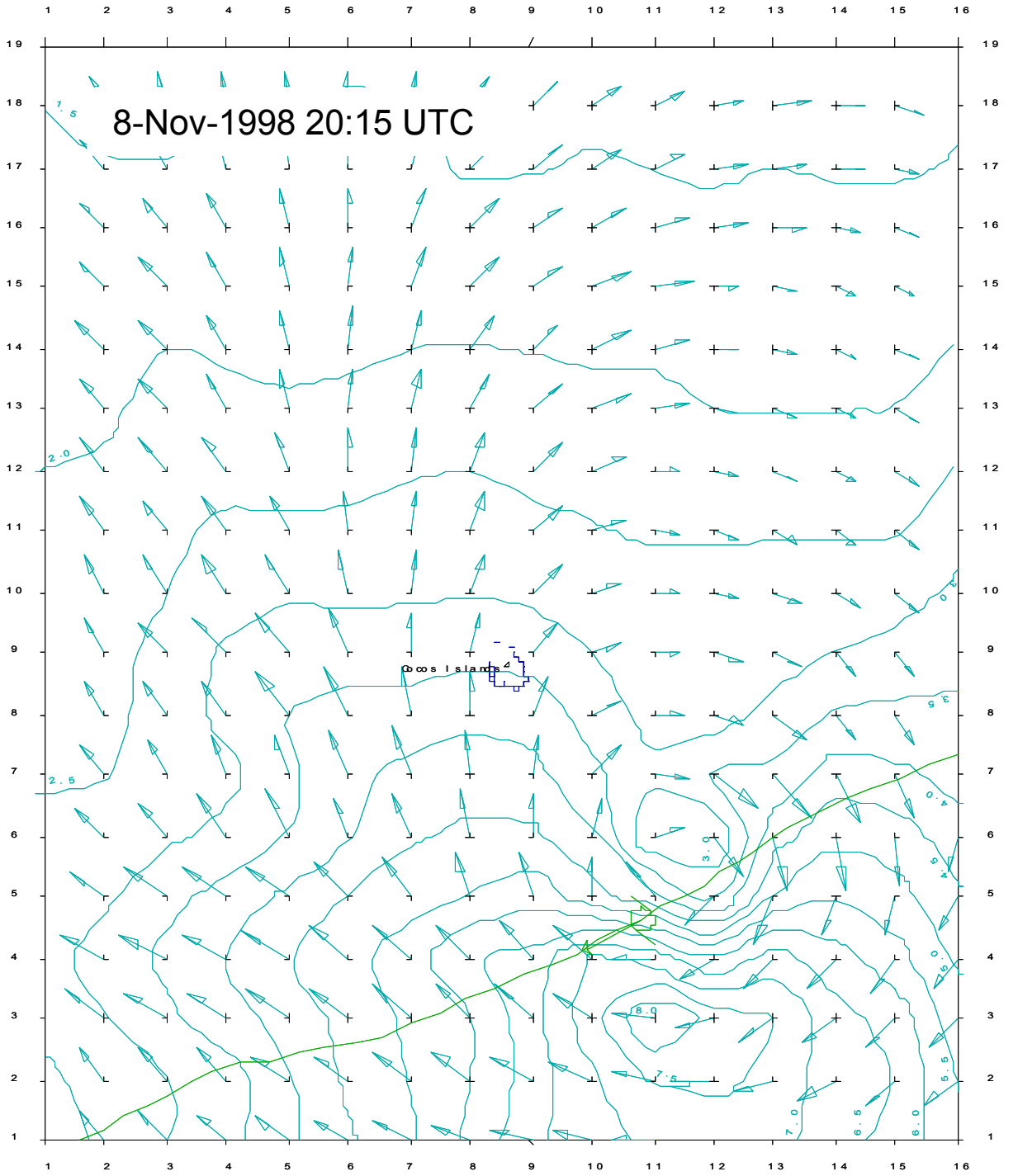

Figure 5.23 "B" grid spectral wave model domain during *Alison*.

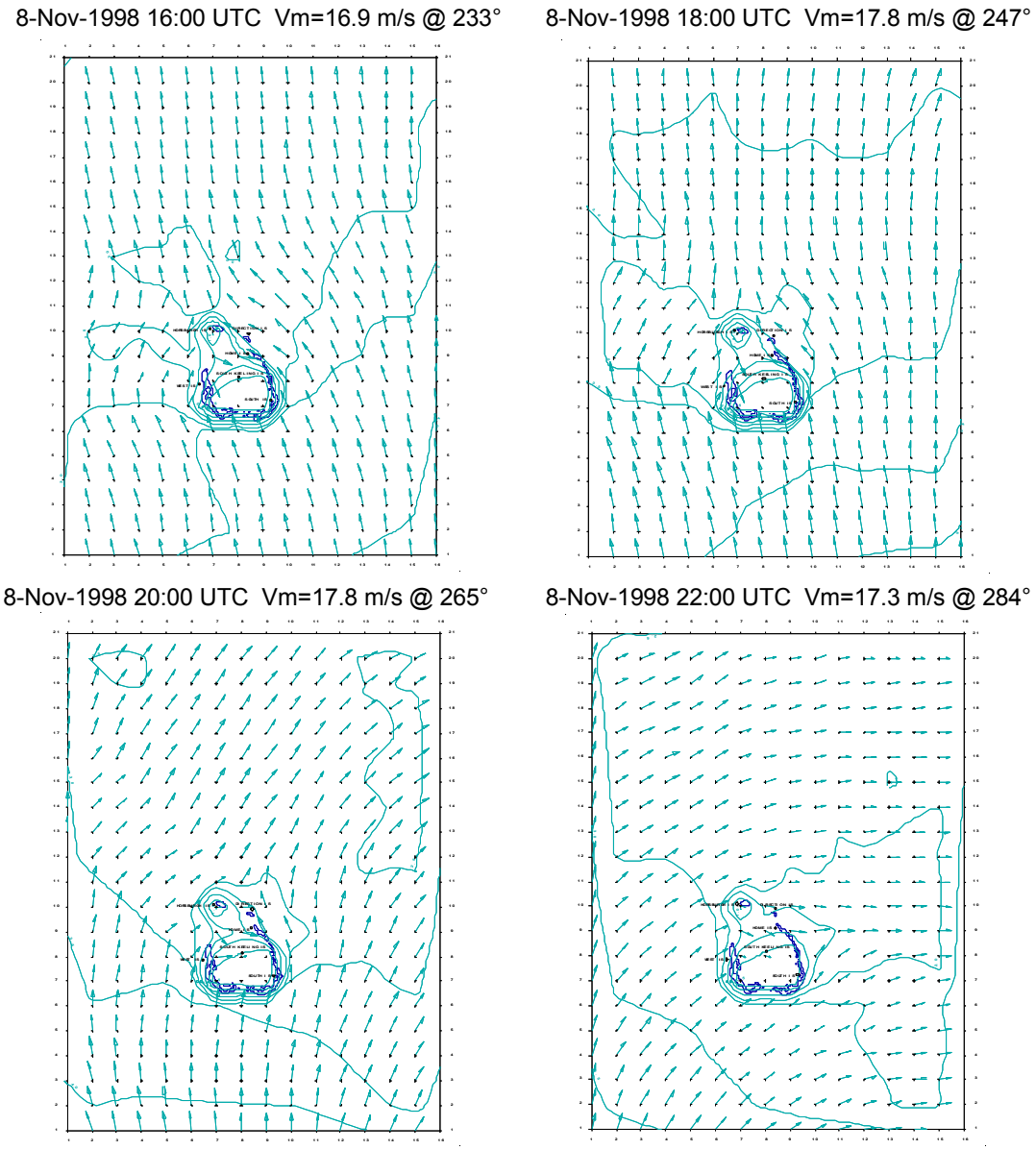

Figure 5.24 "C" grid spectral wave model domain during *Alison*.

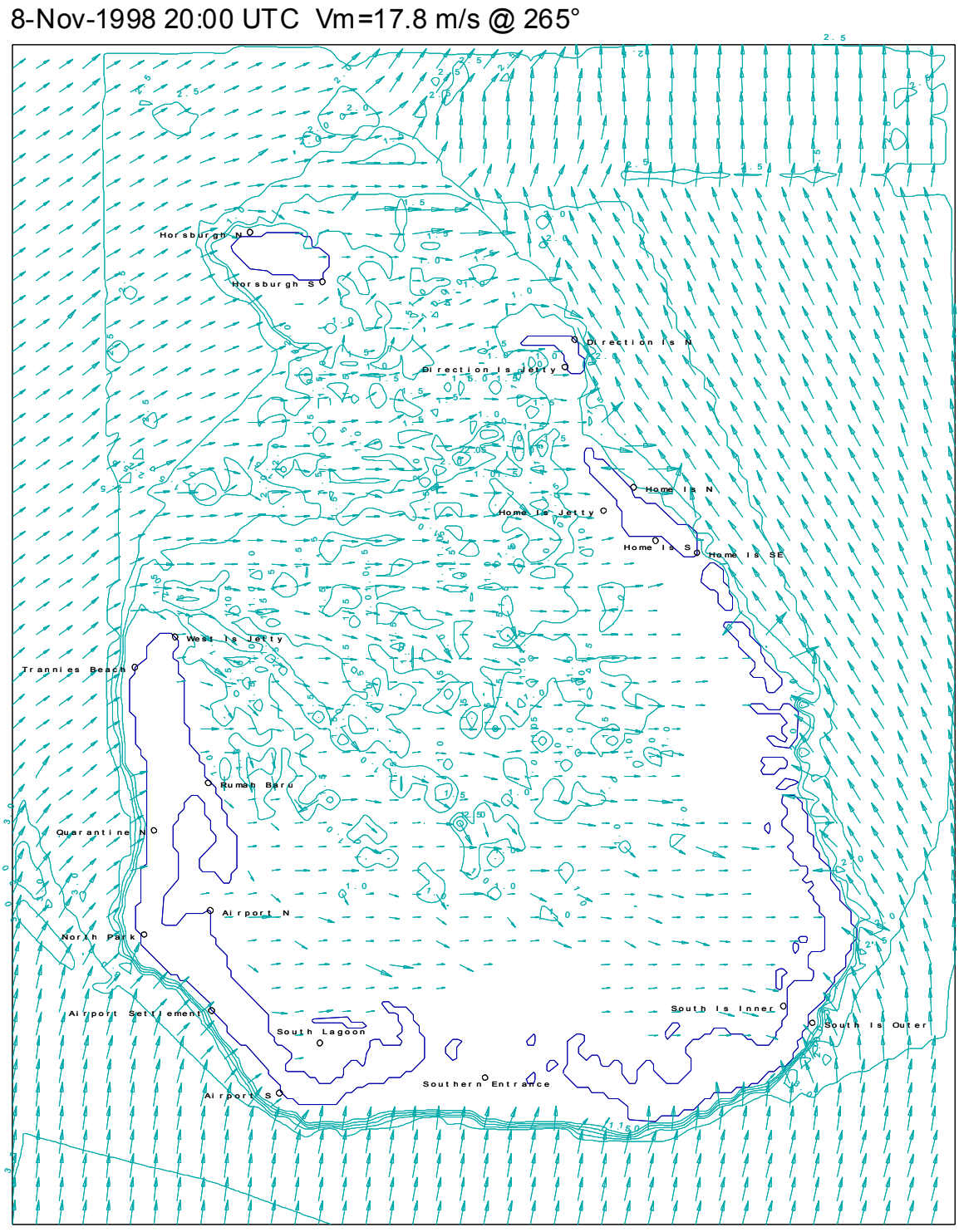

Figure 5.25 "D" grid spectral wave model domain during *Alison*.

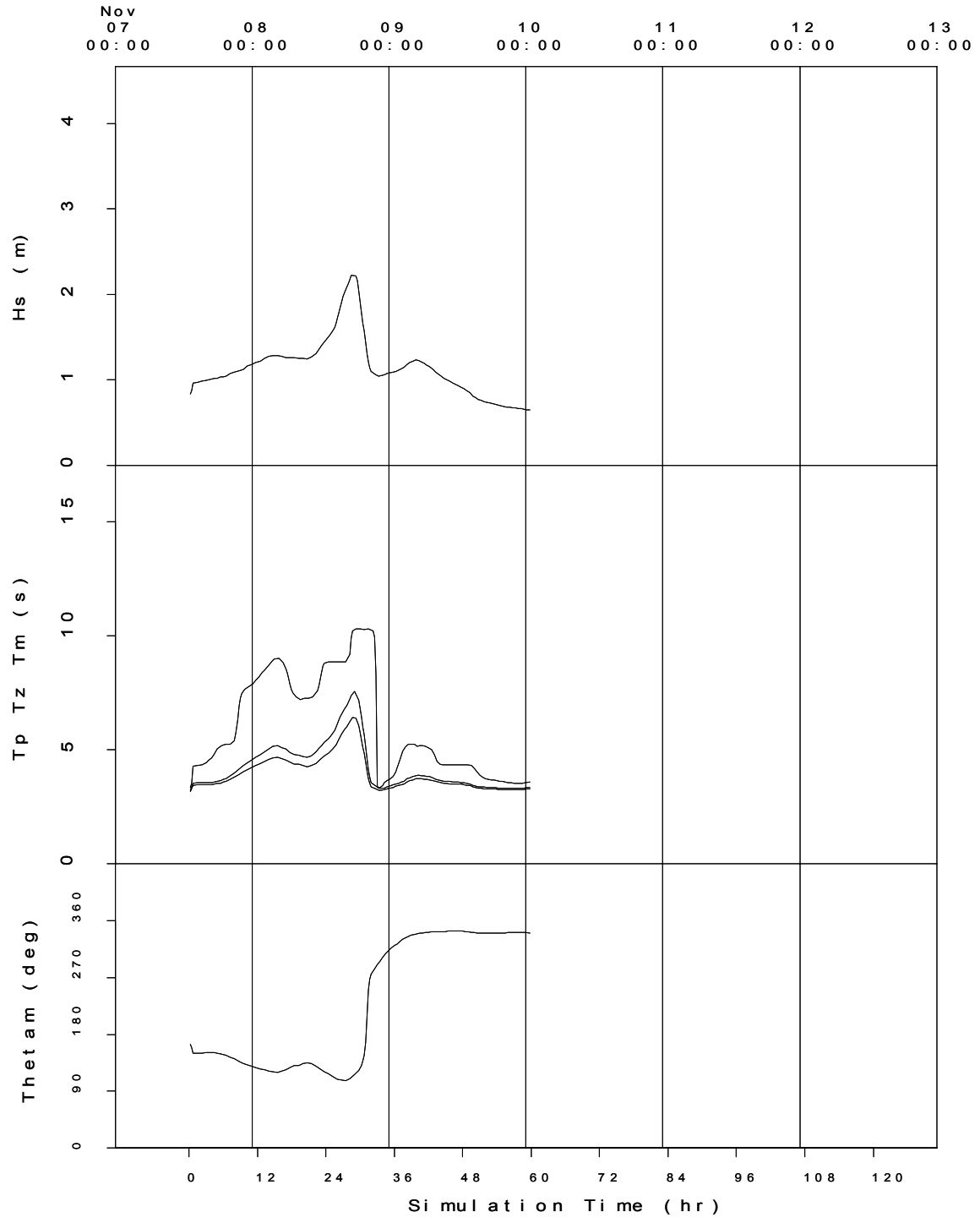

Figure 5.26 Time history of modelled wave parameters at Site 16 during *Alison.*

The time history of offreef wave height, period and direction is given in Figure 5.26 for Site 16 Home Island N. The peak condition occurs at 8/1 16:40 UTC with an H_s of about 2.2 m and a T_p of 10.3 s. The full set of predicted wave time series for Site 16 is given in Appendix J. For completeness, Table 5.8 lists the ADFA1 modelled peak wave conditions (H_s, T_p and θ_m) for all atoll sites and for each of the top 10 storms modelled. Peak conditions at the atoll of about 6 m are estimated to have occurred during *Harriet, Hubert* and *Pedro*, closely followed by *Doreen*. Figure 5.27 provides a visual summary of the values in Table 5.8.

These results are provided to demonstrate the utility of the full ADFA1 spectral wave model in the absence of any measured wave data and to provide perspective on the interpetation of the statistical model results which follow. However, these results are not necessarily highly accurate. In particular, the ADFA1 model has been shown to exhibit a spatial H_s bias which is thought to be related to nonlinear wave-wave interactions in the rotating wind field (Young, *pers comm*). Section 5.6.4.1 later describes a bias correction scheme which is incorporated into the SATSIM parametric model to partially correct this problem. Depending on the relative position of the site and the storm, this scheme can yield H_s correction factors between 0.9 and 1.35 for the top 10 storm set. Later ADFA1 modelled values presented in this report also incorporate the correction factors.

5.6.3 2D Parametric Wave Modelling

The SATSIM model incorporates a 2D parametric tropical cyclone model which provides an estimate of the wave conditions in space and time for an open ocean site remote from land (refer Appendix E for details). This model has been constructed based on a large number of 2D ADFA1 model simulations using a wide range of tropical cyclone parameters.

Although the Cocos Islands are essentially an open ocean site, the atoll represents a finite sized point (e.g. 10 km x 12 km) and for the present study it is necessary to consider the localised shielding effects of the atoll. This was done in an analogous manner to the way the original 2D open ocean parametric wave model was constructed, namely by conducting a series of simulations whose results could be assessed and converted into a parametric approximation.

A large number of simulations were undertaken to explore the impact of the atoll upon the open ocean prediction of wave parameters. Because of the complex manner in which tropical cyclone waves are generated and the varying swell and sea directions, the impact of the atoll on the open ocean condition is also quite complex.

The following method has been adopted to represent the localised impact of the atoll:

1. The atoll sites of interest are separated into either "*outer*" or "*lagoon*" categories;
2. The *outer* class wave response is characterised by
   - A site specific directional response factor e.g. $H_s = f(\theta_{fm})$, and
   - A distance of closest approach factor e.g. $H_s = f(X)$
3. The *lagoon* class is characterised by a directional response factor alone e.g. $H_s = f(\theta_{fm})$

These assumptions are best discussed by examining the series of model results which were used to determine the response. A "direct hit" 900 hPa storm was used to map the directional response at 45° intervals for all sites, compared with a single open ocean site. Figure 2.28 provides a general diagrammatic reference; a direct hit being with X=0. Firstly, Figure 5.29 presents the variation in H_s response factor on the basis of storm track for the *outer* class. The results show a series of site-specific curves plotted as a function of the relative angle between a bearing from the nominal centre of the atoll to each site (θ_s) and the bearing of the storm forward speed (θ_{fm}), i.e. $\theta' = \theta_s - \theta_{fm}$. This

function azimuthally aligns the responses, indicating the maximum wave height factor will tend to occur in the range 180° to 270° clockwise relative to the storm track.

Table 5.8 Summary of "top 10" ADFA1 modelled wave conditions.

		Hazel			*Doreen*			*Daryl*			*Ophelia*			*Frederic*		
Site	Name	H_s	T_p	θ_m	H_s	T_p	θ_m	H_s	T_p	θ_m	H_s	T_p	θ_m	H_s	T_p	θ_m
		m	s	°	m	s	°	m	s	°	m	s	°	m	s	°
1	Trannies_Beach	3.8	8.6	330	4.4	8.7	285	1.9	7.1	261	2.2	7.5	215	1.9	5.3	297
2	West_Is_Jetty	1.8	8.8	347	2.5	10.5	320	1.1	5.2	329	1.3	10.3	9	1.2	5.2	313
3	Rumah_Baru	1.5	9.9	4	2.1	8.3	348	1.2	9.6	227	1.2	5.9	12	1.2	9.6	47
4	Quarantine_N	3.2	8.8	316	4.4	8.7	285	1.7	5.4	295	2.0	7.7	224	1.9	5.4	297
5	Airport_N	0.3	11.7	172	0.4	9.7	199	0.2	11.2	196	0.3	2.9	111	0.2	11.2	252
6	North_Park	3.8	8.7	329	4.4	8.7	289	2.2	7.8	224	2.3	7.6	209	1.9	5.3	298
7	South_Lagoon	0.3	2.9	66	0.4	2.4	340	0.2	2.8	42	0.3	2.8	106	0.2	2.8	35
8	Airport_Settlement	3.6	10.1	230	4.0	8.7	281	2.2	8.5	219	2.3	7.7	207	1.8	5.3	288
9	Airport_S	3.8	10.4	184	4.3	8.6	287	2.8	9.0	159	2.6	7.1	140	2.1	6.6	139
10	Southern_Entrance	4.5	11.1	150	3.6	7.8	124	3.5	10.3	124	2.8	7.7	130	2.3	7.6	130
11	South_Is_Outer	3.9	11.1	130	5.8	10.9	80	3.4	10.3	121	3.6	10.2	100	3.6	10.2	87
12	South_Is_Inner	0.3	6.0	184	0.4	5.0	345	0.2	5.8	13	0.3	3.3	116	0.2	5.8	148
13	Home_Is_SE	3.7	10.6	124	5.8	12.2	72	3.3	10.3	118	3.7	10.2	88	3.7	10.3	77
14	Home_Is_S	0.6	6.0	322	0.8	5.0	152	0.4	5.8	94	0.5	4.7	102	0.5	5.8	291
15	Home_Is_Jetty	0.6	6.0	322	0.8	5.0	152	0.4	5.8	94	0.5	4.7	102	0.5	5.8	291
16	Home_Is_N	3.2	11.5	115	5.7	12.2	71	3.3	10.3	115	3.6	8.9	80	3.6	10.3	76
17	Direction_Is_Jetty	1.3	10.2	259	2.1	17.2	292	1.0	3.5	275	1.5	13.5	250	1.1	5.1	293
18	Direction_Is_N	3.8	7.9	346	5.7	12.2	74	3.2	10.3	117	3.7	9.0	82	3.6	10.3	80
19	Horsburgh_S	3.3	7.7	358	5.0	13.4	36	1.3	9.1	113	3.1	8.9	69	3.0	10.3	66
20	Horsburgh_N	3.9	7.9	341	5.2	13.5	41	3.1	10.3	119	3.5	9.1	80	3.4	10.3	75

		Pedro			*Graham*			*Harriet*			*Hubert*			*Alison*		
Site	Name	H_s	T_p	θ_m	H_s	T_p	θ_m	H_s	T_p	θ_m	H_s	T_p	θ_m	H_s	T_p	θ_m
		m	s	°	m	s	°	m	s	°	m	s	°	m	s	°
1	Trannies_Beach	5.9	10.8	308	3.9	12.6	360	3.0	8.1	183	3.2	10.6	348	2.4	6.3	242
2	West_Is_Jetty	2.2	11.0	343	2.7	13.5	346	2.0	13.9	18	2.3	10.6	347	1.2	6.5	309
3	Rumah_Baru	2.0	6.6	36	1.2	6.8	2	2.2	9.6	203	2.1	9.8	23	1.1	9.6	98
4	Quarantine_N	5.3	10.8	298	1.7	12.9	339	2.1	7.3	205	1.8	10.3	330	2.3	6.3	248
5	Airport_N	0.4	3.2	339	0.3	3.5	24	0.5	11.2	14	0.4	11.5	70	0.2	11.2	181
6	North_Park	6.0	10.5	309	3.2	13.5	346	3.7	8.6	173	3.1	10.8	348	2.5	6.4	235
7	South_Lagoon	0.4	3.1	323	0.3	3.6	24	0.5	2.8	212	0.4	2.8	204	0.2	2.8	108
8	Airport_Settlement	4.0	11.4	280	2.1	6.3	175	3.6	8.6	170	2.0	6.3	157	2.5	8.4	238
9	Airport_S	4.8	11.3	291	2.4	6.5	158	4.7	9.0	145	2.9	7.0	132	2.9	9.7	198
10	Southern_Entrance	2.6	13.5	255	2.5	6.5	155	5.4	10.2	135	3.2	7.8	125	3.3	10.3	163
11	South_Is_Outer	2.5	7.0	47	2.7	7.8	125	6.3	10.3	109	5.6	10.6	82	3.0	10.3	136
12	South_Is_Inner	0.4	3.7	352	0.3	3.7	25	0.5	5.8	343	0.4	5.9	119	0.2	5.8	302
13	Home_Is_SE	4.6	10.3	5	4.8	12.4	18	5.5	10.2	108	6.1	10.4	78	2.4	10.2	122
14	Home_Is_S	0.8	5.3	310	0.6	5.2	22	0.9	5.8	290	0.8	5.9	128	0.4	5.8	255
15	Home_Is_Jetty	0.8	5.3	310	0.6	5.2	22	0.9	5.8	290	0.8	5.9	128	0.4	5.8	255
16	Home_Is_N	4.1	8.8	11	4.6	12.4	21	5.0	10.1	102	6.0	10.4	78	2.2	10.3	116
17	Direction_Is_Jetty	1.4	10.6	304	1.5	12.4	253	1.3	13.4	331	1.3	13.5	305	1.1	7.0	254
18	Direction_Is_N	5.1	10.2	341	4.8	12.4	20	5.1	9.9	112	6.2	10.4	82	2.4	10.1	125
19	Horsburgh_S	4.3	9.1	7	4.3	12.5	17	3.0	9.8	89	5.6	10.3	59	1.6	8.9	105
20	Horsburgh_N	5.5	10.3	329	5.0	12.6	18	3.9	10.3	112	6.0	10.3	77	2.5	10.2	172

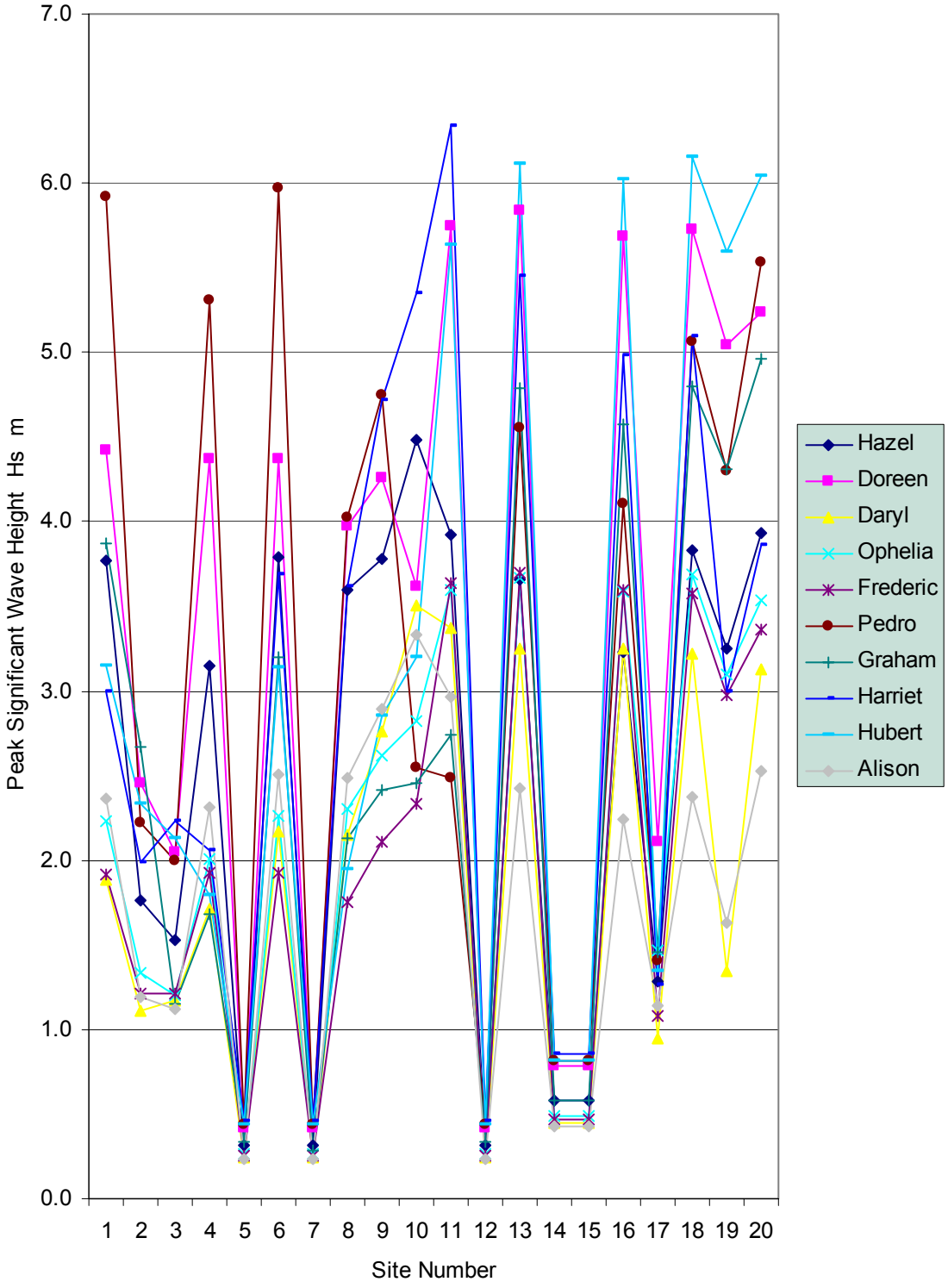

Figure 5.27 Summary of "top 10" modelled ADFA1 wave conditions.

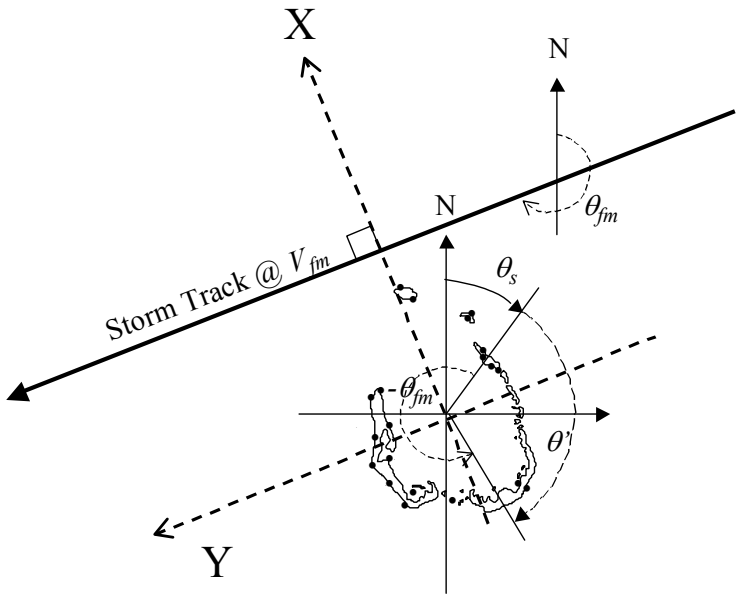

Figure 5.28 Reference system for wave modelling.

Each site-specific response curve then embodies the impact of the special shape of the atoll and also any nearshore effects, although the very deepwater adjacent to the atoll limits these influences. Taking all the data together, the response resembles a $\cos^2$ functional form. Figure 5.30 shows the analogous response factors for peak spectral period T_p. This shows a much more complex pattern with a minimum near 360° but with some sites experiencing multiple variations as a function of relative angle.

Next, a further series of simulations were undertaken by varying the distance of closest approach to the atoll. This yields a series of distance-specific response factors as shown in Figure 5.31, again plotted on the basis of relative angle from the storm track.

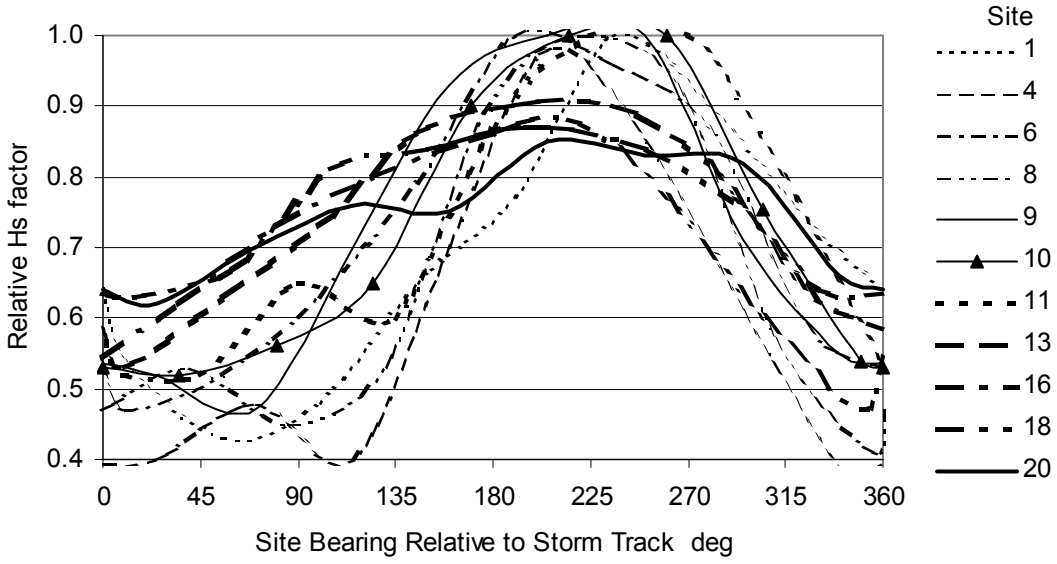

Figure 5.29 Directional Hs response for "outer" sites.

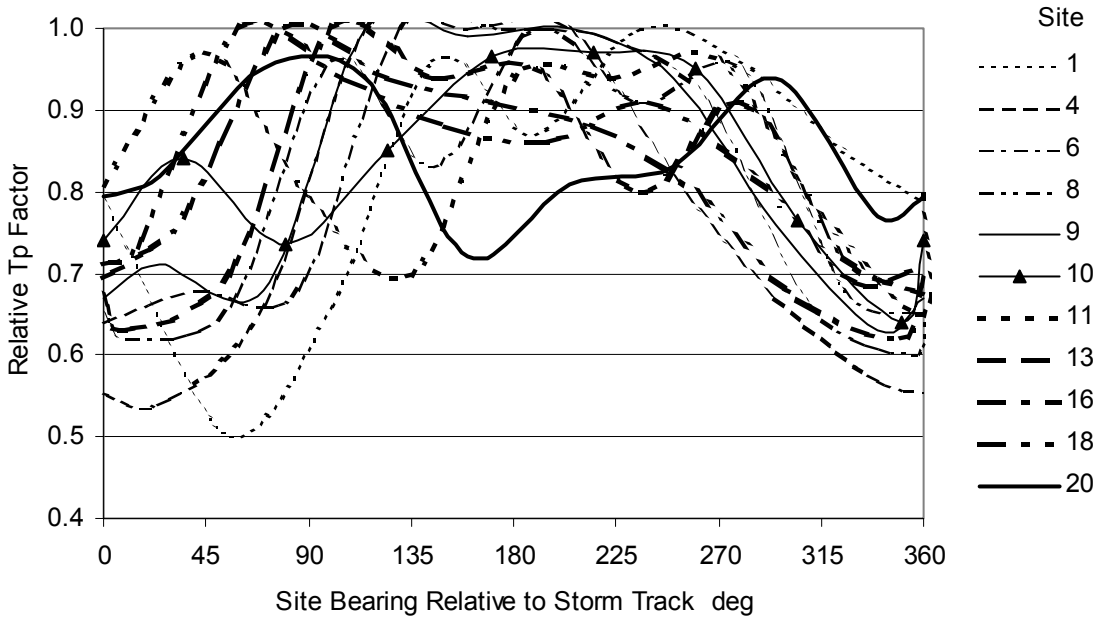

Figure 5.30 Directional Tp response for "outer" sites.

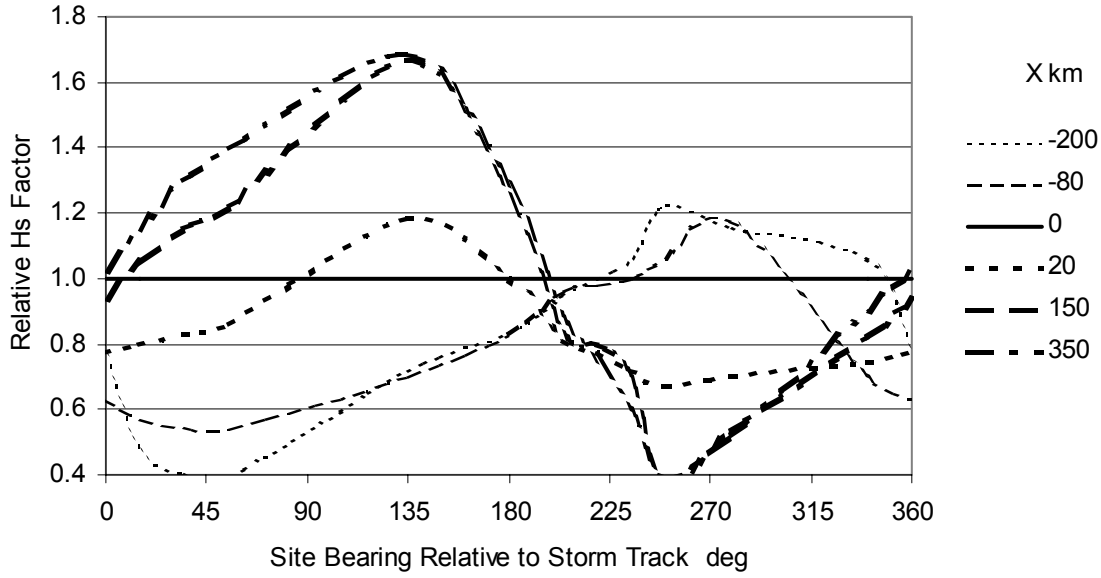

Figure 5.31 Proximity Hs response for "outer" sites.

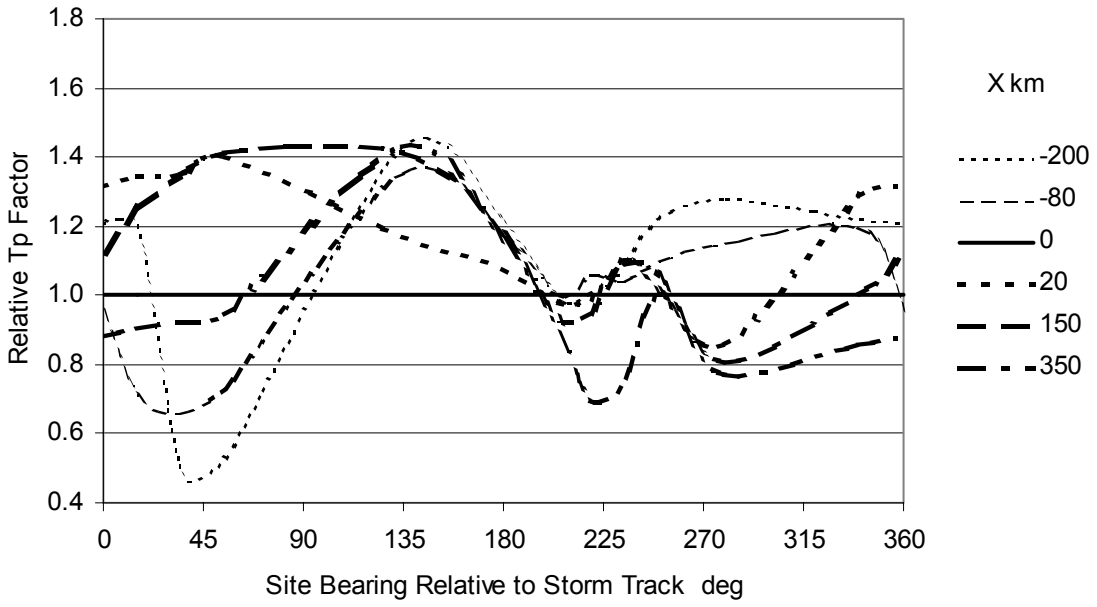

Figure 5.32 Proximity Tp response for "outer" sites.

In this case the factor has been normalised to match the "direct hit" response when X=0. At other distances, relative to the line of the storm track, the response varies as a function of the relative angle of approach. The convention for X is that it is +ve when the atoll is on the LHS of the track (the "strong" side) and -ve when the atoll is on the RHS of the track (refer Figure 5.28). Figure 5.32 presents the analogous result for T_p.

The wave height H_s and period T_p at any site is then calculated as the product of these respective factors, dependent on firstly the relative angle between site and track and secondly the distance normal from the track to the atoll.

In the case of the *lagoon* sites, the response is simplified by the presence of the atoll, leaving the wave conditions at each site essentially a function of the angle of the storm track. This is not the complete variability, since X is also likely to influence the exposure, but this approach is considered reasonable here because the focus is on wave setup at the *outer* sites and the majority of *lagoon* sites will experience very low wave heights due to the shallow water and the high bottom friction. Figures 5.33 and 5.34 show the adopted directional response functions for the *lagoon* sites where it can be seen that sites 19, 2 and 3 experience the greatest response.

5.6.4 Comparison of 2D Spectral and Parametric Modelling

The model comparisons are made in several steps, so as to illustrate the methodology and to introduce the statistical aspects of the parametric modelling approach. Firstly, the parametric model prediction is compared with a 2D spectral model prediction for an open ocean site, i.e. without the atoll present. *Alison* is used as the example storm, both its real or *actual* track and also its *schematised* storm track are considered. Next, the true atoll situation is considered, incorporating the response functions described above and model comparisons for the top 10 storms are considered.

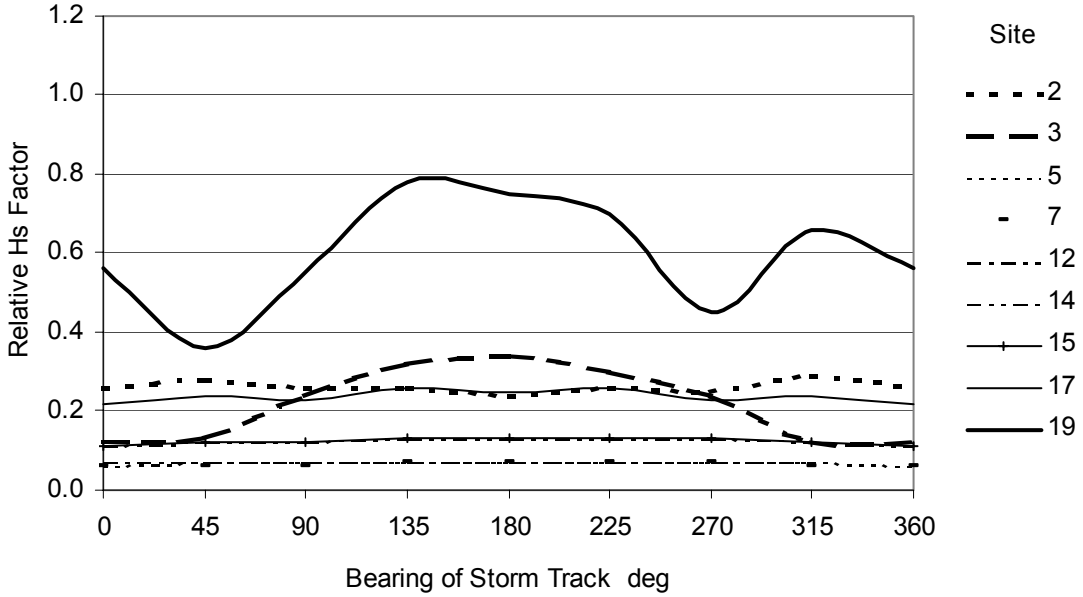

Figure 5.33 Directional Hs response for "lagoon" sites.

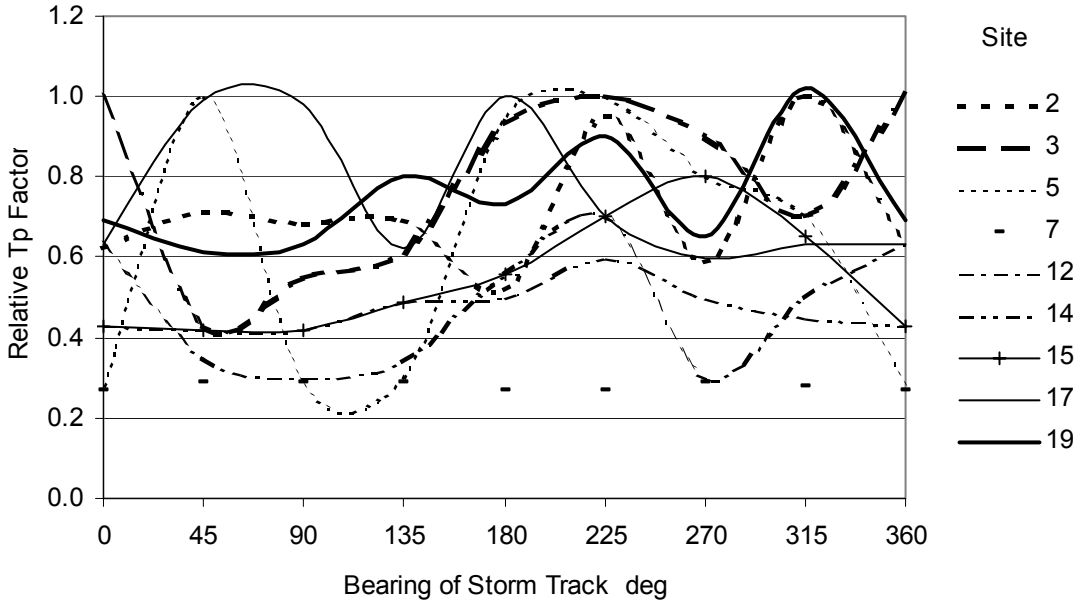

Figure 5.34 Directional Tp response for "lagoon" sites.

5.6.4.1 Open Ocean Wave Model Comparisons

In this comparison, *Alison* is used as an example to illustrate the approach. The basis of the parametric wave model is that it provides estimates of open ocean wave heights and periods relative to the storm position, intensity and size etc. In this regard it is an *approximation* of the prediction which would be obtained directly from a full 2D spectral wave model simulation. It is therefore important to appreciate the degree of approximation actually achievable. Also, as mentioned in Section 5.6.2, the ADFA1 model exhibits some biases of its own, and its predicted H_s values here have been adjusted to match the same bias correction function which is built-in to SATSIM (refer Appendix E). These H_s correction factors are summarised below in Table 5.9 and are applied to all H_s values reported in this and following sections. No adjustment is made to T_p.

Table 5.9 H_s correction factors for the top 10 storms at the Cocos Islands.

Hazel	1.34	*Pedro*	0.91
Doreen	1.09	*Graham*	1.24
Daryl	1.31	*Harriet*	1.09
Ophelia	1.19	*Hubert*	0.90
Frederic	1.09	*Alison*	1.32

For this comparison, the normal spectral wave model "C" grid is replaced by an open sea deepwater grid which does not include the atoll bathymetry and no "D" grid is required. The storm is then modelled as the *actual* Bureau of Meteorology best track (including those parameters determined here by calibration in Section 5.4) and also as a *schematic* storm track which complies with the assumptions embodied in the parametric model. In the schematic case, the storm track is made straightline at constant speed and the pressure variation (from ambient to maximum intenisty) is represented as a Gaussian function. The relative position of the site and the storm is maintained as much as practicable in this context.

Figure 5.35 summarises the spectral model simulations (actual and schematic) and the parametric SATSIM model result for *Alison*. The H_s comparison shows that the peak values for the schematic spectral model and the SATSIM prediction are essentially identical, as expected. The *actual* track result produces a slightly higher peak value. The shape of the wave hydrograph is similar above about 2 m, although the SATSIM result attenuates faster. The T_p comparison shows a greater difference between the actual and schematic spectral model results prior to the arrival of the peak and both indicate a higher peak than the SATSIM model. This highlights the many subtle differences which can occur between actual and schematic track representations. Also, the spectral peak period T_p is a discrete parameter (not subject to averaging such as T_z for example) and tends to flip into adjacent model frequency bands depending on the distribution of spectral wave energy. While the SATSIM result falls short of the indicated peak value of about 10 s, it does provide a wider response and approximates a more stable estimate of T_p as being about 1.3 x T_z.

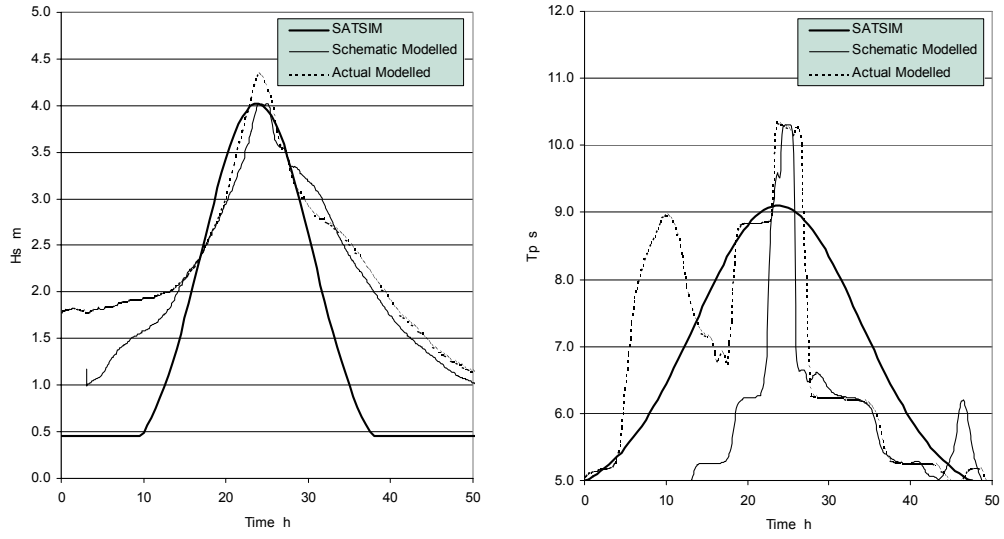

Figure 5.35 Open ocean model comparison for *Alison*.

Time history comparisons of H_s and T_p for the full set of top 10 storms are given later in Figure 5.37, showing the actual spectral model result and the SATSIM result. Some of the storms show an excellent agreement (e.g. *Doreen*, *Ophelia, Frederic, Graham, Hubert)* while others are still reasonable (*Pedro, Daryl*) but *Hazel* and *Harriet* are relatively poor. The mismatches are then due to the actual differences between the real storm track parameters and the schematised versions and include the effects of changes in direction and distance as well as changing intensity etc. The two poorly modelled storms, *Hazel* and *Harriet,* are also the most poorly approximated by their schematic versions. In particular, *Harriet* was nearly-stationary over the island for an extended period and this created an enhanced fetch. In the case of *Hazel*, the change in direction of the actual track has created a tongue of higher wave heights which just manages to intersect the site.

The peak values only are then summarised below in Figure 5.36 as a cross-plot of the SATSIM and ADFA1 results. These plots indicate the ± 0.5 m H_s and ± 1 s T_p ranges. On this basis there is a tendency evident for the parametric model to underpredict H_s for the actual track parameters, although the removal of *Hazel* and *Harriet* significantly improves the comparison, giving a best fit slope of about 0.90. Likewise, the T_p result indicates an underprediction but the actual tracks have a greater tendency to drift to the higher discrete T_p values in the spectral model. This apparent bias will be addressed later, but it must be remembered that the parametric model is not designed to be used for accurate hindcasting of specific storms, but rather to provide a non-biased estimate of the overall population of storms which can be utilised in a statistical simulation.

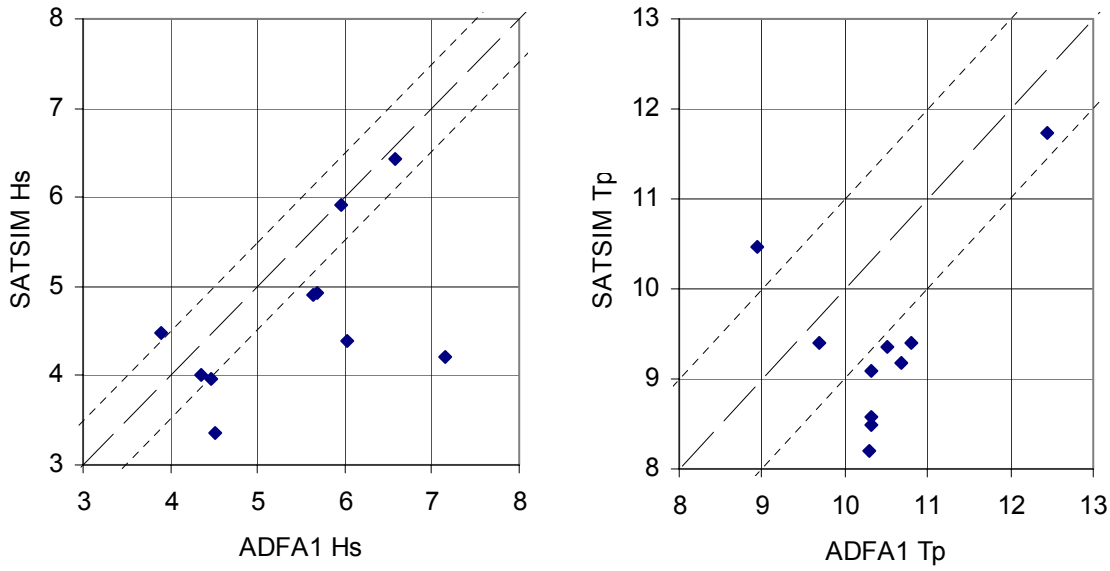

Figure 5.36 Comparison of peak open ocean wave estimates for top 10 storms.

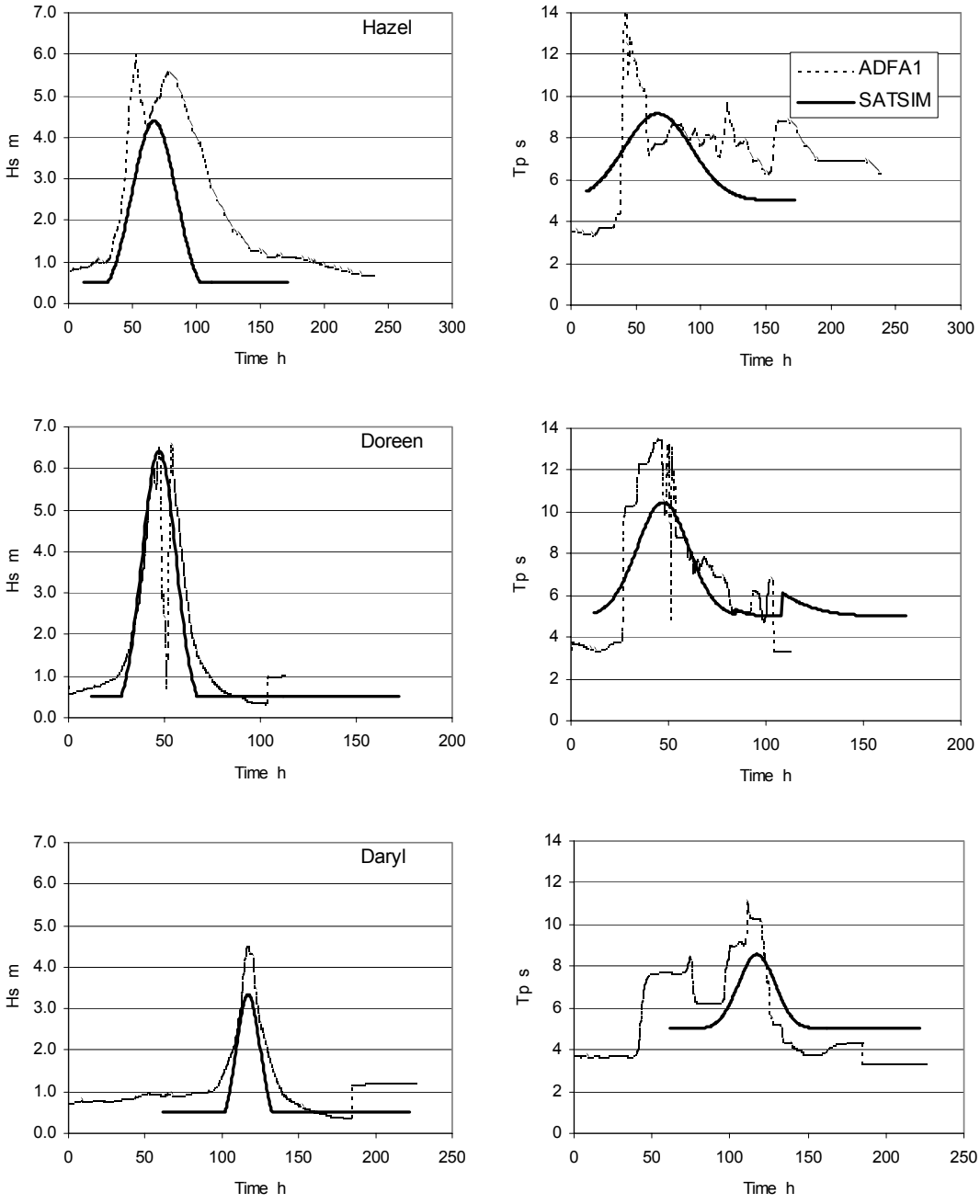

Figure 5.37 Time history comparison of open ocean wave estimates for top 10 storms.

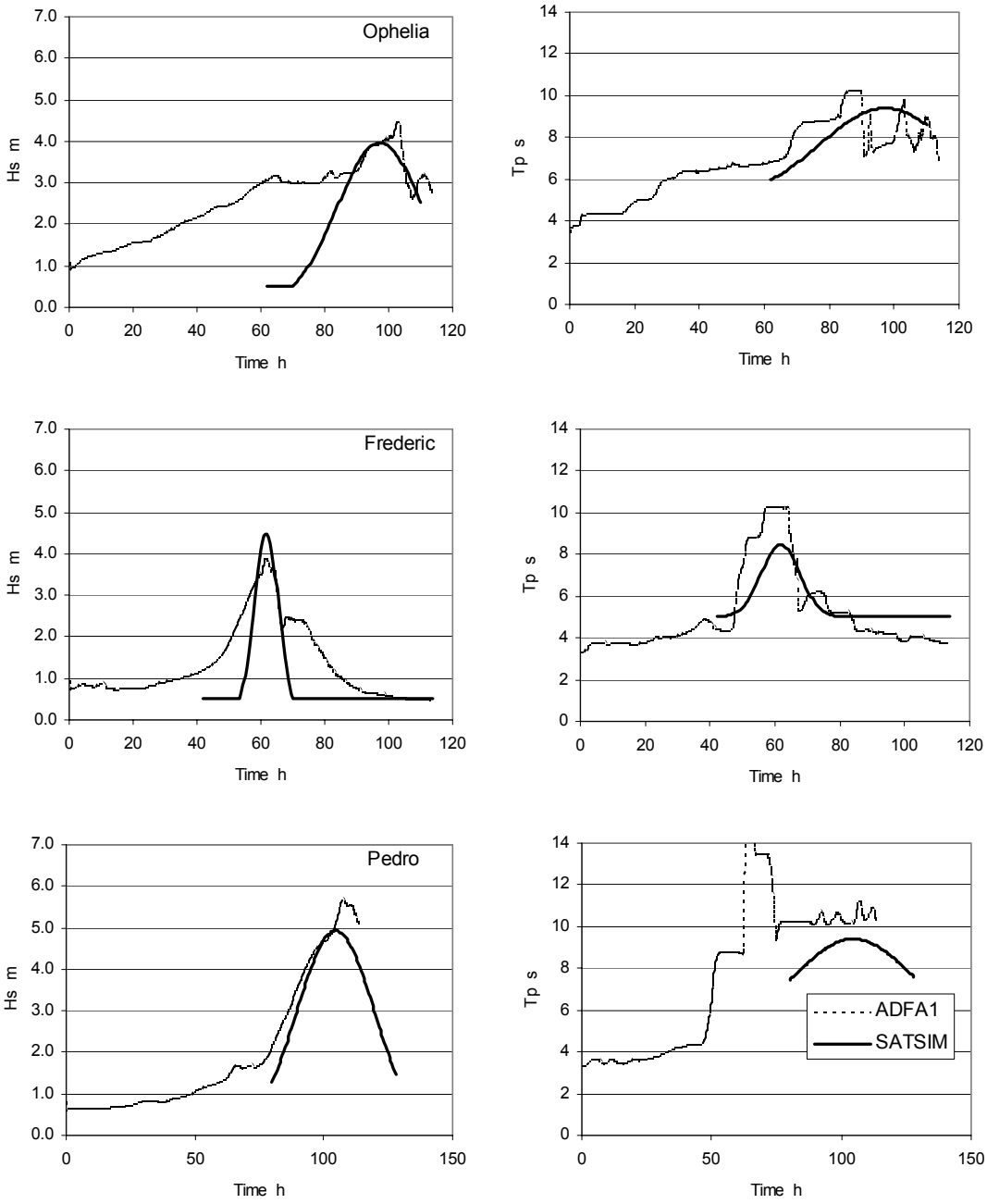

Figure 5.37 (contd.) Time history comparison of open ocean wave estimates for top 10 storms.

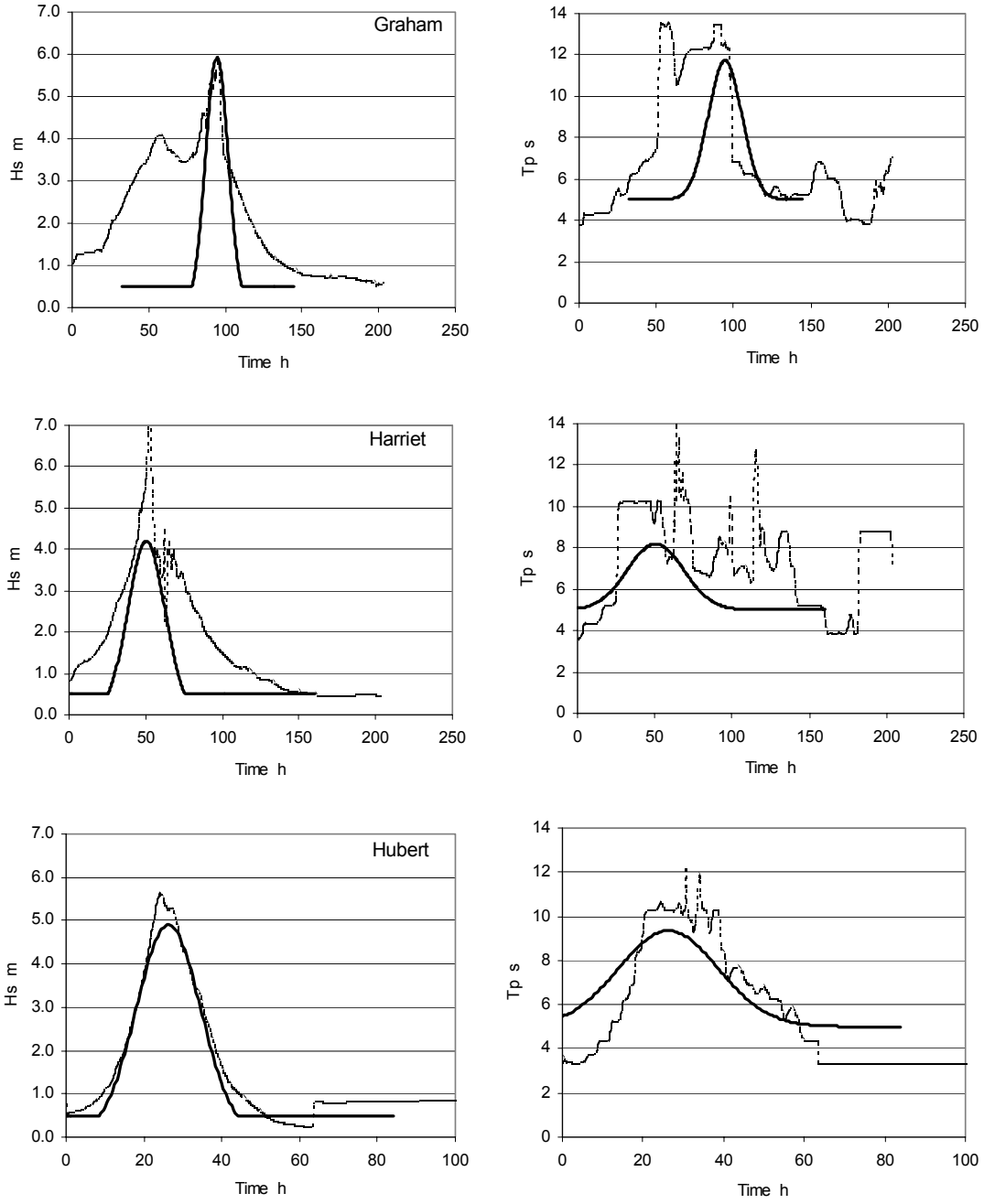

Figure 5.37 (contd.) Time history comparison of open ocean wave estimates for top 10 storms.

5.6.4.2 Atoll-Specific Wave Model Comparisons

The open ocean predicted wave conditions are then modified according to the site-specific atoll variation as discussed in Section 5.6.3 and a parametric time history is constructed for each site of interest. Again, *Alison* is used as an example, with Figure 5.39 showing a selection of SATSIM versus ADFA1 predictions for Sites 10, 11 and 13. In this case the normal "C" and "D" grids are used in the spectral wave model simulation of the actual track parameters for *Alison*. The differences between these two time histories now incorporate both errors due to representation of the open ocean condition (the track schematisation) as well as the approximation of the effect of island shielding. As a result, the agreement between the two methods tends to vary from site to site.

Figure 5.38 below summarises the peak wave conditions anywhere on the atoll during *Alison* for the two modelled cases - each point being the peak attained at one of the 20 sites. In respect of H_s, most but not all sites are modelled by SATSIM within 0.5 m of the ADFA1 result. In the T_p case, greater scatter is evident. However, the highest conditions are generally well represented.

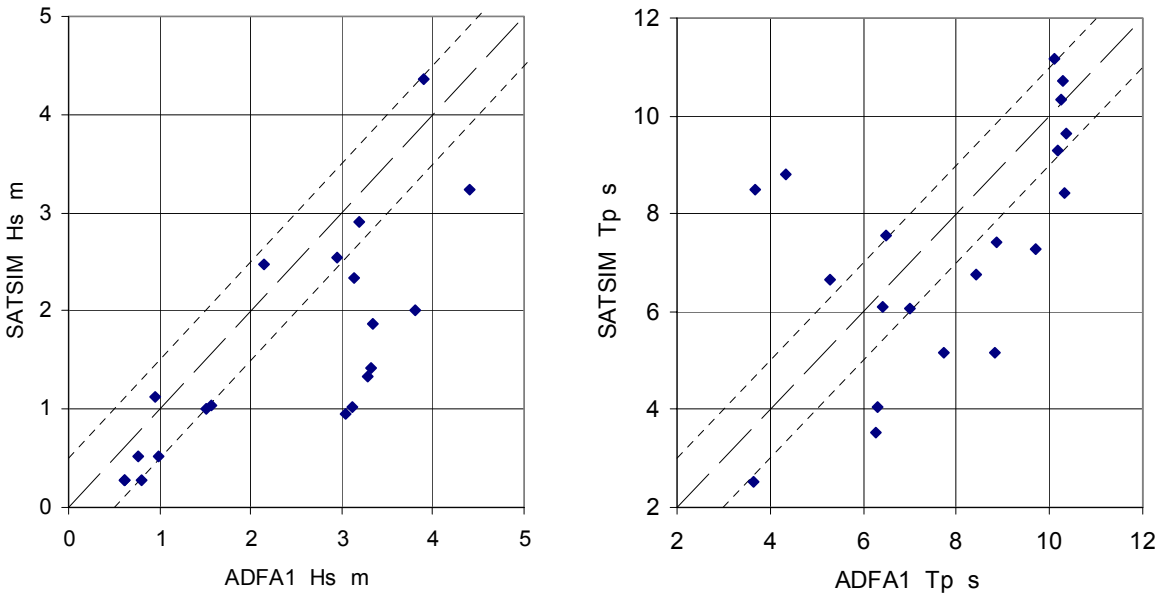

Figure 5.38 Comparison of peak atoll-wide wave estimates for *Alison*.

Taking the whole set of top 10 storms and performing the same comparison of peak site-specific values as above for *Alison*, yields the summary result in Figure 5.40. Here, the SATSIM H_s estimate closely follows the upper envelope 1:1 line but underpredicts many sites relative to the full ADFA1 model. The T_p estimate shows more scatter, with SATSIM often capable of over-estimating the T_p ADFA1 value.

These results illustrate the complexity of modelling tropical cyclone generated waves in such an environment, where small changes in actual storm position, speed and intensity can result in sudden shifts in wave estimates at fixed points close to the island. Further variability would also be seen, for example, if a selection of other nearby points from the "D" grid were chosen for comparison purposes. Also, there are errors due to the approximations needed by the parametric model and the ADFA1 model itself has its own level of accuracy relative to actual measured values, as discussed previously.

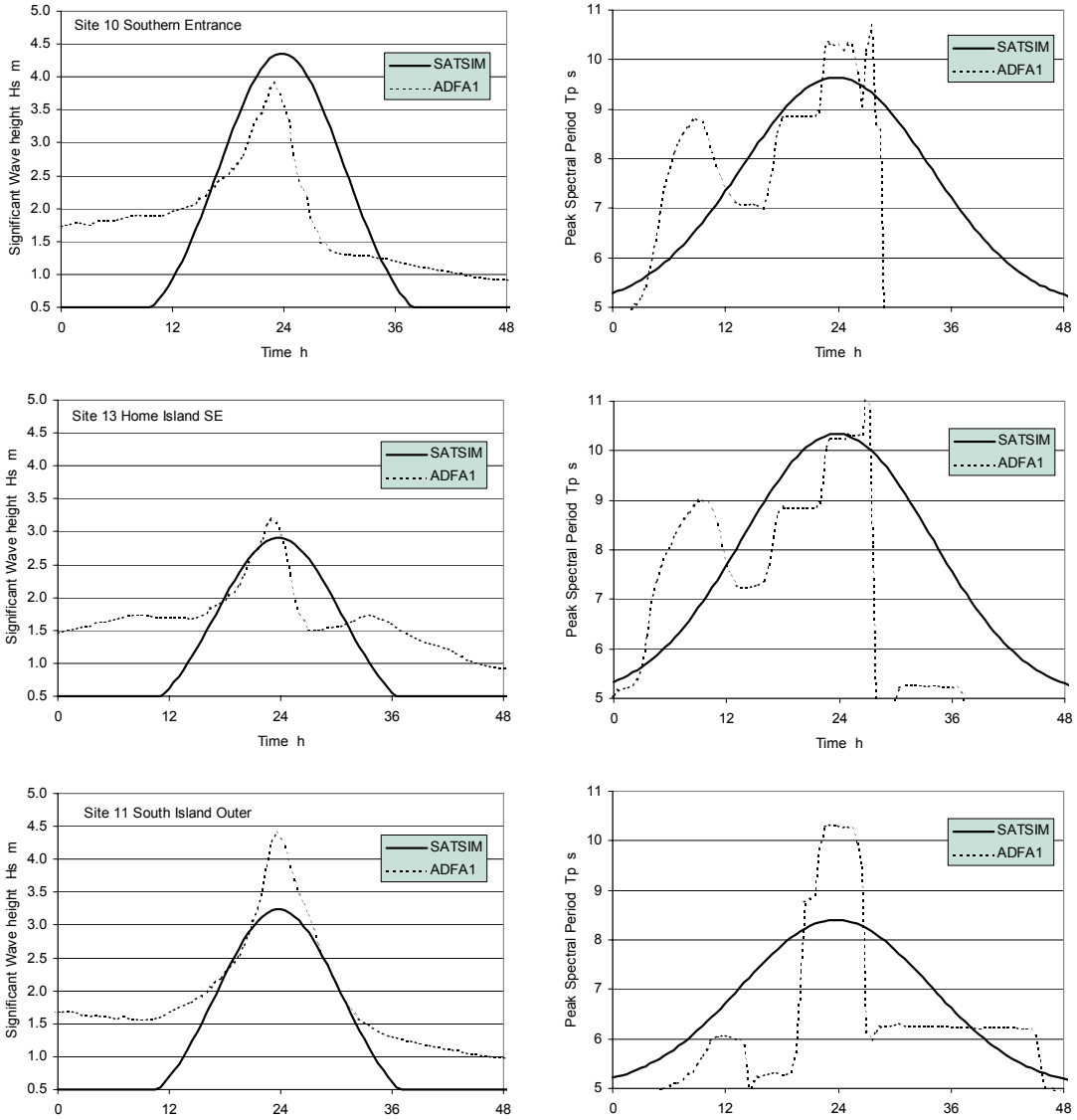

Figure 5.39 Example site-specific wave estimate comparisons for *Alison.*

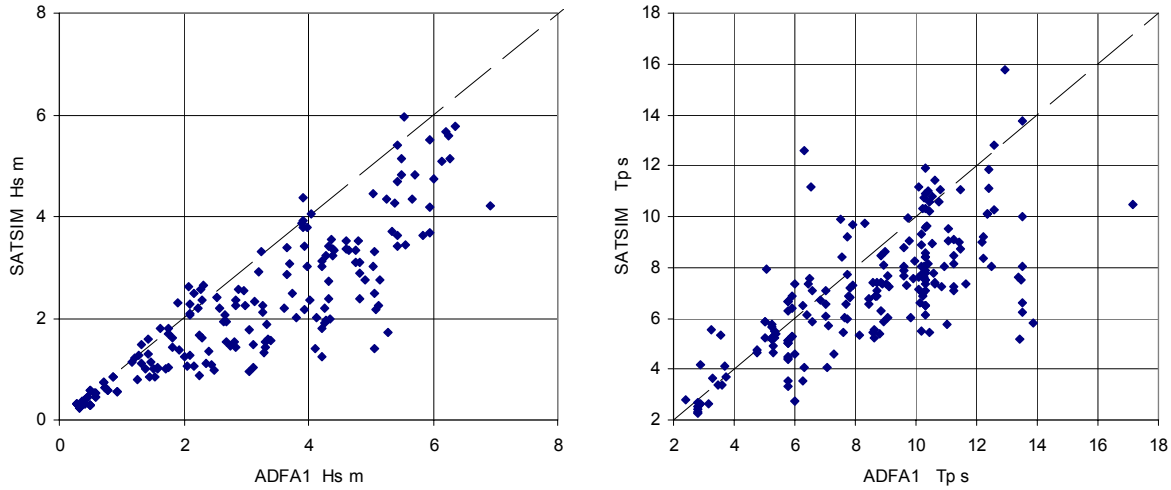

Figure 5.40 Combined wave parameter estimates for the top 10 storms at all sites.

It then remains to interprete these results in terms of the overall accuracy of the parametric model and the purpose for which it is being used in the present study. Firstly, the site-specific attenuation functions in Section 5.6.3 are incorporated so that only the "exposed" sites during any particular storm event receive the full impact of the open ocean wave condition. Otherwise, all sites would show an identical response and yield no site-specific sensitivity. Hence, when judging the accuracy of the overall model and its ability to represent the true response in an unbiased way, we consider more specifically its ability to match the *peak* wave conditions in each of the top 10 storm cases. This comparison is given in Figure 5.41 below, simply being a subset of the previous figure. In this case, the H_s response suggests an underprediction trend of about 15%, based on the best fit line, while the T_p response, although scattered, shows an unbiased best fit. Removing *Harriet* as a special case again returns an approximate 10% underprediction.

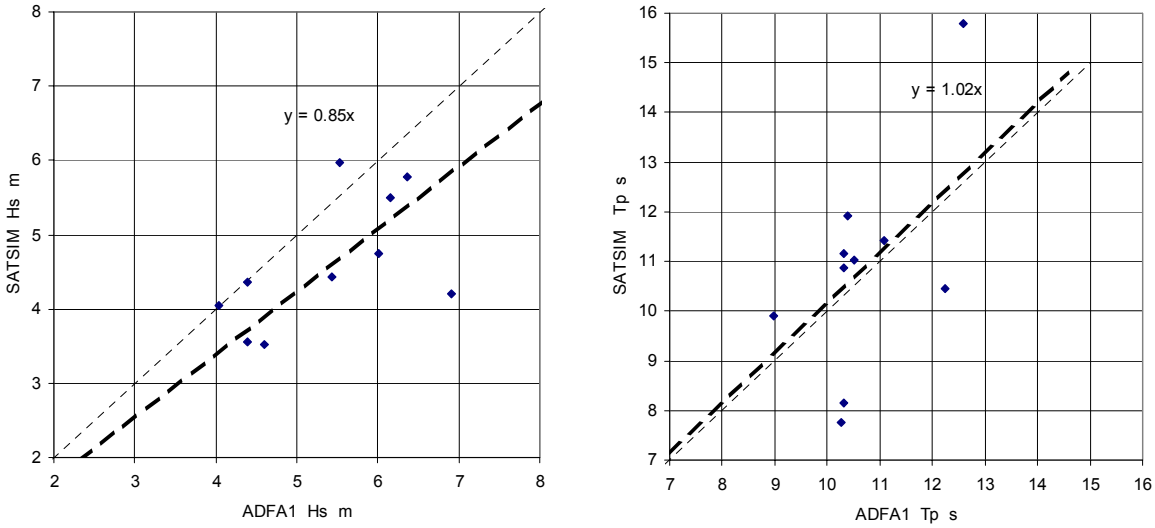

Figure 5.41 Maximum atoll wave parameter estimates for the top 10 storms.

The source of the apparent residual H_s bias is believed due to the finite size of the island, where for some storms and some sites, a site-specific factor greater than unity is indicated, whereas in the Section 5.6.3 simplification, the results were normalised to unity in all cases. Accordingly, whether this represents a true source of bias in the model is open to question, since in the statistical sense these differences will be accommodated by the random selections of track and intensity. However, in order to understand the sensitivity of the final result to a potential bias of this magnitude a specific sensitivity test is reserved in Section 6.3. The values chosen for bias testing are a 10% increase in predicted H_s and, scaling T_p on a constant steepness basis, a 5% increase in $T_{p.}$

As a further conservative assumption, the statistical model ignores the effect of refraction losses at sites other than those directly exposed, i.e. all offreef wave conditions are assumed normal to the local shoreline. This is an engineering approximation which provides a minor level of conservativeness to compensate for the observed tendency to underpredict H_s at relatively shielded sites around the atoll.

5.7 Example of the Operation of the Simulation Model

The foregoing sections have considered the individual mechanisms for generating the time varying wind and pressure forcing and each of the resulting forced water level components, i.e. astronomical tide, inverted barometer effect, bathystrophic storm tide and breaking wave setup. An example of how the various components are combined by the simulation model is given in Figure 5.42, again for the case of *Alison*.

Two atoll sites are considered; Site 15 Home Island Jetty (the tide gauge site), which is typical of a "lagoon" location, and Site 11 South Island Outer, which is typical of an "outer reef" location and also the site of the highest predicted storm tide level during *Alison*. In Figure 5.42, the top two graphs are for Site 14; the lower two graphs are for Site 11.

Considering Site 14 in the lagoon first, the top graph shows the model prediction of mean wind speed and direction. Below this is the simultaneous time history of the astronomical tide, the inverted barometer effect (peaking at 0.09 m only) and the bathystrophic storm tide effect (peaking at 0.06 m only). The wave setup component at lagoon sites is assumed negligible. These water level components are combined by the model with the astronomical tide so as to produce a total peak storm tide level of 0.8 m MSL, some 6 h before the storm was at its closest point. However, the period of peak storm surge occurred around the time of low tide and had a lessened impact as a result. The process of calculating the combined water level ensures that the BST effect is applied last, after the tide and IBE effect are added, thus allowing for non-linear wind stress effects.

The second set of graphs at Site 11 concentrate on the time history of significant wave height and, because it is an open ocean site, the BST component is assumed negligible and replaced now by the breaking wave setup. The peak wave height at Site 11 is predicted to reach 4.4 m and veer from S to W during the passage of the storm. Again, the tide and IBE effect are added first, allowing the correct interaction of the offreef water level and wave height with the reef elevation. In this case the tide and IBE effect are the same as at Site 14 but the wave setup is much greater than the lagoon BST, peaking up to 1.25 m. This also occurs mostly during the period of the falling tide, with the peak storm tide level again occurring earlier and reaching a height of 1.34 m MSL. An almost identical value is reached some 12 h later on the following high tide and after the storm has passed.

In "simulation mode" many thousands of such storms are considered, each with differing parameters, and the next section considers the performance of the simulation model in the probabilistic domain.

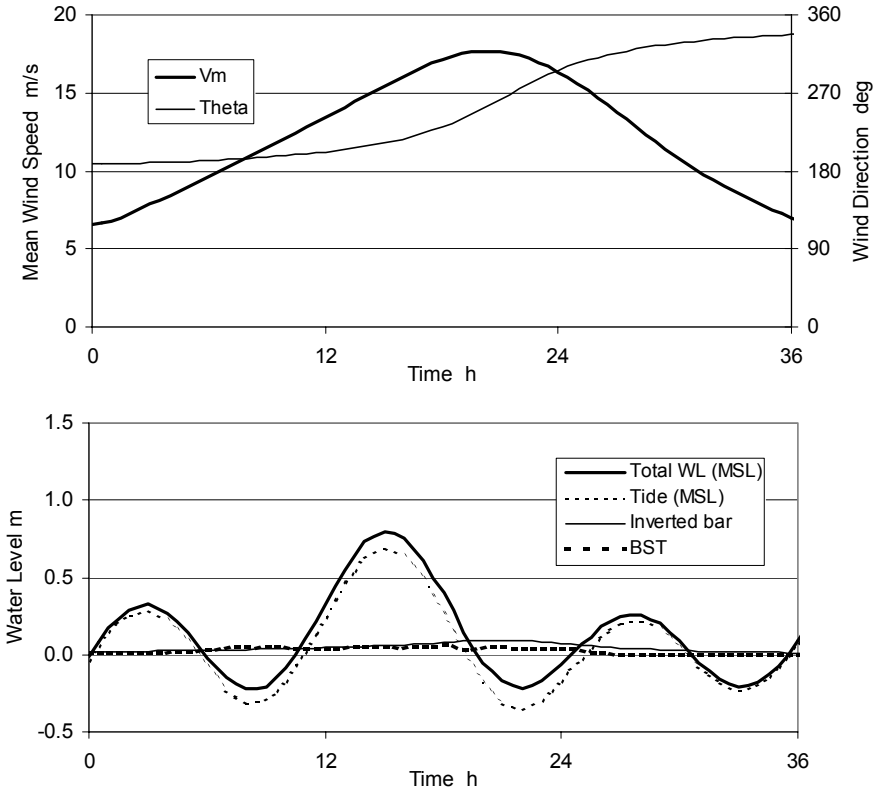

(a) Site 15 - Home Island Jetty

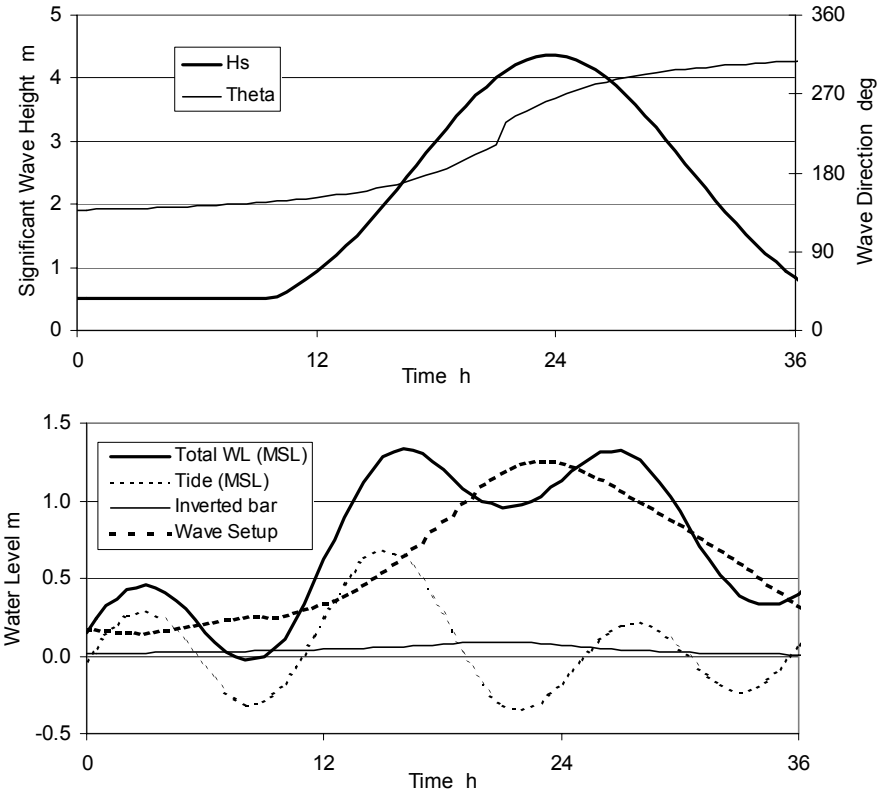

(b) Site 11 - South Island Outer

Figure 5.42 Example model operation for *Alison.*

5.8 Probabilistic Model Verification

The previous sections have dealt with the accuracy of each of the various wind, wave and surge models in terms of their demonstrated *deterministic* accuracy. It is important to also have some confidence in the overall *probabilistic* accuracy of the statistical simulation model SATSIM. The only way this can be done ultimately is to compare model output with long term records of each of these phenomena but since this is not possible, the next best long term data is used, namely wind and tide.

The wind data available for comparison was presented in Section 4, being almost 50 years of measured mean wind speeds from the airport site. Comparison of the SATSIM model output (based on a 10,000 y simulation) with the measured data and the Extreme Value analysis of the data is given in Figure 5.43. The agreement between SATSIM and the EVA analysis is very good, the model result being slightly higher. This provides a high degree of confidence that the model's climatological description, which embodies the *probabilistic* elements, is functioning correctly.

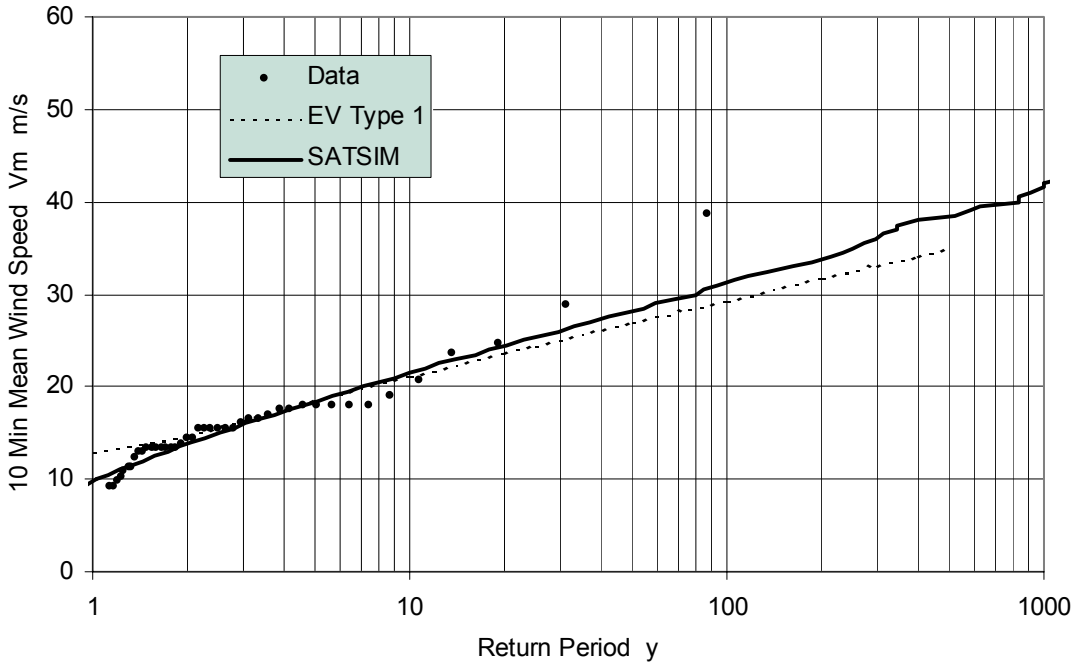

Figure 5.43 Model verification against long-term measured wind data.

The second verification considers the way in which the SATSIM model represents the probabilistic occurrence of the astronomical tide, which is an important modulator of the combined stillwater level and the subsequent wave setup magnitude. Figure 5.44 shows the comparison between the simulated tide levels and the published NTF tidal planes for HAT and MHHW. The heavy curve is the model's sampling of the full tidal signal at an hourly resolution based on 22 harmonic constituents as given in Table 5.10. By comparison, the thin curve shows the sampled tide only during periods when tropical cyclones are actually being generated by the model. With an average of only 2 cyclones per year, each with an average duration of 4 days, this curve samples only around 8 days per year on average. This does not mean that the model is underpredicting the tide levels but simply reflects the fact that the *probability* of attaining any tide level during a tropical cyclone is proportional to the time during which it occurs. Tide levels greater than MHHW are increasingly rare and hence less likely to occur during a cyclone.

Table 5.10 Tidal harmonics for Cocos (South Keeling) Island

Constituent	Amplitude	Phase	Constituent	Amplitude	Phase
	m	°		m	°
S_a	0.0901	197.19	μ_2	0.0116	123.16
S_{sa}	0.0061	142.71	N_2	0.0700	123.30
M_m	0.0065	8.43	ν_2	0.0132	123.21
MS_f	0.0010	111.06	M_2	0.3075	139.99
M_f	0.0132	18.79	L_2	0.0082	151.87
Q_1	0.0197	222.45	T_2	0.0045	175.25
O_1	0.0895	235.93	S_2	0.1133	183.54
P_1	0.0449	249.17	K_2	0.0315	181.78
S_1	0.0099	37.88	M_4	0.0022	341.40
K_1	0.1488	252.60	MS_4	0.0013	52.75
$2N_2$	0.0109	95.69	$2MS_6$	0.0007	297.57

Both of the modelled tidal level curves are asymptotic at about 0.85 m, approximately 0.04 m below the published HAT, which has a theoretical return period of 18.6 y. The slightly lower HAT level obtained by the model is thought to be due to the reduced number of tidal constituents being used and also the hourly sampling. The matching at MHHW (around 3.5 days) appears reasonable. In either case the differences from the theoretical are very small and will not impact on the predictions of total storm tide level.

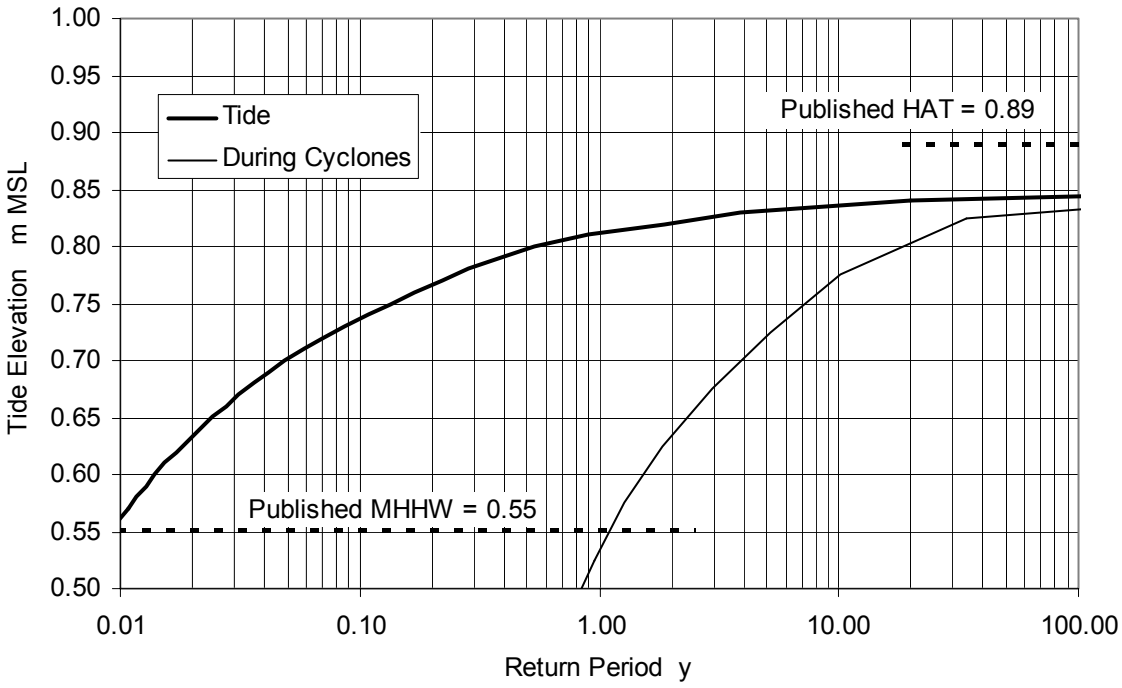

Figure 5.44 Model verification against expected tidal planes.

6 Model Predictions

The previous sections have presented the development and testing of the various sub-models which underpin the construction of the final SATSIM statistical water level model. Here the model predictions are presented based on a series of data scenarios. Firstly, the data sets are discussed.

6.1 Data Sets

The data sets required by the model include:

1. Tropical cyclone climatology (as per Section 4)
2. Tidal harmonics
3. Bathystrophic storm tide fetch definitions for affected sites (as discussed in Section 5)
4. The atoll site-specific wave height and period response functions (from Section 5)
5. Site-specific reef parameters for affected sites

The major site-specific model parameter values (including the adopted "base case" reef parameters) are listed in Table 6.1 below.

Table 6.1 SATSIM site-specific parameter set.

		Type	Site	Tidal	Reef Parameterisation						
		Inner/ Outer	θ_S	Range Ratio	z_r	z_e	W_r	W_{rim}	Rim slope	K_p	K'_p
Site	Name	-	°		m	m	m	m	tanα	-	-
1	Trannies_Beach	outer	280	1.00	-0.60	-14.0	250	380	0.04	0.50	0.49
2	West_Is_Jetty	inner	290	1.00							
3	Rumah_Baru	inner	255	1.05							
4	Quarantine_N	outer	250	1.00	-0.80	-10.0	200	280	0.04	0.50	0.49
5	Airport_N	inner	230	1.10							
6	North_Park	outer	235	1.00	-0.50	-10.0	200	280	0.03	0.50	0.43
7	South_Lagoon	inner	200	1.10							
8	Airport_Settlement	outer	220	1.00	-0.10	-10.0	200	280	0.04	0.50	0.49
9	Airport_S	outer	205	1.00	-0.30	-10.0	200	280	0.03	0.50	0.43
10	Southern_Entrance	outer	180	1.00	-0.35	-10.0	200	250	0.04	0.50	0.49
11	South_Is_Outer	outer	135	1.00	-0.35	-10.0	180	250	0.04	0.50	0.49
12	South_Is_Inner	inner	135	1.10							
13	Home_Is_SE	outer	55	1.00	-0.50	-10.0	100	180	0.05	0.50	0.55
14	Home_Is_S	inner	45	1.00							
15	Home_Is_Jetty	inner	35	1.00							
16	Home_Is_N	outer	35	1.00	-0.50	-10.0	150	200	0.04	0.50	0.49
17	Direction_Is_Jetty	inner	15	1.00							
18	Direction_Is_N	outer	15	1.00	-0.50	-10.0	50	280	0.03	0.50	0.43
19	Horsburgh_S	inner	345	1.00	-0.50	-10.0	100	180	0.05	0.50	0.55
20	Horsburgh_N	outer	340	1.00	-0.50	-10.0	100	180	0.06	0.05	0.56

Each of these is described below, namely:

Inner/Outer Tells the model which type of wave parameterisation to apply

θ_S Is the bearing of the site from the nominal centre of the atoll; used for the wave parameterisation functions.

Range Ratio A tidal range ratio applied at the site to incorporate localised MSL variations (as discussed in Section 5).

Reef Parameterisation

z_r	reef top elevation
z_e	reef edge elevation
W_r	reef top width
W_{rim}	reef rim width
$tan\alpha$	reef rim slope
K_p	reef face breaking parameter
K'_p	reef rim breaking parameter

6.2 Base Case Scenario with 1% Setup levels

The adopted base case scenario is as per Table 6.1, namely that reef parameterisations are based on the "best estimates" from Section 5. The model was then run for a 10,000 year period using the adopted climatology and accumulated a range of water level, wave height, wind and breaking wave setup components. The statistics from this run were then interpreted in terms of the cumulative exceedence above a range of parameter levels and expressed finally in terms of ARI (average recurrence interval) or return period i.e. the average time between equalling or exceeding any given parameter level. Since the model is run for 10,000 years there will be 10 separate estimates of the 1000 year return period values which form the average value as presented. Finally, three different values of the reef induced breaking wave setup have been retained, i.e. the *mean*, the *mean plus standard deviation* and the upper *1%.* For illustration purposes, the results presented here for discussion are for the *1%* reef setup levels.

Figure 6.1 shows the model prediction for the atoll "taken as a whole" - this means that the indicated return period for each water level and wave height parameter is the highest value from any of the 20 sites around the atoll. The upper-most solid line in this graph answers the question e.g. "What is the probability of equalling or exceeding a given storm tide level anywhere on the atoll?" With the other information shown it also addresses the probability of nearshore wave heights (on the RH axis) and the individual water level component magnitudes for IBE, BST and reef setup at the *1*% level. On this basis the 100 year storm tide level is predicted to be approximately 2.9 m MSL and the 1000 year level to be close to 3.5 m MSL. Furthermore, the 1000 year IBE component is seen to be about 0.65 m; the BST component about 1.3 m and the reef setup component is 3.1 m. Reef setup is seen to dominate the total water level estimate. The 1000 year significant wave height (RH axis) is about 10 m and the total water level line can be seen to essentially follow the shape of the wave height line, further indicating the dominance of the wave setup. [Note that the water level curves are not addable in this context due to the amalgamation of results from all 20 sites.]

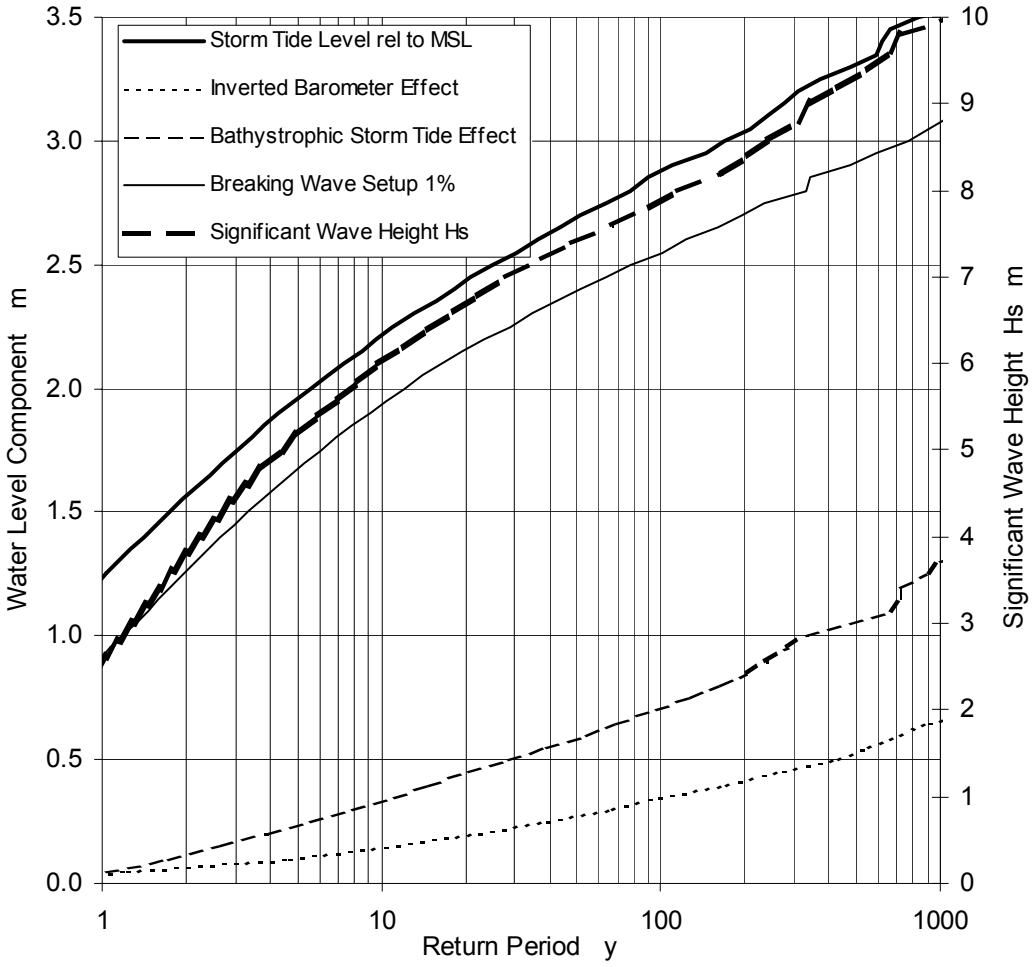

Figure 6.1 Base case water level and wave height return period summary.

While the above summarises the result for the atoll as a whole, the response at the individual sites can be quite variable depending on their level of exposure to each of the forcing mechanisms. Figure 6.2 presents the water level predictions on a site specific basis, where the local ground level (Chris Jones, *pers. comm.*) is also indicated if it is exceeded at a specific site. Note that the lower limit for all curves is set by the astronomical tide where HAT is 0.89 m. These levels are summarised in Table 6.2 for a range of return periods, with *greyed* cells indicating a water level prediction in excess of the local ground level. The highest storm tide levels for any return period are indicated at site 16 Home Island SE, followed by site 20 Horsburgh North. The lowest storm tide levels are indicated at site 17 Direction Island Jetty, followed by 15 Home Island Jetty. The most vulnerable sites are near 10 Southern Entrance and 11 South Island Outer, although Horsburgh Island locations are also vulnerable. While the values in Table 6.2 are given to two significant figures to facilitate graphing it should not be implied that the accuracy of the estimation is to the same precision.

Next, Figures 6.3 through 6.5 show the equivalent statistics for significant wave height, the 1% breaking wave setup component and the local bathystrophic storm tide (BST) component on a site-specific basis. The IBE is essentially a global atoll variable and the curve in Figure 6.1 applies at all sites. The site specific sensitivities are clearly shown whereby the lagoon sites are affected variously by BST while the outer sites are dominated by wave setup.

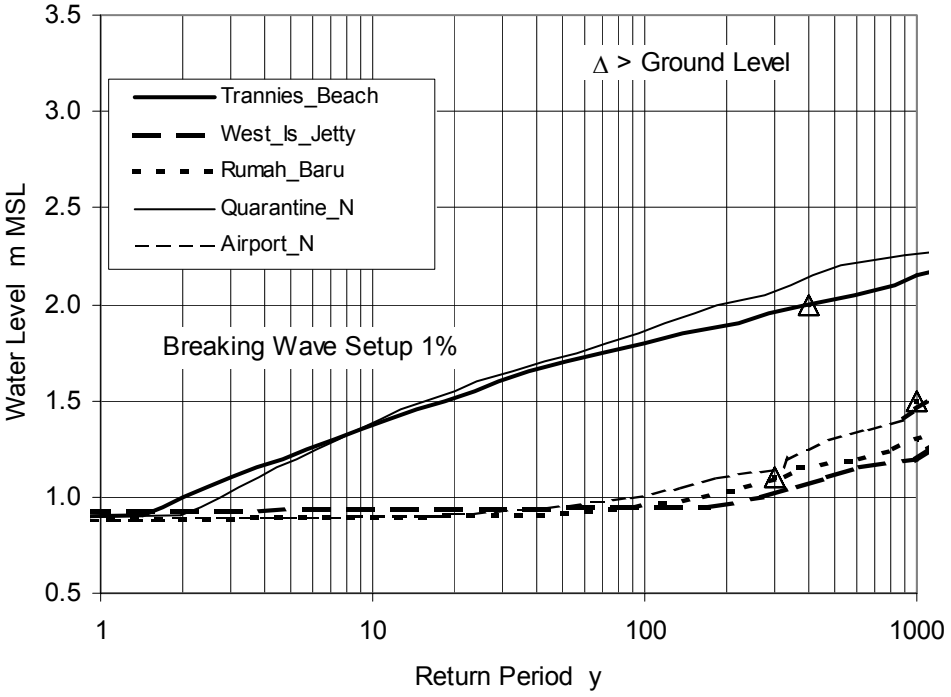

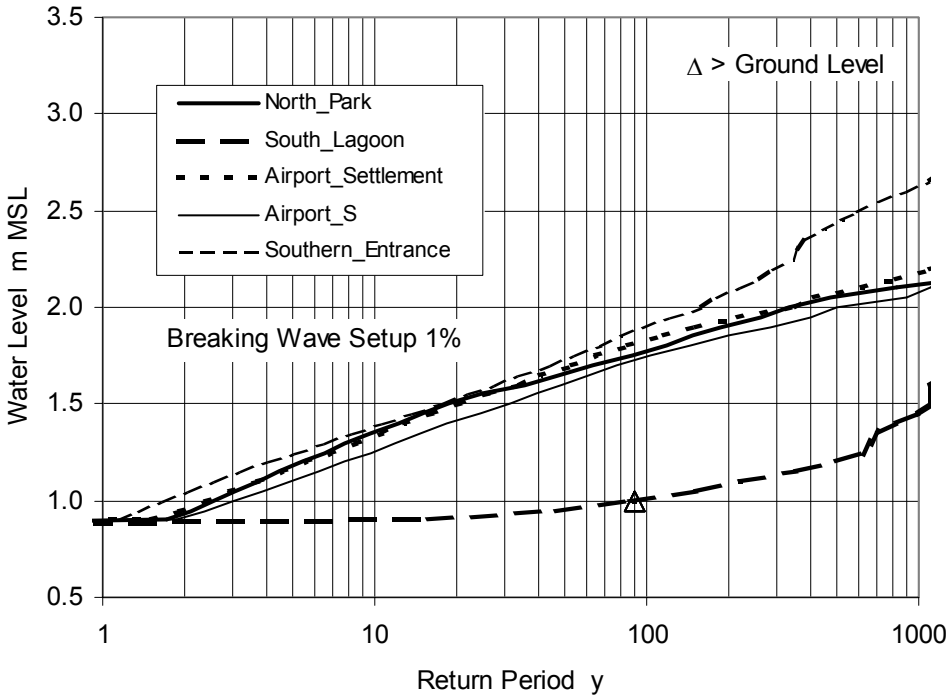

Figure 6.2 Base case storm tide predictions for all sites.

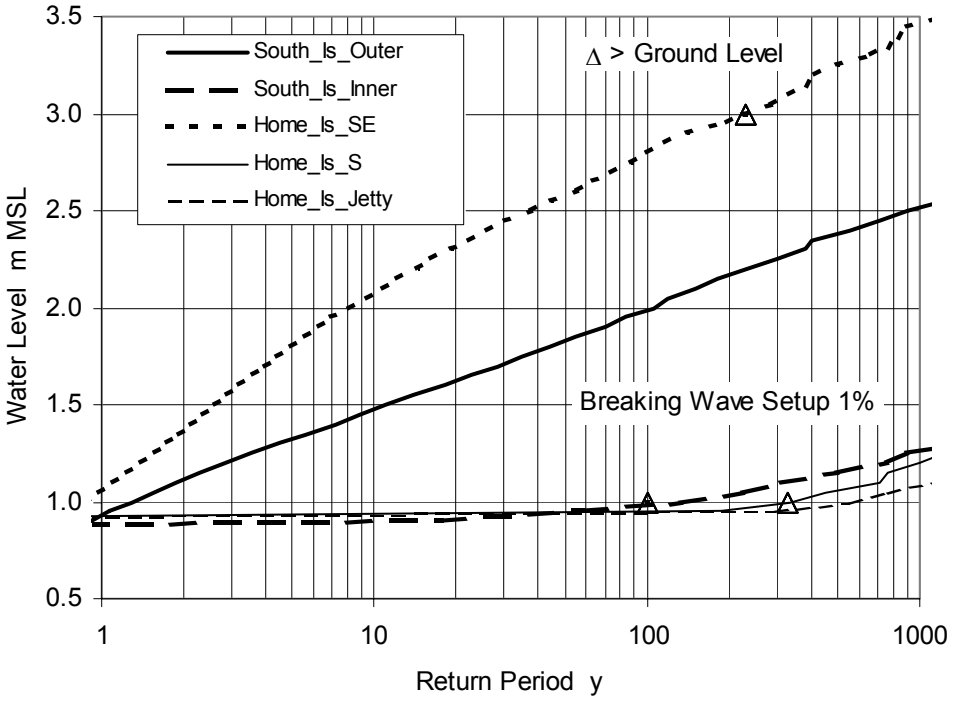

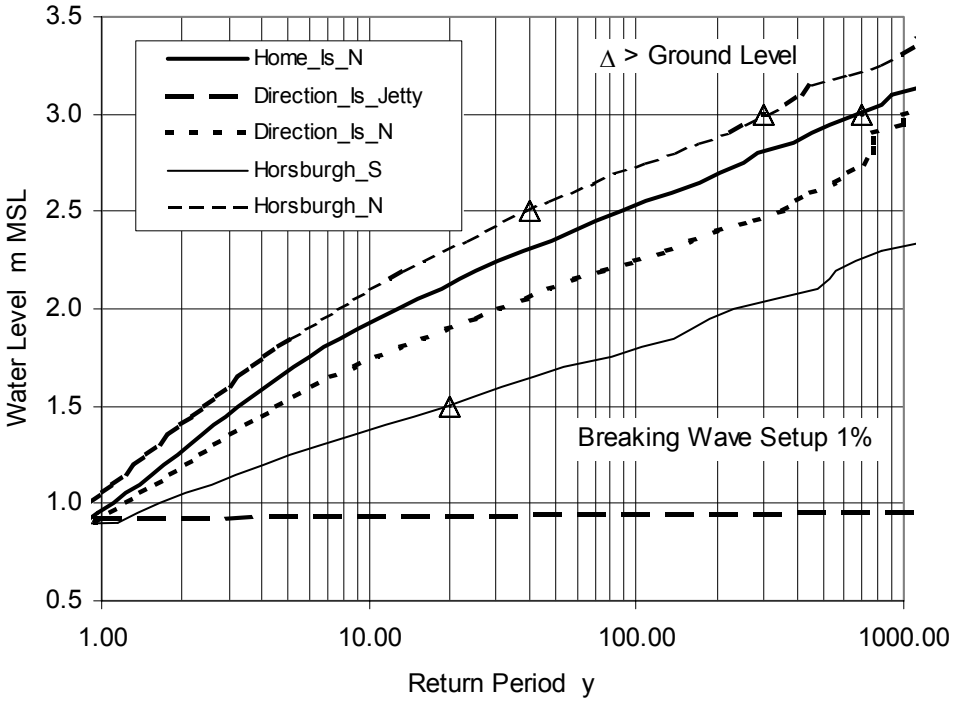

Figure 6.2 (cont) Base case storm tide predictions for all sites.

Table 6.2 Summary of base case 1% storm tide levels.

Site	Name	Typical Local Groundlevel	1% Storm Tide Level at Indicated Return Period				
			10	50	100	500	1000
		m MSL	m	m	m	m	m
	Whole Atoll		2.22	2.69	2.88	3.31	3.52
1	Trannies_Beach	2.0	1.37	1.69	1.80	2.03	2.15
2	West_Is_Jetty	1.5	0.79	0.89	0.90	1.11	1.20
3	Rumah_Baru	1.1	0.89	0.91	0.95	1.18	1.30
4	Quarantine_N	3.2	1.38	1.73	1.86	2.19	2.26
5	Airport_N	2.5*	0.89	0.96	1.01	1.31	1.45
6	North_Park	3.5	1.36	1.66	1.77	2.05	2.11
7	South_Lagoon	1.0	0.89	0.95	1.01	1.20	1.45
8	Airport_Settlement	4.0	1.33	1.69	1.82	2.07	2.18
9	Airport_S	2.8	1.26	1.61	1.74	2.00	2.07
10	Southern_Entrance	0.3	1.39	1.73	1.91	2.43	2.62
11	South_Is_Outer	0.6	1.48	1.83	1.99	2.38	2.51
12	South_Is_Inner	1.0	0.89	0.94	0.98	1.15	1.26
13	Home_Is_SE	3.0	2.07	2.57	2.80	3.25	3.46
14	Home_Is_S	1.0	0.79	0.89	0.90	1.06	1.20
15	Home_Is_Jetty	1.5	0.89	0.89	0.89	0.99	1.08
16	Home_Is_N	3.0	1.93	2.36	2.53	2.93	3.11
17	Direction_Is_Jetty	1.5	0.89	0.89	0.89	0.91	0.94
18	Direction_Is_N	3.0	1.73	2.11	2.25	2.62	3.00
19	Horsburgh_S	1.5	1.37	1.68	1.79	2.12	2.32
20	Horsburgh_N	2.5	2.09	2.56	2.73	3.16	3.30

*near powerhouse and cyclone shelter
NB: Greyed cells indicate storm tide above ground level.

6.2.1 Base Case Mean and Standard Deviation Setup Components

The preceding results are for the *1%* reef setup level, which is an unsteady water level estimated to occur for only 1% of the time. The whole of atoll model results for the *mean* and *mean plus one standard deviation* are shown in Figure 6.6.

It can be seen that there is a large variation in the predicted total water level depending on the choice of reef setup component. The mean water level at the 1000 year return period is only 1.7 m MSL, while the mean plus standard deviation is 2.4 m. This compares with the *1%* estimate of 3.5 m MSL. The choice of appropriate parameter would be dependent on the type of facilities at risk and the extent to which they might withstand inundation and/or erosion.

The assumption in the wave setup calculation (refer Appendix F) is that the unsteady nature of the resulting water level is essentially normally distributed. Clearly, for the *mean* case, this is the average water level predicted due to wave setup and from time to time the level will be above and below this level. For the *mean plus standard deviation* case, 84% of the time the water level will be less than this value and 16% of the time higher. To assist in selection of the appropriate component to consider, the next section presents estimates of water level persistence at the *1%* level.

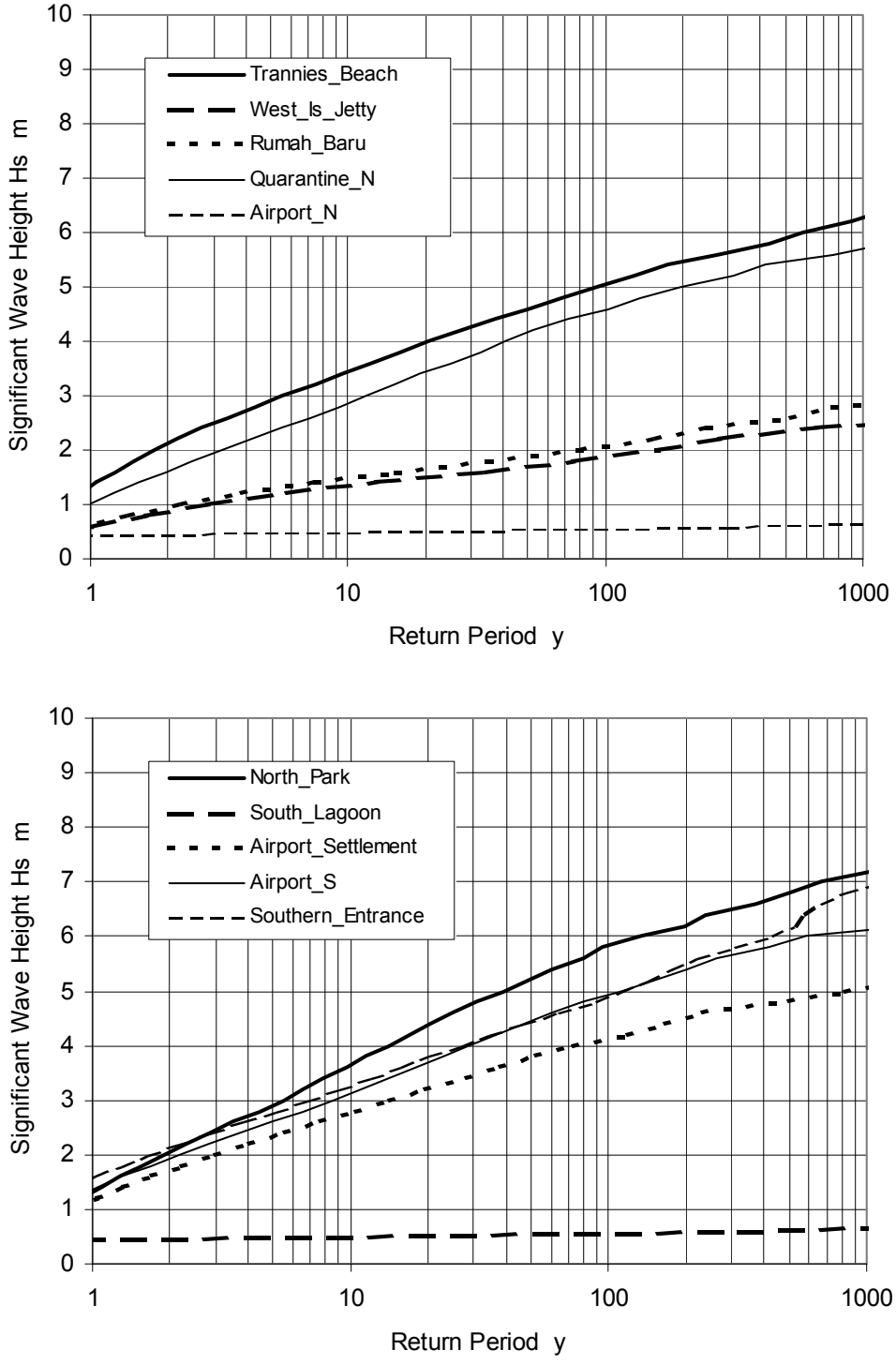

Figure 6.3 Base case significant wave height predictions for all sites.

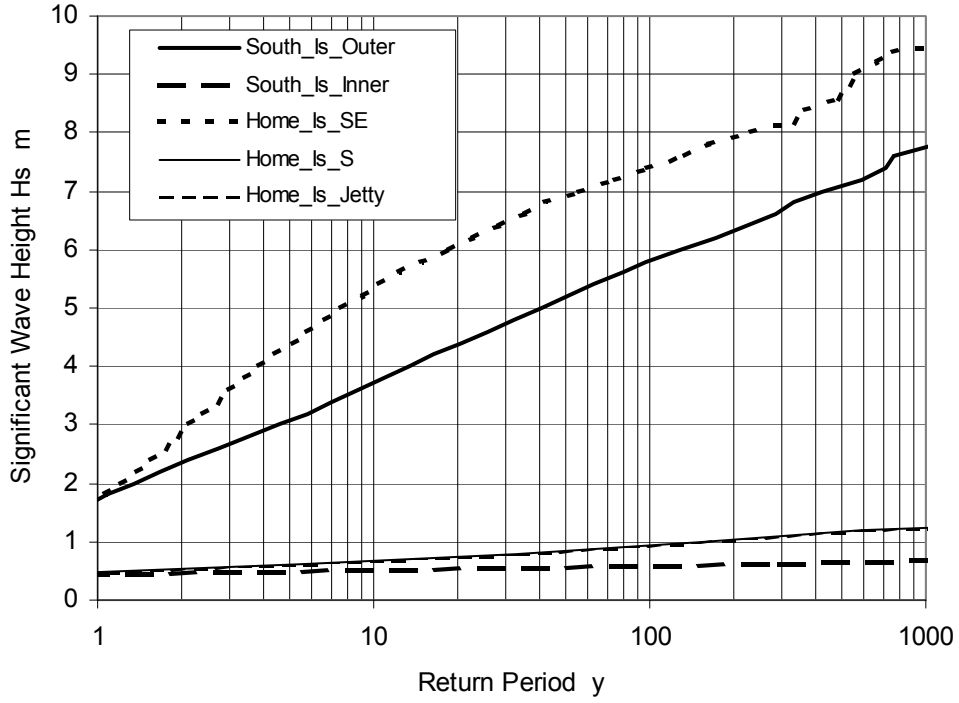

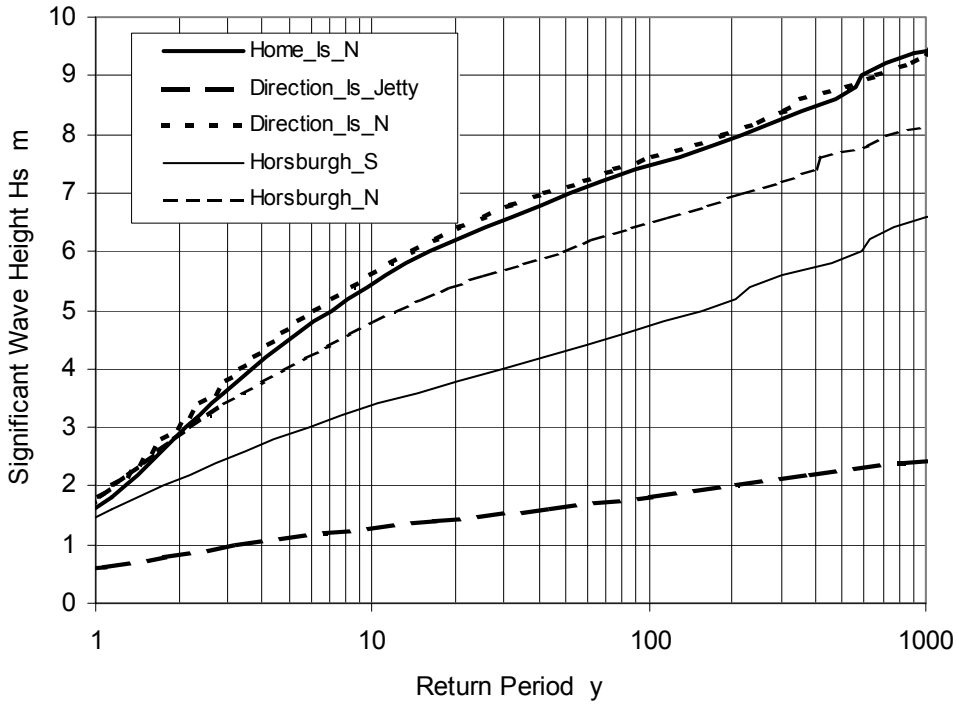

Figure 6.3 (cont) Base case significant wave height predictions for all sites.

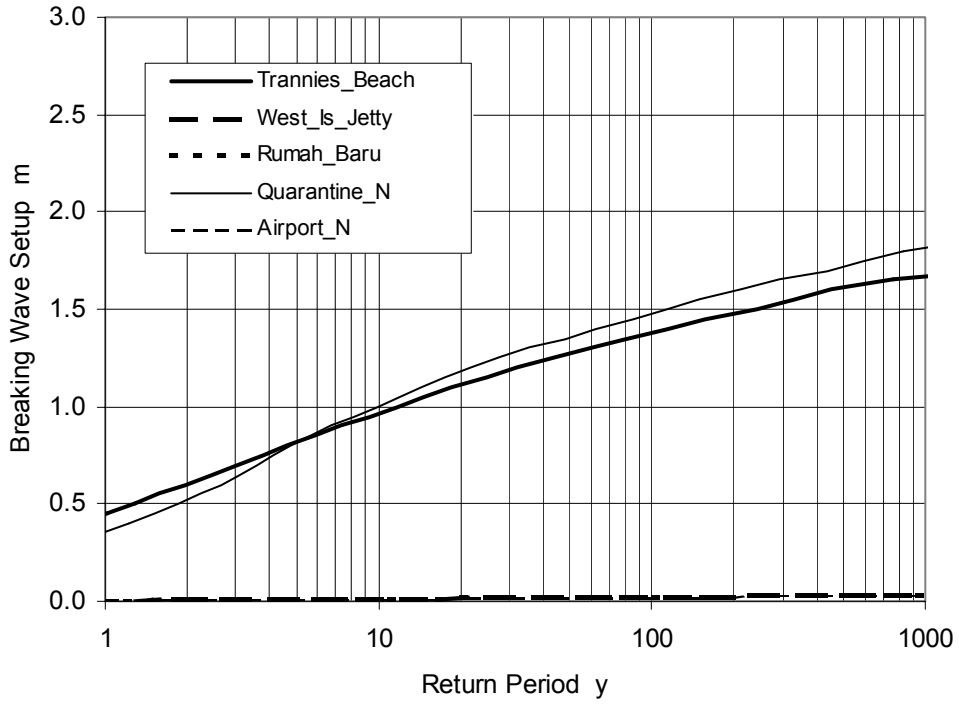

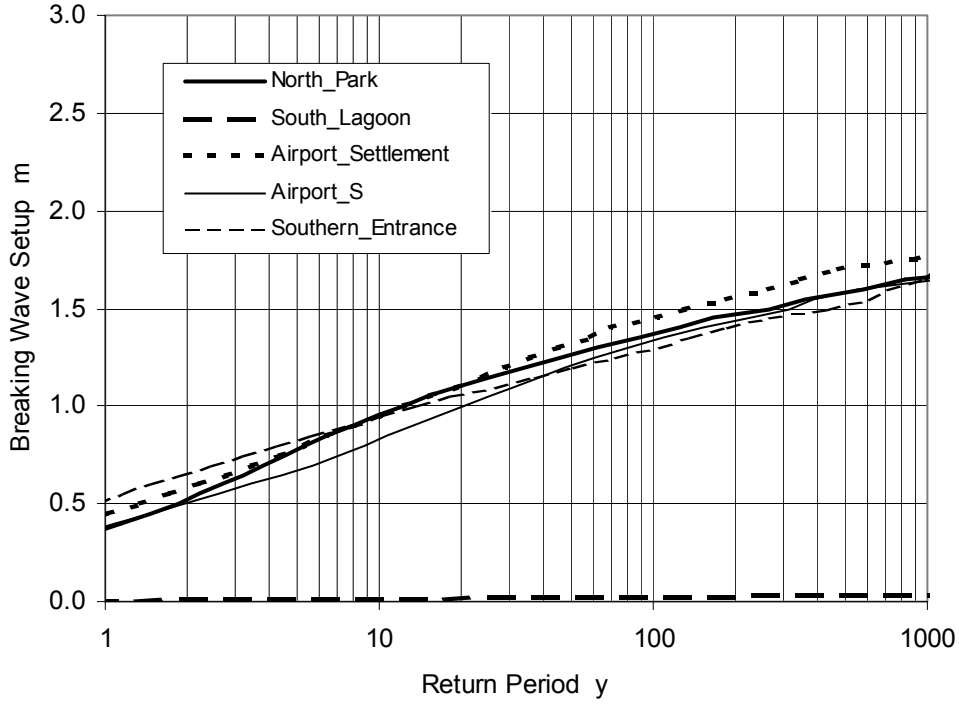

Figure 6.4 Base case breaking wave setup predictions for all sites.

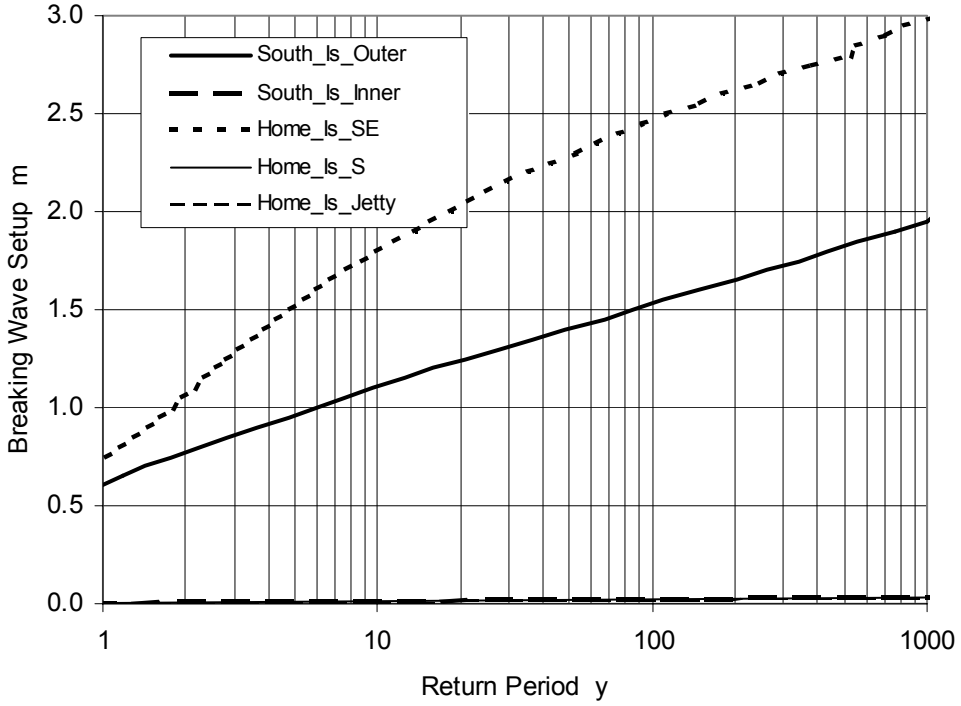

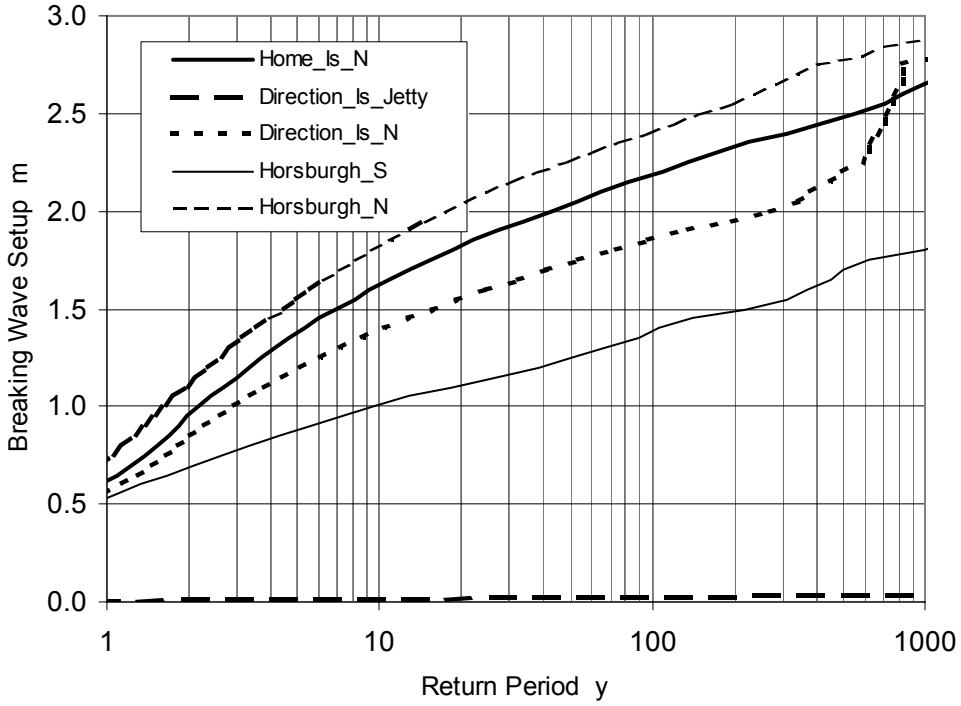

Figure 6.4 (cont) Base case breaking wave setup predictions for all sites.

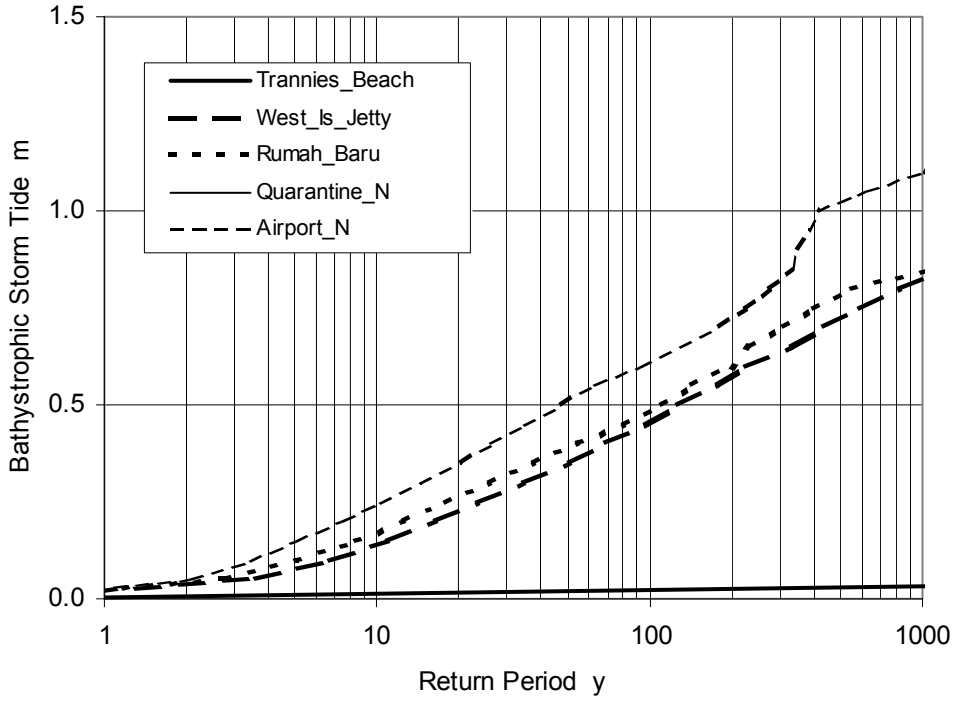

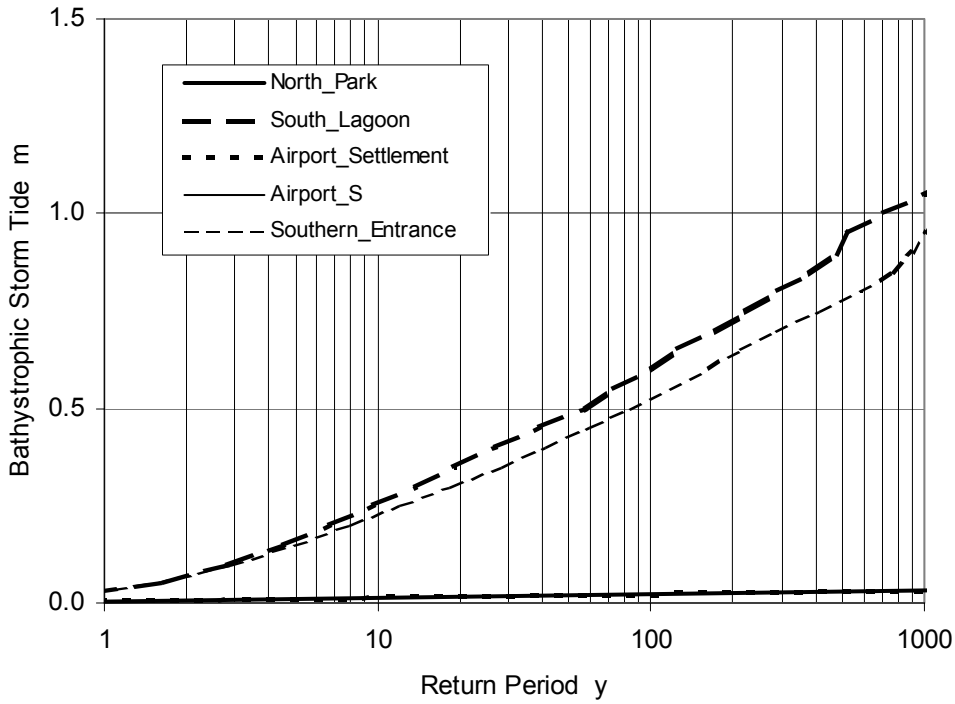

Figure 6.5 Base case bathystrophic storm tide predictions for all sites.

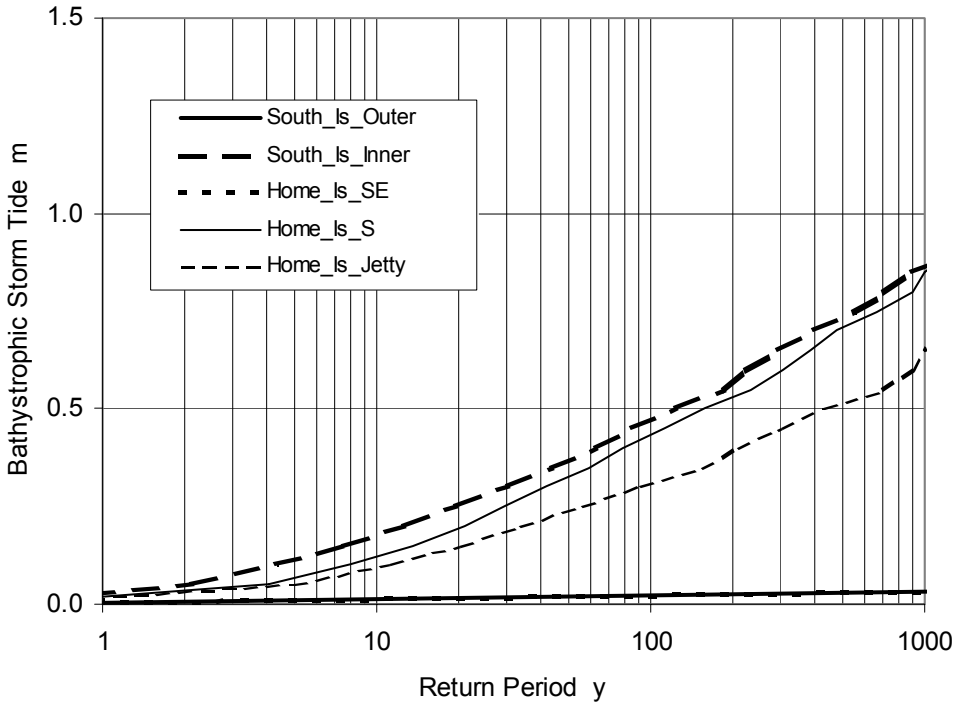

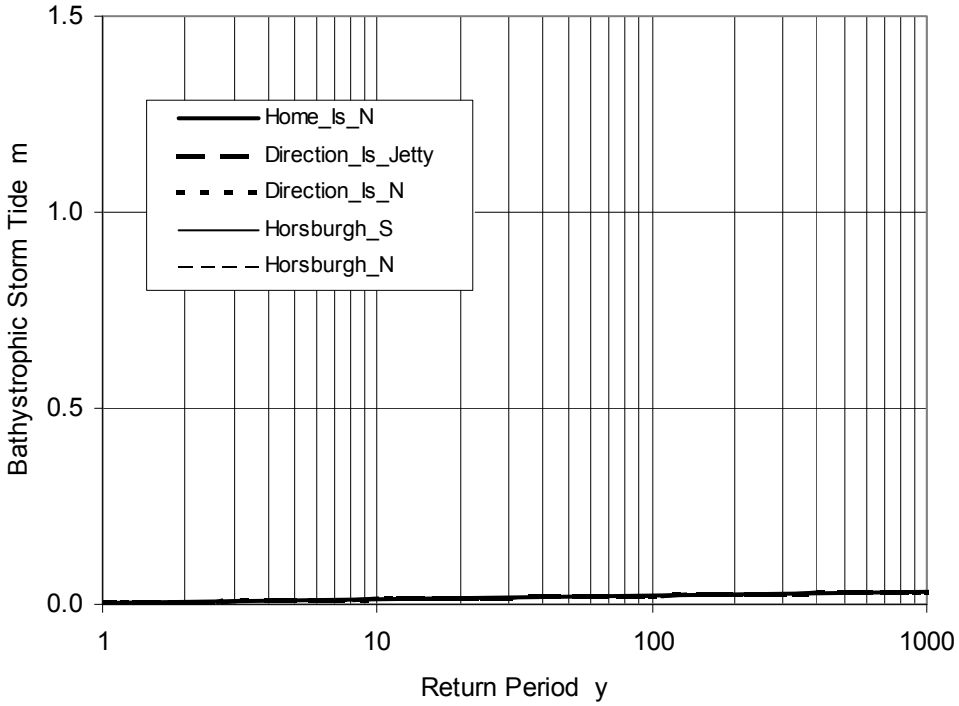

Figure 6.5 (cont) Base case bathystrophic storm tide predictions for all sites.

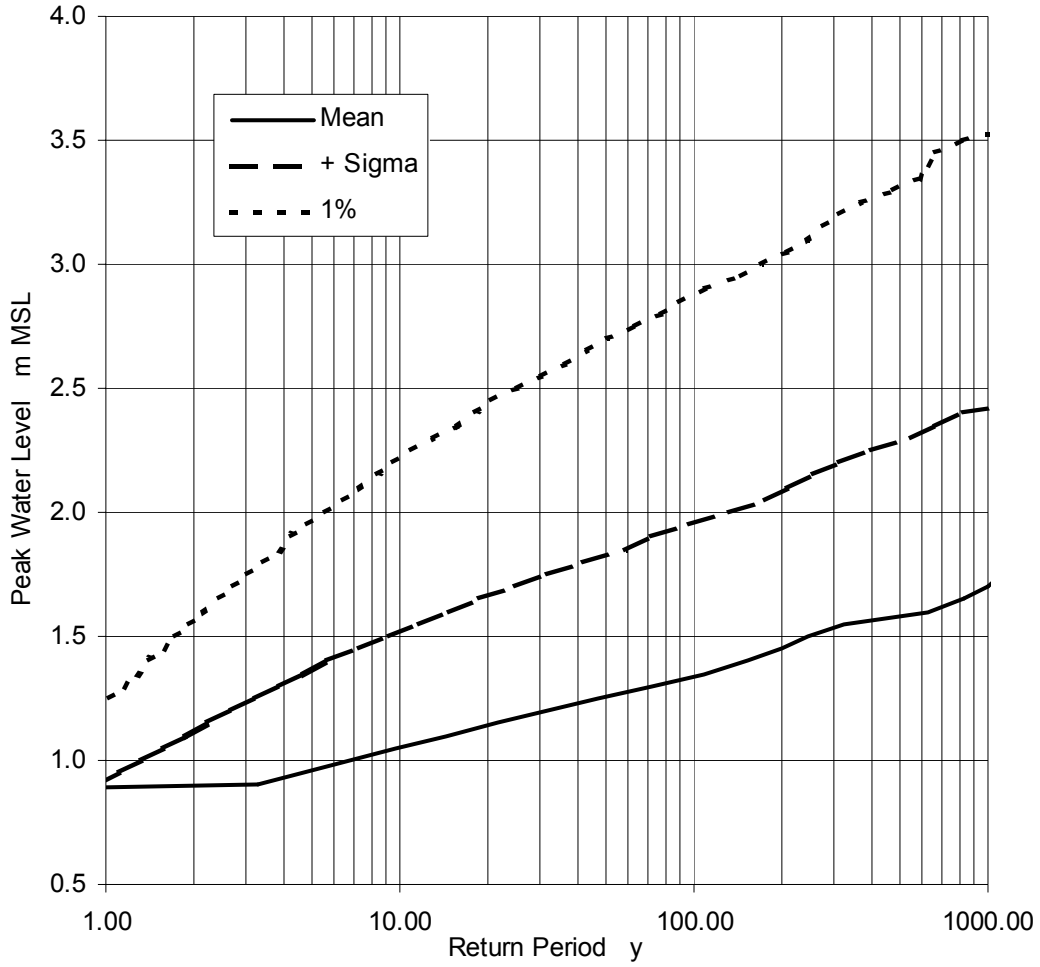

Figure 6.6 Base case storm tide levels depending on the adopted reef setup value.

6.2.2 Persistence of the Base Case 1% Water Level

The model is capable of providing guidance not just on the total water level attained but also the persistence of the water level T_η (i.e. the time for which the water level is exceeded). Figure 6.7 presents this information for the whole-of-atoll case in terms of the persistence, measured in hours, versus both the return period and the water level itself. Each graph displays a series of curves, each of which represents a cumulative level of exceedance of the persistence in steps of 10%. For example, the 50% curve describes the average persistence of a given return period level when it is equalled or exceeded; the 10% curve shows the persistence which is exceeded only on 10% of the occasions when the return period level is equalled or exceeded. This illustrates how the persistence may vary depending on the temporal scale of the event and also the absolute intensity of the event.

Based on Figure 6.7, the 50% persistence at the 1000 year return period level (3.5 m MSL) is 2.6 h and the 10% persistence is 4.4 h. These values must then be nominally reduced further by the 1% wave setup assumption; i.e. water levels would be expected to reach these levels only for 1.56 min and 2.1 min respectively. This indicates a low likelihood of damage at this level.

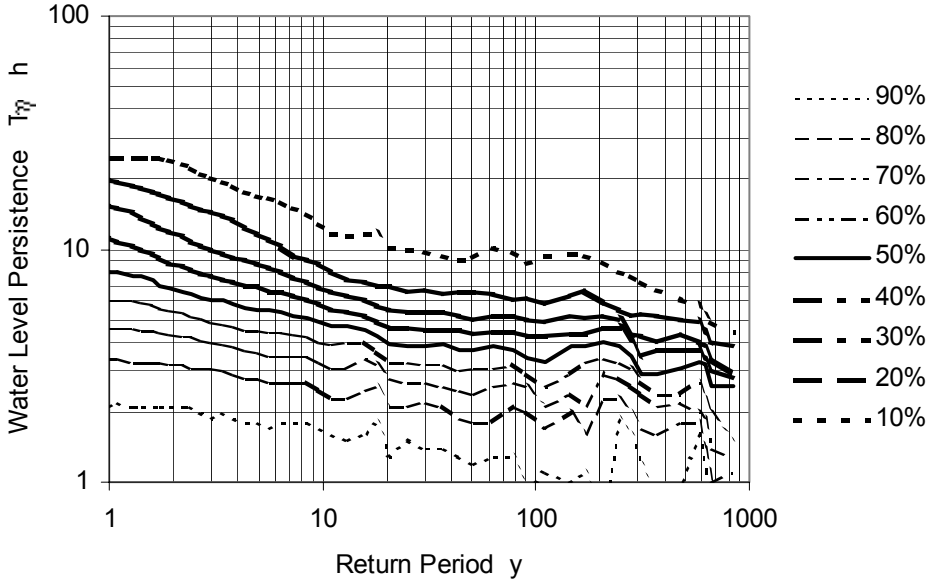

(a) as a function of return period.

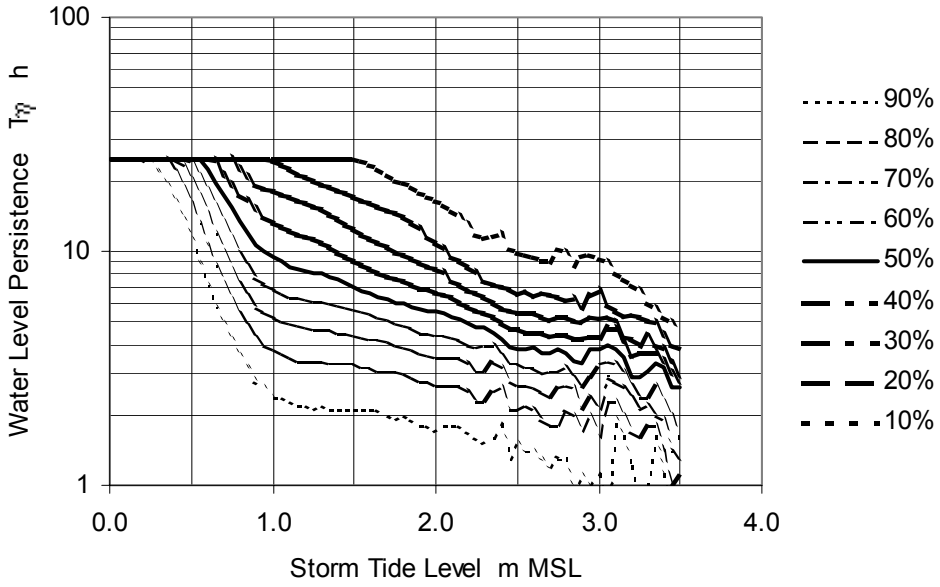

(b) as a function of water level.

Figure 6.7 Persistence of the 1% storm tide level.

6.2.3 Maximum Modelled Base Case 1% Water Level

The simulation is run for a nominal period of 10,000 years of sampled climatology and presentation of the results has been limited to the 1000 year return period only to obtain a finite sample size for averaging purposes. However, the largest single water level modelled for the whole-of-atoll case is **4.95 m MSL**.

6.2.4 Sensitivity Tests of Reef Parameters

A selection of sensitivity tests has been undertaken to determine the likely variability in the water level estimates as a function of:

1. The assumed reef top elevation z_r, and
2. The assumed reef face breaking wave parameter K_p.

These two parameters were chosen as being the most likely sources of error in the analysis of the fringing reef characteristics. In Section 5, the variability in the reef top elevation was determined to represent a standard deviation of 0.1 m, while K_p has a limiting value of about 0.8, compared with the typical value determined for Cocos of 0.5 based on the available (limited) data. Taking the base case as "test a" these limits were then tested, as follows:

Test Case	z_r	K_p
a	base case	base case
b	+ 0.1 m	base case
c	- 0.1 m	base case
d	base case	0.80

These results have been summarised in Figure 6.8 for the whole-of-atoll case and show only a minor sensitivity to the variation in z_r, but a heightened response to K_p which emerges beyond a return period of about 200 years. This is due to the 60% increase in K_p relative to the base case, raising all instances of reef-rim initiated breaking wave setup, which would be the majority of cases.

6.3 Wave Height and Period Sensitivity Test

As presented in Section 5.6, there is some experimental evidence in this study that the SATSIM statistical wave model may be slightly biased towards underpredicting the peak offreef wave conditions at the atoll, at least on the basis of the top 10 storms chosen for detailed comparison. Although this cannot be objectively determined within the statistical context of the model, it remains prudent to consider a nominal safety factor increase of 10% H_s and 5% for T_p (to maintain a constant deepwater steepness). Due to the fact that the reef-top setup is proportional to the square-root of the wave height but directly proportional to the offreef wave period, a nominal increase of about 10.1% could be expected.

The results of this test for the 1% setup base case are shown in Figure 6.9, showing the prescribed 10% increase in predicted H_s at the 1000 year return period from around 9.9 m to 10.8 m. The indicated increase in total water level is from around 3.5 m to 4.0 m, or an increase of 14%. The non-linear increase is predicted to be due to the transition from reef-rim to reef-face wave breaking at or near a nominal 10 m offreef significant wave height.

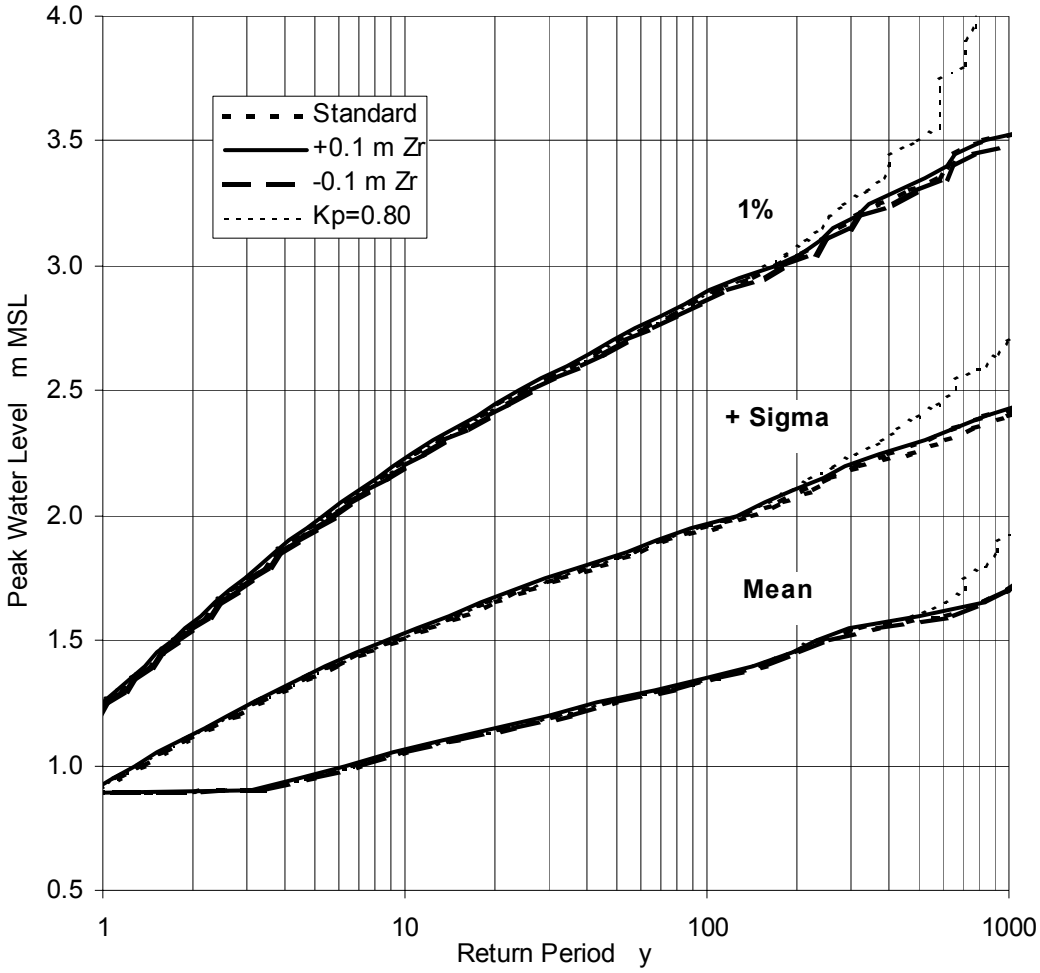

Figure 6.8 Sensitivity to reef parameter assumptions.

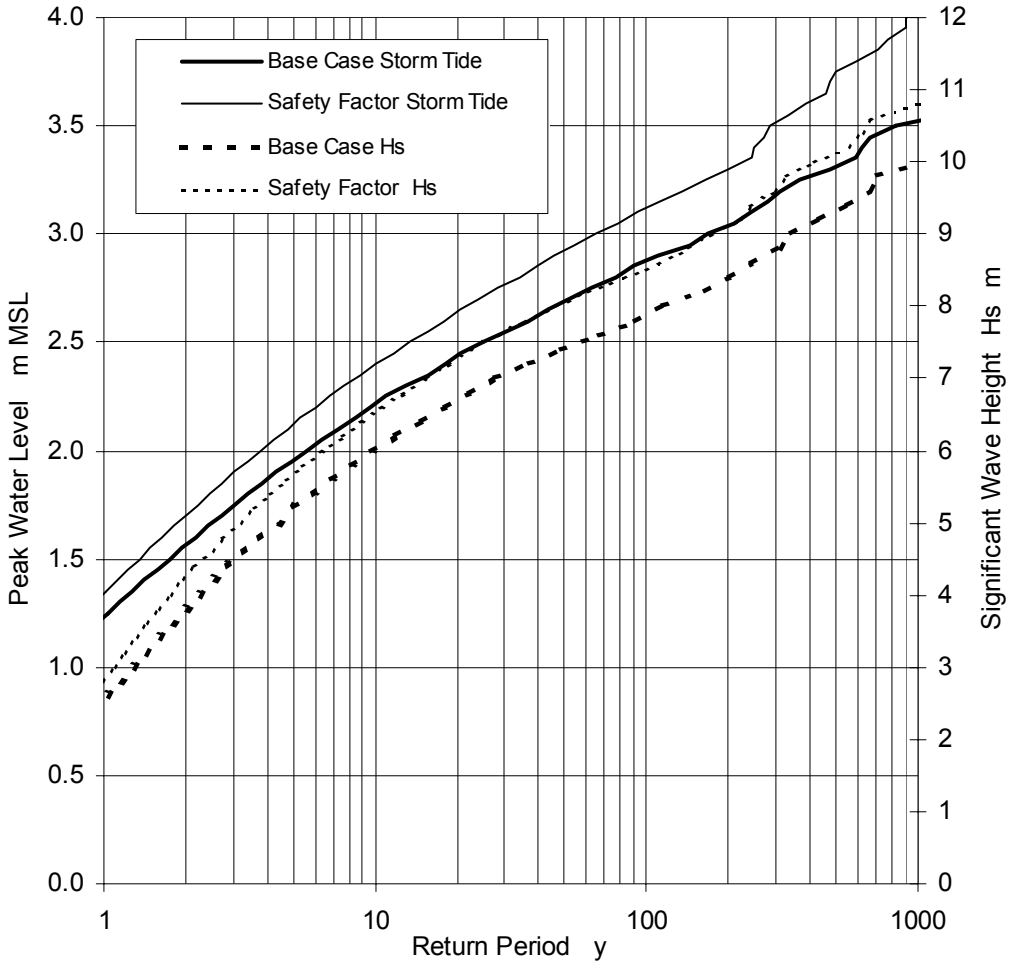

Figure 6.9 Sensitivity to a safety factor of 10% Hs.

6.4 Discussion

Notwithstanding the significant degree of numerical and statistical modelling undertaken in support of the predicted water levels, there is a critical absence of essential data for this region. It has been noted earlier that there is very limited information on reef profiles and reef-top elevations. The present analysis has attempted to locate and use the best available estimates of these parameters within the time available but doubts remain as to the correct reef geometry in many cases. The lack of measured wave data and wave setup elevations in and around the atoll remains as the most critical missing element in terms of model verification. No wave or wave setup validation has been possible and the analysis is completely reliant on past experience of the accuracy of the wave and wave setup modelling approaches in other situations.

In an attempt to overcome the lack of some of the essential data, the methodology has specifically included parameter variability. Accordingly, the results from the modelling provide a range of water level estimates, which are dependent on various assumptions. The most sensitive parameter is the choice of reef-top breaking wave setup component, namely the *mean*, *mean + standard deviation*, or *1%* values as they are presented here following Gourlay (1997). The results are also sensitive to the reef geometry and the uncertainty in the incident wave height and period.

Clearly breaking wave setup is a statistical parameter and it remains to choose a value that is relevant to the application. From the assessment of persistence given earlier, the *1%* level is very much an upper limit to the expected encroachment of saltwater. This component is the least reliable of the three provided (Gourlay, *pers. comm.*) and is based on limited observations by Seelig (1982) at one particular reef. The *1%* assumptions also require that wave grouping is an active contributor to the process, but this phenomenon itself is less likely to be present in the very young and confused sea conditions generated by the close approach of a tropical cyclone. Accordingly, the *1%* level is regarded as relatively conservative in terms of a threat to life and/or property, whereas by comparison, the *mean* level is an elevation that will definitely be exceeded. This leaves a region of uncertainty as to the exact impact of the elevated levels and it is suggested that design criteria be adopted on a case-by-case basis.

It should be noted also that the present study does not consider the possible additional impact of very localised beach wave runup of (generally small) reformed waves over the reef lagoon. While this effect is likely to be small, it will contribute to the occurrence of saltwater at elevated levels. In addition, the possibility of wave resonance has not been considered, which is a potentially very site-specific phenomenon requiring reasonably detailed data and analysis. On the other hand, there may also be significant ground absorption of saltwater into the sandy substrate. These issues should be considered on a case-by-case basis. Based on experience (Gourlay, *pers. comm.*), the *1%* breaking wave setup level is regarded as a reasonable engineering estimate of the sum total of these many unknown influences.

Finally, the values presented in this study have no allowance for possible Greenhouse-induced long-term sea level rise. The latest IPCC scenarios should be consulted in this regard (e.g. IPCC 1996).

7 Conclusions and Recommendations

The study has considered a wide range of potential extreme water level impacts caused by tropical cyclones at the Cocos (South Keeling) Island atoll. A number of complex numerical hydrodynamic models have been constructed as an aid to understanding the relative impacts of potential abnormal water level components, i.e.

- pressure deficit or Inverted Barometer Effect;
- locally generated wind stress effects in the lagoon (Bathystrophic Storm Tide);
- non-linear tide interactions;
- breaking wave setup on fringing reefs.

Secondly, the statistical nature of extreme water level forcing by tropical cyclones has been explored by developing an analytical description of the regional climatology. This considers the probability of exceeding a given instensity, the maximum possible intensity for the region, preferred tracks and directions, forward speed and horizontal scale parameters.

The accuracy of the surface wind and pressure field model which drives the hydrodynamic models has been demonstrated by comparisons with measurements from the "top 10" storms affecting the atoll over the past 30 years. The accuracy of the climatological description has also been verified by comparing long-term model predictions of wind speed with long-term measured wind data (50 years) from the airport weather station.

The results from the numerical hydrodynamic and spectral wave models have been converted into simpler parametric model formulations in order to allow a Monte Carlo statistical simulation of the potential long-term water level climate. The model then simultaneously generated synthetic time histories of:

1. Astronomical tide;
2. Inverted Barometer Effect;
3. Bathystrophic Storm Tide, and
4. Breaking wave setup on reefs

at each of the nominated 20 atoll sites for a period of 10,000 years of assumed climate. These separate water level contributions were added to provide an estimate of the total storm tide level and the statistics of exceedance of that water level were assessed, leading to the estimation of a range of average recurrence (ARI) or return periods of extreme water levels. The sensitivity of the model assumptions to a range of parameters has also been examined.

Wherever possible, recorded data has been used to verify the operation of the various models. However, there is no measured wave data available for comparison and water level verification is limited to the location of the tide gauge on Home Island. Information in regard to reef top levels, widths and slopes is also relatively sparse and remains an area of some uncertainty. Notwithstanding this, the model predictions appear to be consistent with anecdotal experiences of extreme water level episodes on the atoll (C. Jones, *pers. comm.*).

It is recommended that (a) extreme water level predictions be considered with respect to the type of infrastructure requiring protection and that the possible persistence of water levels and the specific reef setup component (*mean*, + *one standard deviation*, *1%*) be considered when establishing design water levels and (b) a long-term measurement programme of waves, reef-top water levels and currents be undertaken to supply essential verification data for any future studies.

8 References

ASO (1987) Cocos Keeling Islands aerial photographs. SOC760 Colour 1:10000 5 April 1987 Runs 1 & 2; CAI/C4003 Colour 1:14000 24-28 August 1987 Runs 2 to 6.

Benjamin J.R. and Cornell C.A. (1970) Probability, statistics and decision for Civil Engineers. *McGraw-Hill.*

BPA (1985) Storm tide statistics - methodology, Prep. for the *Beach Protection Authority of Queensland*, Blain Bremner and Williams Pty Ltd, January, 120 pp.

Colin, P.L. (1977) The reefs of Cocos-Keeling Atoll, Eastern Indian Ocean. Proc. 3rd Int. Coral Reef Symp. *Univ Miami*, Miami, FA, May, 63-68.

DHC (1986) Feasibility study of coastal engineering problems at West Island, Cocos Islands. *Dept Housing and Construction*, Coastal Engin. Branch, Rep No CE86/2, Feb.

Falkland A (1994) Climate, hydrology and water resources of the Cocos (Keeling) Islands. *Atoll Research Bulletin*, No. 400, Feb.

GHD (2000a) Cocos (Keeling) Islands report on seawall upgrade design concept. Prep for Dept. Transport and Regional Services by Gutteridge Haskins and Davey Pty Ltd, Perth Office, Jan.

GHD (2000b) Gridded depth datset 80 m resolution to AGD84.

GHD (2000c) Outfall crossection survey undertaken by CSIRO.

Gourlay, M.R. (1997) Wave setup on coral reefs: some practical applications. Proc. 13th Aust Conf Coastal and Ocean Engin., *Centre for Advanced Engineering*, Christchurch, Sept, 959-964.

Harper B A, Sobey R J and Stark K P, (1977) Numerical simulation of tropical cyclone storm surge along the Queensland coast - Parts I to X. Department of Civil and Systems Engineering, *James Cook University*, November, 90 pp ea.

Harper B.A., Lovell K.F., Chandler B.D. and Todd D.J. (1989) The derivation of environmental design criteria for Goodwyn 'A' platform. Proc 9th Aust Conf Coastal and Ocean Engin, *IEAust*, Dec.

Harper B.A., Mason L.B. and Bode L. (1993) Tropical cyclone Orson - a severe test for modelling. Proc 11th Australian Conference on Coastal and Ocean Engin, *IEAust*, Townsville, Aug, 59-64.

Harper B.A. and Holland G.J. (1999) An updated parametric model of the tropical cyclone. Proc. 23rd Conf. Hurricanes and Tropical Meteorology, *American Meteorological Society*, Dallas, Texas, 10-15 Jan.

Harper B.A. (1999) Numerical modelling of extreme tropical cyclone winds. APSWE Special Edition, *J. Wind Engineering and Industrial Aerodynamics*, 83, 35 - 47.

Holland G.J. (1981) On the quality of the Australian tropical cyclone data base. *Aust Met Mag*, Vol.29, No.4, Dec, 169-181.

Holland G.J. (1997). The maximum potential intensity of tropical cyclones. *J. Atmos. Sci*., 54, Nov, 2519-2541.

IPCC (1996) Climate change 1995 - impacts, adaptations and mitigation of climate change: scientific-technical analyses. Contribution of Working Group II to the Second Assessment Report of the Intergovernmental Panel on Climate Change, *Cambridge University Press*, 879pp.

Kench P.S. (1994) Hydrodynamic observations of the Cocos (Keeling) Islands lagoon. *Atoll Research Bulletin*, 408, Chap 10.,Washington, Feb.

Kench P. (1998a) Physical controls on development of lagoon sand deposits and lagoon infilling in an Indian Ocean atoll. *J. Coastal Research*, Vol. 14, No. 3, 1014-1024.

Kench P.S. (1998b) Physical processes in an Indian Ocean atoll. *Coral Reefs*, 17, 155-168.

Kench P.S. (2000) Personal communication, University of Waikato.

Petrauskas C. and Aagaard P.M. (1971) Extrapolation of historical storm data for estimating design-wave heights. *Soc. Petroleum Engineers Jnl*., March, 23-37.

RAN (1983) Cocos (Keeling) Islands - fair charts from hydrographic survey by HMAS Moresby, Jun-Jul 1983. *RAN Hydrographic Service*, HI-75 21-2-22, Aug.

Ryan P.L. (1968) Cyclone over Cocos. Australian External Territories, Vol. 8, 24-28.

Searle D. (1994) Late quaternary morphology of the Cocos (Keeling) Islands. *Atoll Research Bulletin*, No. 401, Feb.

Seelig W.N. (1982) Wave induced design conditions for reef/lagoon system hydraulics. *US Army Corps of Engineers* (unpublished), Pacific Ocean Division.

Sobey R.J., Harper B.A. and Stark K.P. (1977) Numerical simulation of tropical cyclone storm surge. Department of Civil and Systems Engineering, Research Bulletin No. CS14, *James Cook University*, May, 300 pp.

Sobey R.J. and Harper B.A. (1977) Tropical cyclone surge penetration across the Great Barrier Reef. Proc. 3rd Aust Conf Coastal and Ocean Eng, *IEAust*, Melbourne, 58-63.

US Navy (1994) Global tropical / extratropical cyclone climatic atlas. *US Navy*, V1.0, CD media, March.

Smithers S.G. and Woodroffe C.D. (2000) Microatolls as sea-level indicators on a mid-ocean atoll. *Marine Geology*, 168, 61-78.

Woodroffe C.D. and Falkland A.C (1997) Geology and hydrogeology of the Cocos (Keeling) Islands. In Vacher, H.L. and Quinn, T. (eds) Geology and Hydrogeology of Carbonate Islands. Developments in Sedimentology, 54, *Elsevier*, Amsterdam.

Woodroffe C.D. and McLean R.F. (1994) Reef islands of the Cocos (Keeling) Islands. *Atoll Research Bulletin*, 403, Feb.

Woodroffe C.D., McLean R.F. and Wallensky E. (1994) Geomorphology of the Cocos (Keeling) Islands. *Atoll Research Bulletin*., No. 402, Feb.

Woodroffe C.D., McLean R., Polach H. and Wallensky E. (1990) Sea level and coral atolls: Late Holocene emergence in the Indian Ocean. *Geology*, Vol. 18, 62-66.

Woodroffe C.D., McLean R.F, Smithers S.G. and Lawson E. M. (1999) Atoll reef-island formation and response to sea-level change; West Island, Cocos (Keeling) Islands. *Marine Geology*, Vol. 160, 85-104.

Woodroffe C.D., Veeh M.H., Falkland H.H., McLean R.F. and Wallensky E. (1991) Last interglacial reef and subsidence of the Cocos (Keeling) Islands, Indian Ocean. *Marine Geology*, 96, 137-143.

Young I.R. and Sobey R.J. (1986) Hurricane wind waves - a discrete spectral model. *J. Waterway, Port, Coastal and Ocean Engineering*, ASCE, Vol. 112, No. 3, 370-389.

Young I.R. (1987a) A general purpose spectral wave prediction model. Res Rep No 16, Univ College, *Australian Defence Force Academy*, Canberra, Jan.

Young I.R. (1987b) Validation of the spectral wave model ADFA1. Res Rep No 17, Univ College, *Australian Defence Force Academy*, Canberra, Jan.

APPENDIX A

SCOPE OF WORK

COCOS (KEELING) ISLANDS

METEOROLOGICAL AND OCEANOGRAPHIC RISK ASSESSMENT

General

Following a review of previous investigations of storm surge levels at Cocos (Keeling) Islands it was concluded that:

- There have been considerable advances in technology in relation to computer modelling of storm surge and wave effects;
- A new cyclone surge and wave setup study should be undertaken for Cocos (Keeling) Islands using contemporary methods; and
- The primary focus of the new study should be the extreme water levels created by storm surge or wave setup and resultant inundation of, or flow across landforms at Cocos (Keeling) Islands.

A number of earlier studies have investigated the issue of cyclone related storm surge, notably in 1976, 1986 and 1995. These studies were carried out by or in conjunction with the Australian Construction Services, Maritime Works Branch.

The 1976 Cyclone Storm Surge Study was based on cyclone parameters used for Darwin storm surge computations. The 1986 study re-examined the design cyclone parameters based on cyclones occurring in the vicinity of Cocos (Keeling) Islands between 1951 and 1984.

In 1995 a review of earlier storm surge calculations was undertaken. This review added a further allowance for wave crest height and under floor clearances to set minimum floor levels for community refuge shelters. This showed that the floor levels of both the Home Island and West Island Cyclone Shelters were above the minimum floor levels.

It is believed prudent for a new study of storm surge levels at Cocos (Keeling) Islands using updated numerical modelling techniques to be carried out. This shall include the assessment of storm surge levels in the lagoon (dominated by effects of reduced atmospheric pressure, tide, and wind) as well as an assessment of the effects of wave setup on the external near-horizontal reef flats, (dominated by breaking wave effects which can lead to maximum waterlevels at the shore associated with ocean waterlevels near mean sea level), is also required. This would improve knowledge in relation to the risk of inundation of Cocos (Keeling) Islands and its infrastructure.

Select tenders are being sought from the following four (4) consultant organisations:

1. Bureau of Meteorology
2. Global Environmental Modelling Solutions (GEMS)
3. WNI Science and Engineering

4. Systems Engineering Australia (SEA)

Scope of Works

The following tasks will be performed:

1. Analysis of tropical cyclone climatology;
2. Modelling of storm surge, cyclone wave conditions and inundation levels resulting from cyclone wind and barometric pressure fields, as well as wave setup on external reef flats ;
3. Determination of return periods for combined storm surge - tide still water levels using probability analysis;
4. Determination of return periods for wave setup levels on external reef flats using probability analysis;
5. Assessment of inundation levels at a number of locations on Home Island and West Island, including cyclone refuge shelters, power generation facilities and other nominated sites as shown on Figure1; and
6. Assessment of meteorological and oceanographic risk for the above key sites, including 10, 50, 100, 500 and 1000 year recurrence levels at each location;

Timing

The following timetable is anticipated.

Receive Proposals	5 April, 2000
Appointment of Sub- Consultant	26 April, 2000
Delivery of Draft Report	19 July , 2000
Delivery of Final Report	16 August July, 2000

Reporting Requirements

The Successful Consultant shall provide copies of the report as follows ;

- four (4) bound copies of the draft report including any maps and diagrams are to be supplied for review and comment.
- a presentation of the draft report to a review panel (in Perth) will be required approximately 1 week after submission of the draft (Cost option for presentation via video link from GHD offices)
- agreement to the revised report incorporating review comments shall be obtained prior to production of the final report

Cocos Storm Surge Study 3
\611\850120\00

- fifteen (15) bound copies, one unbound copy for photocopying and one electronic copy of the final report plus any maps and diagrams compatible with Microsoft Office 95 Software. Documents shall be also provided in .RTF format.

- reports and supporting maps and diagrams are to be of a high professional standard .

Tender Submission Requirements

The following information is required to be submitted with the submission.

Storm Surge Modelling.

1. Details of similar modelling tasks carried out by the modeller(s) including details of time of commission, client contact details, scope of modelling work required and model(s) used.
2. Details of model(s) proposed for use in this study and capabilities and limitations of the models.
3. Proposed methodology for carrying out the study including; proposed method of calibration and verification of the model, establishing design cyclones and tracks.

Reef Flat Wave Setup Modelling:

1. Details of similar tasks carried out by the modeller(s) including details of time of commission, client contact details, scope of work required and method(s) used.
2. Details of theoretical basis of model(s) proposed for use in this study and capabilities and limitations of the models.
3. Proposed methodology for carrying out the study including; proposed method of verification of the model, establishing design wave statistics, and establishing overflow rates where this occurs.

Program

Gant chart showing proposed activities of; data assembly, establishment and verification of model(s), operation of models and statistical analysis, reporting and review processes.

Price

1. Lump Sum Price for the study inclusive of all disbursments. The price is to be inclusive of all costs associated with the terms of engagement outlined in the attached GHD sub-consultancy agreement.

2. Breakdown of Lump Sum price including; Data acquisition, Client meeting attendance, Model operation, Reporting, Presentations, and Reimbursibles.

Data available for consultants.

1. The following information will be provided to tenderers during the tender period:

- Earlier studies carried out by or in conjunction with the Australian Construction Services, investigating the issue of cyclone related storm surge, in 1976, 1986 and 1995.

- Cocos (Keeling) Islands, Seawall Upgrade Design Concept., GHD,1999.

These documents must be returned with tender submissions or the submissions will not be considered.

2. The following information will be provided to the successful tenderer for use during the term of the consultancy:.

- Hourly Water Levels 1986 - 1999 recorded by the National Tidal Facility.

- 6 Hourly wave hindcast information produced by the UK Met office July 1993 - April 1999.

Terms of Engagement

The successful consultant will be engaged under a GHD subconsultancy agreement and the terms of engagement between GHD and subconsultant are attached.

Confidentiality

The successful consultant will be required to sign a deed of non-disclosure and privacy. At the end of the project the consultant shall return all copies of data and information supplied specifically for the execution

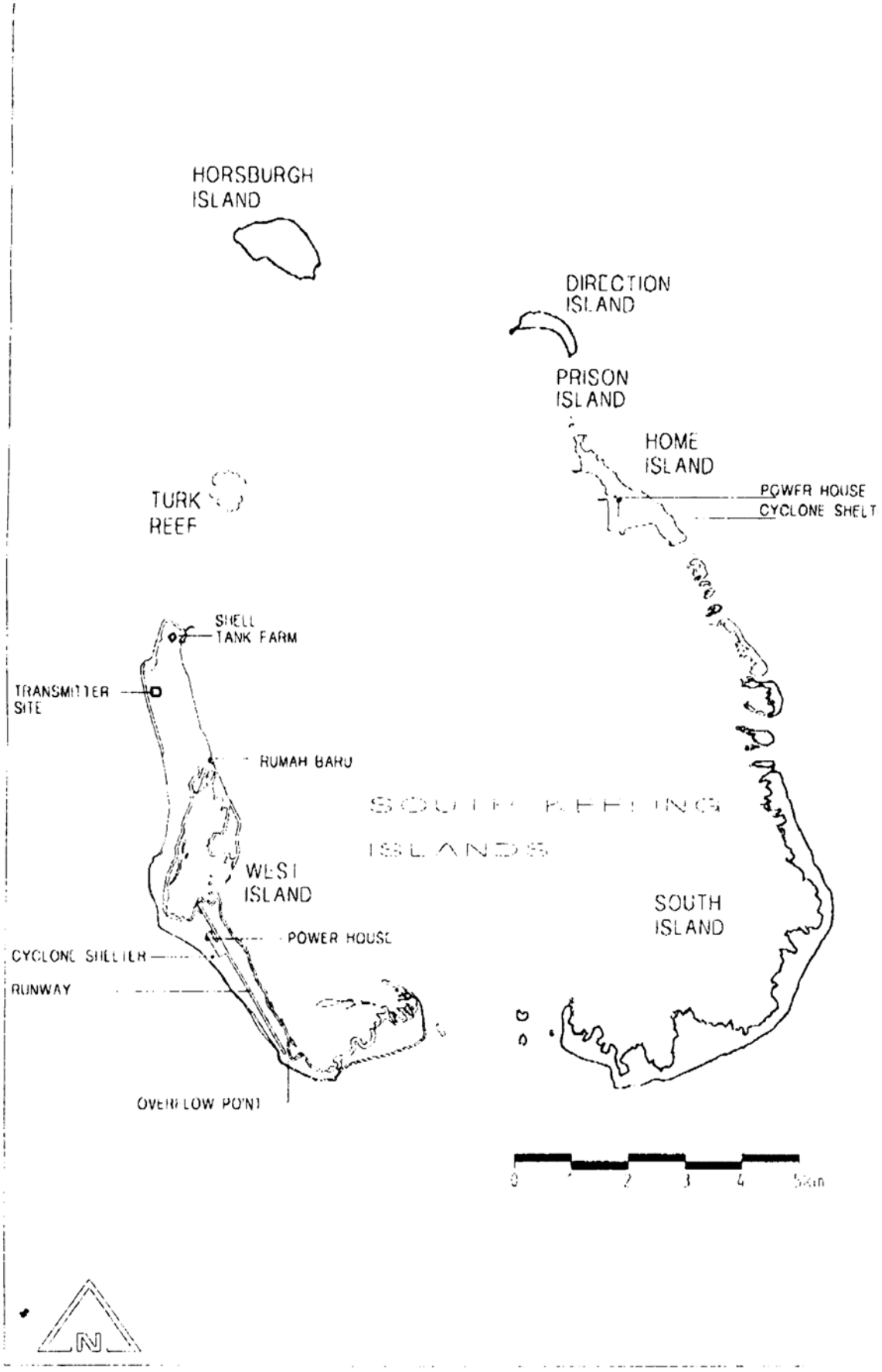

COCOS (KEELING) ISLANDS
STORM SURGE STUDY

FIGURE 1

APPENDIX B

TROPICAL CYCLONE WIND AND PRESSURE FIELD MODEL

Appendix B - Tropical Cyclone Wind and Pressure Model

The following provides an overview of the parametric tropical cyclone wind and pressure model adopted for this study, which is similar to Harper and Holland (1999). Further elaboration is provided here of specific formulations which have been developed over a number of years as a result of extensive wind, wave and current hindcasting, e.g. Harper *et al.* (1989, 1993) and Harper (1999).

B.1 Definitions and Background

A tropical cyclone (hurricane or typhoon) is defined as a non-frontal cyclonically rotating (clockwise in the Southern Hemisphere) low pressure system (below 1000 hPa) of tropical origin, in which 10 minute mean wind speeds at +10 m MSL (V_m) exceed gale force (63 km h^{-1}, 34 kn, or 17.5 ms^{-1}). In view of the complex nature of tropical cyclones and their interaction with surrounding synoptic scale mechanisms, most empirical wind and pressure models (Lovell 1990) represent the surface wind field by considering the storm as a steady axisymmetric vortex which is stationary in a fluid at rest.

The vortex solution is based on the Eulerian equations of motion in a rotating frame of reference (Smith 1968). The analysis begins with a consideration of force balance at the geostrophic, or gradient, wind level above the influence of the planetary boundary layer. The gradient wind speed can be expressed as a function of storm pressure, size, air density and latitude. The gradient wind speed is then reduced to the surface reference level of +10 m MSL (mean sea level) by consideration of gross boundary layer effects, wind inflow (also due to frictional effects) and asymmetric effects due to storm forward motion or surrounding synoptic pressure gradients.

B.2 Radial Pressure Field

A primary assumption of almost all empirical tropical cyclone models is that the radial pressure field at gradient wind speed level can be expressed as:

$$p(r) = p_0 + (p_n - p_0) \exp(-R/r) \qquad \text{(B.1)}$$

where r = radial distance from storm centre
$p(r)$ = pressure at r
p_0 = pressure at the storm centre (central pressure)
p_n = ambient surrounding pressure field
and R = radius to maximum winds

This exponential pressure profile was first proposed by Schloemer (1954). Holland (1980) noted deficiencies in the ability of Eqn B.1 to represent many observed pressure profiles and that the Schloemer base-profiles resembled a family of rectangular hyperbolae, viz:

$$r^B \ln [p/(p_n - p_0)] = A \qquad \text{(B.2)}$$

where A and B are storm-dependent scaling parameters.

This modification leads to the following radial pressure field, which forms the basis of the 'Holland' model:

$$p(r) = p_0 + (p_n - p_0) \exp(-A/r^B) \qquad \text{(B.3)}$$

B.3 Gradient Wind Speed

The gradient level winds are derived by considering the balance between centrifugal and Coriolis forces acting outwards and the presence gradient force acting inwards, leading to the so-called gradient wind equation:

$$V_g^2(r)/r + f V_g = 1/\rho_a \; dp(r)/dr \qquad \text{(B.4)}$$

where $V_g(r)$ = gradient level wind at distance r from the centre
ρ_a = air density
f = Coriolis parameter
= $2\omega \sin \phi$
and ω = radial rotational speed of the earth
ϕ = latitude

The pressure gradient term for the Holland model is:

$$dp(r)/dr = p / r \; (AB/r^B) \; exp \; (-A/r^B) \qquad \text{(B.5)}$$

and substituting into Eqn B.4 gives

$$V_g(r) = -r f/2 + [(p_n - p_0)/ \rho_a \; (AB/r^B) \; exp \; (-A/r^B) + r^2 f^2/4]^{1/2} \qquad \text{(B.6)}$$

The so-called cyclostrophic wind equation, which neglects the Coriolis components, is then

$$V_c(r) = [(p_n - p_0)/ \rho_a \; (AB/r^B) \; exp \; (-A/r^B)]^{1/2} \qquad \text{(B.7)}$$

with $V_c(r)$ attaining its maximum value when $dV_c(r)/dr = 0$ which, after differentiating, is satisfied when

$$-A/r^B + 1 = 0$$

and since, by definition, $r = R$ when $V_c(r)$ is a maximum

$$R = A^{1/B}$$
or $$A = R^B \qquad \text{(B.8)}$$

Back-substituting into the model equations yields:

$$p(r) = p_0 + (p_n - p_0) \; exp \; (-R/r)^B \qquad \text{(B.9)}$$

$$V_g(r) = -r f/2 + [(p_n - p_0)/\rho_a \; B(R/r)^B \; exp \; (-R/r)^B + r^2 f^2/4]^{1/2} \qquad \text{(B.10)}$$

which, for the particular case of B=1 the basic set of relationships reduces to the Schloemer model.

The influence of B is one of a 'peakedness' parameter which in the region of R causes an increase in pressure gradient as B increases and a corresponding increase in peak wind speed of $B^{1/2}$ near R and with lower wind speeds at increasing r. Holland (1980) uses conservation of angular momentum and a review of pressure gradient and R data to propose restricting the dynamic range of B as 1.0 to 2.5. Furthermore, based on the climatological work of Atkinson and Holliday (1977) and Dvorak (1975), Holland suggested 'standard' B values might be inferred of the form

$$B = 2.0 - (p_0 - 900)/160 \quad \text{(B.11)}$$

making B a direct function of the storm intensity.

However, due to the inherent scatter in the climatological data it is reasonable to allow further variability whilst still maintaining the identified parameter trend, viz:

$$B = B_0 - p_0/160 \quad \text{(B.12)}$$

where B_0 is the so-called intercept value of B.

B.4 Open Ocean Atmospheric Boundary Layer

Following Powell (1980), a gross simplification of the complex atmospheric boundary later is made by transferring gradient level wind speeds (V_g) to the +10 m MSL reference level (V_m) by way of a boundary layer coefficient (K_m) viz:

$$V_m = K_m V_g \quad \text{(B.13)}$$

Additionally, variation with height above the ground is derived on the basis of a traditional roughness height and logarithmic deficit law approach whereby the near-surface boundary layer profile at any height z is a function of the surface roughness and the reference speed at +10 m MSL, ie:

$$V_m (z) = V_m (10) \ ln(z/z_0)/ln(10/z_0) \quad \text{(B.14)}$$

which is terminated at a nominal gradient height z_g such that

$$V_m (z_g) = V_g = V_m (10) \ ln(z_g/z_0)/ln(10/z_0) \quad \text{(B.15)}$$

hence

$$V_m (10) = V_g \ ln(10/z_0)/ln(z_g/10) \quad \text{(B.16)}$$

$$K_m = ln (10/z_0)/ln(z_g/z_0) \quad \text{(B.17)}$$

requiring a priori selection of z_0 and z_g which are both known to vary; the former as a function of wave height (wind speed and fetch) and the latter as a function of storm energetics.

North West Cape data sets presented by Wilson (1979) give a lower limit estimate of z_g as 60 m for the open ocean environment, yielding a typical z_0 of 0.3 m for wind speeds of the order of 30 m s^{-1}. Garratt (1977) provides a functional form for z_0 at lower wind speeds (generally agreed to around 20 m s^{-1}) and nominal z_g values form Standards Australia (1989) allow the following representation of the variation of z_0 and z_g:

$$\begin{aligned} \ln(z_0) &= 0.367 V_m - 12 \quad & 0 < V_m < 30 \\ \ln(z_0) &= -1.204 \quad & V_m \geq 30 \end{aligned} \quad \text{(B.18)}$$

$$\begin{aligned} z_g &= 228 - 5.6 V_m \quad & 0 < V_m < 30 \\ z_g &= 60 \quad & V_m \geq 30 \end{aligned} \quad \text{(B.19)}$$

which, when combined into Eqn B.17 and referenced to the V_g level, yield

$$\begin{aligned} K_m &= 0.81 && 0 < V_g < 6 \\ K_m &= 0.81 - 2.96 \times 10^{-3} (V_g - 6) && 6 \le V_g < 19.5 \\ K_m &= 0.77 - 4.31 \times 10^{-3} (V_g - 19.5) && 19.5 \le V_g < 45 \\ K_m &= 0.66 && V_g \ge 45 \end{aligned} \qquad \text{(B.20)}$$

The above speed-dependent formulation for K_m was devised in an attempt to try to improve wind speed calibrations from a number of tropical cyclones in the North West Shelf region of Australia where measured wind, wave and current data was available. It embodies the observation that winds from more remote storms and/or winds on the "weak" side of storms was generally underpredicted using a constant K_m. This can also be interpreted as an attempt to devise a spatially varying K_m formulation, which has some similarity with, for example, the findings of Kepert and Wang (2000). For practical purposes in strong winds, this Eqn B.20 yields a K_m of about 0.7, which is in the range observed by Powell (1980) and subsequently, for a number of US hurricanes. In Australia, McConochie *et al.* (1999) report favourable results using the above formulation on the east coast of Queensland.

B.5 Inflow Angle and Windfield Asymmetry

In addition to direct boundary layer attenuation, frictional effects cause the inflow of winds across the line of the isobars, towards the centre of the storm. This inflow (β) is typically of the order of 25º but decreases towards the storm centre, viz:

$$\beta = \begin{cases} (10\ (r/R) & 0 \le r < R \\ (10 + 75\ (r/R\text{-}1) & R \le r < 1.2R \\ (25 & r \ge 1.2R \end{cases} \qquad \text{(B.21)}$$

following Sobey *et al.* (1977).

The observed gross features of moving storms is accounted for by including an asymmetry effect which, on one side of the storm adds the forward speed of the storm centre (V_{fm}) and subtracts it from the other side, relative to an assumed line of maximum wind θ_{max}, ie

$$V_m (r,\theta) = K_m V_g (r) + V_{fm} \cos (\theta_{max} - \theta) \qquad \text{(B.22)}$$

Where θ_{max} is commonly taken to be in the range of either 65º to 70º (left forward quadrant for Southern Hemisphere) or as 115º (left rear quadrant for Southern Hemisphere) measured upwind from the line of V_{fm} to which θ is referenced.

Figure B.1 presents the geometry of the wind field model in detail, including consideration of north point references for θ_{fm} and V_b (the bearing of V_m).

B.6 Wind Gust Formulae

The wind speed gust factor, G, is defined as the largest value of the average peak gust speed, of a given duration, to the mean wind speed averaged over a specified period. It is related to the longitudinal turbulence intensity Iu as follows:

$$G = 1 + g\, I_u \qquad \text{(B.23)}$$

where g is a 'peak' factor normally determined from the power spectral density of the wind speed record. However, in the absence of measured data the following empirical formula after Ishizaki (1983) are used:

$$G = 1 + 0.5\, I_u \ln (T_m/T_g) \qquad \text{(B.24)}$$

where T_m = mean speed reference time
T_g = gust speed reference time

such that

$$V(T_g) = G\, V(T_m) \qquad \text{(B.25)}$$

and

$$I_u = I_u\,'/\ln(V_m) \qquad \text{(B.26)}$$

where I_u ' = 0.6 for "peak gusts" and 0.4 for "mean gusts" based on the assessment of over-water wind gusts on the North West Shelf.

B.7 Radius to Maximum Wind Estimates

Estimates of R are rarely available for storms which are remote from measurement sites and outside radar range but this parameter can have an important influence on, for example, the fetch available for wind-wave generation. As an aid in determining suitable *R* values in the absence of any direct information, an empirical relationship has been developed based on available data from Australian and US sources.

The *R* hypothesis is based on the proposition (Myers 1954) that the storm spatial scale and the central pressure differential are related throughout the life of a given storm. The evidence for this appears reasonably substantial but the physical basis is by no means established. Myers presented an argument based on conservation of kinetic energy within a nominal radius of the storm centre which showed a hyperbolic relationship linking radius to maximum winds and the central pressure deficit viz:

$$R = \boldsymbol{F}\, [p_n - p_0] \qquad \text{(B.27)}$$

An analysis of over 20 separate tropical cyclones in the north-west Australian sector was undertaken using the time history of *R* values throughout each storm for both the intensifying and decaying legs and a series of best fit relationships were developed of the form:

$$R(t) = R_c / (p_n - p_0)(t) \qquad \text{(B.28)}$$

where R_c represents a scaling parameter with units of hPa.km and *t* is time.

Based on the Australian experience R_c values for the intensifying leg are likely to be in the range of 650 to 3000, with a mean value around 1850 hPa.km. Using US Gulf Coast data from NOAA (1979) a range of 900 to 4300 is indicated with a mean of 2100 hPa.km. Other regions may exhibit slightly different characteristics.

It should be noted that no relationship between R_c and (p_n-p_0) is itself proposed but rather that for any given storm intensity it is reasonable to ascribe a particular trend in spatial variation over time. On this basis storms of vastly different intensities might still share a common R_c value. In the model the R_c value is applied only to the intensifying leg and is made monatonically decreasing in R towards minimum p_0 such that any minor fluctuations in pressure are ignored. Also, based on Holland (1990), R is held constant in the decaying leg and is always limited to a practical maximum value in the range of 80 to 100 km.

Where radar eye data is available, the radar radius to the eyewall echo is taken and a constant 5 km added to estimate the position of the radius to maximum winds. This is based on experience and is consistent with available data from historical storms, e.g. Hurricane *Andrew* in 1992.

B.10 References

Atkinson G.D. and Holliday C.R. (1977) Tropical cyclone minimum sea level pressure/maximum sustained wind relationship for the Western North Pacific. *Monthly Weather Review*, 105, 421-427.

Dvorak V.F. (1975) Tropical cyclone intensity analysis and forecasting from satellite imagery. *Monthly Weather Review*, 103, 420-430.

Garratt J.R. (1977) Review of drag coefficients over oceans and continents. *Monthly Weather Review*, 105, 915-929.

Harper B.A., Lovell, K.F., Chandler B.D. and Todd D.J. (1989) The derivation of environmental design criteria for Goodwyn 'A' Platform, Proc. 9th Aust Conf. Coastal and Ocean Engin., *Institution of Engineers Australia*, Adelaide, Dec.

Harper B.A., Mason L.B. and Bode L. (1993) Tropical cyclone Orson - a severe test for modelling, Proc. 11th Australian Conf. on Coastal and Ocean Engin., *Institution of Engineers Australia*, Townsville, Aug, 59-64.

Harper B.A. (1999) Numerical modelling of extreme tropical cyclone winds. APSWE Special Edition, *Journal of Wind Engineering and Industrial Aerodynamics*, 83, 35 - 47.

Harper B.A. and Holland G.J. (1999) An updated parametric model of the tropical cyclone. Proc. 23rd Conf. Hurricanes and Tropical Meteorology, *American Meteorological Society*, Dallas, Texas, 10-15 Jan.

Holland G.J (1980) An analytic model of the wind and pressure profiles in hurricanes. *Monthly Weather Review*, 108, 1212-1218.

Holland G.J (1990) Personal communication.

Ishizaki H. (1983) Wind profiles, turbulence intensities and gust factors for design in typhoon-prone regions. *J. Wind Engineering and Industrial Aerodynamics*, Vol 13, pp 55-66.

Kepert J.D. and Wang Y. (2000) The dynamics of boundary layer jets within the tropical cyclone core. Part II: Nonlinear enhancement. To appear *Jnl Atmospheric Science*.

Lovell K.F. (1990) Review of empirical tropical cyclone wind and pressure models. MEngSt Thesis, Dept Civil Engineering, *University of Western Australia*.

McConochie J.D., Mason L.B. and Hardy T.A. (1999) A Coral Sea wind model intended for wave modelling. Proc. 14th Australasian Conf. Coastal and Ocean Enginering, *IEAust*, Perth, April, 413-418.

Myers V A (1954) Characteristics of United States Hurricanes Pertinent to Levee Design for Lake Okeechobee, Florida. US Weather Bureau, *Hydrometeor*, Report No. 32, March.

NOAA (1979) Meteorological criteria for standard project hurricane and probable maximum hurricane windfields, Gulf and East Coasts of the United States", NOAA Tech Rep NWS23, *US Dept of Commerce*, Sept.

Powell M.D. (1980) Evaluations of diagnostic marine boundary-layer models applied to hurricanes. *Monthly Weather Review,* 108, 757-766.

Schloemer R.W. (1954) Analysis and synthesis of hurricane wind patterns over Lake Okeechobee, Florida. *US Weather Bureau*, March.

Smith R.K. (1968) The surface boundary layer of a hurricane. *Tellus*, 0, 473-484.

Sobey R.J., Harper B.A. and Stark K.P. (1977) Numerical simulation of tropical cyclone storm surge. Research Bulletin CS-14, Dept Civil and Systems Engineering, *James Cook University*, March.

Standards Australia (1989) AS 1170.2 - 1989 SAA loading code part 2: wind loads. 96 pp.

Wilson K.J. (1979) Wind observations from an instrumented tower during tropical cyclone Karen, 1977. 12th Tech Conf on Hurricanes and Tropical Meteorology, *American Meteorological Society,* New Orleans, April.

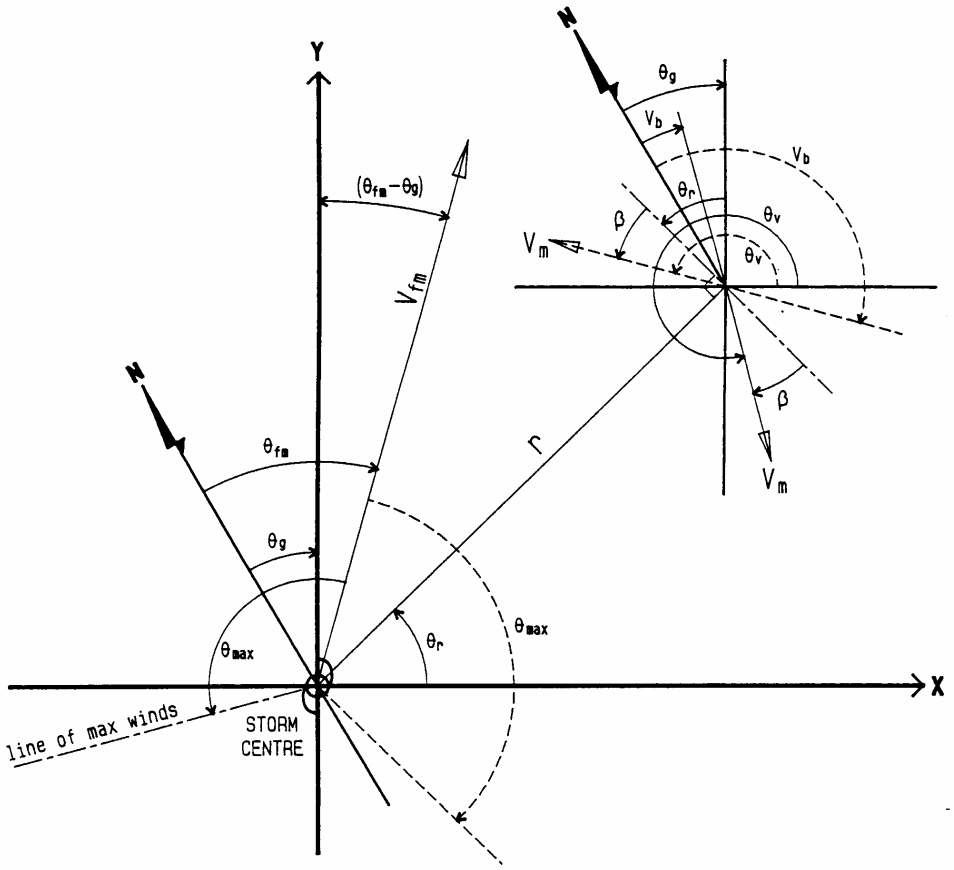

	SOUTHERN HEMISPHERE	NORTHERN HEMISPHERE
θ_{max}	+ 115	- 115
θ_v	$270 + \theta_r - \beta$	$90 + \theta_r + \beta$
V_b	$-\theta_r + \beta + \theta_g$	$180 - \theta_r - \beta + \theta_g$

TROPICAL CYCLONE MODEL
WIND FIELD GEOMETRY

Figure B.1

APPENDIX C

2D NUMERICAL HYDRODYNAMIC MODEL SURGE

Appendix C - 2D Numerical Hydrodynamic Model - SURGE

C.1 Background

SURGE is a general numerical hydrodynamic model for the generation and propagation of tropical cyclone storm surge, the first of its type developed in Australia (Sobey *et al.* 1977; Harper *et al.* 1977a; Harper and Sobey 1983). It solves the two-dimensional (2-D) depth-integrated form of the *Long Wave Equations* using an explicit finite difference procedure on a regular Cartesian grid, with increasingly finer spatial resolution obtained by utilising nested grids.

The model has been used extensively for deterministic storm surge modelling throughout Australia (Sobey and Harper 1977; Harper *et al.* 1977b-k; James Cook University 1979; Sobey *et al.* 1980; Harper and Sobey 1983; McMonagle 1995) as well as underpinning extensive statistical analyses of storm tide (Harper and Robinson 1997; Harper 1999). The model is generalised and can be used to represent any coastal location, including reef features and overland flow (in special configurations, e.g. Sobey *et al.* 1980).

The model includes the effect of undersea bathymetry, offshore islands, sand spits, reefs and other coastal features at any desired resolution in space and time. Tidal effects can be introduced at the open boundaries to simultaneously include tide and cyclone influences. Tropical cyclone size, intensity and track can be varied continuously throughout a simulation to produce water flow patterns, contours of water level, coastal surge profiles at any time and water level and flow velocity time histories anywhere within the model area.

C.2 Tropical Cyclone Forcing

Prior to 1999, the model surface wind and pressure forcing of tropical cyclones was represented by an adaptation of available models based on US hurricanes (Sobey *et al.* 1977). After 1999 the model was updated in accordance with the Holland model (Holland 1980) as modified by Harper and Holland (1999). Refer relevant Appendix for details.

C.3 Numerical Aspects

The response of a homogeneous sea to the meteorological influence of a tropical cyclone is described by the full Navier Stokes Equations for a homogeneous, incompressible fluid. For long wave propagation (astronomical tides, tsunami, storm surge) a number of approximations to the full equations are justified. The flow can be considered nearly-horizontal with little vertical motion, wave amplitude can be considered small compared with depth, the horizontal component of the Coriolis acceleration and the spherical geometry of the earth can be neglected and frictional effects can be confined to vertical shear only. These simplifications lead to the two-dimensional vertically-integrated form of the Reynolds Equations, called the Long Wave Equations, which represent the conservation of mass and momentum in spatial directions x and y:

$$\frac{\partial \eta}{\partial t} + \frac{\partial U}{\partial x} + \frac{\partial V}{\partial y} = 0 \qquad \text{(C.1)}$$

$$\frac{\partial U}{\partial t} + \frac{\partial}{\partial x}\left(\frac{U^2}{h+\eta}\right) + \frac{\partial}{\partial y}\left(\frac{U\,V}{h+\eta}\right) - f\,V = -g\,(h+\eta)\frac{\partial \eta}{\partial x} - \frac{(h+\eta)}{\rho_w}\frac{\partial p_s}{\partial x} + \frac{1}{\rho_w}(\tau_{sx} - \tau_{bx}) \quad \text{(C.2)}$$

$$\frac{\partial V}{\partial t} + \frac{\partial}{\partial x}\left(\frac{U\,V}{h+\eta}\right) + \frac{\partial}{\partial y}\left(\frac{V^2}{h+\eta}\right) + f\,U = -g\,(h+\eta)\frac{\partial \eta}{\partial y} - \frac{(h+\eta)}{\rho_w}\frac{\partial p_s}{\partial y} + \frac{1}{\rho_w}(\tau_{sy} - \tau_{by}) \quad \text{(C.3)}$$

The *x-y* datum plane is located at the mean water level with the *z* axis directed vertically upwards; ρ_w is seawater density. The water surface elevation w.r.t. datum is η *(x,y,t),* the seabed is *h (x,y)* below datum, *U* (*x,y,t)* and *V* (*x,y,t)* are depth integrated flows per unit width in the *x* and *y* directions respectively. The forcing influence of the tropical cyclone is represented through the surface wind shear stress vector τ_s (*x,y,t)* resolved into components τ_{sx} and τ_{sy} and the *x* and *y* gradients of the MSL atmospheric surface pressure $p_s(x,y,t)$. The effect of bottom stress is represented by the bottom shear stress vector τ_b (*x,y,t)* resolved into components τ_{bx} and τ_{by}, and *f* is the Coriolis parameter:

$$f = 2\,\omega \sin\phi \quad \text{(C.4)}$$

where ω is the rotational speed of the earth and ϕ is latitude north (+ve) or south (-ve).

The surface pressure term is conveniently expressed in terms of an equivalent barometric head of water *B* :

$$B = \frac{p_s}{\rho_w\, g} \quad \text{(C.5)}$$

and this term can then be considered together with the hydrostatic pressure of the superelevated water such that:

$$-g\,(h+\eta)\frac{\partial \eta}{\partial x} - \frac{(h+\eta)}{\rho_w}\frac{\partial p_s}{\partial x} = -g\,(h+\eta)\left[\frac{\partial \eta}{\partial x} + \frac{\partial B}{\partial x}\right] \quad \text{(C.6)}$$

The local magnitude of *B is* commonly referred to as the *Inverted Barometer Effect,* i.e.

$$\Delta B = \frac{(p_n - p_s)}{\rho_w\, g} \quad \text{(C.7)}$$

where p_n is the ambient or surrounding MSL atmospheric pressure. The magnitude of ΔB is then typically 10 mm for each 1 hPa pressure difference.

The surface wind stress forcing is parameterised w.r.t. the 10-minute mean wind speed W_{10} at the standard reference height of +10 m MSL by

$$\tau_s = C_{10}\, \rho_a\, W_{10}^{\,2} \qquad \text{(C.8)}$$

where ρ_a is the air density and C_{10} is an empirical coefficient whereby (Wu 1982)

$$10^3\, C_{10} = 0.8 + 0.065\, W_{10} \qquad \text{(C.9)}$$

The effect of bottom stress is parameterised by a Darcy-Weisbach equation with Q the total flow $\sqrt{U^2 + V^2}$ and λ the Darcy-Weisbach friction factor, e.g.

$$\tau_{bx} = \frac{\lambda}{8}\, \rho_w\, \frac{QU}{(h+\eta)^2} \qquad \text{(C.10)}$$

for the x component, with λ assumed depth-dependent according to the hydraulically rough Colebrook-White formula, with roughness height k_b, e.g.

$$\frac{1}{\lambda} = -2 \log_{10} \left[\frac{k_b}{14.8\, (h+\eta)} \right] \qquad \text{(C.11)}$$

where k_b is typically set at 0.025 m for coastal areas.

Numerical integration of the above partial differential equations is accomplished through appropriate finite difference equation representations on a square grid of unit dimension Δs and application of a "leap frog" explicit procedure. Discrete values of the variables are specified on a space (x,y) and time (t) staggered computational grid, whose node points are defined as ($i\Delta x$, $j\Delta y$, $n\Delta t$). Water surface elevation η, depth of water below MSL h and barometric head B are located at points (i,j,n), depth integrated flow U and the surface wind stress term τ_{sx} at ($i+½$, j, $n+½$) and depth integrated flow V and surface wind stress term τ_{sy} at (i, $j+½$, $n+½$) points.

The explicit solution procedure relies on appropriate selection of space and time steps for numerical stability, such that the Courant-Friedrichs-Lewy (CFL) criterion must be satisfied at all times:

$$\Delta t \leq \frac{\Delta s}{\sqrt{2\, g\, h_{\max}}} \qquad \text{(C.12)}$$

This may require adoption of appropriate depth cut-offs in situations where both shallow and deep water situations exist with the one model grid. This must be based on judgement and should be confirmed by numeical sensitivity testing, but typical depth cut-offs of order 60 to 100 m have been used successfully in a variety of situations.

The model has a number of options for both internal and open boundary conditions, e.g.

- Coastal (no-flow) boundaries; U or $V = 0$.
- Reefs and low barriers; U or $V = f(h,t)$ etc
- Open tidal boundaries; $\eta = f(x,t)$ etc

- Open inverted barometer boundaries; $\eta = f(B,t)$ etc
- Open bathystrophic storm tide boundaries; $\eta = f(\tau_{sx},B,t)$ etc

C.4 References

Harper B.A. and Holland G.J. (1999) An updated parametric model of the tropical cyclone. Proc. 23rd Conf. Hurricanes and Tropical Meteorology, *American Meteorological Society*, Dallas, Texas, 10-15 Jan.

Harper B.A. and Robinson D.A. (1997) Storm tide threat in Queensland, Proc 13th Australasian Conf Coastal and Ocean Engin, *IPENZ/IEAust*, Christchurch, Sept.

Harper B.A. and McMonagle C.M. (1996) Storm tide statistics - Cardwell region, Beach Protection Authority of Queensland, *Rust PPK Pty Ltd*, 1996, 50pp.

Harper B.A. (1999) Storm tide threat in Queensland - history, prediction and relative risks, Qld Dept of Environment and Heritage, Conservation Technical Report No. 10, ISSN 1037-4701, RE208-2, Jan, 23pp.

Harper B.A. and Sobey R.J. (1983) Open boundary conditions for open coast hurricane storm surge, *Coastal Engineering,* 7, 41-60.

Harper B.A., Sobey R.J. and Stark K.P. (1978) Sensitivity analysis of a tropical cyclone surge model, in Noye B J (ed) Numerical Simulation of Fluid Motion, *North-Holland*, 371-381.

Harper B.A., Sobey R.J. and Stark K.P. (1977a) Users guide to SURGE, Department of Civil and Systems Engineering, *James Cook University*, Nov, 250 pp.

Harper B.A., Sobey R.J. and Stark K.P. (1977b) Numerical simulation of tropical cyclone storm surge along the Queensland coast - Part I: Weipa, Department of Civil and Systems Engineering, *James Cook University*, November, 90 pp.

Harper B.A., Sobey R.J. and Stark K.P. (1977c) Numerical simulation of tropical cyclone storm surge along the Queensland coast - Part II: Cooktown, Department of Civil and Systems Engineering, *James Cook University*, November, 90 pp.

Harper B.A., Sobey R.J. and Stark K.P. (1977d) Numerical simulation of tropical cyclone storm surge along the Queensland coast - Part III: Cairns, Department of Civil and Systems Engineering, *James Cook University*, November, 90 pp.

Harper B.A., Sobey R.J. and Stark K.P. (1977e) Numerical simulation of tropical cyclone storm surge along the Queensland coast - Part IV: Innisfail, Department of Civil and Systems Engineering, *James Cook University*, November, 90 pp.

Harper B.A., Sobey R.J. and Stark K.P. (1977f) Numerical simulation of tropical cyclone storm surge along the Queensland coast - Part V: Ingham, Department of Civil and Systems Engineering, *James Cook University*, November, 90 pp.

Harper B.A., Sobey R.J. and Stark K.P. (1977g) Numerical simulation of tropical cyclone storm surge along the Queensland coast - Part VI: Townsville, Department of Civil and Systems Engineering, *James Cook University*, November, 90 pp.

Harper B.A., Sobey R.J. and Stark K.P. (1977h) Numerical simulation of tropical cyclone storm surge along the Queensland coast - Part VII: Bowen, Department of Civil and Systems Engineering, *James Cook University*, November, 90 pp.

Harper B.A., Sobey R.J. and Stark K.P. (1977i) Numerical simulation of tropical cyclone storm surge along the Queensland coast - Part VIII: Mackay, Department of Civil and Systems Engineering, *James Cook University*, November, 90 pp.

Harper B.A., Sobey R.J. and Stark K.P. (1977j) Numerical simulation of tropical cyclone storm surge along the Queensland coast - Part IX: Rockhampton, Department of Civil and Systems Engineering, *James Cook University*, November, 90 pp.

Harper B.A., Sobey R.J. and Stark K.P. (1977k) Numerical simulation of tropical cyclone storm surge along the Queensland coast - Part X: Gold Coast, Department of Civil and Systems Engineering, *James Cook University*, November, 90 pp.

Holland G.J. (1980) An analytic model of the wind and pressure profiles in hurricanes. *Monthly Weather Review*, Vol 108, No 8, Aug, 1212-1218.

James Cook University (1979) Mermaid Sound extreme water level study. Report prep for Woodside Offshore Petroleum Pty Ltd, *James Cook University*, May.

McMonagle C.J. (1995) Numerical simulation of storm surge along the Queensland coast - Part XI Cardwell Region. Report prepared by Rust PPK Pty Ltd for *The Beach Protection Authority Queensland*. Nov.

Sobey R.J. and Harper B.A. (1977) Tropical cyclone surge penetration across the Great Barrier Reef, Proc 3rd Aust Conf Coastal and Ocean Engg, *IEAust*, Melb, 58-63.

Sobey R.J., Harper B.A. and Mitchell G.M. (1980) Numerical modelling of tropical cyclone storm surge, Proc 17th International Conf Coastal Engg, *ASCE*, Sydney, 725-745.

Sobey R.J., Harper B.A. and Stark K.P. (1977) Numerical simulation of tropical cyclone storm surge, Department of Civil and Systems Engineering, Research Bulletin No. CS14, *James Cook University*, May, 300 pp.

Wu J. (1982) Wind stress coefficients over sea surface from sea breeze to hurricane. *Jnl Geophysical Research*, 87, 9704-9706.

APPENDIX D

ADFA1 SPECTRAL WAVE MODEL

Appendix D - ADFA1 Spectral Wave Model

D.1 Overview of the Model

A comprehensive description of the numerical spectral wave model ADFA1 can be found in Young (1987a, 1987b). ADFA1 is a further development by the original author of the 2nd generation model SPECT (Sobey and Young 1986), originally from James Cook University, having enhanced shallow water and non-linear source terms.

The complex sea state is described by the model in terms of the directional wave energy spectrum $E(f,\theta,x,y,t)$. At each position x,y and time t, E represents the superposition of free linear wave components of all frequencies f and all directions θ. The evolution of the energy spectrum is then described by the *Radiative Transfer Equation*:

$$\frac{\partial}{\partial t}(C\,C_g\,E) + C_g \cos\theta \frac{\partial}{\partial x}(C\,C_g\,E) + C_g \sin\theta \frac{\partial}{\partial y}(C\,C_g\,E)$$

$$+ \frac{C_g}{C}\left[\sin\theta \frac{\partial C}{\partial x} - \cos\theta \frac{\partial C}{\partial y}\right] \frac{\partial}{\partial\theta}(C\,C_g\,E) = C\,C_g\,S \qquad \text{(D.1)}$$

Where $C(x,y,f)$ = the individual wave phase speed

$C_g(x,y,f,\theta)$ = the wave group speed

$S(f,\theta,x,y,t)$ = a source term representing the net transfer of energy to, from or within the spectrum

The kinematics of wave propagation are described in the model by ray theory, neglecting the effects of currents. This allows wave propagation to be represented by characteristic equations.

The net source term S is represented as the summation of a number of separate influences:

(i) atmospheric input
(ii) non-linear wave-wave interactions
(iii) white cap energy dissipation
(iv) bottom friction
(v) shallow water wave breaking

Atmospheric forcing is provided by specification of the 10 minute average wind speed and direction at the standard reference height of +10 m SWL (V_m). In the present investigation, this is provided by the Holland (1980) tropical cyclone wind field model. This was incorporated into ADFA1 and updates wind speed and direction at each x, y location and at each time step t based on the position of the storm centre, and the various storm parameters, central pressure, radius to maximum winds and ambient pressure.

Eqn D.1 is solved numerically using a fractional step method consisting of separation of propagation and forcing mechanisms. This method avoids the penalty of numerical dispersion in the solution. The propagation solution (which includes refraction and shoaling) is obtained from the

method of characteristics, assuming only the influence of bathymetry. A separate wave characteristic is constructed for each frequency and direction component of the discrete representation of the spectrum and at each model point within the computational grid. The set of characteristic paths need be only determined once for each particular computational grid, provided changes in water depth will not be significant throughout a storm simulation.

Boundary conditions are either of the radiation type where there are no significant generation areas beyond the computational limits, or a system of sub-grids may be used to provide greater geographical detail where necessary. Boundary data for the finer sub-grid are provided post-hoc from the coarser parent grid.

Model output can be either the time history of the relevant spectral parameters ($H_s, T_p, T_z, T_m, \theta_m$) at particular computational grid locations, contours of H_s and vector fields of T_p and θ_m over the entire region, one-dimensional spectral energy plots at particular locations and times or full directional energy density contours throughout the simulation.

D.2 References

Holland G J (1980) An analytic model of the wind and pressure profiles in hurricanes. *Monthly Weather Review*, Vol 108, No 8, Aug, 1212-1218.

Sobey R J and Young I R (1986) Hurricane wind waves - a discrete spectral model. ASCE *Jnl Waterway, Port, Coastal and Ocean Engineering*, Vol 112, No 3, 370-389.

Young I R (1987a) A general purpose spectral wave prediction model. Res Rep No 16, Univ College, *Australian Defence Force Academy*, Canberra, January.

Young I R (1987b) Validation of the spectral wave model ADFA1. Res Rep No 17, Univ College, *Australian Defence Force Academy*, Canberra, January.

APPENDIX E

STATISTICAL SIMULATION MODEL SATSIM

Appendix E - Statistical Simulation Model - SATSIM

E.1 Background

SATSIM (Surge And Tide SIMulation) is a discrete *Monte-Carlo* statistical model employing tide generation and a parametric tropical cyclone storm surge model, which can be applied to arbitrary coastal or open ocean areas. The early model was based on techniques first described by Stark (1976, 1979) and Harper and Stark (1977) and is similar to Russell (1971) as applied in the Gulf of Mexico. SATSIM was formalised by Harper and McMonagle (1983) and used to establish design water levels along the Queensland coast (Harper 1983, 1985), the Northern Territory (Harper and McMonagle 1983) and parts of Western Australia (Stark and McMonagle 1982). The model was further extensively developed in the late 1980s to include parametric tropical cyclone wave, wind and 3-D current models (Harper *et al.* 1989). More recently, the same basic technique has been further extended to include wind estimation and building damage in an even more complex model (MIRAM) which includes severe thunderstorms as well as tropical cyclone wind and storm surge (Harper 1996ab, 1997, 1999). The latest variant of SATSIM includes breaking wave setup over coral reefs and shallow water bathystrophic storm tide effects (SEA 2001).

E.2 Definitions

The total water level experienced at a coastal, ocean or estuarine site during the passage of a severe meteorological event such as a tropical cyclone, is made up of contributions from some or all of the following components. The combined water level is termed the *storm tide,* refer Figure E.1.

(a) The Astronomical Tide

This is the regular periodic variation in water levels due to the gravitational effects of the Moon and Sun. With a suitably long period of tide measurements at a specific location, combined with harmonic analysis, the tide can be predicted with very high accuracy at any point in time (past and present). The highest expected tide level is termed *Highest Astronomical Tide* (HAT) and occurs once each 18.6 y period, although at some sites tide levels similar to HAT may occur several times per year.

(b) Storm Surge

This is the combined result of the severe atmospheric pressure gradients and wind shear stresses of a significant meteorological event such as a tropical cyclone acting on the underlying water body. The storm surge is a long period wave capable of sustaining above-normal water levels over a number of hours. The wave travels with and ahead of the storm and may be amplified as it progresses into shallow waters or is confined by coastal features. Typically the length of coastline which is severely affected by a tropical cyclone storm surge is of order 100 km either side of the track although some influences may extend many hundreds of kilometres. The magnitude of the surge is affected by many factors such as storm intensity, size, speed and angle of approach to the coast and the coastal bathymetry.

(c) Breaking Wave Setup

Severe wind fields create abnormally high sea conditions and extreme waves may propagate large distances from the centre of the storm as ocean swell. These waves experience little or no attenuation in deepwater regions and an offshore storm can impact several hundred kilometres of coastline. As the waves enter shallower waters they refract and steepen under the action of shoaling until their stored energy is dissipated by wave breaking either offshore or at a beach or reef. Just

prior to breaking, a phenomenon known as *wave setdown* occurs where the average stillwater level is slightly lower than the same level further offshore. After breaking, a portion of the wave energy is converted into forward momentum which, through the continuous action of many waves, is capable of sustaining shoreward water levels which are above the stillwater level further offshore. This quasi-steady increase in stillwater level after breaking is known as *breaking wave setup* and applies to most natural beaches and reefs.

There remain other related phenomena which can also affect the local water level. These may include long period shelf waves, unsteady surf beat, wave runup, stormwater and/or river runoff etc. Any phenomenon which can be deterministically described in space and time with respect to the incident storm parameters can be incorporated into the SATSIM methodology.

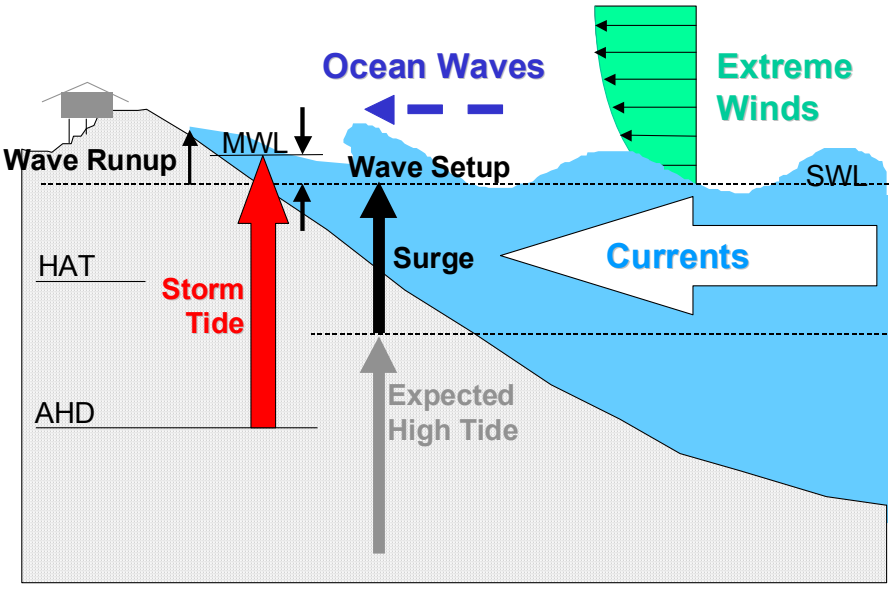

Figure E.1 Components of total water level.

E.2 Basic Methodology

(a) Deterministic Phase

SATSIM consists of a series of water level forcing modules which can provide an estimate of the time history of each of the water level components of interest. In the case of the astronomical tide, the time history of water levels is provided directly from a set of harmonic constituents for the site under consideration and tidal planes (e.g. AHD) provide a base water level datum. The storm surge and breaking wave setup time histories are provided by a series of *parametric* models which describe the likely behaviour of the respective component as a function of the incident storm parameters (e.g. distance of approach, intensity, track, size etc). These parametric models are derived from a combination of complex numerical hydrodynamic models (e.g. SURGE, ADFA1) as well as analytical approximations such as those for breaking wave setup (e.g. Nielsen and Hanslow 1991; Gourlay 1997).

The model typically considers a 36 h "window" for each storm tide event and generates simultaneous and independent estimates of each of the water level components at a time interval of 30 mins. These are then linearly combined using superposition to provide the estimated total *storm*

tide level over that time as shown schematically in Figure E.2, which closely approximates the Cyclone *Althea* storm tide at Townsville in 1971 (Stark 1972).

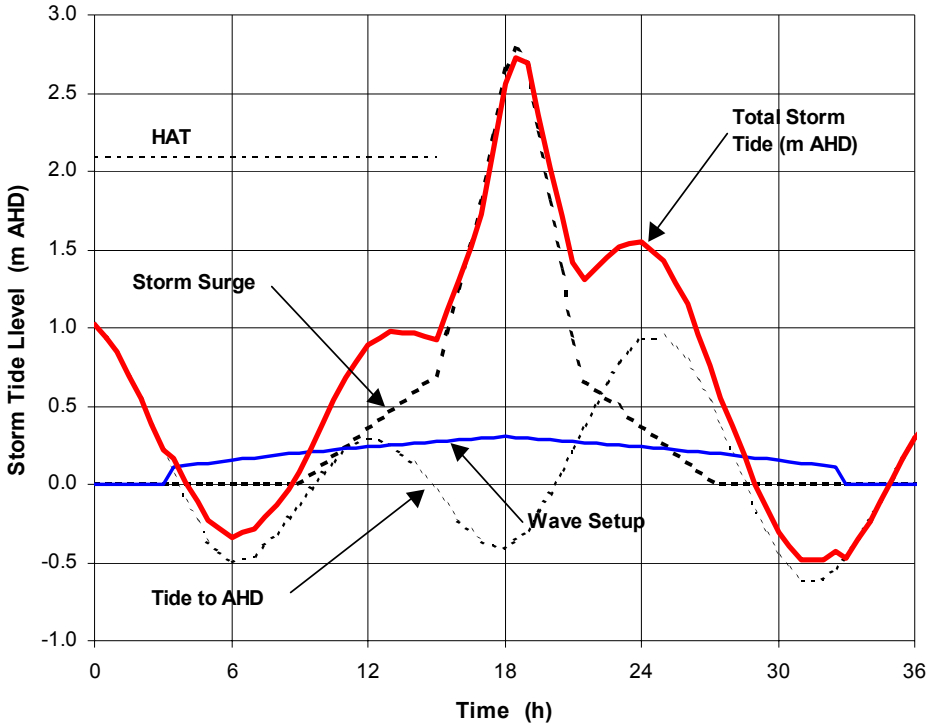

Figure E.2 Example of the superposition process.

(b) Probabilistic Phase

A number of different probabilistic variants of the model have been developed. All approaches are based on the concept of defining a statistical *control volume* around the site of interest. This may be in any geometric form such as a square or rectangular domain or a radius from the site, termed the *target site* (refer Figure E.3). The climatology of the meteorological forcing within that control volume is then determined based on either the analysis and interpretation of historical data or, where no data exists, hypothetical statistical distributions of the parameters of interest.

In Australia, tropical cyclone tracks and estimates of central pressure have been variously recorded and archived by the Bureau of Meteorology since the early 1900s. The quality of the data is quite variable in space and time (e.g. Holland 1981) and as a general rule is only suitable for statistical analysis from around 1959/60 onwards. This marks the commencement of routine satellite imagery and the adoption of objective intensity estimation methods. Individual storms which passed close to recording sites prior to this time are still suitable for inclusion but care must be taken not to bias the overall statistical descriptions.

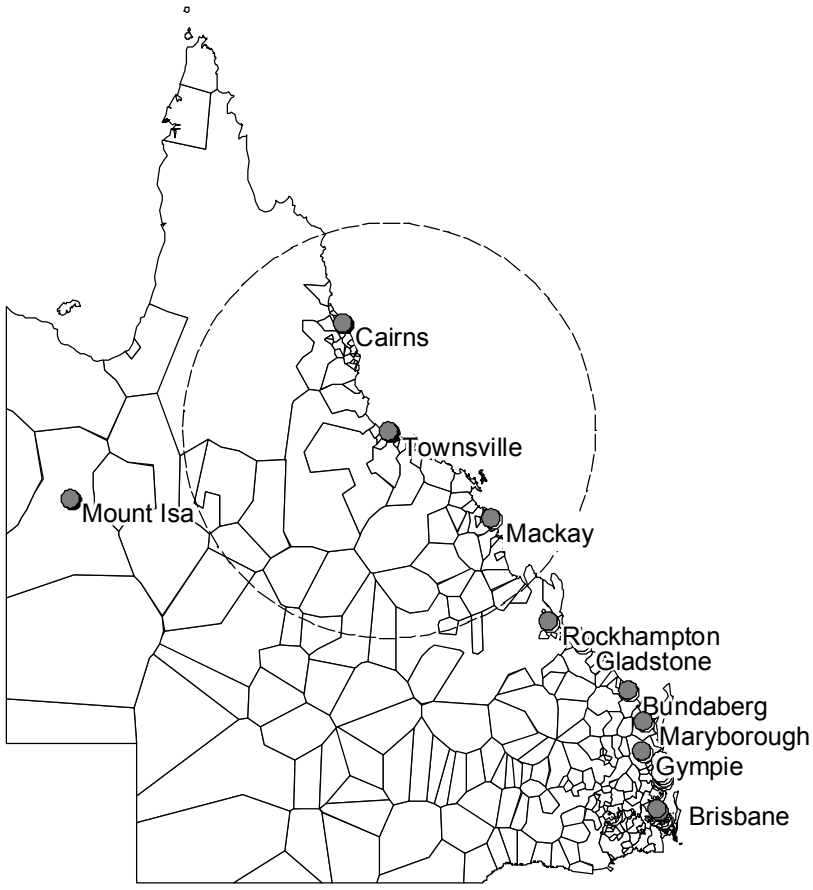

Figure E.3 Example of a 500 km radius statistical control volume with Townsville as the target site.

The climatology of storms within the control volume then is normally expressed in terms of the following major components:

Population class

At any single location it is common for the incidence of tropical cyclones to be due to two or more separate storm populations. These can normally be clearly identified by origin and track but other more complex discriminators may be required.

Frequency of occurrence

The relative frequency of occurrence between populations is often a further discriminator.

Intensity

Different populations often exhibit varying intensity behaviour which is typically related to the origin and track of the storms relative to the prevailing atmospheric patterns and landmass effects.

Scale

This typically relates to the radius of maximum winds or the radius to gales and influence the extent of storm surge or wave generation fetch etc.

Forward speed and track

The speed of approach to the coast and the angle of crossing, for example, influence the

generation of storm surge.

Distance of closest approach

This is one of the principal determinants of impact at any site, the tropical cyclone structure is spatially variable and the region of maximum effect is typically within 2 to 3 radius to maximum winds of the centre.

E.3 Statistical Model

The model utilises a discrete Monte Carlo approach, whereby a random number generator is used to provide a source of unbiased probability, and a series of individual storm events are created based on the climatological description. The deterministic output from each hypothetical storm event is then created, based on the relationships determined between the storm parameters and the impacts of interest (surge, waves, wave setup etc). A 36 h window is typically allowed for each event and simultaneous time histories of each impact at a resolution of 0.5 h are assembled and combined as required to yield the output of interest (e.g. storm tide level). The statistics of each event are then recorded in terms of the frequency of exceedance of a range of given magnitude levels. After many thousands of samples from the control volume, the statistical exceedance function becomes smoothed and simulation ends when the function has converged sufficiently at the desired probability level. For example, to estimate the 100 year return period (or 1% annual exceedance), at least 1000 years of simulation is recommended so that there will be at least 10 estimates of the 100 year magnitude. Figure E.4 illustrates the basic model structure in flowchart format.

The forms of the statistical representations used are typically:

Frequency of Occurrence	Poisson
Storm Intensity	Gumbel (EV Type I)
Forward Speed	Smoothed Data CDF
Track	Smoothed Data CDF
Closest Approach	Smoothed Data CDF
Radius to Maximum Winds	Normal CDF
Windfield Peakedness	Normal CDF

Any of the input statistical distributions may then be altered to test the sensitivity of the model results to the input assumptions.

E.4 Model Variants

SATSIM has been variously developed over a number of years according to the needs of the particular analysis. The following provides an introduction to some of the specific versions which were used in major or landmark studies. Individual study reports should be consulted for further details.

V3 through V4

These versions were used for the series of studies conducted during the early 1980s (e.g. Harper 1983; Harper and McMonagle 1983, 1985). It considers a rectangular control volume of nominally 5º of latitude alongshore (556 km) and 2.5º of longitude offshore (278 km). Tidal constituent data for the target site was provided and extended to up to 10 secondary sites by the use of published range ratios. The coastal storm surge response was parameterised according to intensity, track, closest approach and forward speed based on the results of a series of numerical hydrodynamic

model tests (e.g Harper 1977 for each of 10 locations along the Queensland coast). Some versions incorporated breaking wave setup and also coastal wave height, these being derived from a series of model tests using the SPECT model (Sobey and Young 1986).

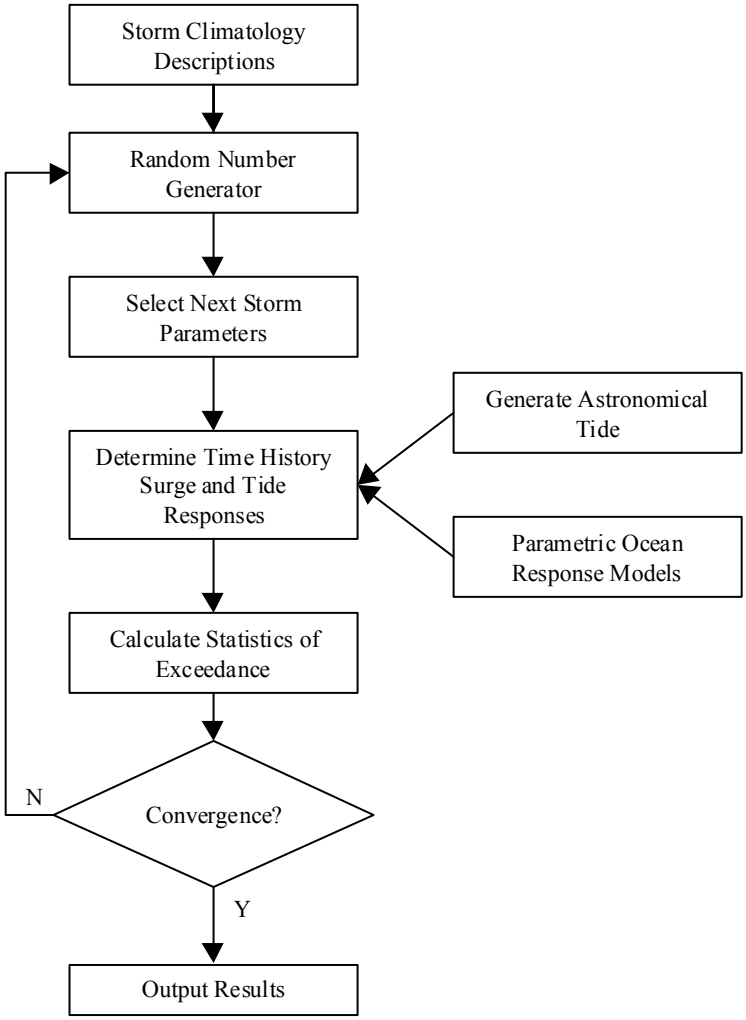

Figure E.4 Flowchart of the model simulation process.

V5 through V8

These versions were developed under licence by Woodside Offshore Petroleum Pty Ltd in the late 1980s to provide design criteria for the Goodwyn 'A' offshore production platform on the North West Shelf of Western Australia (Harper *et al.* 1989, 1990). A radius of influence of 1000 km was taken to represent the statistical control volume around a single site. These versions provided full (contemporaneous) statistical descriptions of environmental loadings on an offshore platform allowing phase separation at very long return periods (10,000yr). Hurricane wind fields could be specified as NHRP circa 1970 or according to a modified and extended Holland (1980). Each site impact of interest was separately modelled, e.g.

V5 deepwater storm surge (inverted barometer effect) driven directly from the parametric wind and pressure field model dependent upon the relative position of the site and the storm centre.

V6 wind speed and direction (mean and gust) driven directly from the parametric wind and pressure field model, as above.

V7 wave height (H_s, H_{max}), period (T_z, T_m, T_p), direction (θ_m) parameterised based on over 200 separate spectral wave model tests using the ADFA1 model (Young 1987) - an updated version of the SPECT model. A two-stage nested-model domain system was used with resolutions of 54 km and 10.8 km. Results were summarised in terms of a series of complex tabular functions describing the wave conditions of straightline tracks as a function of various storm parameters and position relative to the target site. Long-term directional wave counts were also estimated for structural fatigue considerations. Maximum wave heights and associated periods were determined by numerical integration of the time history of significant wave heights and periods (e.g. Sobey *et al.* 1990).

V8 3D currents (barotropic, baroclinic, pulsed) were similarly parameterised on the basis of a series of sensitivity tests using a hydrodynamic model after Fandry (CSIRO Division of Marine Research.

The Woodside developments included significant calibration and verification testing of the various parametric model components against extensive measured wind, wave and current datasets.

V9a

This version was developed to represent storm tide impacts at the Cocos (Keeling) Islands in the Southern Indian Ocean on behalf of GHD Pty Ltd, acting for the Commonwealth Department of Transport and Regional Services (SEA 2001). The selected radius of influence was 500 km. The model combines a number of aspects of previous models, namely:

- Astronomical tide
- Deepwater inverted barometer effect
- Mean and gust wind speed
- Parametric open ocean tropical cyclone waves

As well as some additional capabilities:

- Ability to represent up to 20 sites around the island by a directionally sensitive wave sub-model, further modifying the V7 open ocean model
- Breaking wave setup over the fringing reefs based on Gourlay (1997)
- Bathystrophic storm tide effects within the island lagoon

This version of the model simultaneously generates estimates of all impacts for all sites.

E.5 Algorithms

E.5.1 Astronomical Tide

The astronomical tide is specified only for the target site and secondary sites may have an associated range ratio to allow variation from the target site. No phase differences are incorporated, with phase being regarded as a random variable in this context. The target site tide is specified by up to 36 harmonic constituents (amplitudes , phases) together with the relevant datum planes for z_0, MSL and HAT.

E.5.2 Tropical Cyclone Winds and Pressures

The Holland (1980) model formulation is used, as modified and extended by Harper and Holland (1999).

E.5.3 Inverted Barometer Effect (IBE)

This is represented by

$$\Delta B = \frac{(p_n - p_s)}{\rho_w \, g}$$

where p_s is the local MSL atmospheric pressure; p_n is the ambient or surrounding MSL atmospheric pressure; ρ_w is seawater density; g is gravity. The magnitude of ΔB is then typically 10 mm for each 1 hPa pressure difference.

E.5.4 Bathystrophic Storm Tide (BST)

This is the first-order 1D momentum balance for a steady-state wind stress scenario which, considering the x direction is given by:

$$0 = -g\,(h+\eta)\frac{\partial \eta}{\partial x} - \frac{(h+\eta)}{\rho_w}\frac{\partial p_s}{\partial x} + \frac{1}{\rho_w}(\tau_{sx} - \tau_{bx})$$

where the x-y datum plane is located at the mean water level with the z axis directed vertically upwards; the water surface elevation w.r.t. datum is $\eta\,(x,y,t)$, the seabed is $h\,(x,y)$ below datum. The forcing influence of the tropical cyclone is represented through the surface wind shear stress vector component τ_{sx} and the x gradient of the MSL atmospheric surface pressure $p_s(x,y,t)$. The effect of bottom stress is represented by the bottom shear stress vector component τ_{bx}.

Following the SURGE model (Sobey *et al.* 1977), the surface stress and bottom stress components are represented parametrically. For example, the surface wind stress forcing is parameterised w.r.t. the 10-minute mean wind speed component W_{x10} at the standard reference height of +10 m MSL by

$$\tau_{sx} = C_{10}\,\rho_a\,W_{x10}{}^2$$

where ρ_a is the air density and C_{10} is an empirical coefficient whereby (Wu 1982)

$$10^3\,C_{10} = 0.8 + 0.065\,W_{x10}$$

The effect of bottom stress is parameterised by a Darcy-Weisbach equation with U the x component of flow and λ the Darcy-Weisbach friction factor, e.g.

$$\tau_{bx} = \frac{\lambda}{8}\,\rho_w\,\frac{U^2}{(h+\eta)^2}$$

with λ assumed depth-dependent according to the hydraulically rough Colebrook-White formula, with roughness height k_b, e.g.

$$\frac{1}{\lambda} = -2\log_{10}\left[\frac{k_b}{14.8\,(h+\eta)}\right]$$

where k_b is typically set at 0.025 m for coastal areas.

However, U remains an unknown in this context and is therefore further parameterised by the surface wind speed

$$U = k_u W_{x10}$$

assuming k_u is a fixed nominal value of 0.03 (e.g. Bishop 1979).

The surface elevation η is then calculated based on a given fetch and depth profile using a Runge-Kutta integration technique.

E.5.5 Coastal Storm Surge

This follows the method outlined in Harper and McMonagle (1985).

E.5.6 Tropical Cyclone Waves and Currents

This follows the tabular look-up methodology described in Harper *et al.* (1989), which is based on a schematised storm reference system as shown in Figure E.5. Straightline tracks of constant speed are assumed but with a symmetric variation in central pressure based on a Gaussian function. Radius to maximum winds varies as a function of pressure differential for a given R_c constant.

Some examples of the tabular functions which comprise the open ocean tropical cyclone wave model are shown in Figure E.6. Clockwise from top left these are: peak wave height as a function of central pressure; modification due to forward speed; modification due to along-track position; modification due to across-track position. Similar functions describe the variation of wave periods, direction and shape of the hydrograph.

The model incorporates a bias adjustment for H_s determined from detailed calibration studies with 23 tropical cyclones which identified an apparent cross-track bias in the ADFA1 spectral wave model, thought to be due to non-linear wave-wave interactions in the rotating wind field (Young *pers. comm.*). The adjustment is implemented here as a linear function according to the relative x position within a nominal y domain, as follows:

$$H_s^{'} = \frac{H_s}{E_r}$$

where

$$E_r = 0.00196\, x + 0.92089 \qquad -100 < x < 100$$

with x in km and a clipped linear return to unity at -200 and +200 . The applicable y domain is defined by

$y0 < -100$ and $y2 > 0$

E.5.7 Breaking Wave Setup

The method of Nielsen and Hanslow (1991) is applied for plane beaches while that of Gourlay (1997) is applied for reefs.

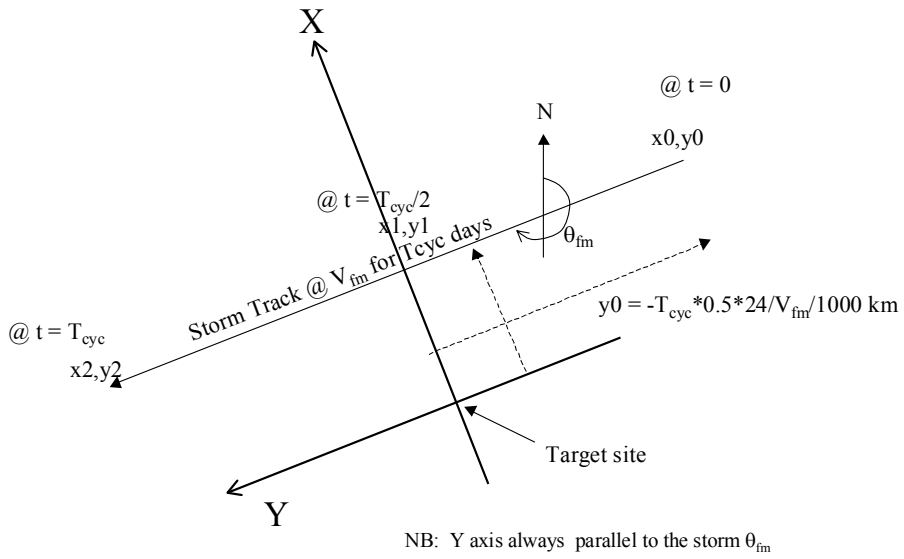

Figure E.5 Model reference system for schematised tropical cyclones.

E. 6 References

Bishop J.M. (1979) A note on surface wind-driven flow. *Ocean Engineering*, 6, 273-284.

Gourlay M.R. (1997) Wave setup on coral reefs: some practical applications. Proc. 13th Australasian Conf Coastal and Ocean Engin., *IEAust*, Christchurch, Sep, 959-964.

Harper B.A. (1983) Half Tide tug harbour extreme water level study. Report prepared by *Blain Bremner and Williams Pty Ltd* for DBCT-UDC Joint Venture. Sept.

Harper B.A. (1985) Storm tide statistics - Parts 1 to 8. Reports prepared by Blain Bremner and Williams Pty Ltd for the *Beach Protection Authority Queensland*, Jan.

Harper B.A. (1996a) Risk modelling of cyclone losses, Proc Annual Engineering Conf, *IEAust*, Darwin, April.

Harper B.A. (1996b) The application of numerical modelling in natural disaster risk management, Proc Conf Natural Disaster Reduction NDR'96, *IEAust*, Gold Coast, Sep.

Harper B.A. (1997) Numerical modelling of extreme tropical cyclone winds, Proc 4th Asia Pacific Sympos on Wind Engin, Gold Coast, July.

Harper B.A. (1999) Numerical modelling of extreme tropical cyclone winds. APSWE Special Edition, *Journal of Wind Engineering and Industrial Aerodynamics*, 83, 35 - 47.

Harper B.A. and Holland G.J. (1999) An updated parametric model of the tropical cyclone. Proc. 23rd Conf. Hurricanes and Tropical Meteorology, *American Meteorological Society*, Dallas, Texas, 10-15 Jan.

Harper B.A., Lovell K.F., Chandler B.D. and Todd D.J. (1989) The derivation of environmental design criteria for Goodwyn 'A' platform, Proc 9th Aust Conf Coastal and Ocean Engin, *IEAust*, Dec.

Harper B.A. and McMonagle C.J. (1983) Greater Darwin storm surge study - part 3: extreme water level frequencies, Northern Territory Department of Lands under direction Maritime Works Branch Department of Housing and Construction, *Blain Bremner and Williams Pty Ltd*, Sept, 120 pp.

Harper B.A. and McMonagle C.J. (1985) Storm tide statistics - methodology, Report prep by Blain Bremner and Williams Pty Ltd, *Beach Protection Authority of Queensland*, Jan, 120 pp.

Harper B.A. and Stark K.P. (1977) Probabilities of water levels at Townsville resulting from the combined effects of cyclone storm surge, tide and waves. Dept of Civil and Systems Engin., *James Cook University*, Dec.

Holland G.J. (1980) An analytic model of the wind and pressure profiles in hurricanes. *Monthly Weather Review*, Vol 108, No 8, Aug, 1212-1218.

Holland G J (1981) On the quality of the Australian tropical cyclone data base, *Aust Met Mag*, Vol.29, No.4, Dec, pp. 169-181.

Holland G.J. (1997). The maximum potential intensity of tropical cyclones. *J. Atmos. Sci*., 54, Nov, 2519-2541.

Stark K.P. and McMonagle C.J. (1982) Karratha storm surge plus tide levels. Report prepared for WA Dept of Resource Development, Dept of Civil and Systems Engin, James Cook University,April.

McMonagle C.J. (1995) Storm tide statistics Cardwell region. Report prepared by Rust PPK Pty Ltd for *The Beach Protection Authority Queensland*, Oct.

Nielsen P. and Hanslow D.J. (1991) Wave runup distributions on natural beaches. *J Coastal Res,* Vol 7, No 4, pp 1139-1152.

Russell, L.R. (1971) Probability distributions for hurricane effects. *J. Waterways, Harbors and Coastal Eng. Div. A.S.C.E.,* Paper 7886, February 1971.

SEA (2001) Cocos Island storm surge study. Prep for GHD Pty Ltd on behalf of the Dept of Transport and Regional Services, *Systems Engineering Australia Pty Ltd*, Jan.

Sobey R.J., Harper B.A. and Stark K.P. (1977) Numerical simulation of tropical cyclone storm surge, Department of Civil and Systems Engineering, Research Bulletin No. CS14, *James Cook University*, May, 300 pp.

Sobey R.J. and Young I.R. (1986) Hurricane wind waves - a discrete spectral model. Jnl Waterways, Port, Coastal and Ocean Engin, *ASCE*, 113, 3, 370-389.

Sobey R.J., Chandler B.D. and Harper B.A., Extreme waves and wave counts in a hurricane, Proc 22nd Int Conf Coastal Engin, *ASCE*, 1990.

Stark K.P. (ed.) (1972) Cyclone Althea - Part II storm surge and coastal effects. *James Cook University*. Oct.

Stark K.P. (1976) Rosslyn Bay boat harbour surge investigation. Report prepared by Dept of Civil and Systems Engin *James Cook University*.

Stark K.P. (1979) Cairns storm surge plus tide levels. Report prepared by Dept of Civil and Systems Engin *James Cook University* for Cairns City Council. Dec.

Wu J. (1982) Wind stress coefficients over sea surface from sea breeze to hurricane. *Jnl Geophysical Research*, 87, 9704-9706.

Young I.R. (1987) A general purpose spectral wave prediction model. Research Report No. 16, University College, Australian Defence Force Academy, Canberra, Jan.

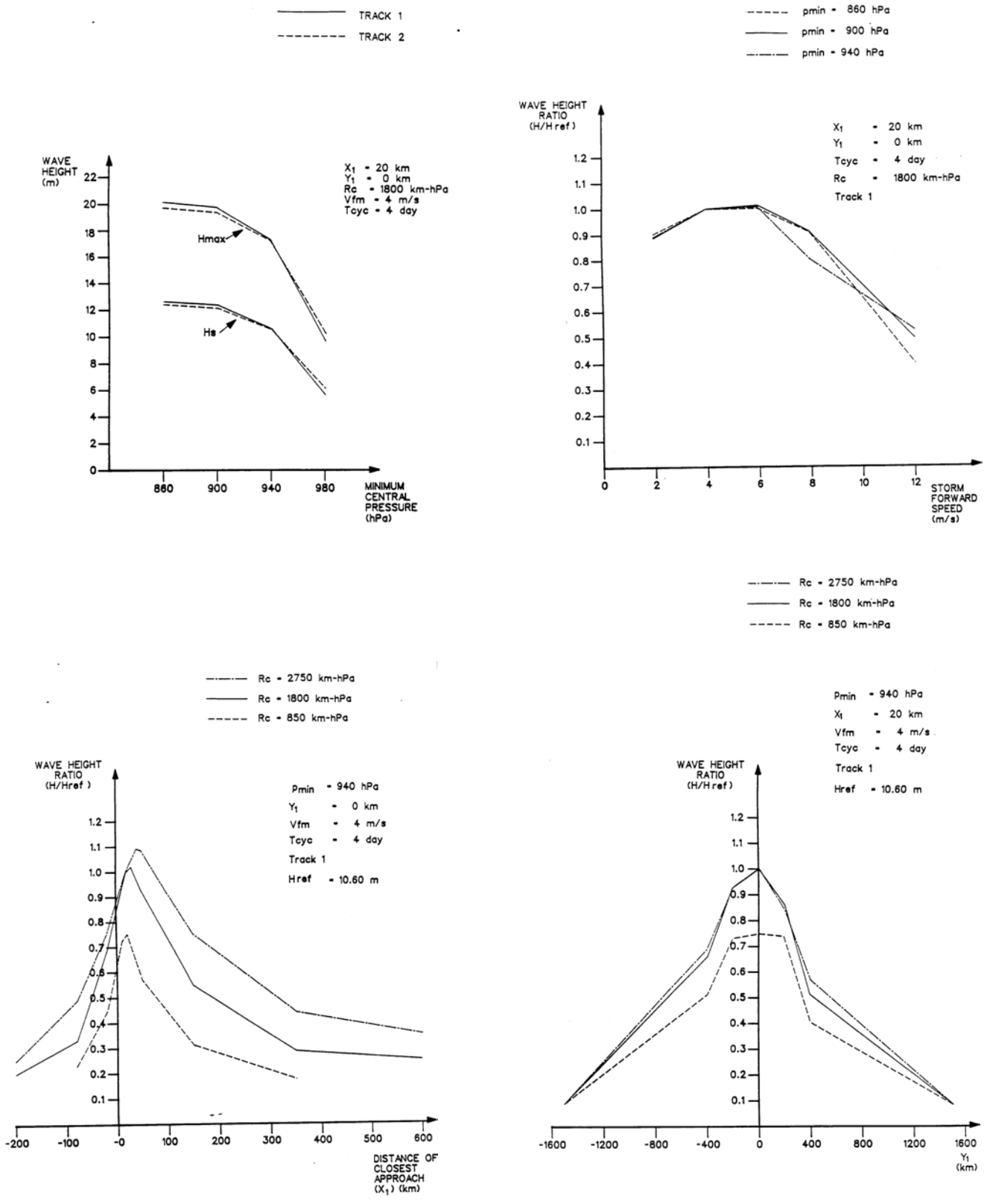

Figure E.6 Example open ocean tropical cyclone parametric wave model functions.

APPENDIX F

BREAKING WAVE INDUCED SETUP ON CORAL REEFS

Appendix F - Breaking Wave-Induced Setup on Coral Reefs

Coral reef environments present a specific set of physical characteristics which can often create very significant nearshore wave setup, raising the water levels on the reef-top, and driving reef-top current systems that may control lagoon flushing and sediment transport processes. In extreme situations, wave setup can be responsible for overtopping and flooding of low lying islands and is likely to be the largest component of storm tide at some offshore island sites. In particular, the combination of astronomical tide variation, storm surge and incident wave height and period present a very dynamic and sensitive wave setup environment.

F.1 Definitions

Figure F.1 presents a schematic view of a typical coral reef nearshore environment (Gourlay 1997), where:

Reef-face is the relatively steep seaward facing underwater slope of the reef;
Reef-top the skyward facing surface of the reef, usually submerged except at low tides;
Reef-rim the relatively flat seaward inclined surface between the reef-top and the reef-face;
Reef-edge the intersection between the reef-face and the reef-rim;
Reef-crest the highest part of the reef-rim or the intersection between the reef-rim and the reef-top;
Lagoon a body of water ponded on or enclosed by a reef or by a reef and a continental or island land mass.

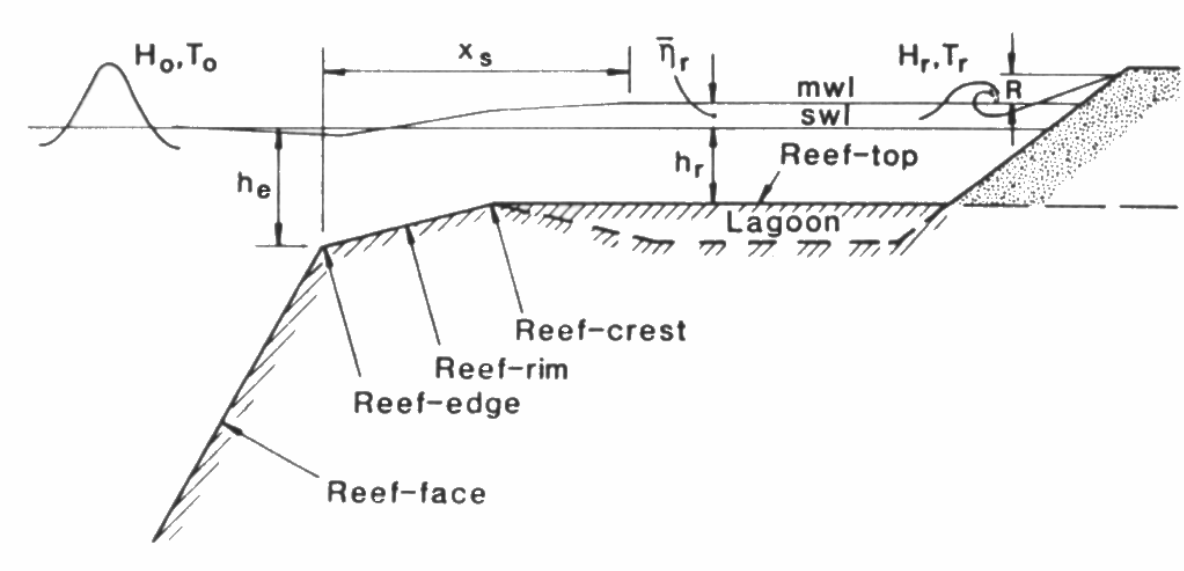

Figure F.1 Coral reef wave setup definitions (after Gourlay 1997).

Clearly, reefs and reef platforms represent potentially very complex shorelines which, being living environments, have evolved at any specific location to be in equilibrium with the incident wave and tide conditions. Even relatively small areas of reef platforms may display a myriad of channels, ridges and holes. Any estimate of wave setup must therefore be considered in a very generalised manner and applied with caution to specific locations. In particular, accurate information on reef-top water levels and slopes will be seen to be critical to any accurate assessment of reef setup.

F.2 Estimation of Wave Setup

Using an analysis combining wave energy flux and radiation stress concepts and assuming deepwater conditions offreef and shallow water conditions on the reef-top, Gourlay (1994b) derived the following equation for the wave setup $\overline{\eta}_r$ on a reef-top as a function of the offreef wave conditions H_o and T and the stillwater depth h_r on the reef-top:

$$\overline{\eta}_r = \frac{3}{64\pi} K_p \frac{g^{1/2} H_o^2 T}{(\overline{\eta}_r + h_r)^{3/2}} \left[1 - K_r^2 - 4\pi K_R^2 \frac{1}{T} \sqrt{\frac{(\overline{\eta}_r + h_r)}{g}} \right] \qquad \text{(F.1)}$$

where K_p is a reef profile factor (varies according to reef profile up to approximately 0.8)

K_R is the reflection coefficient (0 to 1)

K_r is the transmission coefficient (0 to 1)

and the term in **[...]** is subsequently referred to as the *transmission parameter* P_T .

Laboratory experiments (Gourlay 1996a) indicate that for steep reef-faces $K_R \le 0.3$, whereas for flatter slopes (Gourlay 1994) $K_R \le 0.1$. Hence wave reflection at most decreases the wave setup by about 10% and can be reasonably neglected.

The influence of wave transmission on wave setup however is a function of the relative submergence *S*, viz.

$$S = \frac{(\overline{\eta}_r + h_r)}{H_o} \qquad \text{(F.2)}$$

and is also relatively small when S < 1. However it becomes increasingly significant as the submergence increases until, when S 〈 2.5, waves pass over the reef *without* breaking and hence without generating any setup (Gourlay 1996a).

To facilitate analysis, the transmission coefficient K_r $(\equiv H_r / H_o)$ can be expressed in terms of the reef-top wave height to depth ratio γ_r $(\equiv H_r / (\overline{\eta}_r + h_r))$ The resulting form of the transmission parameter P_T , neglecting K_R, is then:

$$P_T = \left[1 - 4\pi \gamma_r^2 \frac{1}{T} \sqrt{\frac{(\overline{\eta}_r + h_r)}{g}} \left(\frac{(\overline{\eta}_r + h_r)}{H_o} \right)^2 \right] \qquad \text{(F.3)}$$

or

$$P_T = \left[1 - 4\pi \gamma_r^2 \; S^2 / D \right] \qquad \text{(F.4)}$$

where *D* is the inverse of the relative depth of the reef-top waves, i.e.:

$$D = T\sqrt{\frac{g}{(\overline{\eta}_r + h_r)}} \qquad \text{(F.5)}$$

On a horizontal or near-horizontal reef-top $\gamma_r \leq 0.55$ (Gourlay 1994; Nelson 1994),i.e. maximum wave heights never exceed 0.55 times the reef-top water depth $(\overline{\eta}_r + h_r)$. For regular waves with significant dissipation at the reef-edge, laboratory studies show $\gamma_r = 0.4$ (Gourlay 1994) and this value also has been found to apply for significant wave heights in the field (Hardy *et al.* 1991). Hence, when P_T is calculated with typical values of $\gamma_r = 0.4$ and $D = 12.5$, it can be simplified to the following form:

$$P_T = \left[1 - 0.16\ S^2\right] \qquad \text{(F.6)}$$

thus correctly representing the observed condition that full transmission (and hence zero setup) occurs when S $\langle$ 2.5. Alternatively, $P_T = 1$ when S=0 (or rather $K_R = 0$ and $K_r = 0$), and the maximum reef-top wave setup is estimated as:

$$\overline{\eta}_{r\max} = \frac{3}{64\pi} K_p \frac{g^{1/2} H_o^2 T}{(\overline{\eta}_r + h_r)^{3/2}} \qquad \text{(F.7)}$$

with typically achievable maximum setup values in the range 0.25 to 0.80 m even for average swell conditions at many exposed coral atolls, and potentially increasing above 3 m in extreme wave conditions, being modulated significantly by the tide and/or incident storm surge levels.

The reef profile factor K_p depends upon the roughness, permeability and shape of the reef. Gourlay (1996b) provides a range of K_p values derived from laboratory studies which increase with increasing profile slope tan α. For waves breaking at the reef-edge, the reef-face slope determines the value of K_p, whereas for waves breaking on a seaward sloping reef-rim, the reef-rim slope determines K_p. In the latter case it was found (Gourlay 1997) that an average water depth h_a determined over the reef-rim surf zone, was more appropriate than the reef-top water depth h_r for calculating the wave setup and use of a modified K_p' is recommended. Both relationships with respect to tan α are presented in Figure F.2.

Hence, two situations are possible:

(a) Wave breaking occurs at the reef-edge:
- tan α is taken as the reef-face slope (i.e. into deepwater)
- S is calculated using either h_r for a horizontal reef-top or the average depth h_a over the reef-rim (assuming that the surf zone x_S extends over the full width of the reef-rim).
- the appropriate reef profile factor is K_p taken from Figure F.2

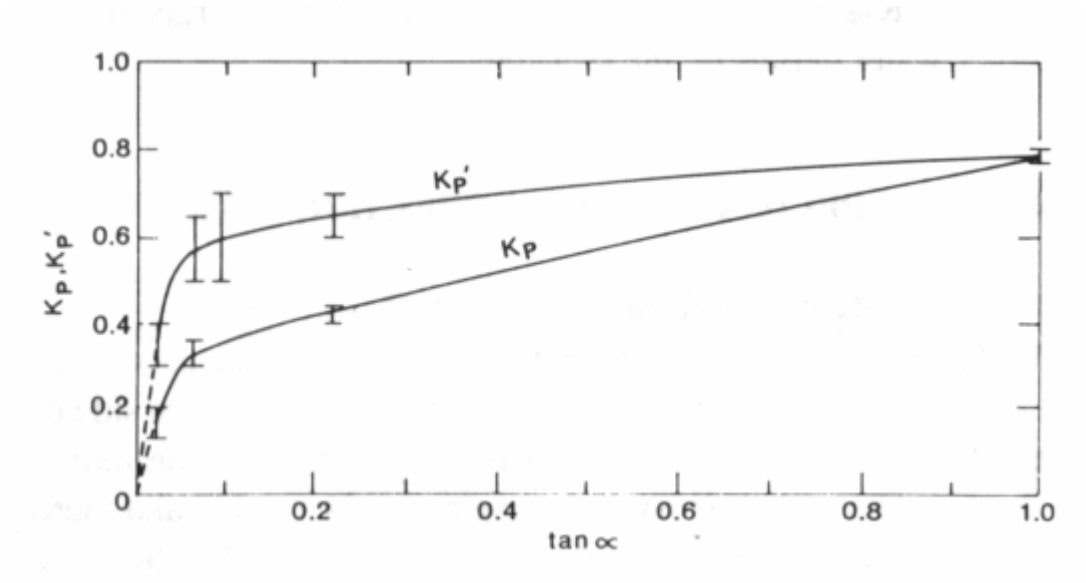

Figure F.2 K_p and K_p' as a function of tan α (after Gourlay 1997).

(b) Wave breaking occurs on the reef-rim:

- tan α is taken as the reef-rim slope
- the breakpoint should be calculated (i.e. the breaker depth related to the reef-rim slope)
- S is calculated using the average depth h_{ba} on the reef-rim between the breakpoint and the reef-crest (for tan α > 0.1, refer Gourlay 1997)
- the appropriate reef profile factor is K_p' taken from Figure F.2

In the latter situation, the breakpoint depth ($d = d_b$) on the reef-rim can be estimated as proposed by Gourlay (1992), ignoring possible wave-setdown, viz:

$$\frac{d_b}{H_o} = 0.259 \left[\tan^2 \alpha \left(\frac{H_o}{L_o} \right) \right]^{-0.17} \qquad \text{(F.8)}$$

Furthermore, calculation of h_a or h_{ba} implies knowledge of the surf zone width x_S which can be estimated by the following equation from Gourlay (1994):

$$x_S = \left(2 + 1.1 \frac{H_o}{h_e} \right) T \sqrt{g\, h_e} \qquad \text{(F.9)}$$

where h_e is the reef-edge depth.

F.3 Irregular Waves

Finally, irregular waves may be considered in an analogous manner, substituting the offreef wave parameters as follows, e.g.

$$H_o = H_{0rms} \equiv \frac{H_{os}}{\sqrt{2}} \qquad \text{(F.10)}$$

where H_{os} is the offreef significant wave height, and

$$T_o = T_{0p} \tag{F.11}$$

where T_{op} is the peak spectral wave period, yielding a maximum reef-top setup value from Eqn F.7 of:

$$\overline{\eta}_{r\max} = 0.023\, K_p\, \frac{H_{os}^2\, T_{op}}{(\overline{\eta}_r + h_r)^{3/2}} \tag{F.12}$$

This maximum condition also assumes that wave crests approach normal to the reef profile and that H_{oS} is a measure of the shore-normal wave energy. This will not always be the case since the reefs are often surrounded by very deep water and refraction generally will be limited. Accordingly, in specific situations the direction of wave approach relative to the orientation of the reef-shore should also be considered and, given the overall level of approximations involved, a simple transference is preferred, e.g.

$$H_{oS}(\theta{=}0) = H_{oS}(\theta{=}\vartheta_o)\, \cos\theta_o \tag{F.13}$$

where υ_o is the angle between the offshore deepwater wave energy and the shore-normal reef profile.

Gourlay (1996b) also examined the variability in setup values due to the irregular wave condition (or *surf beat* phenomenon), utilising laboratory data from Seelig (1982, 1983) and Nielsen and Rasmussen (1990). These analyses considered the variability in water levels in terms of the standard deviation $\sigma_{\overline{\eta}}$ of setup magnitudes relative to the mean setup and also an estimate of the extreme setup level $\overline{\eta}_{1\%}$, i.e. equaled or exceeded only 1% of the time. Gourlay's analysis of these data sets showed that the relative values of $\sigma_{\overline{\eta}} / \overline{\eta}_r$ and $\overline{\eta}_{1\%} / \overline{\eta}_r$ were functions of the submergence *S* and the reef-top width W_r, and presented the ralationships in graphical form, as shown in Figure F.3. This allows estimation of the wave induced water level z_L on a reef-top lagoon, variously:

$$z_L = z_o + \overline{\eta}_r \pm \sigma_{\overline{\eta}} \tag{F.14}$$

within the expected range of one standard deviation, or

$$z_L = z_o + \overline{\eta}_{1\%} \tag{F.15}$$

an estimate of the extreme wave setup level; where z_0 is an offshore SWL datum which includes astronomical tide, inverted barometer effect and/or wind setup.

Depending on the reef-top characteristics, it may also be necessary to consider the possibility of re-formed waves and bores in the lagoon and additional beach setup and runup. Gourlay (1997) provides further advice on such matters.

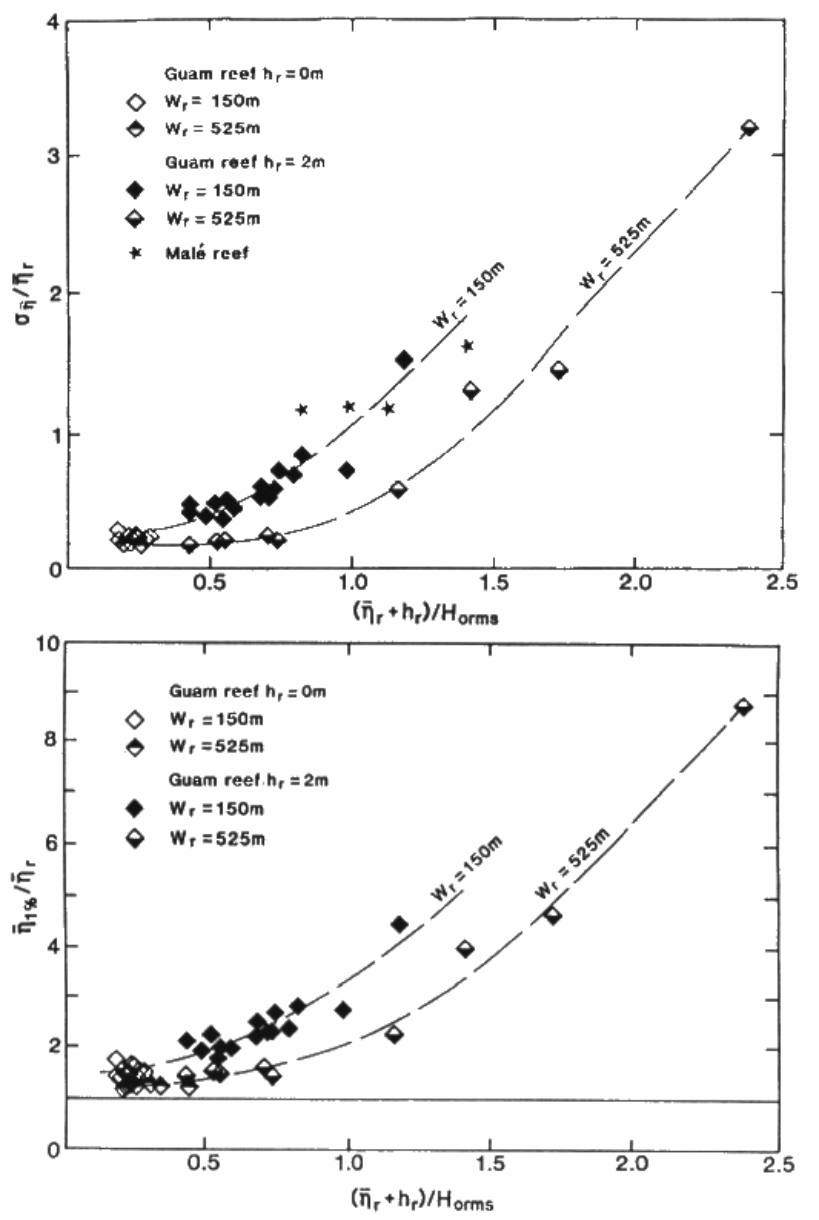

Figure F.3 Effect of irregular waves on reef-top wave setup. (after Gourlay 1996b)

F.4 References

Gourlay M.R. (1992) Wave set-up, wave run-up and beach water table: Interaction between surf zone hydraulics and groundwater hydraulics. *Coastal Engineering*, 17, 93-144.

Gourlay M.R. (1994) Wave transformation on a coral reef. *Coastal Engineering*, 23,17-42.

Gourlay M.R. (1996a) Wave setup on coral reefs. 1. Set-up and wave-generated flow on an idealised two dimensional horizontal reef. *Coastal Engineering*, 27,161-193.

Gourlay M.R. (1996b) Wave setup on coral reefs. 1. Set-up on reefs with various profiles. *Coastal Engineering*, 28,17-55.

Gourlay M.R. (1997) Wave setup on coral reefs: some practical applications. Proc. 13th Australasian Conf Coastal and Ocean Engin., *IEAust*, Christchurch, Sep, 959-964.

Hardy, T.A., Young I.R., Nelson R.C. and Gourlay M.R. (1991) Wave attenuation on an offshore coral reef. Proc. 22nd Intl Conf Coastal Engin., Delft, 1990, *ASCE*, New York, Vol 1, 330-344.

Nelson R.C. (1994) Depth limited design wave heights in very flat regions. *Coastal Engineering*, 23, 43-59.

Nielsen P. and Rasmussen A. (1990) Waves on coral reefs. Thesis-report, *Danish Engineering Academy* (in Danish).

Seelig W.N. (1982) Wave induced design conditions for reef/lagoon system hydraulics. *US Army Corps of Engineers* (unpublished), Pacific Ocean Division.

Seelig W.N. (1983) Laboratory study of reef-lagoon system hydraulics. *J. Waterways Port and Coastal Engin*, ASCE, 109, 380-391.

APPENDIX G

SUMMARY TROPICAL CYCLONE PARAMETERS WITHIN 500 Km COCOS ISLANDS

		Start				Finish				At Maximum Intensity Within Radius							At Closest Approach to Site						
No.	Name	Date	Time	Lat	Long	Date	Time	Lat	Long	p0	Date	Time	Dist	Bear	Vfm	Theta	p0	Date	Time	Dist	Bear	Vfm	Theta
			hh mm	S	E		hh mm	S	E	hPa		hh mm	km	deg	m/s	deg	hPa		hh mm	km	deg	m/s	deg
196002	665	29-Dec-1960	0100	7.0	96.0	03-Jan-1961	0100	17.0	98.0	1000	29-Dec-1960	1000	496	338	4.8	211	1000	01-Jan-1961	200	218	243	2.3	153
196009	666	12-Feb-1961	0100	9.0	99.0	17-Feb-1961	0100	19.0	99.0	990	14-Feb-1961	0100	201	174	2.0	180	991	13-Feb-1961	1130	18	93	4.1	180
196011	667	21-Feb-1961	0100	13.0	95.0	01-Mar-1961	2200	12.0	105.0	994	27-Feb-1961	0400	492	99	3.2	71	997	24-Feb-1961	1600	179	174	3.0	90
196108	668	02-Mar-1962	0100	15.0	101.0	06-Mar-1962	0100	16.0	93.0	1001	03-Mar-1962	0100	482	151	1.0	270	1003	04-Mar-1962	1200	421	180	5.9	270
196213	673	21-Jan-1963	0100	11.0	101.0	24-Jan-1963	1900	17.0	107.0	1000	22-Jan-1963	0100	494	113	1.4	135	1003	21-Jan-1963	1130	453	90	4.1	180
196225	676	15-Mar-1963	0100	10.0	101.0	24-Mar-1963	0100	23.0	98.0	994	18-Mar-1963	1000	380	215	5.7	224	999	17-Mar-1963	930	139	161	3.2	251
196308	HAZEL	07-Mar-1964	0100	14.0	106.0	17-Mar-1964	0100	30.0	95.0	980	10-Mar-1964	2200	413	225	2.3	205	988	09-Mar-1964	1000	89	182	4.0	270
196504	CAROL	25-Dec-1965	1000	9.0	100.0	28-Dec-1965	0100	13.2	93.3	997	27-Dec-1965	0700	244	277	2.9	224	998	26-Dec-1965	2200	150	323	5.1	232
196505	UNNAMED	30-Dec-1965	1600	11.3	92.8	01-Jan-1966	0100	13.9	87.2	999	30-Dec-1965	1600	450	282	10.3	258	999	30-Dec-1965	1600	450	282	10.3	258
196512	MARTHA	24-Feb-1966	0100	11.0	99.0	08-Mar-1966	0100	24.7	64.8	997	25-Feb-1966	1000	299	195	2.9	238	1003	24-Feb-1966	1130	37	134	3.6	224
196513	NANCY	14-Mar-1966	0100	13.0	101.0	24-Mar-1966	0100	19.0	60.0	995	14-Mar-1966	1600	142	3	7.3	267	996	14-Mar-1966	1330	126	29	7.0	300
196514	NELLIE	21-Mar-1966	0700	10.0	100.0	28-Mar-1966	0100	29.0	101.0	997	21-Mar-1966	1000	242	4	5.2	258	997	21-Mar-1966	1330	233	348	5.2	258
196604	DELILAH	26-Dec-1966	0100	11.0	100.0	31-Dec-1966	0100	22.0	91.0	995	28-Dec-1966	2200	383	221	5.4	247	998	28-Dec-1966	400	133	147	5.9	238
196614	LAURA	06-Apr-1967	0100	10.0	96.0	15-Apr-1967	0100	38.0	119.0	1000	07-Apr-1967	0400	476	284	4.5	243	1003	06-Apr-1967	100	258	339	4.2	255
196708	DOREEN	19-Jan-1968	0700	7.0	97.0	24-Jan-1968	0100	19.0	92.0	970	21-Jan-1968	0700	27	41	3.7	213	970	21-Jan-1968	900	4	107	3.7	213
197005	JANET	19-Dec-1970	0000	8.0	97.0	25-Dec-1970	0000	20.0	87.0	987	21-Dec-1970	0600	434	109	12.0	160	990	20-Dec-1970	1400	300	56	3.7	146
197007	MYRTLE	15-Jan-1971	0000	12.0	99.5	19-Jan-1971	0000	15.0	78.0	997	16-Jan-1971	0600	413	240	8.6	248	1003	15-Jan-1971	1230	77	157	6.4	251
197008	POLLY	20-Jan-1971	0000	11.0	93.5	29-Jan-1971	0000	25.0	90.0	998	20-Jan-1971	0000	386	289	2.0	270	998	20-Jan-1971	0	386	289	2.0	270
197017	YVONNE	19-Feb-1971	0000	13.0	93.0	24-Feb-1971	0000	19.0	76.5	1002	19-Feb-1971	0000	425	257	1.0	90	1002	19-Feb-1971	2100	355	247	18.1	266
197112	ANGELA	29-Feb-1972	0000	8.0	97.0	03-Mar-1972	0000	13.3	109.8	1000	01-Mar-1972	0600	492	81	6.4	108	1002	29-Feb-1972	1600	338	45	5.8	135
197113	BELINDA	20-Mar-1972	0000	10.0	105.0	29-Mar-1972	0600	23.3	89.8	980	23-Mar-1972	0000	359	149	4.3	224	982	22-Mar-1972	1800	355	138	2.9	224
197212	PAULA	26-Mar-1973	0000	8.6	103.5	01-Apr-1973	0000	14.0	86.5	997	29-Mar-1973	0000	215	235	3.6	235	999	28-Mar-1973	1000	4	306	3.7	235
197302	ANNIE	21-Nov-1973	0001	9.0	91.0	08-Dec-1973	0001	19.0	85.0	994	25-Nov-1973	0001	17	304	1.4	135	994	25-Nov-1973	401	1	164	1.0	90
197305	CECILY	11-Dec-1973	0001	9.9	100.1	19-Dec-1973	0001	28.8	91.5	976	14-Dec-1973	1200	455	198	5.1	215	983	13-Dec-1973	1801	192	134	7.9	219
197307	DEIDRE	20-Dec-1973	0001	10.0	98.0	26-Dec-1973	0001	15.8	79.5	985	22-Dec-1973	0900	164	289	4.0	270	995	21-Dec-1973	1131	25	334	2.2	243
197401	MARCIA	17-Oct-1974	0000	8.8	88.8	25-Oct-1974	0000	17.0	86.0	988	19-Oct-1974	2100	447	281	2.3	116	999	21-Oct-1974	900	282	238	2.3	153
197402	NORAH	28-Oct-1974	0000	8.0	105.1	04-Nov-1974	0000	11.3	76.6	983	31-Oct-1974	1800	471	268	3.2	251	995	30-Oct-1974	1730	192	338	5.5	247
197403	PENNY	06-Nov-1974	1500	5.9	96.9	16-Nov-1974	0000	12.6	80.0	981	10-Nov-1974	0000	390	317	3.7	236	981	10-Nov-1974	0	390	317	3.7	236
197413	VIDA	16-Mar-1975	0000	14.1	95.5	20-Mar-1975	1200	36.8	117.0	992	17-Mar-1975	1200	448	105	5.5	95	994	16-Mar-1975	2230	219	124	7.3	33
197416	CLARA	20-Apr-1975	0100	9.0	100.6	26-Apr-1975	0100	27.5	111.5	995	20-Apr-1975	1900	486	78	4.6	153	998	20-Apr-1975	1300	467	67	4.6	153
197417	DENISE	18-May-1975	1800	12.0	106.2	25-May-1975	0000	13.7	90.4	992	21-May-1975	2100	475	91	4.0	270	995	22-May-1975	2230	34	176	5.0	270
197501	RAY	17-Nov-1975	0000	7.0	102.2	25-Nov-1975	0000	23.7	92.0	973	22-Nov-1975	0000	376	276	3.7	213	985	20-Nov-1975	1100	247	341	3.2	251
197512	ALICE	02-Mar-1976	0100	15.0	115.4	13-Mar-1976	0100	13.5	83.0	1000	10-Mar-1976	1300	293	209	8.6	291	1000	10-Mar-1976	1300	293	209	8.6	291
197601	HARRY	15-Dec-1976	0000	8.4	103.0	21-Dec-1976	0000	17.0	80.4	955	17-Dec-1976	1800	223	326	3.7	213	985	17-Dec-1976	2100	211	316	3.7	235
197609	JACK	13-Feb-1977	0000	9.0	99.4	20-Feb-1977	0000	13.0	80.0	991	16-Feb-1977	0600	468	253	4.3	224	996	14-Feb-1977	1200	207	334	3.2	251

		Start				Finish				At Maximum Intensity Within Radius							At Closest Approach to Site						
No.	Name	Date	Time	Lat	Long	Date	Time	Lat	Long	p0	Date	Time	Dist	Bear	Vfm	Theta	p0	Date	Time	Dist	Bear	Vfm	Theta
			hh mm	S	E		hh mm	S	E	hPa		hh mm	km	deg	m/s	deg	hPa		hh mm	km	deg	m/s	deg
197703	TRUDY	10-Jan-1978	0000	10.6	129.0	20-Jan-1978	0000	25.2	89.2	968	14-Jan-1978	1200	497	150	6.7	242	968	14-Jan-1978	1300	496	153	6.7	242
197706	WINNIE	16-Mar-1978	0000	13.6	83.8	29-Mar-1978	0000	37.7	89.5	967	22-Mar-1978	0600	493	213	5.4	112	981	24-Mar-1978	900	441	205	2.9	223
197810	JANE	08-Apr-1979	0000	7.2	91.2	14-Apr-1979	0000	18.9	100.3	988	11-Apr-1979	1200	313	221	2.5	127	988	11-Apr-1979	1430	312	217	2.5	127
197811	KEVIN	02-May-1979	0000	4.3	94.7	12-May-1979	0000	12.0	88.0	990	10-May-1979	0000	498	300	2.8	158	990	10-May-1979	1200	427	287	1.8	235
197903	WILF	23-Dec-1979	0000	9.8	94.9	01-Jan-1980	0000	16.0	81.2	999	24-Dec-1979	1800	463	283	2.7	247	1004	23-Dec-1979	600	335	316	1.8	235
197907	CLARA	21-Jan-1980	0000	9.7	89.7	29-Jan-1980	0000	22.2	103.1	992	22-Jan-1980	1200	482	281	6.2	125	1001	23-Jan-1980	830	41	165	8.1	67
197911	FRED	20-Feb-1980	0000	11.6	102.3	28-Feb-1980	0000	25.6	87.5	930	23-Feb-1980	1800	234	175	7.3	253	932	23-Feb-1980	1600	230	164	6.2	255
198001	ALICE	03-Nov-1980	0000	4.9	102.0	10-Nov-1980	1200	13.4	78.8	958	06-Nov-1980	1800	484	325	7.3	257	972	06-Nov-1980	900	450	348	5.2	258
198003	CAROL	12-Dec-1980	0000	10.8	122.3	24-Dec-1980	1200	15.5	78.9	991	21-Dec-1980	0600	492	187	6.8	313	991	21-Dec-1980	1330	424	210	8.1	300
198004	DAN	14-Dec-1980	0000	8.6	99.6	18-Dec-1980	0000	13.6	105.4	1006	14-Dec-1980	0000	499	37	3.6	81	1006	14-Dec-1980	0	499	37	3.6	81
198005	EDNA	20-Dec-1980	0000	10.1	117.4	27-Dec-1980	0000	10.1	93.0	994	25-Dec-1980	0000	456	76	6.1	265	1003	25-Dec-1980	1830	104	15	6.7	283
198014	PADDY	24-May-1981	0300	6.0	89.0	30-May-1981	0000	16.6	95.4	1002	29-May-1981	1800	499	207	4.0	120	1002	29-May-1981	1800	499	207	4.0	120
198105	CHRIS	05-Jan-1982	0000	10.3	105.1	11-Jan-1982	1200	12.5	80.3	973	08-Jan-1982	1200	432	245	7.0	270	984	07-Jan-1982	1930	178	181	8.0	270
198106	DAPHNE	10-Jan-1982	1800	7.1	94.0	21-Jan-1982	0900	20.2	120.4	986	16-Jan-1982	0600	189	73	5.0	90	994	15-Jan-1982	1030	81	13	2.1	104
198206	NAOMI	21-Apr-1983	0000	13.7	81.5	02-May-1983	0600	12.0	88.5	960	27-Apr-1983	1800	459	227	1.8	124	964	28-Apr-1983	600	444	214	1.4	135
198207	MONTY	22-Apr-1983	0600	9.8	96.0	29-Apr-1983	1200	28.0	106.0	994	23-Apr-1983	1800	437	66	5.7	116	1004	22-Apr-1983	1430	275	0	3.0	90
198302	PEARL	11-Nov-1983	0900	8.4	91.6	14-Nov-1983	1200	18.0	101.0	998	12-Nov-1983	1200	446	302	1.6	198	999	13-Nov-1983	830	227	226	8.6	135
198312	ANNETTE	03-Feb-1984	1200	9.4	101.1	16-Feb-1984	0300	19.5	80.0	985	06-Feb-1984	1200	405	226	4.7	219	994	05-Feb-1984	1130	34	303	6.5	218
198319	DARYL	06-Mar-1984	1200	8.6	101.4	20-Mar-1984	0600	28.2	88.9	977	12-Mar-1984	0600	413	247	6.2	255	984	11-Mar-1984	1130	80	160	5.3	252
198401	EMMA	03-Dec-1984	1800	5.3	102.0	13-Dec-1984	0600	21.9	119.8	986	08-Dec-1984	1200	486	63	3.7	106	990	07-Dec-1984	1500	447	45	2.2	135
198408	ISOBEL	11-Feb-1985	0600	7.6	100.6	22-Feb-1985	0000	31.5	94.2	976	14-Feb-1985	0600	410	109	7.1	98	976	14-Feb-1985	530	410	108	3.2	198
198412	KIRSTY	01-Mar-1985	0000	10.5	112.0	19-Mar-1985	0000	33.6	113.0	986	07-Mar-1985	0000	485	276	4.4	233	997	05-Mar-1985	1900	175	0	5.1	270
198416	MARGOT	10-Apr-1985	0300	6.8	103.8	25-Apr-1985	0000	19.4	106.9	959	14-Apr-1985	0000	455	71	5.4	139	966	13-Apr-1985	600	333	37	1.8	123
198502	OPHELIA	07-Jan-1986	0000	8.6	97.6	12-Jan-1986	0000	12.9	98.1	986	10-Jan-1986	0900	188	338	2.0	90	989	11-Jan-1986	830	41	68	3.2	161
198512	ALISON	04-Apr-1986	1800	11.3	105.2	09-Apr-1986	1800	14.1	89.8	984	09-Apr-1986	0000	364	275	7.9	242	991	08-Apr-1986	630	87	359	5.1	270
198514	BILLY	04-May-1986	1800	4.7	89.3	15-May-1986	0300	32.0	131.8	960	08-May-1986	1800	497	277	5.1	232	980	08-May-1986	0	465	306	2.9	224
198702	FREDERIC	28-Jan-1988	0000	6.9	99.5	02-Feb-1988	0000	18.6	95.0	961	31-Jan-1988	1200	452	191	6.5	197	989	30-Jan-1988	1600	20	115	5.9	210
198703	GWENDA	06-Feb-1988	0000	12.8	109.0	12-Feb-1988	0000	17.1	90.0	966	10-Feb-1988	0600	484	214	4.5	276	982	09-Feb-1988	1200	410	180	5.0	270
198705	HERBIE	17-May-1988	0300	6.8	91.6	19-May-1988	0840	13.6	97.5	990	18-May-1988	1200	227	330	5.8	164	992	19-May-1988	100	44	229	5.8	142
198803	JOHN	23-Jan-1989	0600	7.6	103.3	02-Feb-1989	0600	25.9	104.1	990	27-Jan-1989	0000	123	264	3.6	261	997	26-Jan-1989	230	20	5	3.0	270
198805	LEON	13-Feb-1989	0600	12.0	102.0	19-Feb-1989	1200	12.8	89.0	992	18-Feb-1989	1800	454	261	6.1	274	999	17-Feb-1989	1430	89	181	3.5	270
198901	PEDRO	06-Nov-1989	0000	7.8	97.2	13-Nov-1989	0600	20.9	96.3	982	10-Nov-1989	0600	146	260	3.3	141	982	10-Nov-1989	1200	128	232	2.3	153
198903	ROSITA	04-Jan-1990	1800	12.7	111.7	17-Jan-1990	1200	11.2	98.1	998	12-Jan-1990	0600	475	78	3.0	149	1001	17-Jan-1990	700	160	77	4.2	346
198908	WALTER	03-Mar-1990	1800	14.6	94.0	14-Mar-1990	1200	11.6	87.8	990	13-Mar-1990	0000	395	268	7.1	278	997	12-Mar-1990	800	101	196	6.8	287
199007	ERROL	23-Mar-1991	1200	11.0	99.6	31-Mar-1991	0600	17.4	92.6	950	26-Mar-1991	0600	425	75	4.8	148	988	24-Mar-1991	1200	282	56	0.5	0

		Start				Finish				At Maximum Intensity Within Radius							At Closest Approach to Site						
No.	Name	Date	Time	Lat	Long	Date	Time	Lat	Long	p0	Date	Time	Dist	Bear	Vfm	Theta	p0	Date	Time	Dist	Bear	Vfm	Theta
			hh mm	S	E		hh mm	S	E	hPa		hh mm	km	deg	m/s	deg	hPa		hh mm	km	deg	m/s	deg
199101	GRAHAM	02-Dec-1991	0000	5.0	95.0	10-Dec-1991	1200	15.0	104.5	915	05-Dec-1991	0900	287	336	3.7	146	926	05-Dec-1991	2200	132	20	5.5	112
199105	HARRIET	24-Feb-1992	1800	11.5	101.8	09-Mar-1992	0000	45.0	124.5	935	29-Feb-1992	0000	464	250	2.9	224	973	27-Feb-1992	800	9	50	9.1	266
199110	JANE	08-Apr-1992	0000	7.6	97.7	17-Apr-1992	0600	17.8	83.1	948	13-Apr-1992	0000	421	228	6.1	260	976	09-Apr-1992	1800	221	66	3.0	149
199201	KEN	18-Dec-1992	0000	10.7	99.7	24-Dec-1992	0000	11.6	81.0	990	19-Dec-1992	0600	57	172	3.6	235	993	19-Dec-1992	400	51	145	3.6	235
199207	MONTY	06-Apr-1993	0000	10.5	101.0	13-Apr-1993	0600	19.3	107.6	1006	06-Apr-1993	0000	491	67	2.0	108	1006	06-Apr-1993	0	491	67	2.0	108
199304	PEARL	11-Jan-1994	0000	15.4	121.4	21-Jan-1994	0000	24.1	88.8	955	16-Jan-1994	0600	467	154	5.9	270	955	16-Jan-1994	1200	427	170	6.5	260
199309	TIM	28-Mar-1994	0000	10.2	115.0	03-Apr-1994	0000	11.7	94.3	1005	02-Apr-1994	0000	209	54	5.2	261	1006	02-Apr-1994	1000	93	350	5.2	261
199311	WILLY	27-Apr-1994	1200	6.8	93.7	02-May-1994	0000	17.4	87.3	985	28-Apr-1994	2100	336	332	3.1	180	990	29-Apr-1994	1500	91	262	2.9	224
199501	DARYL	16-Nov-1995	0100	7.0	95.5	25-Nov-1995	0100	17.0	77.5	985	18-Nov-1995	1300	331	285	5.1	270	996	17-Nov-1995	2130	200	321	3.3	230
199502	EMMA	01-Dec-1995	2200	10.0	105.9	16-Dec-1995	1600	13.0	115.0	990	04-Dec-1995	1900	219	341	4.3	315	998	04-Dec-1995	900	125	25	4.5	296
199506	HUBERT	06-Jan-1996	2200	10.2	99.6	12-Jan-1996	1300	15.0	75.5	960	08-Jan-1996	2200	441	255	6.5	230	977	07-Jan-1996	2330	97	341	3.2	251
199601	LINDSAY	09-Jul-1996	1000	9.3	93.3	13-Jul-1996	0000	15.3	95.3	996	11-Jul-1996	0900	493	267	1.4	135	998	12-Jul-1996	1530	359	225	4.3	135
199602	MELANIE	28-Oct-1996	1000	9.1	97.8	06-Nov-1996	1600	11.7	80.2	995	31-Oct-1996	1600	499	315	5.3	286	1000	30-Oct-1996	400	266	333	1.5	243
199609	PANCHO	18-Jan-1997	0700	9.6	96.2	07-Feb-1997	0700	18.8	76.2	915	21-Jan-1997	0700	223	278	4.3	224	960	20-Jan-1997	2030	156	314	2.9	224
199613	RHONDA	10-May-1997	0100	11.0	84.5	17-May-1997	1000	27.3	112.2	935	14-May-1997	0400	410	180	7.8	130	954	13-May-1997	1630	313	219	6.5	129
199703	SELWYN	25-Dec-1997	1600	11.9	110.9	02-Jan-1998	2200	19.7	88.3	1000	31-Dec-1997	1600	479	173	5.0	264	1000	31-Dec-1997	1600	479	173	5.0	264
199801	ZELIA	07-Oct-1998	0600	11.3	93.0	10-Oct-1998	0900	13.9	95.3	990	08-Oct-1998	0900	345	219	2.2	117	1003	10-Oct-1998	530	246	214	3.6	304
199802	ALISON	07-Nov-1998	0100	10.2	98.2	13-Nov-1998	1000	15.9	88.8	955	09-Nov-1998	0700	197	222	5.1	232	967	08-Nov-1998	2030	88	153	4.5	242
199805	CATHY	22-Dec-1998	1900	11.1	100.6	28-Dec-1998	0400	15.9	90.1	980	25-Dec-1998	0400	468	157	2.8	223	1002	22-Dec-1998	2200	422	76	2.3	153
199808	DAMIEN	21-Jan-1999	0700	12.8	112.8	28-Jan-1999	1000	16.7	89.5	950	24-Jan-1999	2200	462	155	6.9	270	984	26-Jan-1999	630	351	225	1.4	315
199814	HAMISH	19-Apr-1999	1000	10.5	93.6	21-Apr-1999	2200	15.9	89.1	985	20-Apr-1999	1300	491	252	3.6	235	1002	19-Apr-1999	1230	396	290	5.5	201
199901	ILSA	08-Dec-1999	2200	9.0	95.0	17-Dec-1999	1000	20.2	121.3	985	11-Dec-1999	1000	438	74	3.7	106	997	10-Dec-1999	1000	315	32	3.4	116
199903	KIRRILY	24-Jan-2000	0400	11.5	99.8	01-Feb-2000	2200	22.7	104.8	1000	24-Jan-2000	0400	332	76	6.1	90	1000	24-Jan-2000	400	332	76	6.1	90
199905	MARCIA	14-Feb-2000	1000	13.8	99.7	18-Feb-2000	1000	16.5	104.2	1000	14-Feb-2000	1000	358	119	7.0	87	1000	14-Feb-2000	1000	358	119	7.0	87
199911	PAUL	10-Apr-2000	2200	13.0	127.5	20-Apr-2000	0800	15.0	94.3	930	16-Apr-2000	0400	448	110	4.0	270	955	17-Apr-2000	400	217	157	3.2	230

APPENDIX H

TROPICAL CYCLONE WIND AND PRESSURE MODEL CALIBRATION

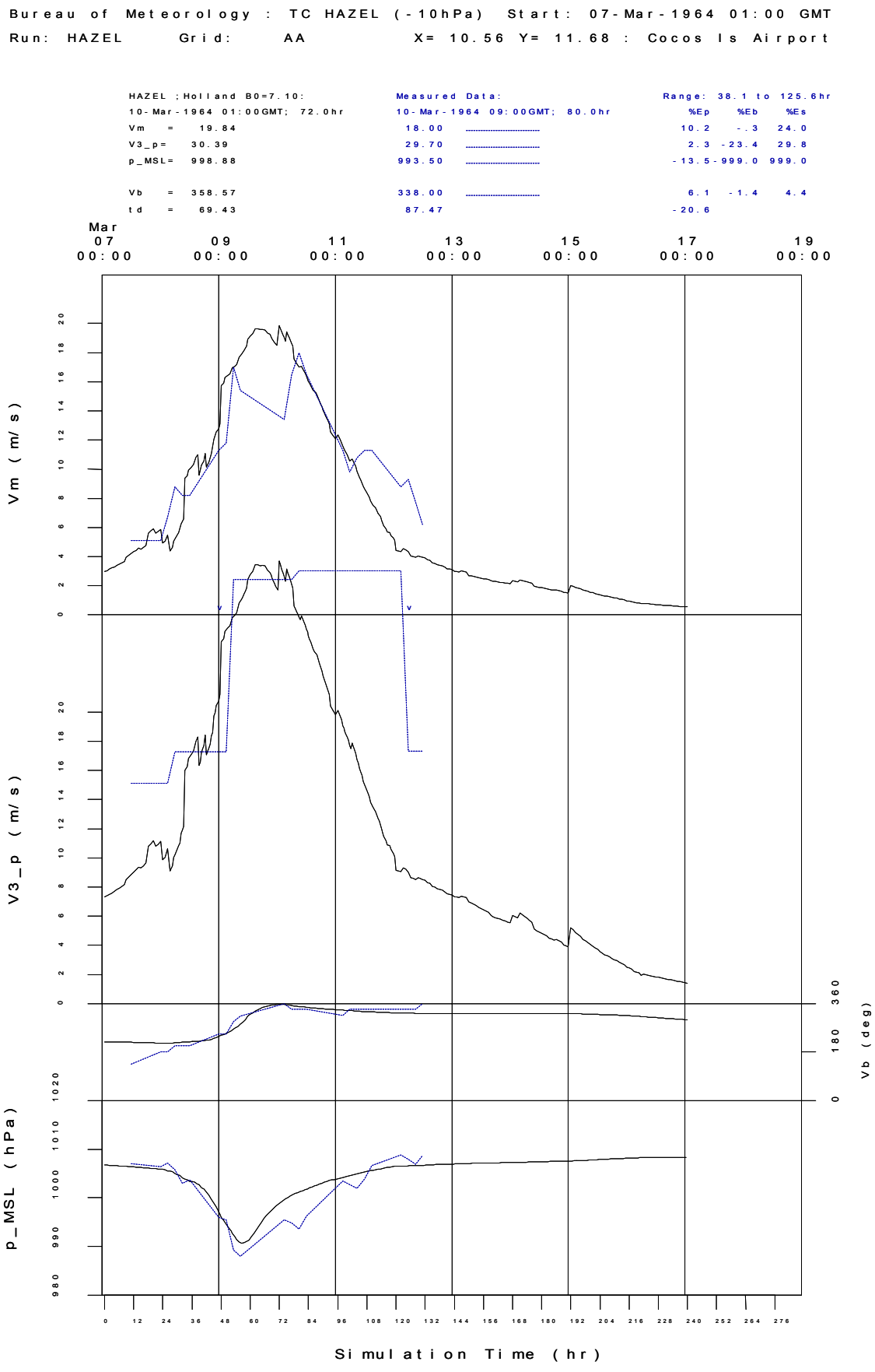
Bureau of Meteorology : TC HAZEL (-10hPa) Start: 07-Mar-1964 01:00 GMT
Run: HAZEL Grid: AA X= 10.56 Y= 11.68 : Cocos Is Airport
HAZEL ;Holland B0=7.10:
10-Mar-1964 01:00GMT; 72.0hr
Vm = 19.84
V3_p= 30.39
p_MSL= 998.88
Vb = 358.57
td = 69.43
Measured Data:
10-Mar-1964 09:00GMT; 80.0hr
18.00
29.70
993.50
338.00
87.47
Range: 38.1 to 125.6hr
%Ep %Eb %Es
10.2 -.3 24.0
2.3 -23.4 29.8
-13.5 -999.0 999.0
6.1 -1.4 4.4
-20.6
Mar
07 09 11 13 15 17 19
00:00 00:00 00:00 00:00 00:00 00:00 00:00
Vm (m/s)
V3_p (m/s)
p_MSL (hPa)
Vb (deg)
Simulation Time (hr)

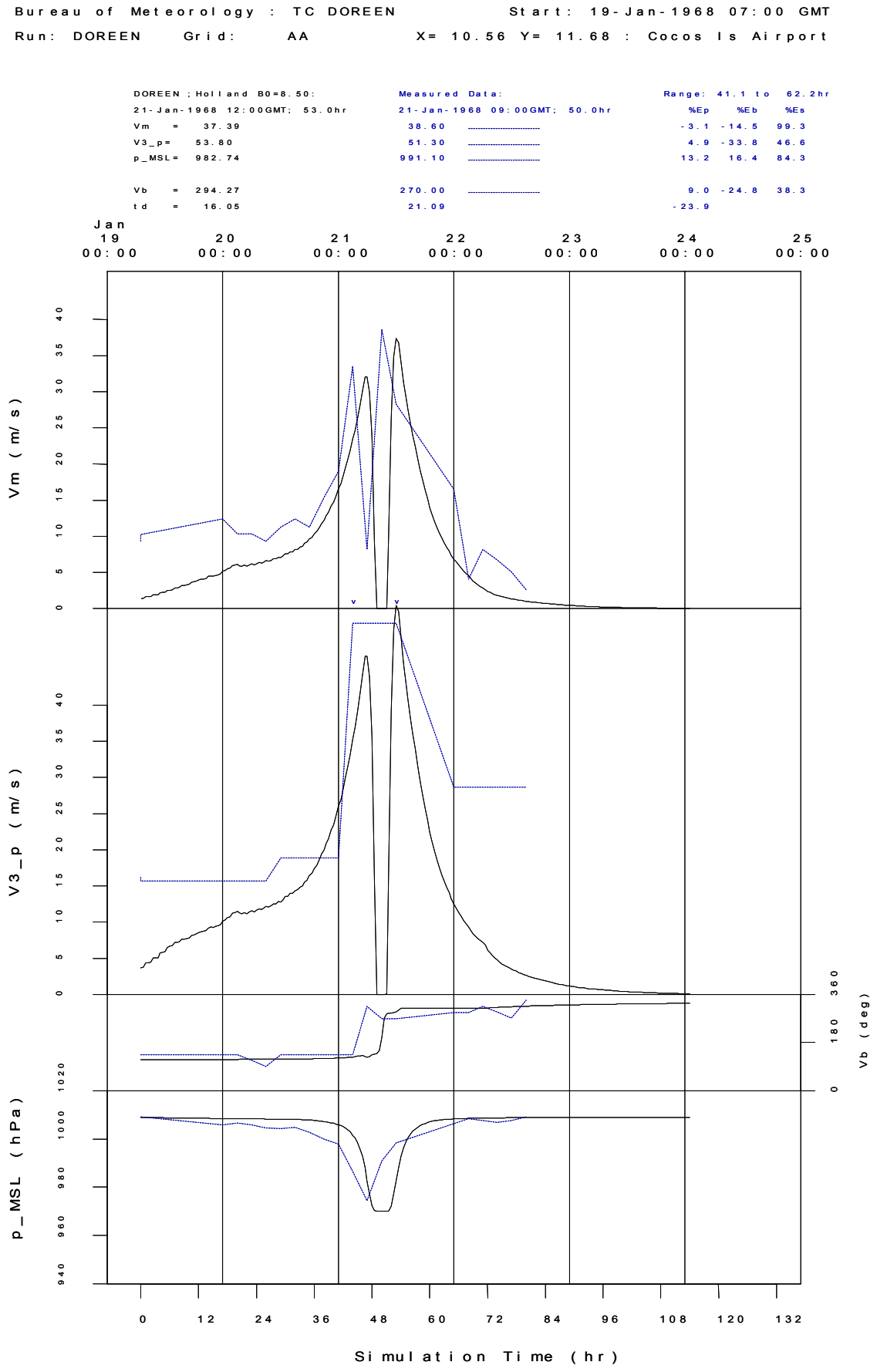
Bureau of Meteorology : TC DOREEN
Start: 19-Jan-1968 07:00 GMT
Run: DOREEN Grid: AA
X= 10.56 Y= 11.68 : Cocos Is Airport
DOREEN ; Holland B0=8.50:
21-Jan-1968 12:00GMT; 53.0hr
Vm = 37.39
V3_p= 53.80
p_MSL= 982.74
Vb = 294.27
td = 16.05
Measured Data:
21-Jan-1968 09:00GMT; 50.0hr
38.60
51.30
991.10
270.00
21.09
Range: 41.1 to 62.2hr
%Ep %Eb %Es
-3.1 -14.5 99.3
4.9 -33.8 46.6
13.2 16.4 84.3
9.0 -24.8 38.3
-23.9
Jan
19 00:00
20 00:00
21 00:00
22 00:00
23 00:00
24 00:00
25 00:00
Vm (m/s)
V3_p (m/s)
p_MSL (hPa)
Vb (deg)
0 5 10 15 20 25 30 35 40
940 960 980 1000 1020
0 180 360
0 12 24 36 48 60 72 84 96 108 120 132
Simulation Time (hr)

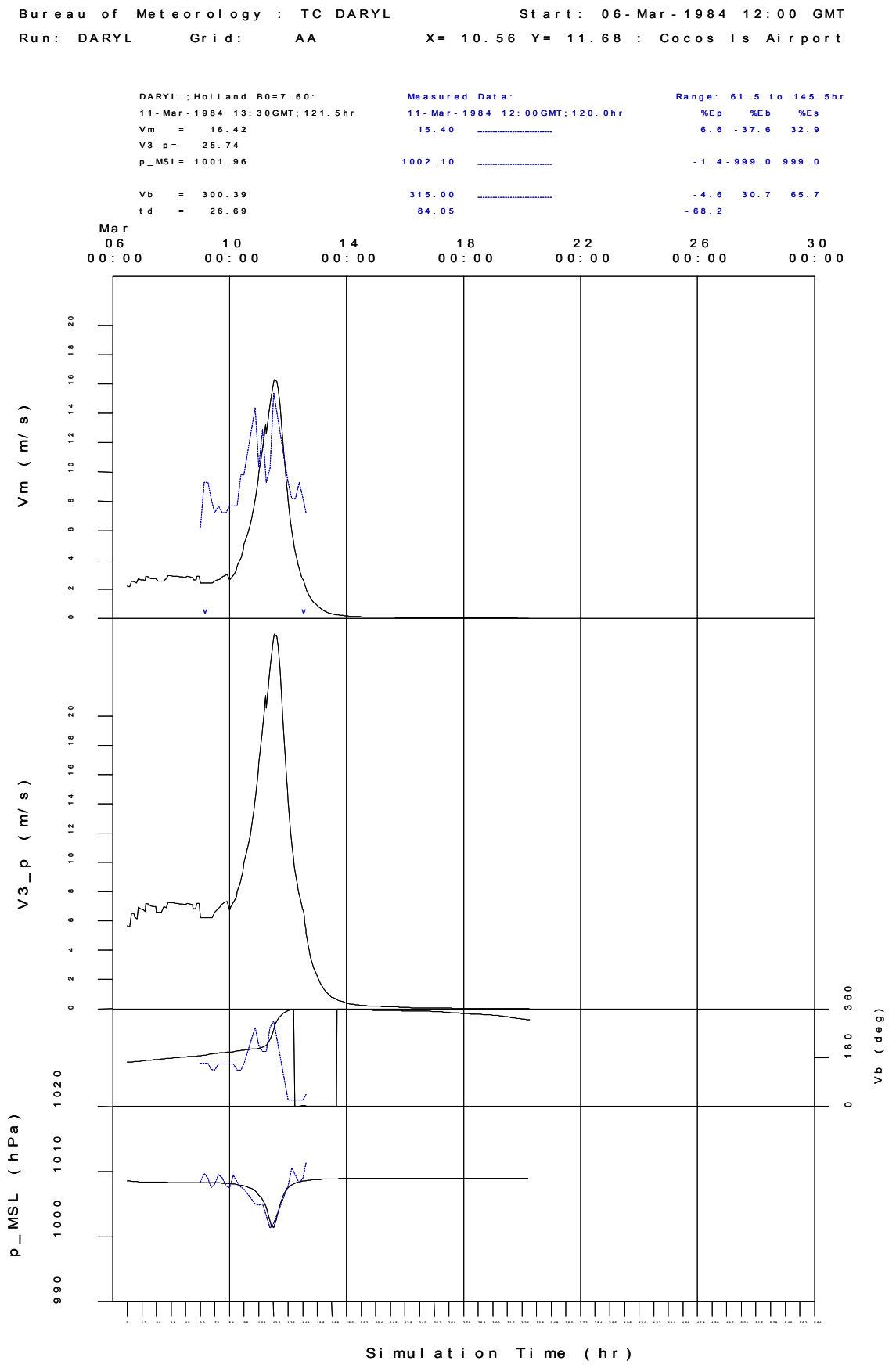
Bureau of Meteorology : TC DARYL
Start: 06-Mar-1984 12:00 GMT
Run: DARYL Grid: AA
X= 10.56 Y= 11.68 : Cocos Is Airport
DARYL ;Holland B0=7.60:
11-Mar-1984 13:30GMT;121.5hr
Vm = 16.42
V3_p= 25.74
p_MSL= 1001.96
Vb = 300.39
td = 26.69
Measured Data:
11-Mar-1984 12:00GMT;120.0hr
15.40
1002.10
315.00
84.05
Range: 61.5 to 145.5hr
%Ep %Eb %Es
6.6 -37.6 32.9
-1.4 -999.0 999.0
-4.6 30.7 65.7
-68.2
Mar
06 10 14 18 22 26 30
00:00 00:00 00:00 00:00 00:00 00:00 00:00
Vm (m/s)
V3_p (m/s)
p_MSL (hPa)
Vb (deg)
Simulation Time (hr)

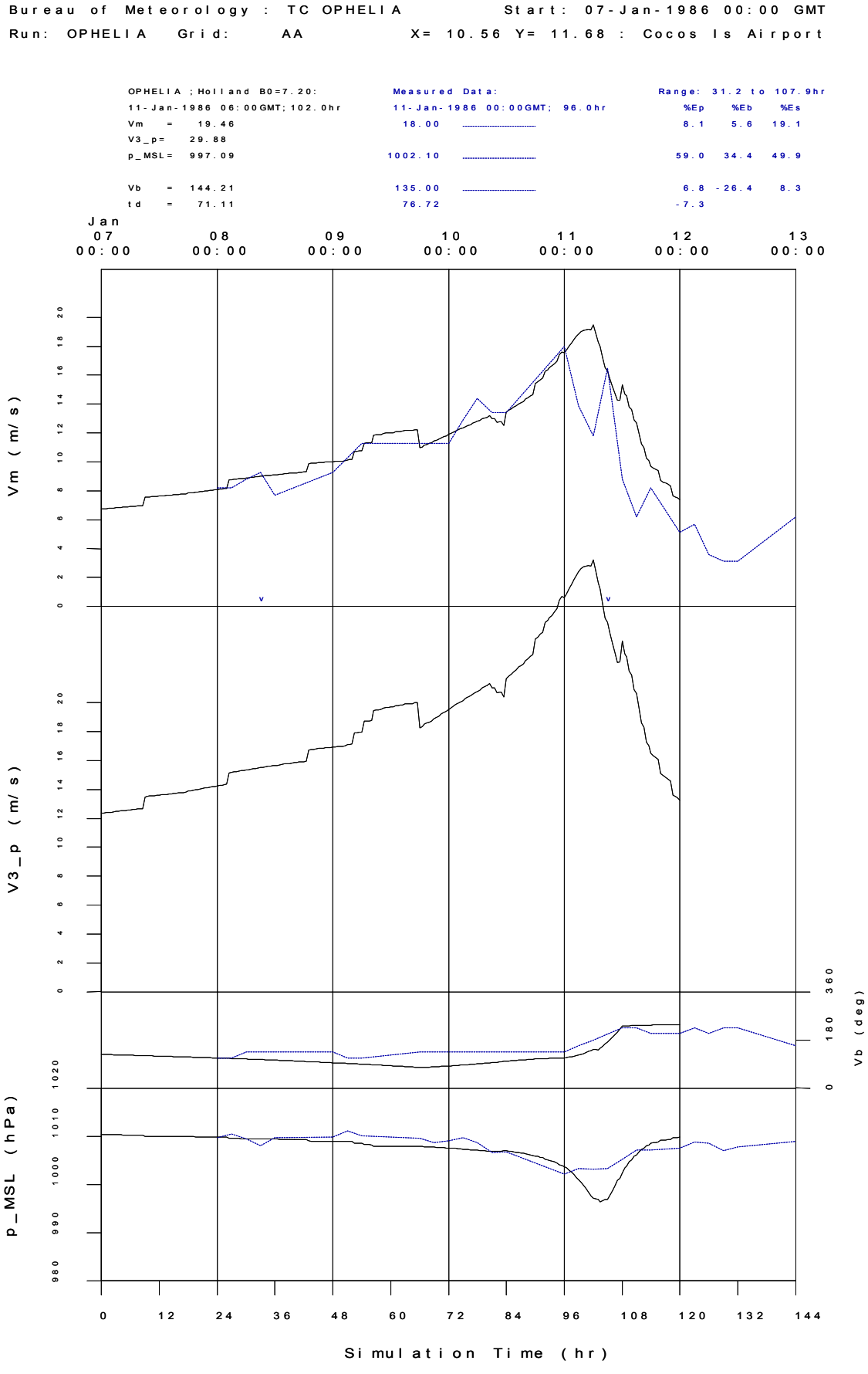
Bureau of Meteorology : TC OPHELIA Start: 07-Jan-1986 00:00 GMT
Run: OPHELIA Grid: AA X= 10.56 Y= 11.68 : Cocos Is Airport
OPHELIA ; Holland B0=7.20:
11-Jan-1986 06:00GMT; 102.0hr
Vm = 19.46
V3_p= 29.88
p_MSL= 997.09
Vb = 144.21
td = 71.11
Measured Data:
11-Jan-1986 00:00GMT; 96.0hr
18.00
1002.10
135.00
76.72
Range: 31.2 to 107.9hr
%Ep %Eb %Es
8.1 5.6 19.1
59.0 34.4 49.9
6.8 -26.4 8.3
-7.3
Jan
07 00:00
08 00:00
09 00:00
10 00:00
11 00:00
12 00:00
13 00:00
Vm (m/s)
V3_p (m/s)
p_MSL (hPa)
Vb (deg)
Simulation Time (hr)

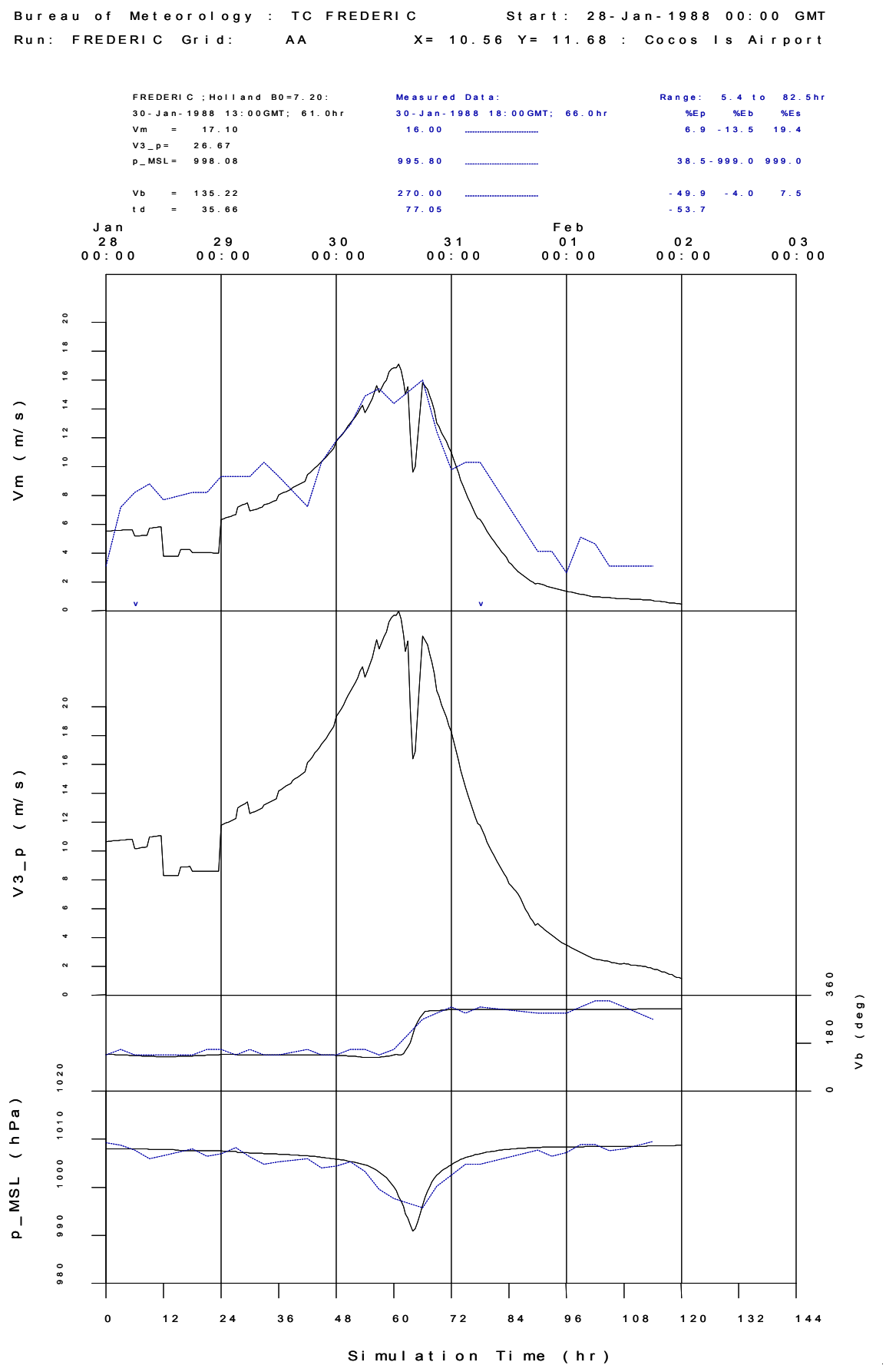
Bureau of Meteorology : TC FREDERIC Start: 28-Jan-1988 00:00 GMT
Run: FREDERIC Grid: AA X= 10.56 Y= 11.68 : Cocos Is Airport
FREDERIC ;Holland B0=7.20:
30-Jan-1988 13:00GMT; 61.0hr
Vm = 17.10
V3_p= 26.67
p_MSL= 998.08
Vb = 135.22
td = 35.66
Measured Data:
30-Jan-1988 18:00GMT; 66.0hr
16.00
995.80
270.00
77.05
Range: 5.4 to 82.5hr
%Ep %Eb %Es
6.9 -13.5 19.4
38.5 999.0 999.0
-49.9 -4.0 7.5
-53.7
Jan
28 00:00
29 00:00
30 00:00
31 00:00
Feb
01 00:00
02 00:00
03 00:00
Vm (m/s)
V3_p (m/s)
p_MSL (hPa)
Vb (deg)
0 2 4 6 8 10 12 14 16 18 20
980 990 1000 1010 1020
0 180 360
0 12 24 36 48 60 72 84 96 108 120 132 144
Simulation Time (hr)

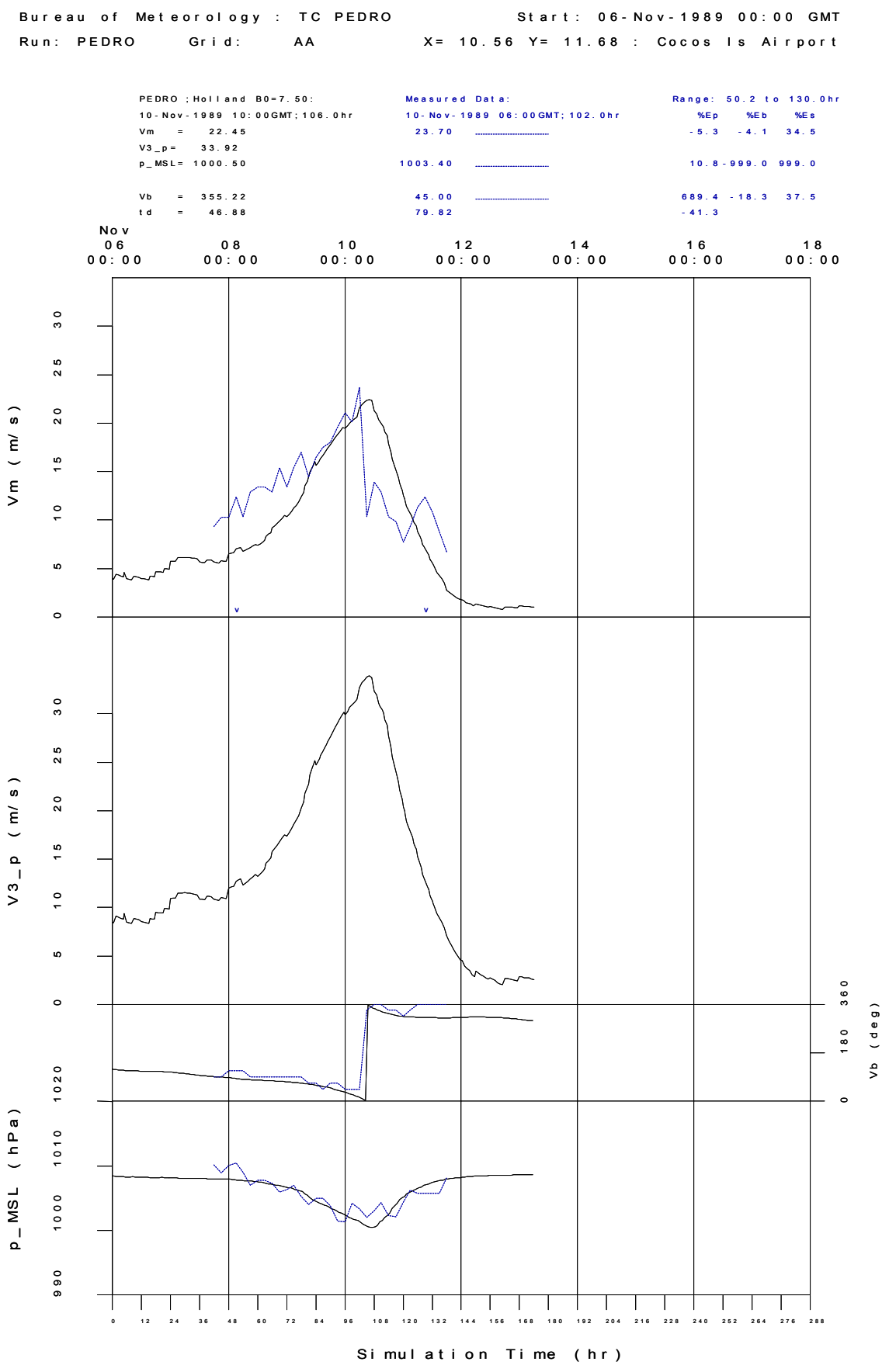
Bureau of Meteorology : TC PEDRO
Start: 06-Nov-1989 00:00 GMT
Run: PEDRO Grid: AA
X= 10.56 Y= 11.68 : Cocos Is Airport
PEDRO ; Holland B0=7.50:
10-Nov-1989 10:00GMT; 106.0hr
Vm = 22.45
V3_p= 33.92
p_MSL= 1000.50
Vb = 355.22
td = 46.88
Measured Data:
10-Nov-1989 06:00GMT; 102.0hr
23.70
1003.40
45.00
79.82
Range: 50.2 to 130.0hr
%Ep %Eb %Es
-5.3 -4.1 34.5
10.8 -999.0 999.0
689.4 -18.3 37.5
-41.3
Nov
06 00:00
08 00:00
10 00:00
12 00:00
14 00:00
16 00:00
18 00:00
Vm (m/s)
V3_p (m/s)
p_MSL (hPa)
Vb (deg)
Simulation Time (hr)

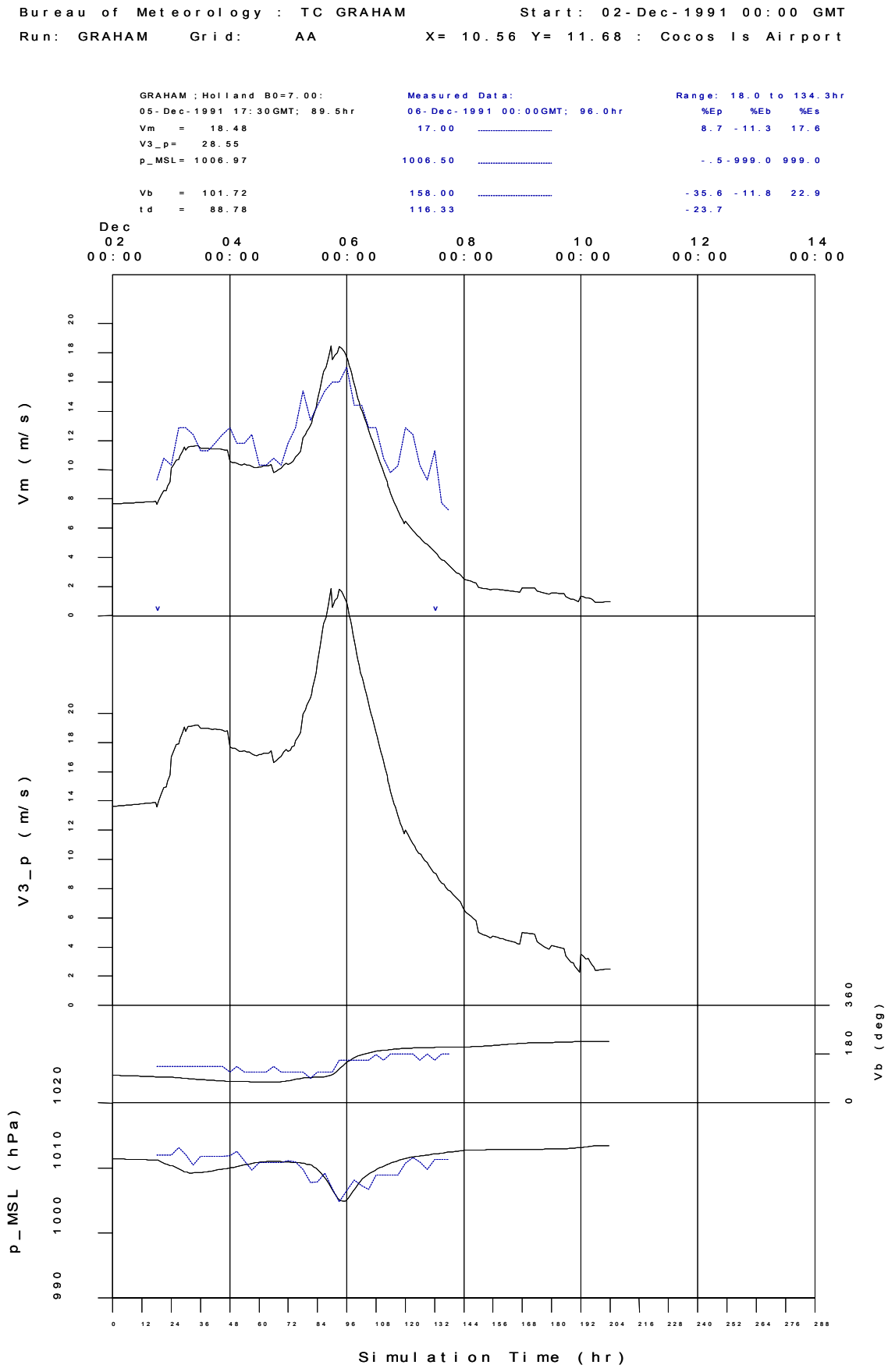
Bureau of Meteorology : TC GRAHAM
Start: 02-Dec-1991 00:00 GMT
Run: GRAHAM Grid: AA
X= 10.56 Y= 11.68 : Cocos Is Airport
GRAHAM ; Holland B0=7.00:
05-Dec-1991 17:30GMT; 89.5hr
Vm = 18.48
V3_p= 28.55
p_MSL= 1006.97
Vb = 101.72
td = 88.78
Measured Data:
06-Dec-1991 00:00GMT; 96.0hr
17.00
1006.50
158.00
116.33
Range: 18.0 to 134.3hr
%Ep %Eb %Es
8.7 -11.3 17.6
--.5-999.0 999.0
-35.6 -11.8 22.9
-23.7
Dec
02 00:00
04 00:00
06 00:00
08 00:00
10 00:00
12 00:00
14 00:00
Vm (m/s)
V3_p (m/s)
p_MSL (hPa)
Vb (deg)
Simulation Time (hr)

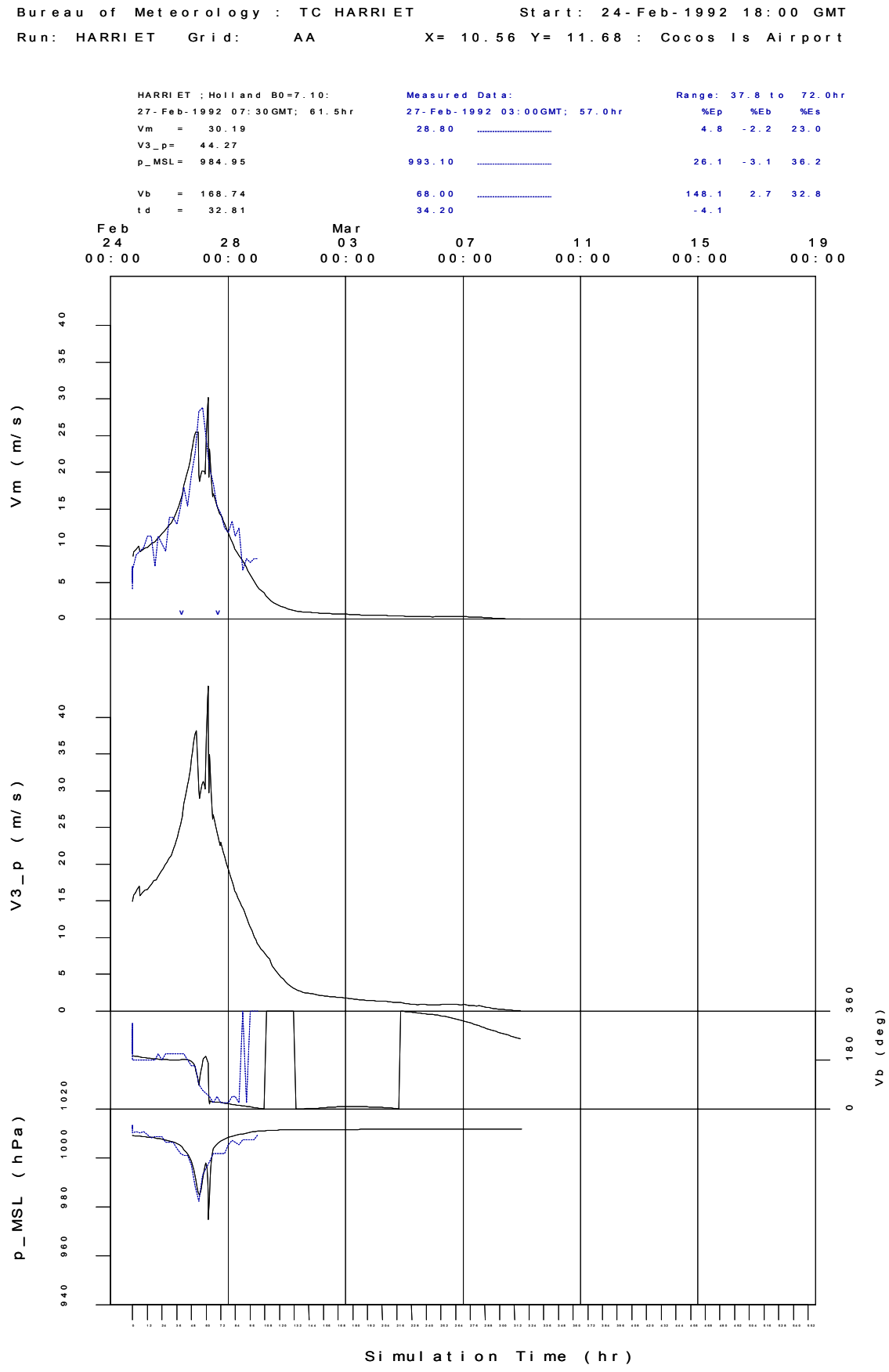
Bureau of Meteorology : TC HARRIET Start: 24-Feb-1992 18:00 GMT
Run: HARRIET Grid: AA X= 10.56 Y= 11.68 : Cocos Is Airport
HARRIET ; Holland B0=7.10:
27-Feb-1992 07:30GMT; 61.5hr
Vm = 30.19
V3_p= 44.27
p_MSL= 984.95
Vb = 168.74
td = 32.81
Measured Data:
27-Feb-1992 03:00GMT; 57.0hr
28.80
993.10
68.00
34.20
Range: 37.8 to 72.0hr
%Ep %Eb %Es
4.8 -2.2 23.0
26.1 -3.1 36.2
148.1 2.7 32.8
-4.1
Feb
24 28 Mar 03 07 11 15 19
00:00 00:00 00:00 00:00 00:00 00:00 00:00
Vm (m/s)
V3_p (m/s)
p_MSL (hPa)
Vb (deg)
Simulation Time (hr)

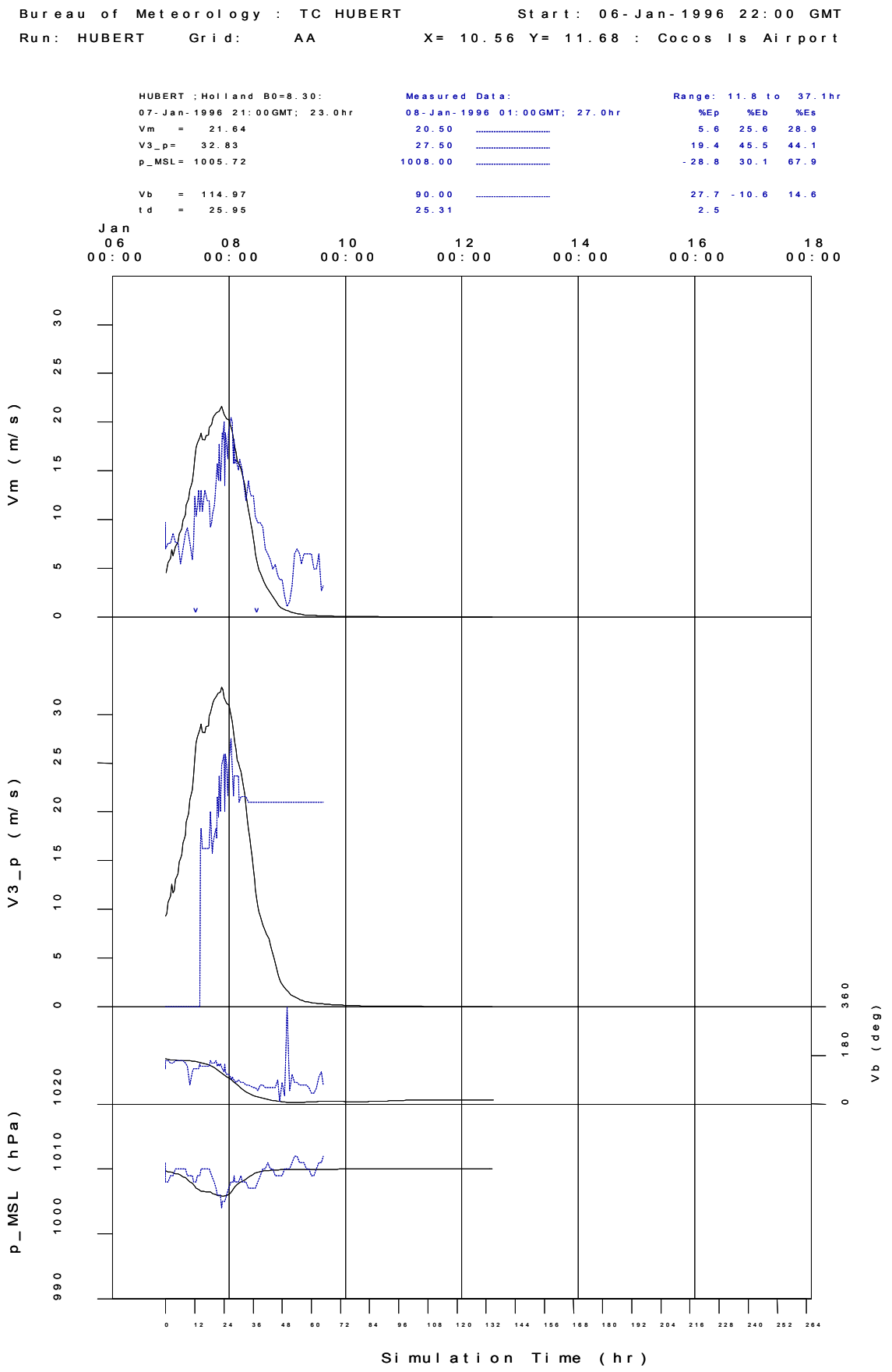
Bureau of Meteorology : TC HUBERT
Start: 06-Jan-1996 22:00 GMT
Run: HUBERT Grid: AA
X= 10.56 Y= 11.68 : Cocos Is Airport
HUBERT ;Holland B0=8.30:
07-Jan-1996 21:00GMT; 23.0hr
Vm = 21.64
V3_p= 32.83
p_MSL= 1005.72
Vb = 114.97
td = 25.95
Measured Data:
08-Jan-1996 01:00GMT; 27.0hr
20.50
27.50
1008.00
90.00
25.31
Range: 11.8 to 37.1hr
%Ep %Eb %Es
5.6 25.6 28.9
19.4 45.5 44.1
-28.8 30.1 67.9
27.7 -10.6 14.6
2.5
Jan
06 00:00
08 00:00
10 00:00
12 00:00
14 00:00
16 00:00
18 00:00
Vm (m/s)
V3_p (m/s)
p_MSL (hPa)
Vb (deg)
Simulation Time (hr)

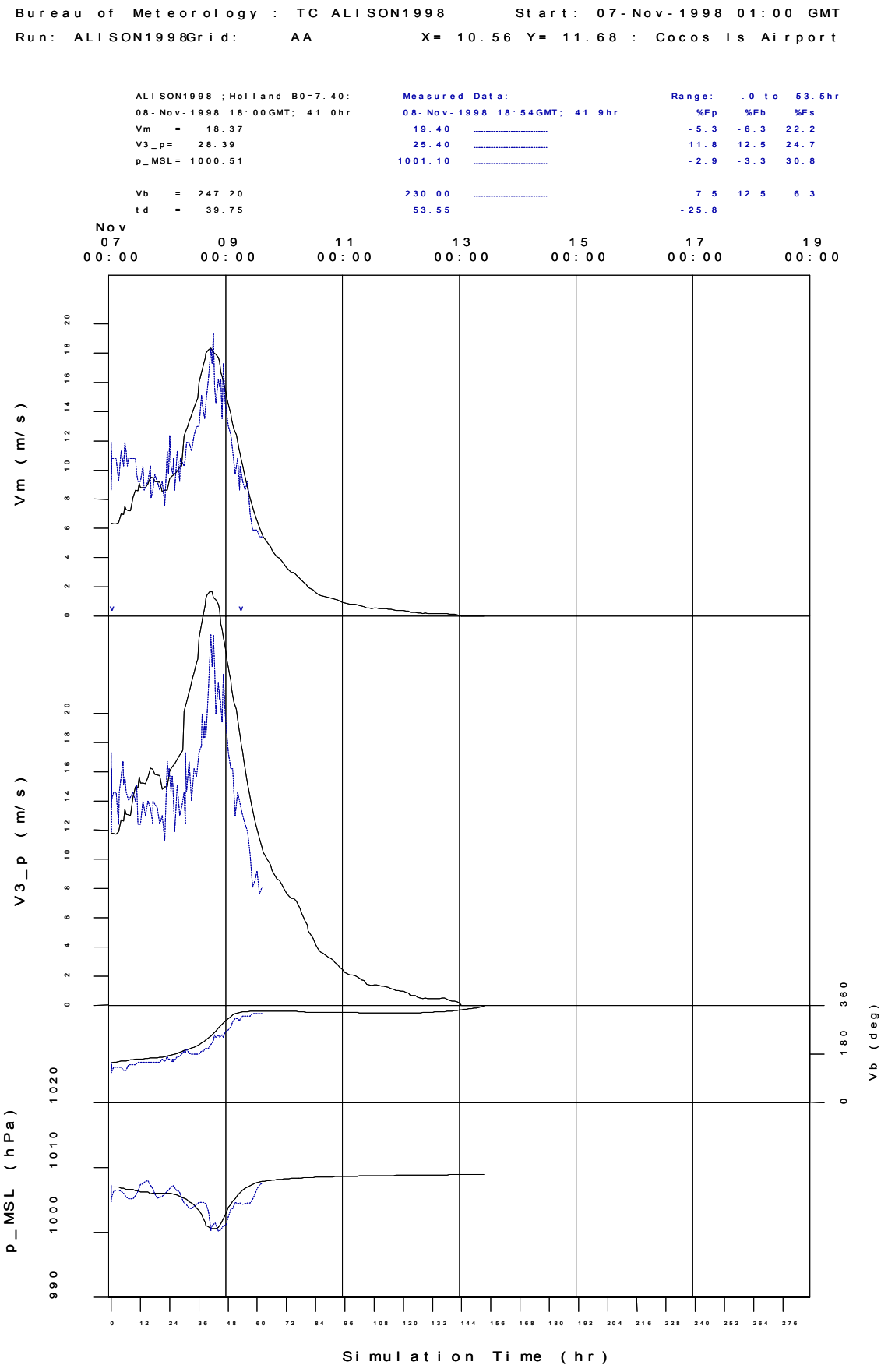
Bureau of Meteorology : TC ALISON1998 Start: 07-Nov-1998 01:00 GMT
Run: ALISON1998Grid: AA X= 10.56 Y= 11.68 : Cocos Is Airport
ALISON1998 ;Holland B0=7.40:
08-Nov-1998 18:00GMT; 41.0hr
Vm = 18.37
V3_p= 28.39
p_MSL= 1000.51
Vb = 247.20
td = 39.75
Measured Data:
08-Nov-1998 18:54GMT; 41.9hr
19.40
25.40
1001.10
230.00
53.55
Range: .0 to 53.5hr
%Ep %Eb %Es
-5.3 -6.3 22.2
11.8 12.5 24.7
-2.9 -3.3 30.8
7.5 12.5 6.3
-25.8
Nov
07 00:00
09 00:00
11 00:00
13 00:00
15 00:00
17 00:00
19 00:00
Vm (m/s)
V3_p (m/s)
p_MSL (hPa)
Vb (deg)
Simulation Time (hr)

APPENDIX I

2D SURGE MODEL COMPARISONS

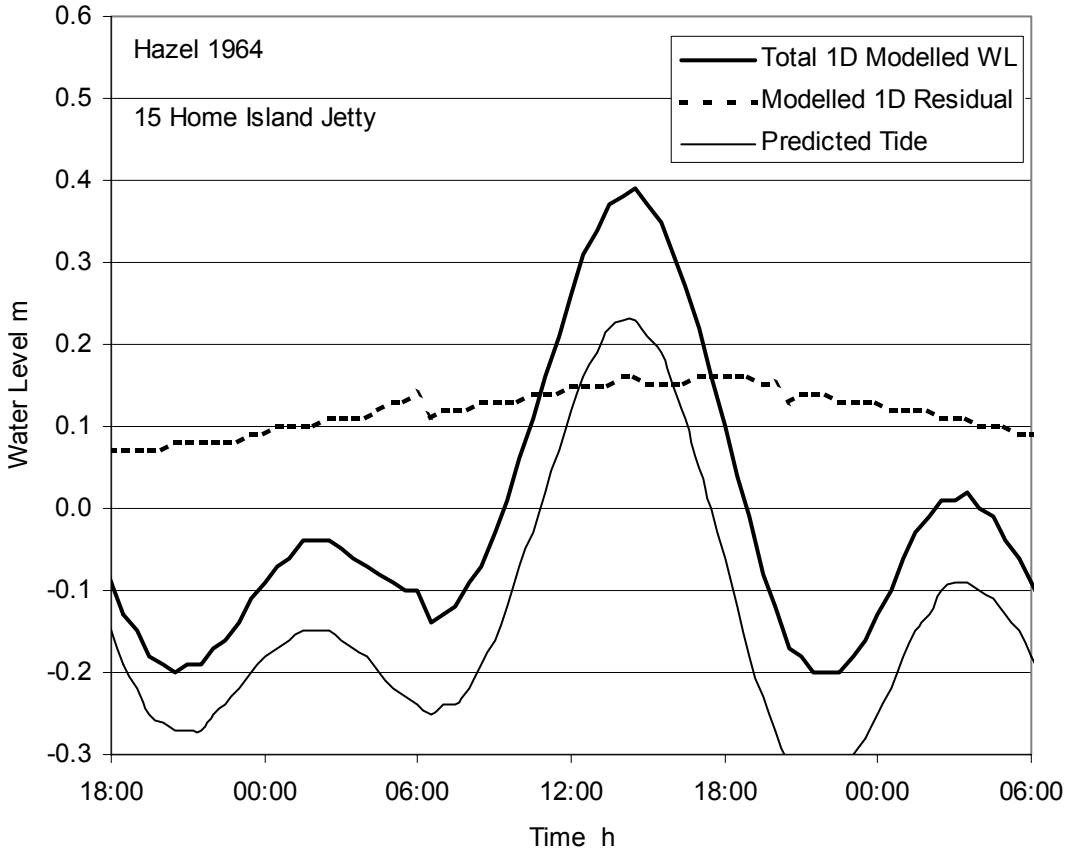
Hazel 1964
15 Home Island Jetty
Total 1D Modelled WL
Modelled 1D Residual
Predicted Tide
Water Level m
0.6
0.5
0.4
0.3
0.2
0.1
0.0
-0.1
-0.2
-0.3
18:00
00:00
06:00
12:00
18:00
00:00
06:00
Time h

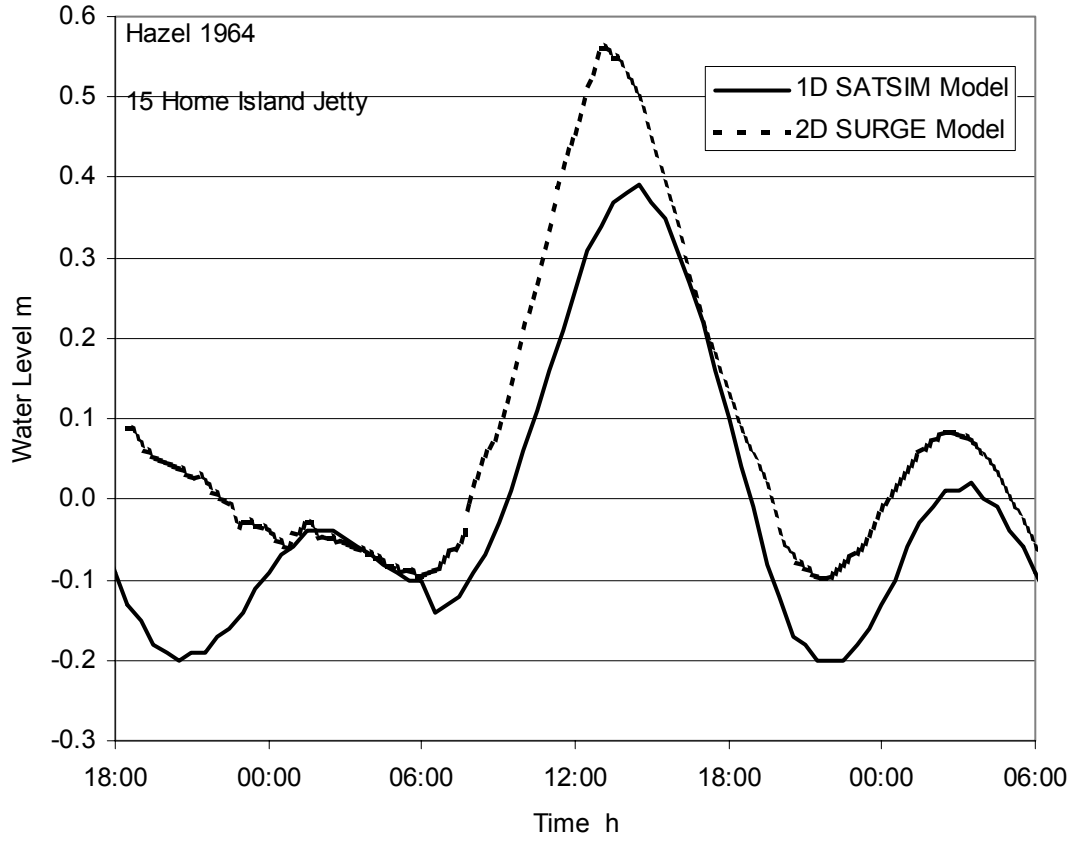
Hazel 1964
15 Home Island Jetty
1D SATSIM Model
2D SURGE Model
Water Level m
0.6
0.5
0.4
0.3
0.2
0.1
0.0
-0.1
-0.2
-0.3
18:00
00:00
06:00
12:00
18:00
00:00
06:00
Time h

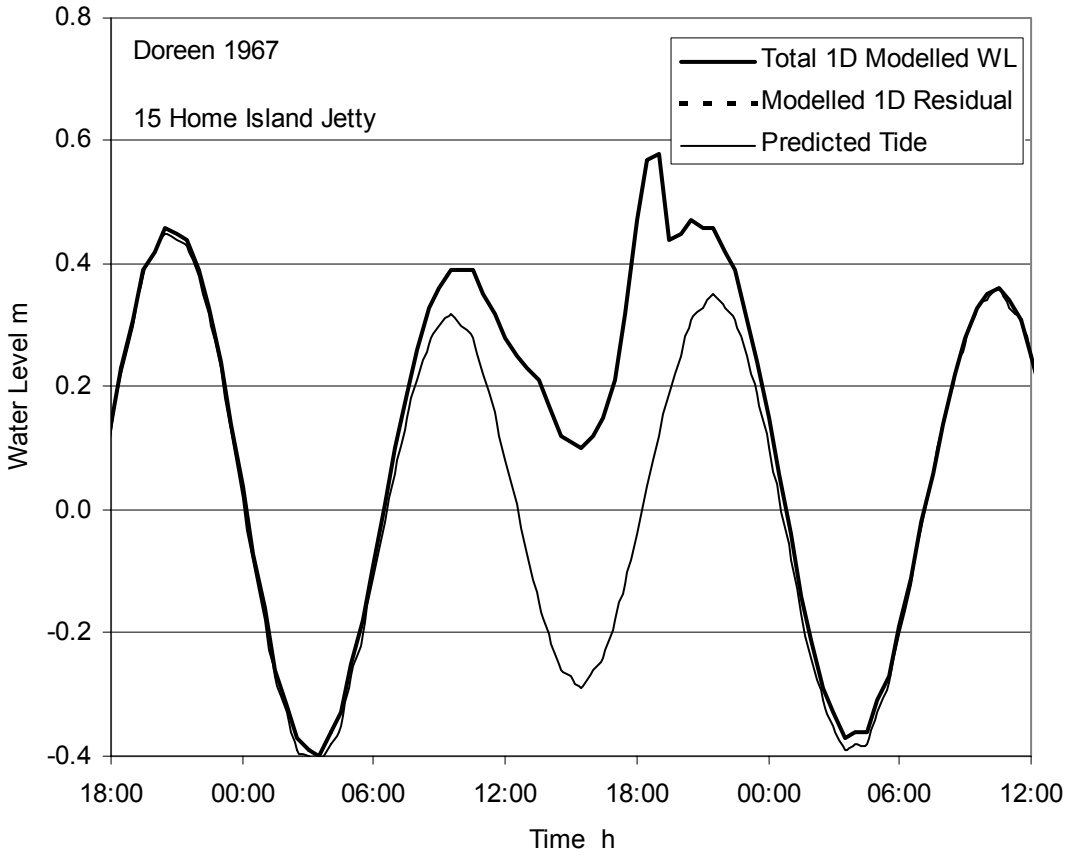
Doreen 1967
15 Home Island Jetty
Total 1D Modelled WL
Modelled 1D Residual
Predicted Tide
Water Level m
0.8
0.6
0.4
0.2
0.0
-0.2
-0.4
18:00
00:00
06:00
12:00
18:00
00:00
06:00
12:00
Time h

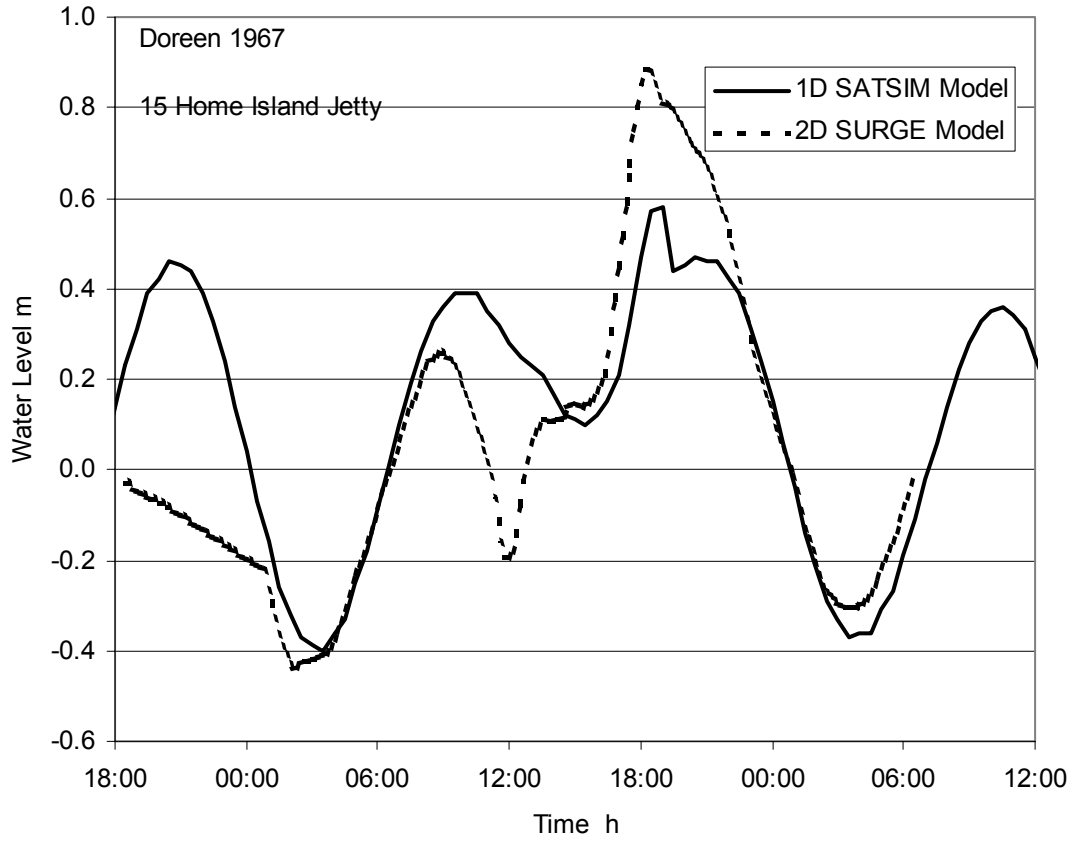
Doreen 1967
15 Home Island Jetty
1D SATSIM Model
2D SURGE Model
Water Level m
1.0
0.8
0.6
0.4
0.2
0.0
-0.2
-0.4
-0.6
18:00
00:00
06:00
12:00
18:00
00:00
06:00
12:00
Time h

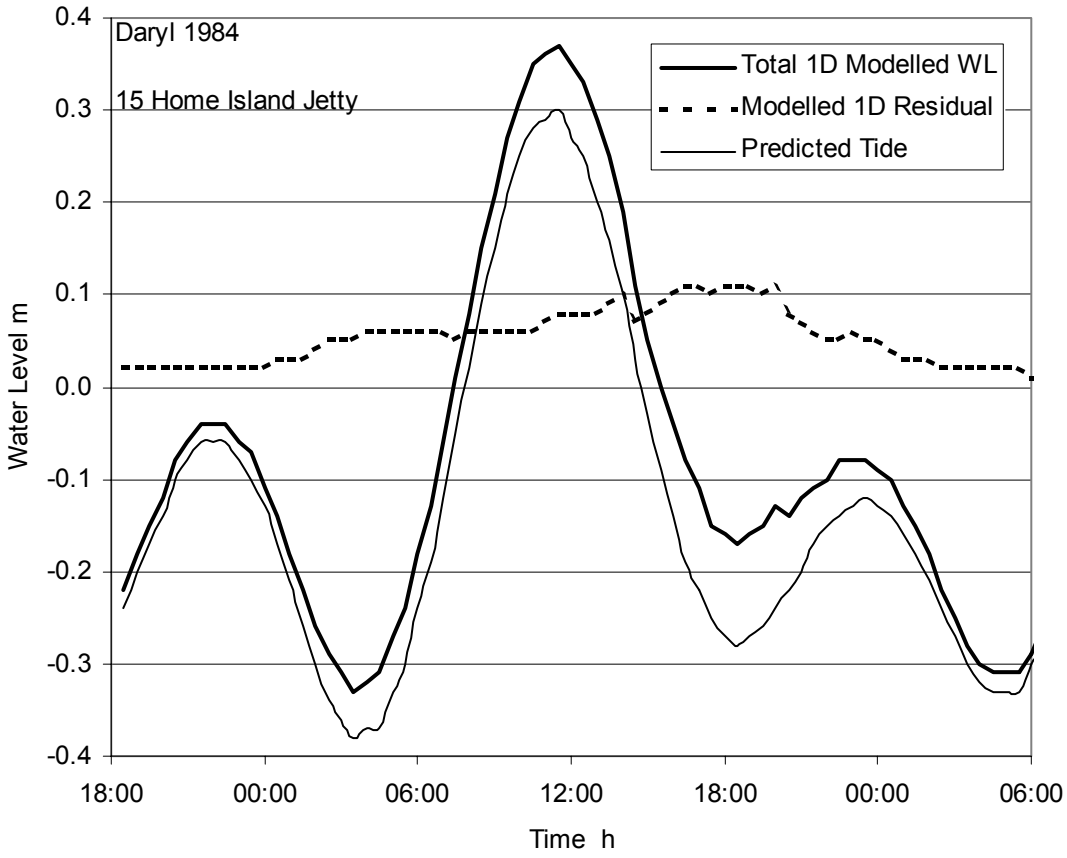
Daryl 1984
15 Home Island Jetty
Total 1D Modelled WL
Modelled 1D Residual
Predicted Tide
Water Level m
0.4
0.3
0.2
0.1
0.0
-0.1
-0.2
-0.3
-0.4
18:00
00:00
06:00
12:00
18:00
00:00
06:00
Time h

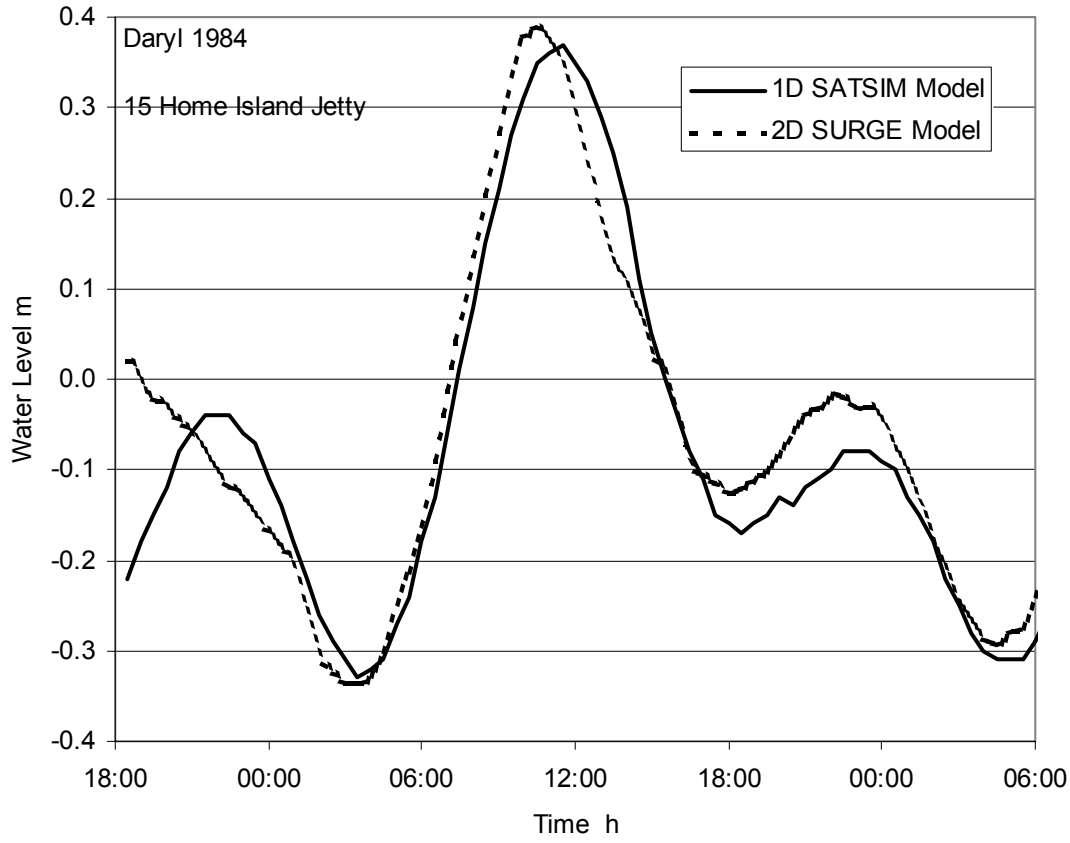
Daryl 1984
15 Home Island Jetty
1D SATSIM Model
2D SURGE Model
Water Level m
0.4
0.3
0.2
0.1
0.0
-0.1
-0.2
-0.3
-0.4
18:00
00:00
06:00
12:00
18:00
00:00
06:00
Time h

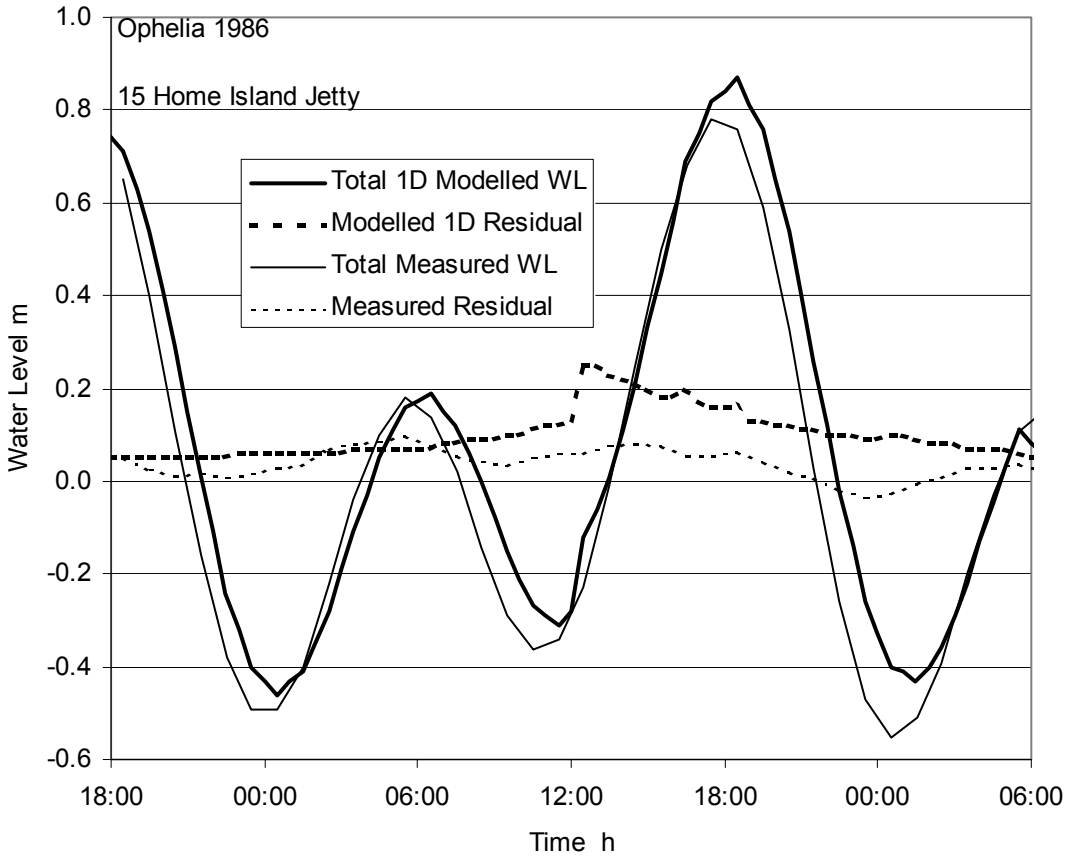
Ophelia 1986
15 Home Island Jetty
Total 1D Modelled WL
Modelled 1D Residual
Total Measured WL
Measured Residual
Water Level m
1.0
0.8
0.6
0.4
0.2
0.0
-0.2
-0.4
-0.6
18:00
00:00
06:00
12:00
18:00
00:00
06:00
Time h

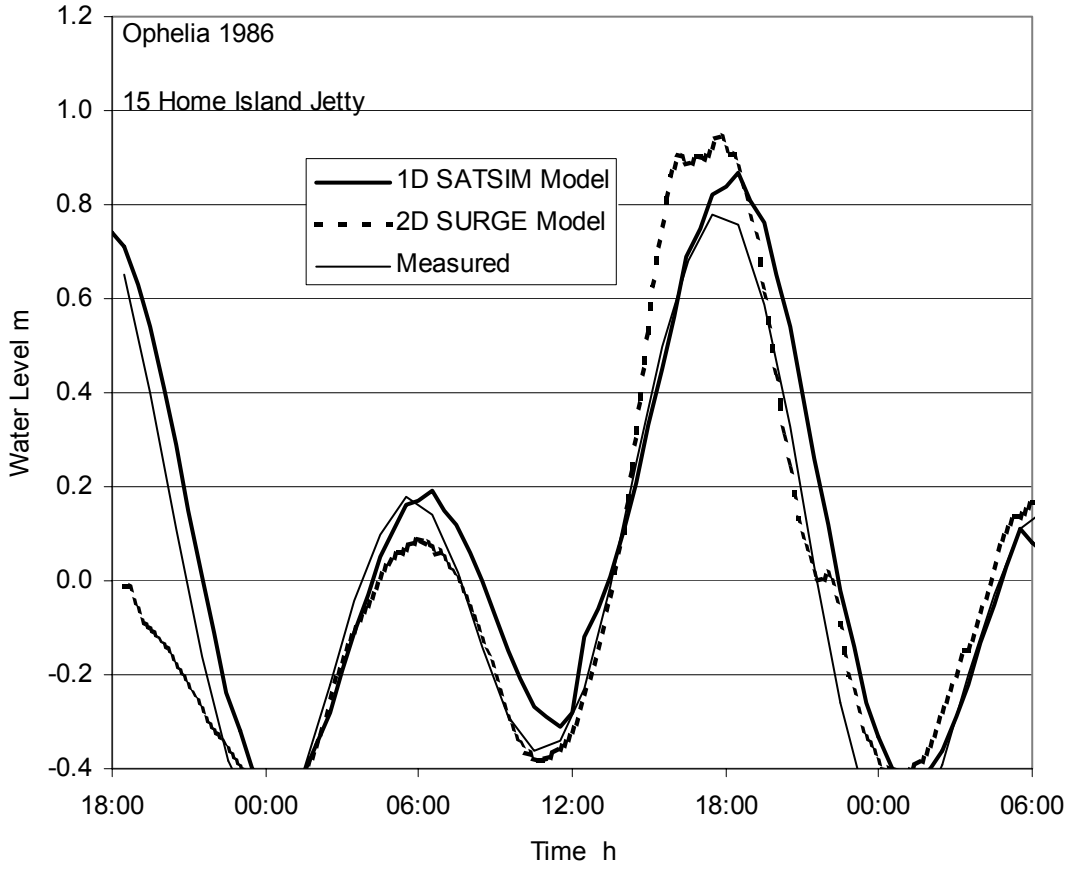
Ophelia 1986
15 Home Island Jetty
1D SATSIM Model
2D SURGE Model
Measured
Water Level m
1.2
1.0
0.8
0.6
0.4
0.2
0.0
-0.2
-0.4
18:00
00:00
06:00
12:00
18:00
00:00
06:00
Time h

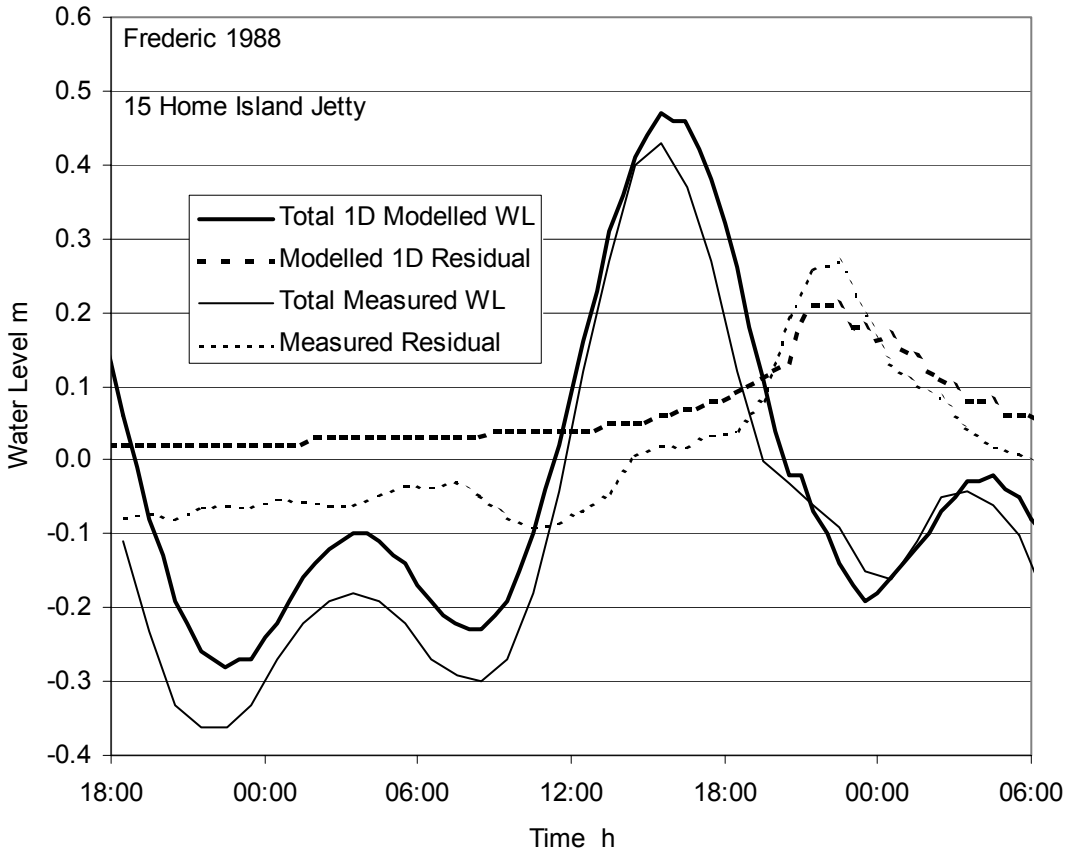
Frederic 1988
15 Home Island Jetty
Total 1D Modelled WL
Modelled 1D Residual
Total Measured WL
Measured Residual
Water Level m
0.6
0.5
0.4
0.3
0.2
0.1
0.0
-0.1
-0.2
-0.3
-0.4
18:00
00:00
06:00
12:00
18:00
00:00
06:00
Time h

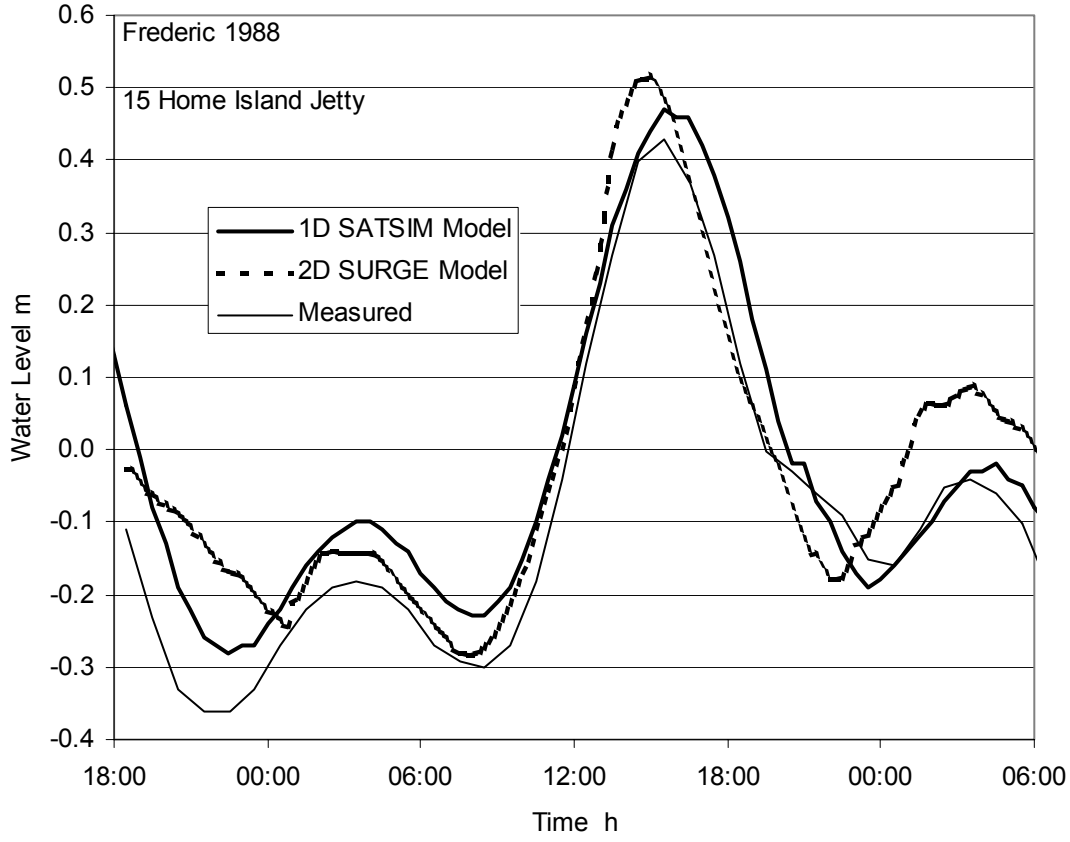
Frederic 1988
15 Home Island Jetty
1D SATSIM Model
2D SURGE Model
Measured
Water Level m
0.6
0.5
0.4
0.3
0.2
0.1
0.0
-0.1
-0.2
-0.3
-0.4
18:00
00:00
06:00
12:00
18:00
00:00
06:00
Time h

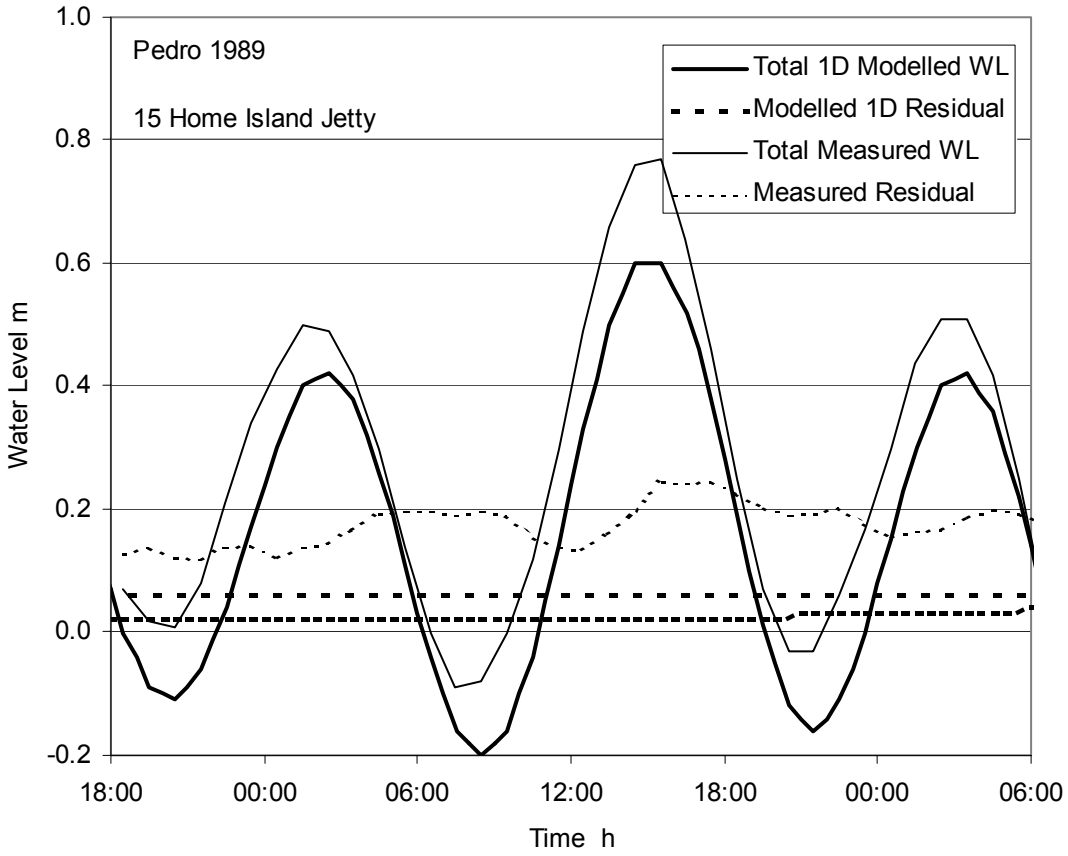
Pedro 1989
15 Home Island Jetty
Total 1D Modelled WL
Modelled 1D Residual
Total Measured WL
Measured Residual
Water Level m
1.0
0.8
0.6
0.4
0.2
0.0
-0.2
18:00
00:00
06:00
12:00
18:00
00:00
06:00
Time h

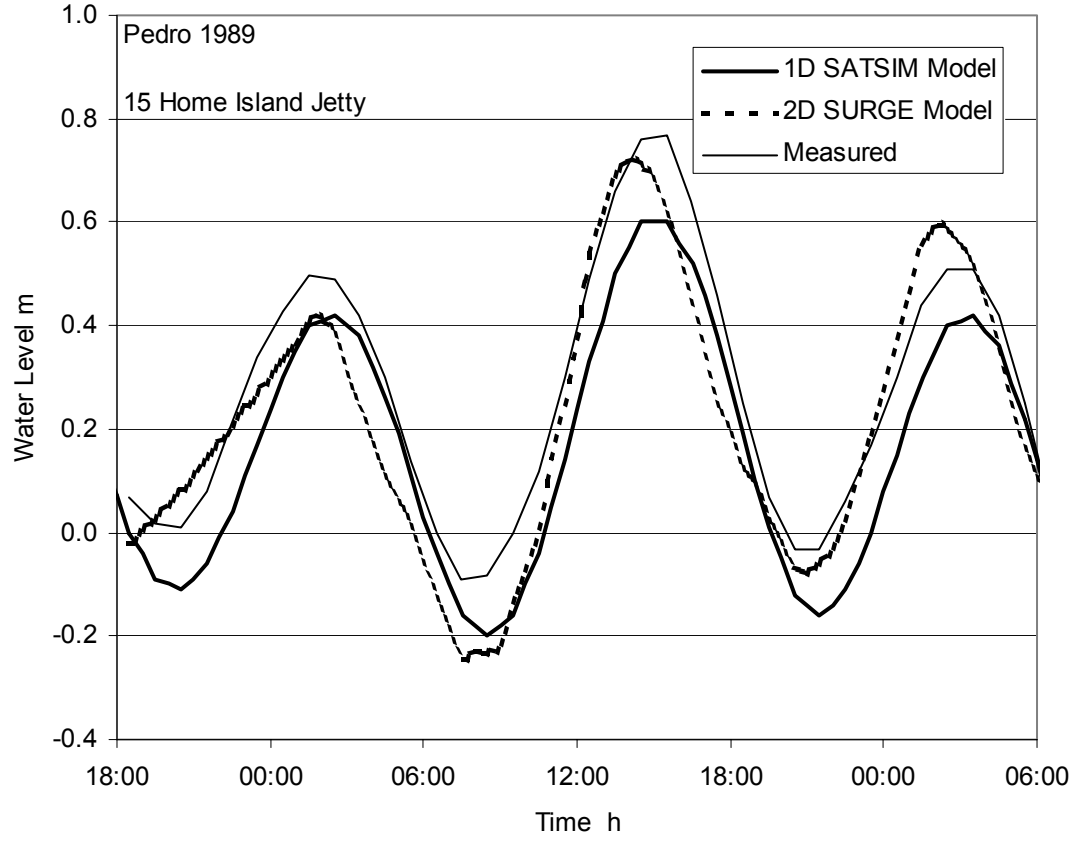
Pedro 1989
15 Home Island Jetty
1D SATSIM Model
2D SURGE Model
Measured
Water Level m
1.0
0.8
0.6
0.4
0.2
0.0
-0.2
-0.4
18:00
00:00
06:00
12:00
18:00
00:00
06:00
Time h

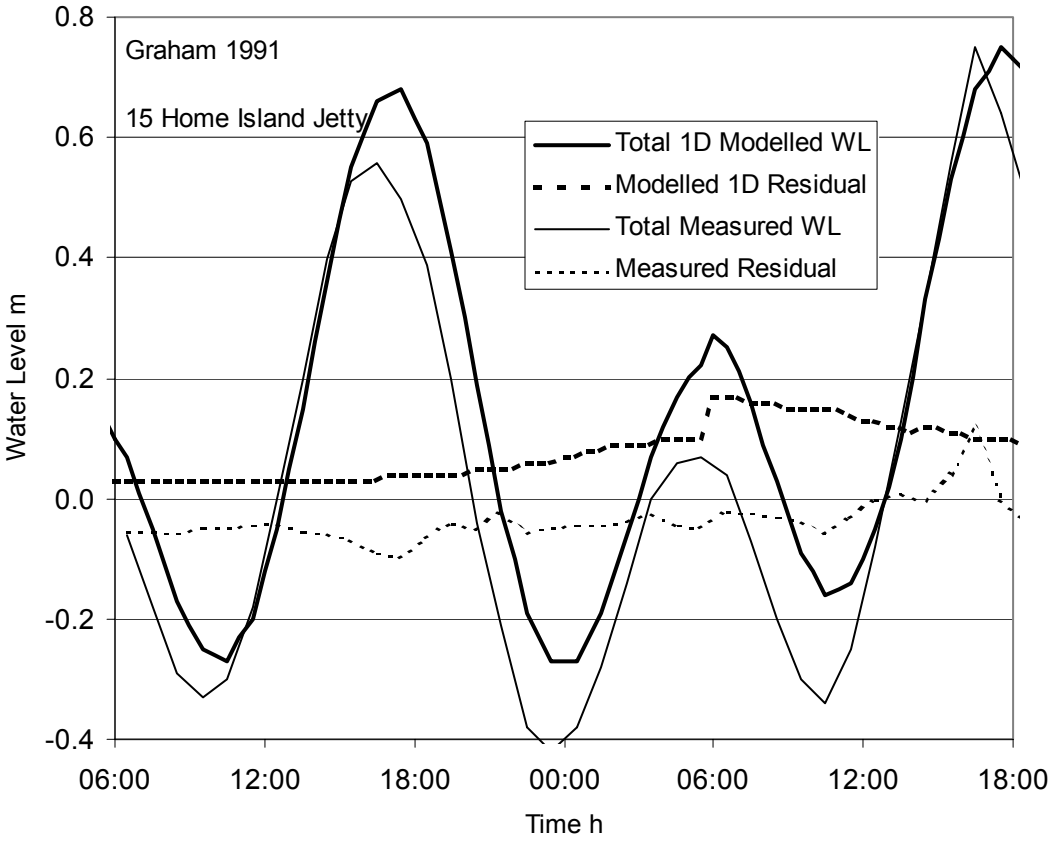
Graham 1991
15 Home Island Jetty
Total 1D Modelled WL
Modelled 1D Residual
Total Measured WL
Measured Residual
Water Level m
0.8
0.6
0.4
0.2
0.0
-0.2
-0.4
06:00
12:00
18:00
00:00
06:00
12:00
18:00
Time h

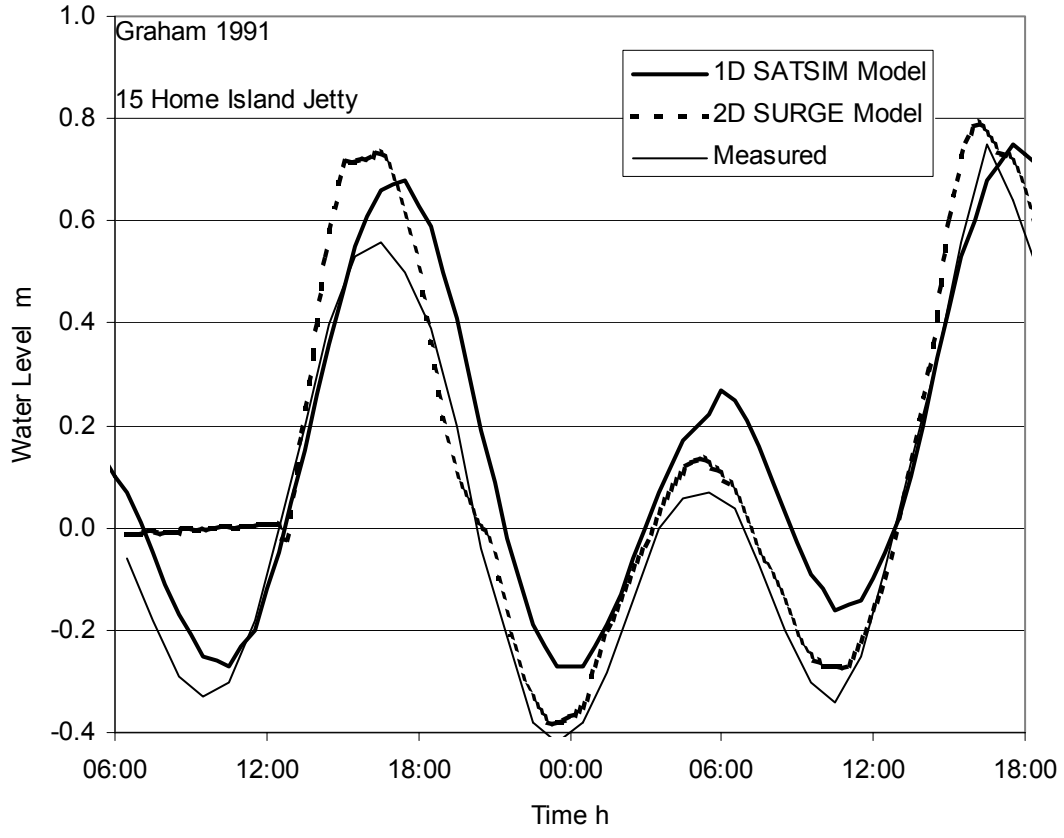
Graham 1991
15 Home Island Jetty
1D SATSIM Model
2D SURGE Model
Measured
Water Level m
1.0
0.8
0.6
0.4
0.2
0.0
-0.2
-0.4
06:00
12:00
18:00
00:00
06:00
12:00
18:00
Time h

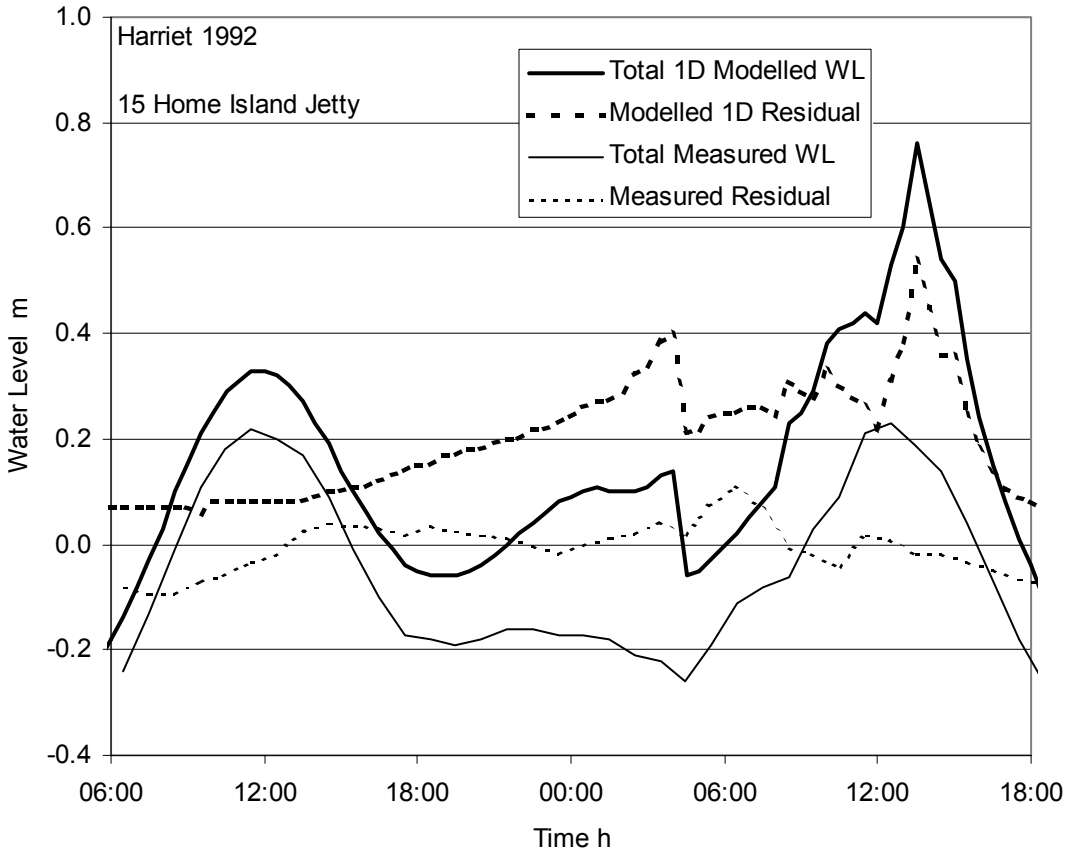
Harriet 1992
15 Home Island Jetty
Total 1D Modelled WL
Modelled 1D Residual
Total Measured WL
Measured Residual
Water Level m
1.0
0.8
0.6
0.4
0.2
0.0
-0.2
-0.4
06:00
12:00
18:00
00:00
06:00
12:00
18:00
Time h

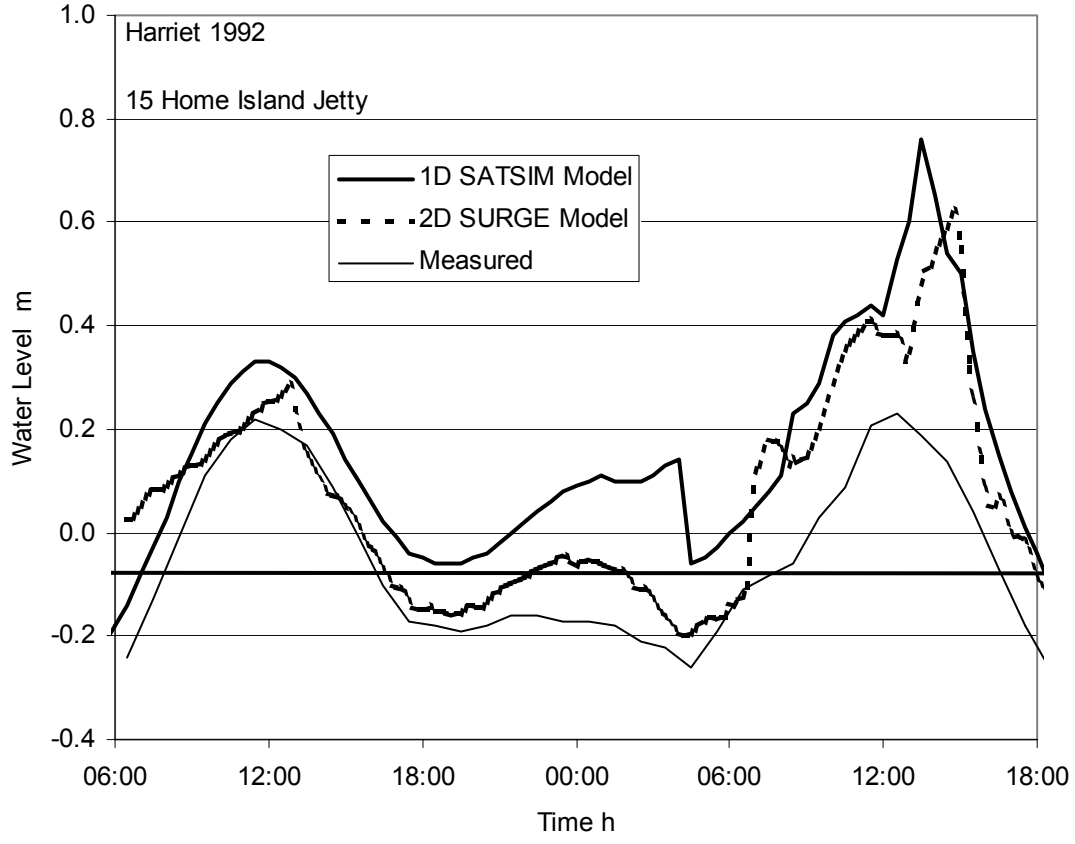
Harriet 1992
15 Home Island Jetty
1D SATSIM Model
2D SURGE Model
Measured
Water Level m
1.0
0.8
0.6
0.4
0.2
0.0
-0.2
-0.4
06:00
12:00
18:00
00:00
06:00
12:00
18:00
Time h

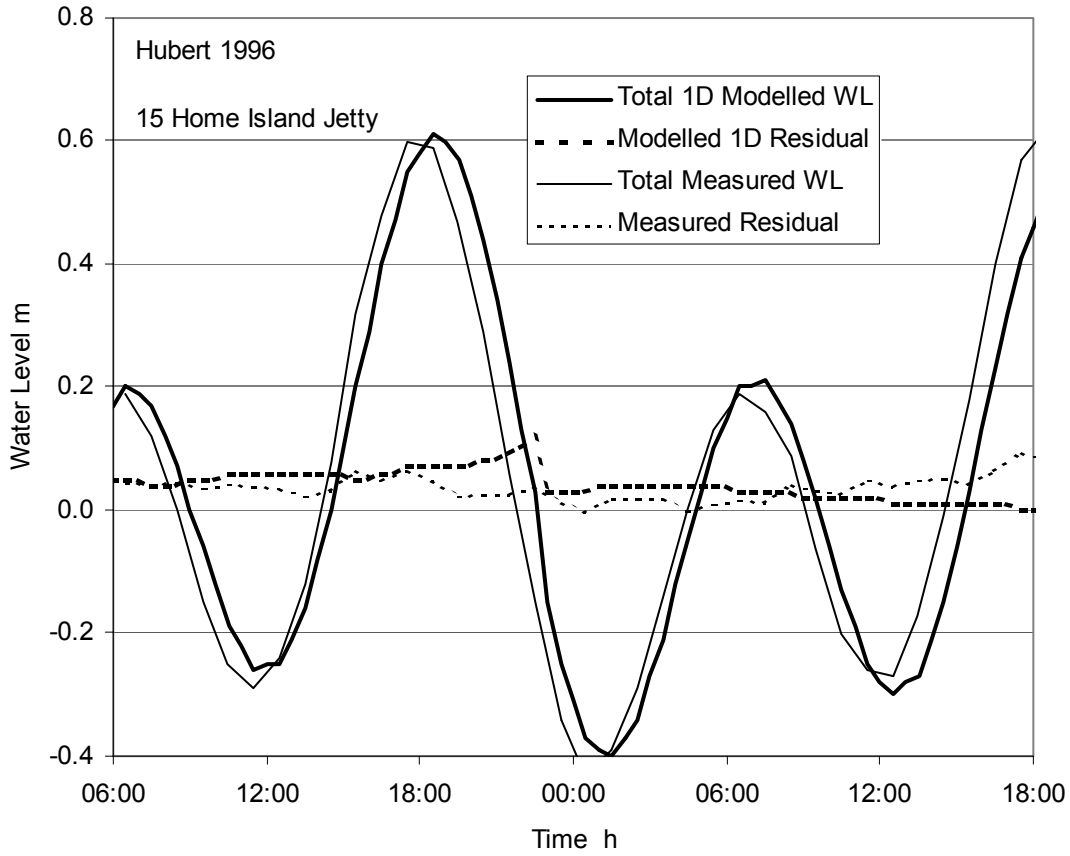
Hubert 1996
15 Home Island Jetty
Total 1D Modelled WL
Modelled 1D Residual
Total Measured WL
Measured Residual
Water Level m
0.8
0.6
0.4
0.2
0.0
-0.2
-0.4
06:00
12:00
18:00
00:00
06:00
12:00
18:00
Time h

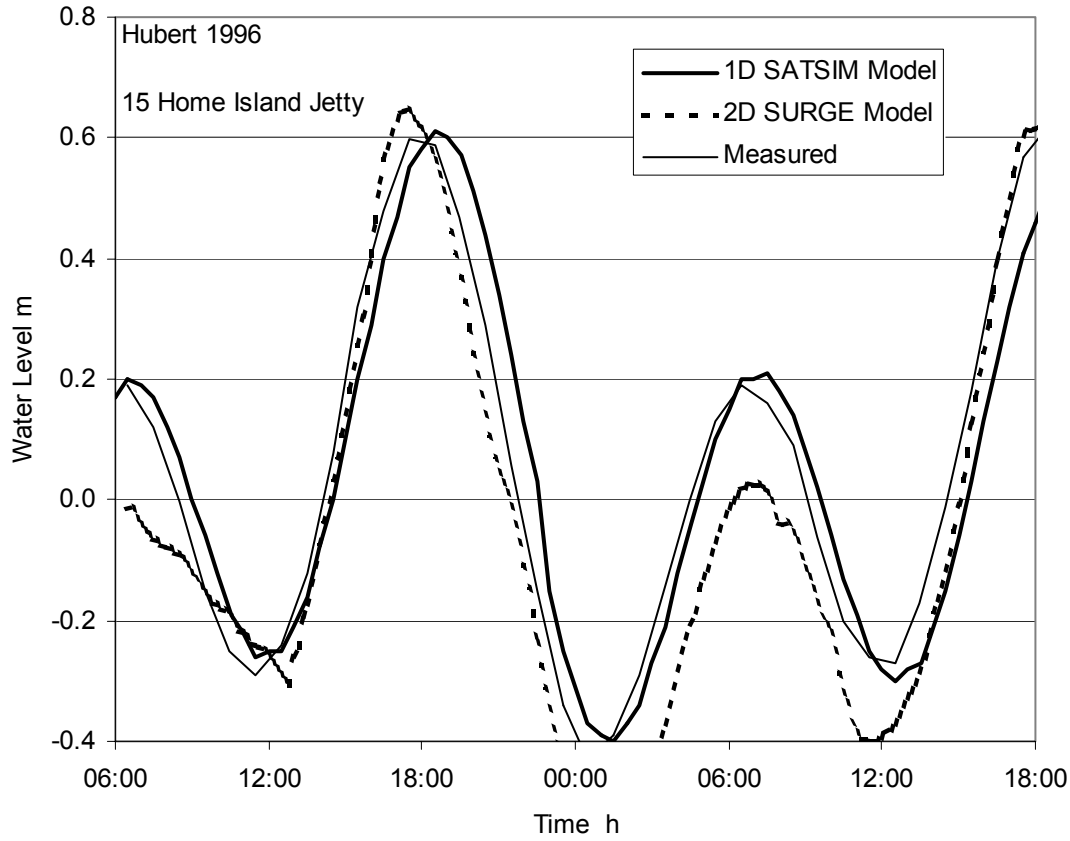
Hubert 1996
15 Home Island Jetty
1D SATSIM Model
2D SURGE Model
Measured
Water Level m
0.8
0.6
0.4
0.2
0.0
-0.2
-0.4
06:00
12:00
18:00
00:00
06:00
12:00
18:00
Time h

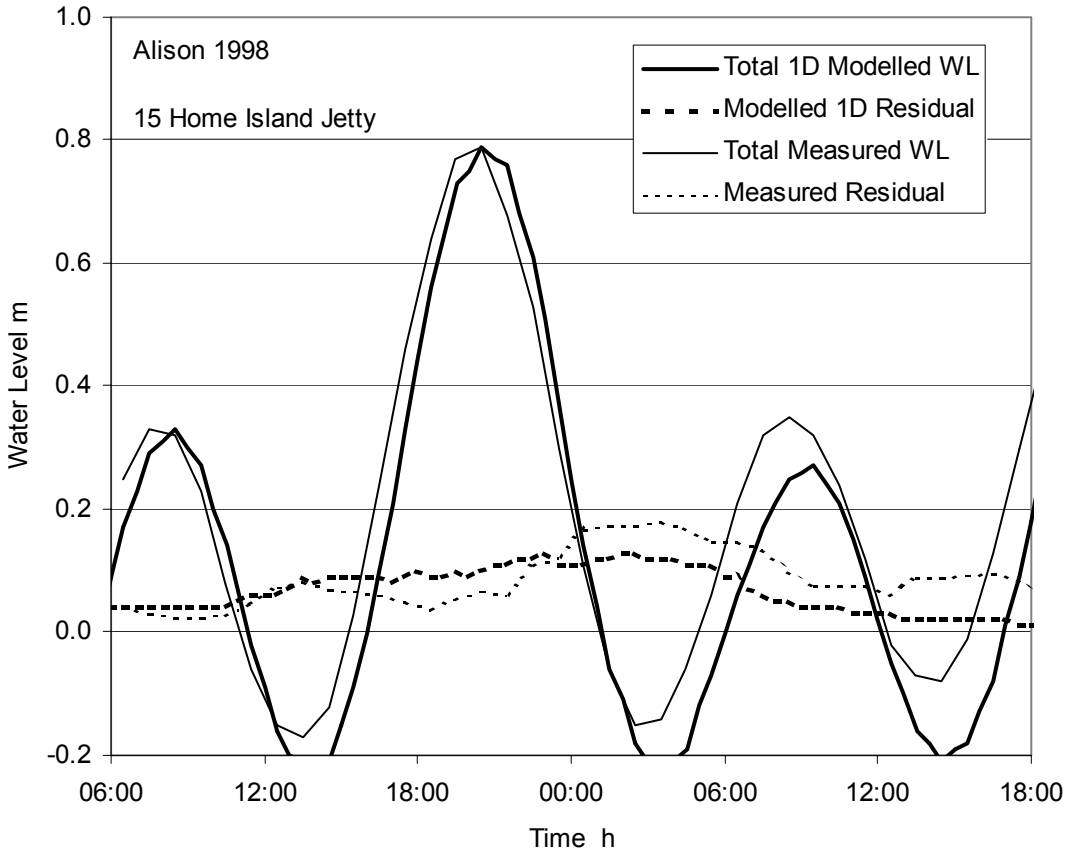
Alison 1998
15 Home Island Jetty
Total 1D Modelled WL
Modelled 1D Residual
Total Measured WL
Measured Residual
Water Level m
1.0
0.8
0.6
0.4
0.2
0.0
-0.2
06:00
12:00
18:00
00:00
06:00
12:00
18:00
Time h

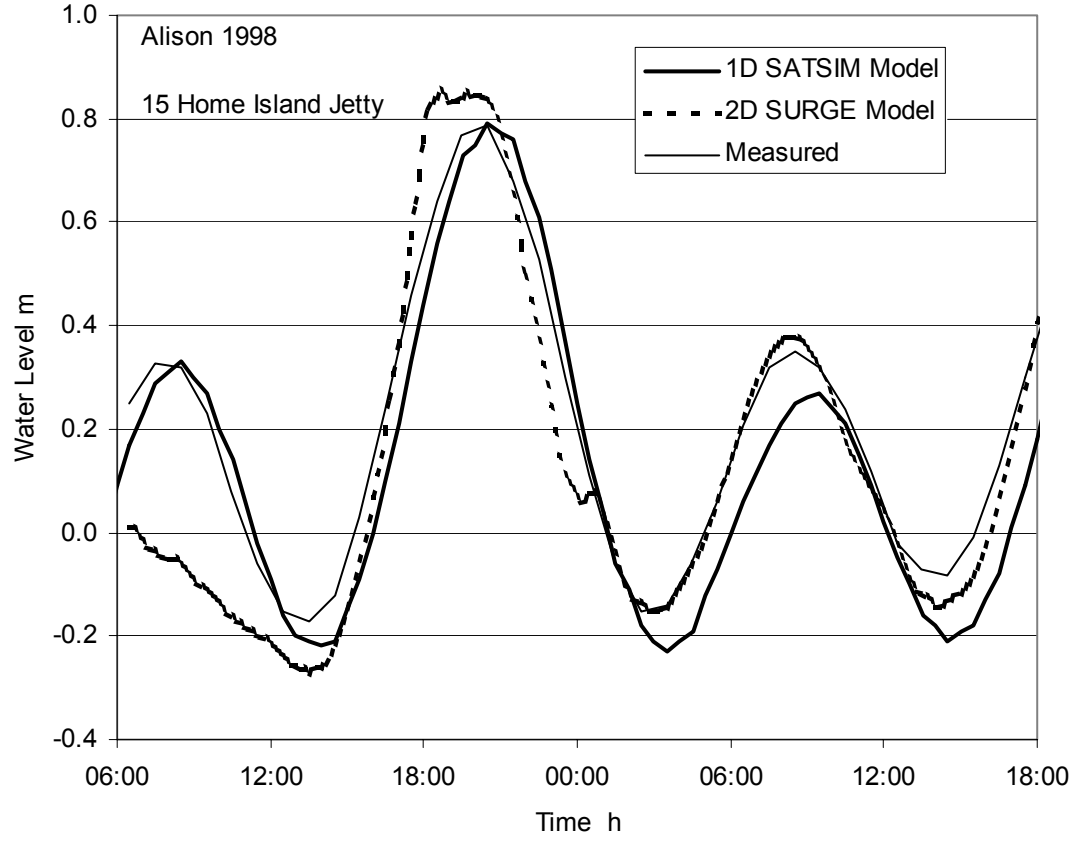
Alison 1998
15 Home Island Jetty
1D SATSIM Model
2D SURGE Model
Measured
Water Level m
1.0
0.8
0.6
0.4
0.2
0.0
-0.2
-0.4
06:00
12:00
18:00
00:00
06:00
12:00
18:00
Time h

APPENDIX J

SPECTRAL WAVE MODEL EXAMPLES

Site 16 - Home Island North

CS CC CB CA: Cocos Islands: TC HAZEL [Prod Start: 08-Mar-1964 00:54 GMT
Run: HAZ115 Grid: CS X= 55.00 Y= 65.00 : Home Is N

HAZ115
09-Mar-1964 00:23GMT; 23.5hr
Hs = 3.23
Tp = 11.48
Tz = 8.67
Tm = 9.86
Thtm= 115.14
td = 57.95

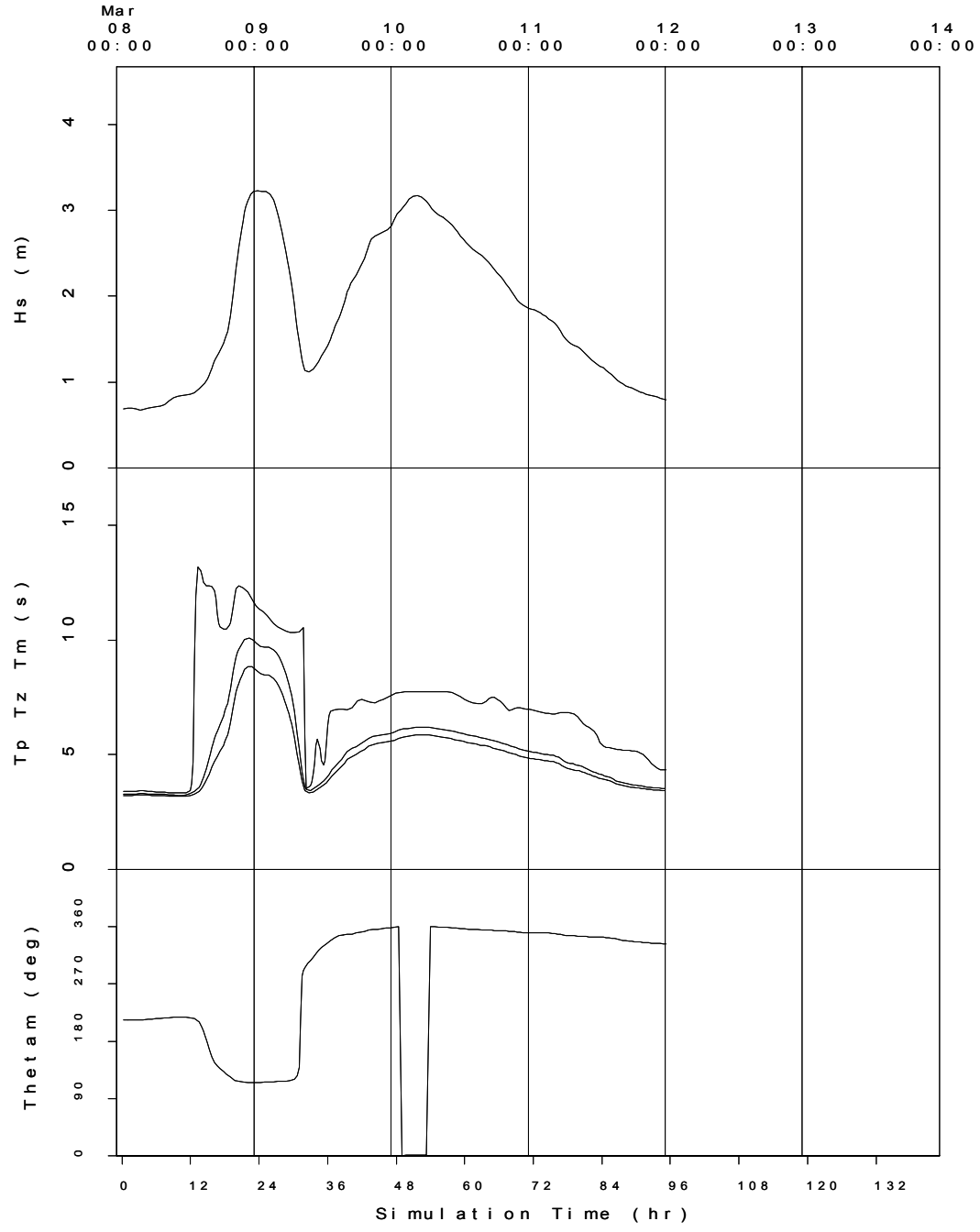

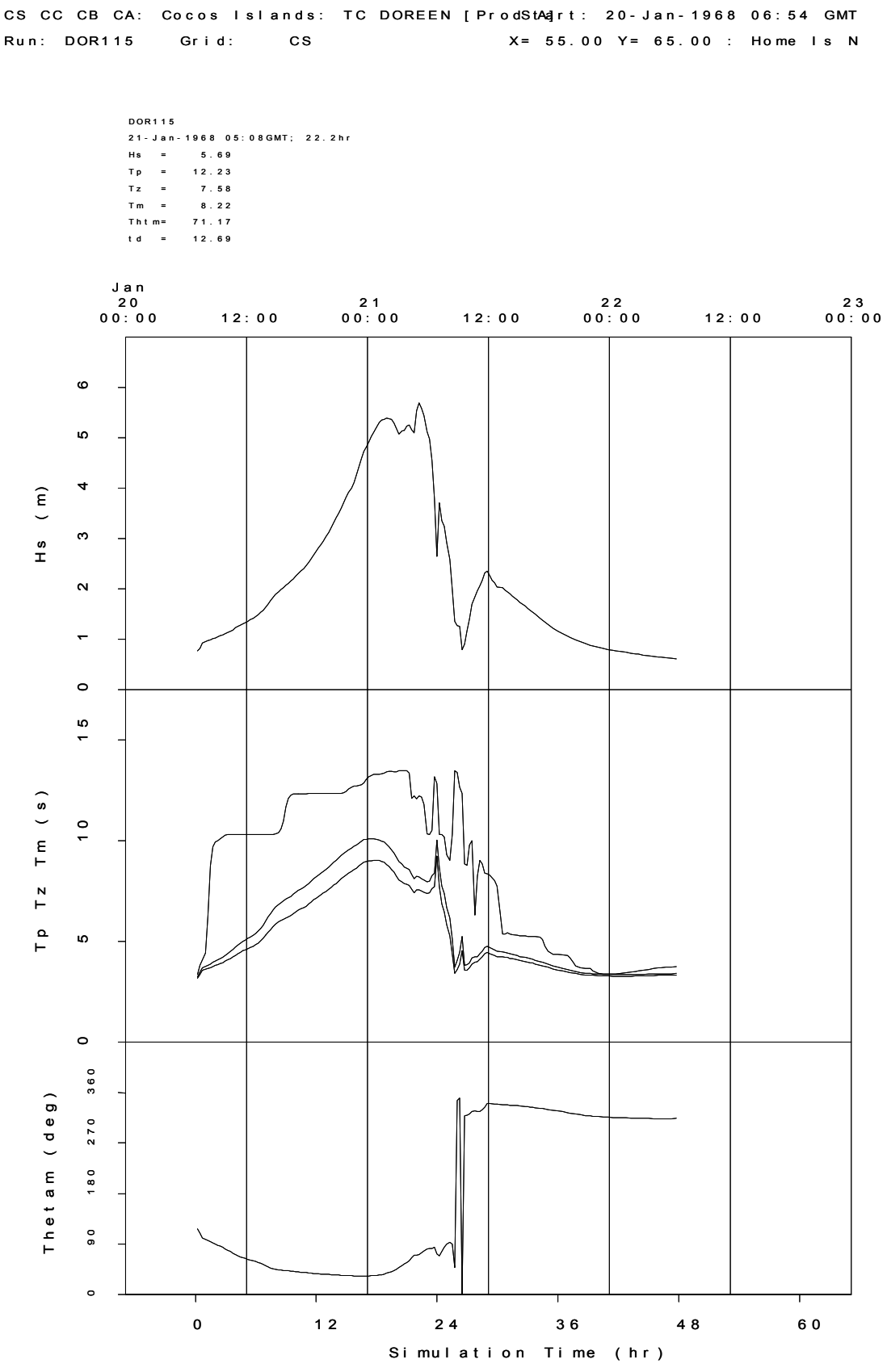
CS CC CB CA: Cocos Islands: TC DOREEN [ProdStart: 20-Jan-1968 06:54 GMT
Run: DOR115 Grid: CS X= 55.00 Y= 65.00 : Home Is N
DOR115
21-Jan-1968 05:08GMT; 22.2hr
Hs = 5.69
Tp = 12.23
Tz = 7.58
Tm = 8.22
Thtm= 71.17
td = 12.69
Jan
20
00:00
12:00
21
00:00
12:00
22
00:00
12:00
23
00:00
Hs (m)
Tp Tz Tm (s)
Thetam (deg)
0
90
180
270
360
0
12
24
36
48
60
Simulation Time (hr)

CS CC CB CA: Cocos Islands: TC DARYL [Prod 34] Start: 09-Mar-1984 23:54 GMT
Run: DAR115 Grid: CS X= 55.00 Y= 65.00 : Home Is N

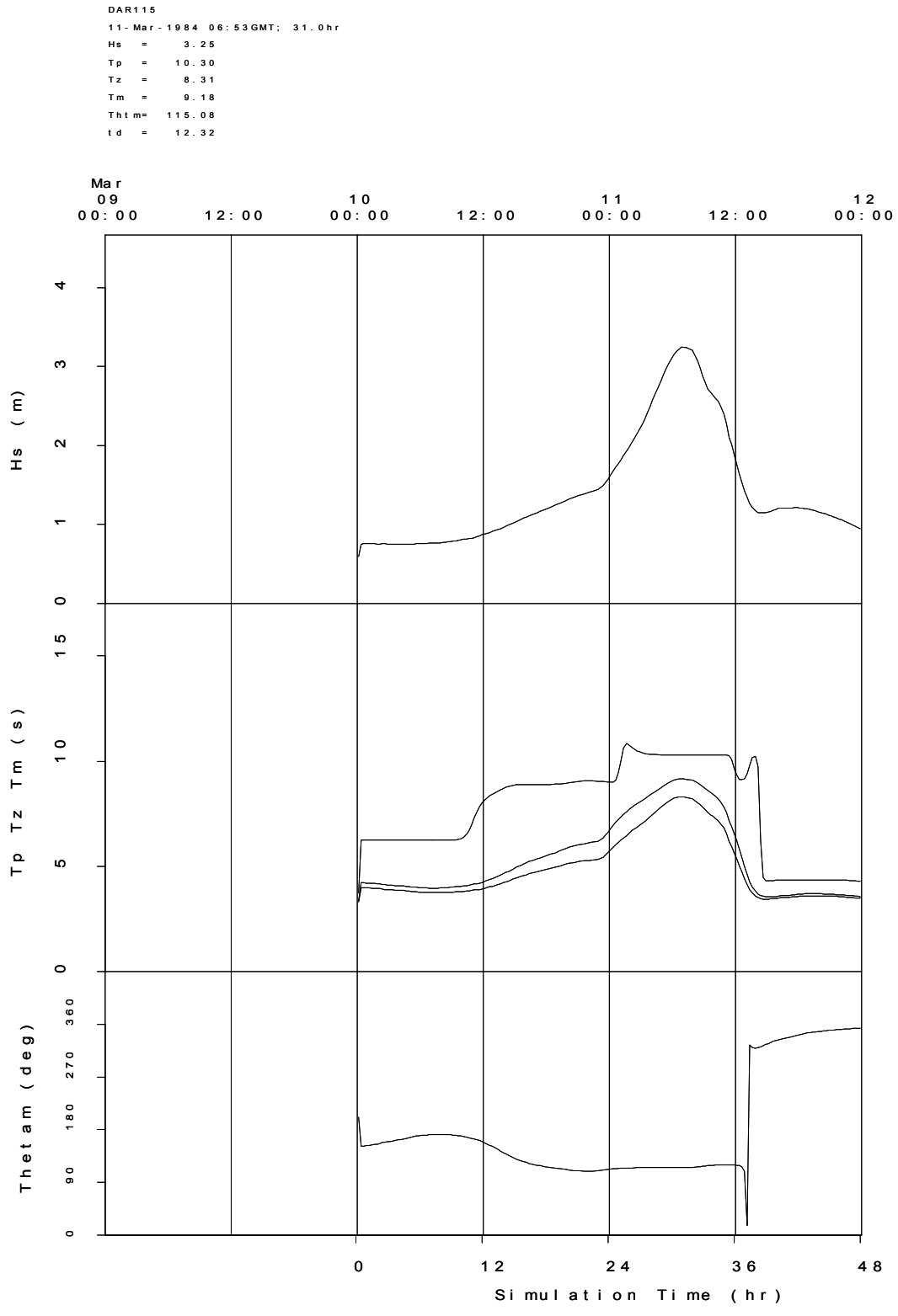

CS CC CB CA: Cocos Islands: TC OPHELIA [Prost] Start: 07-Jan-1986 11:54 GMT
Run: OPH115 Grid: CS X= 55.00 Y= 65.00 : Home Is N

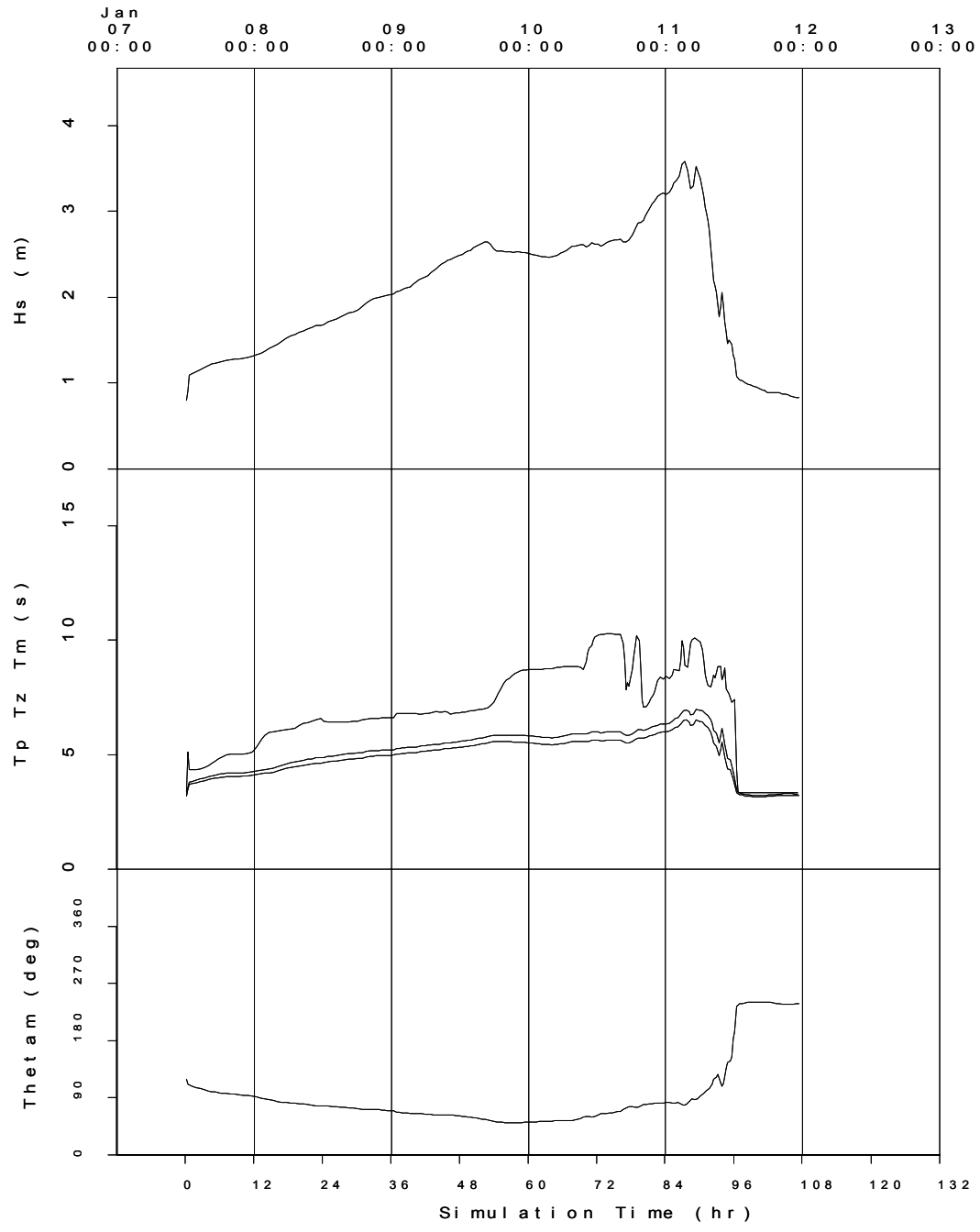

CS CC CB CA: Cocos Islands: TC FREDERIC [PrStdarAt]: 28-Jan-1988 23:54 GMT
Run: FRE115 Grid: CS X= 55.00 Y= 65.00 : Home Is N

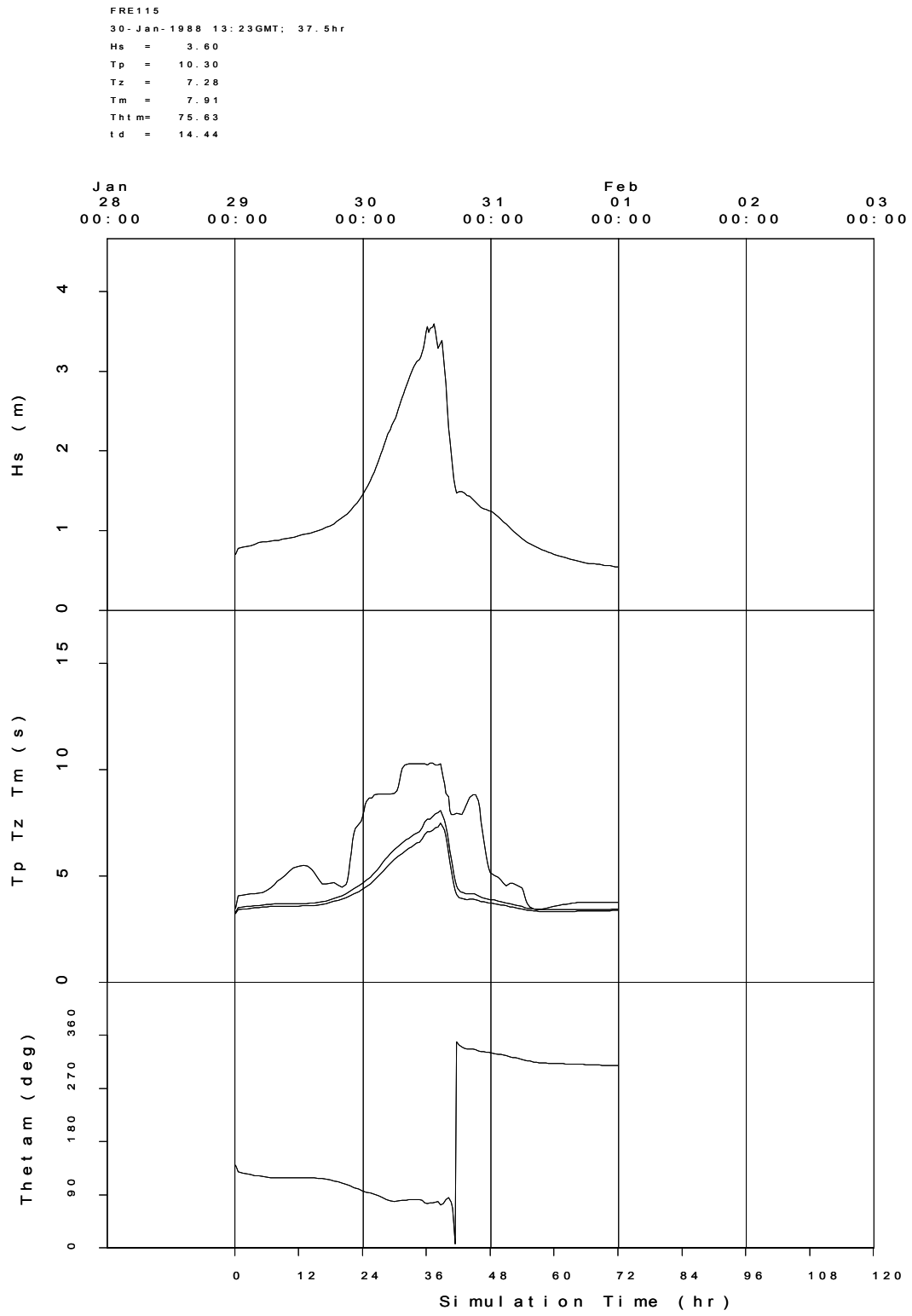

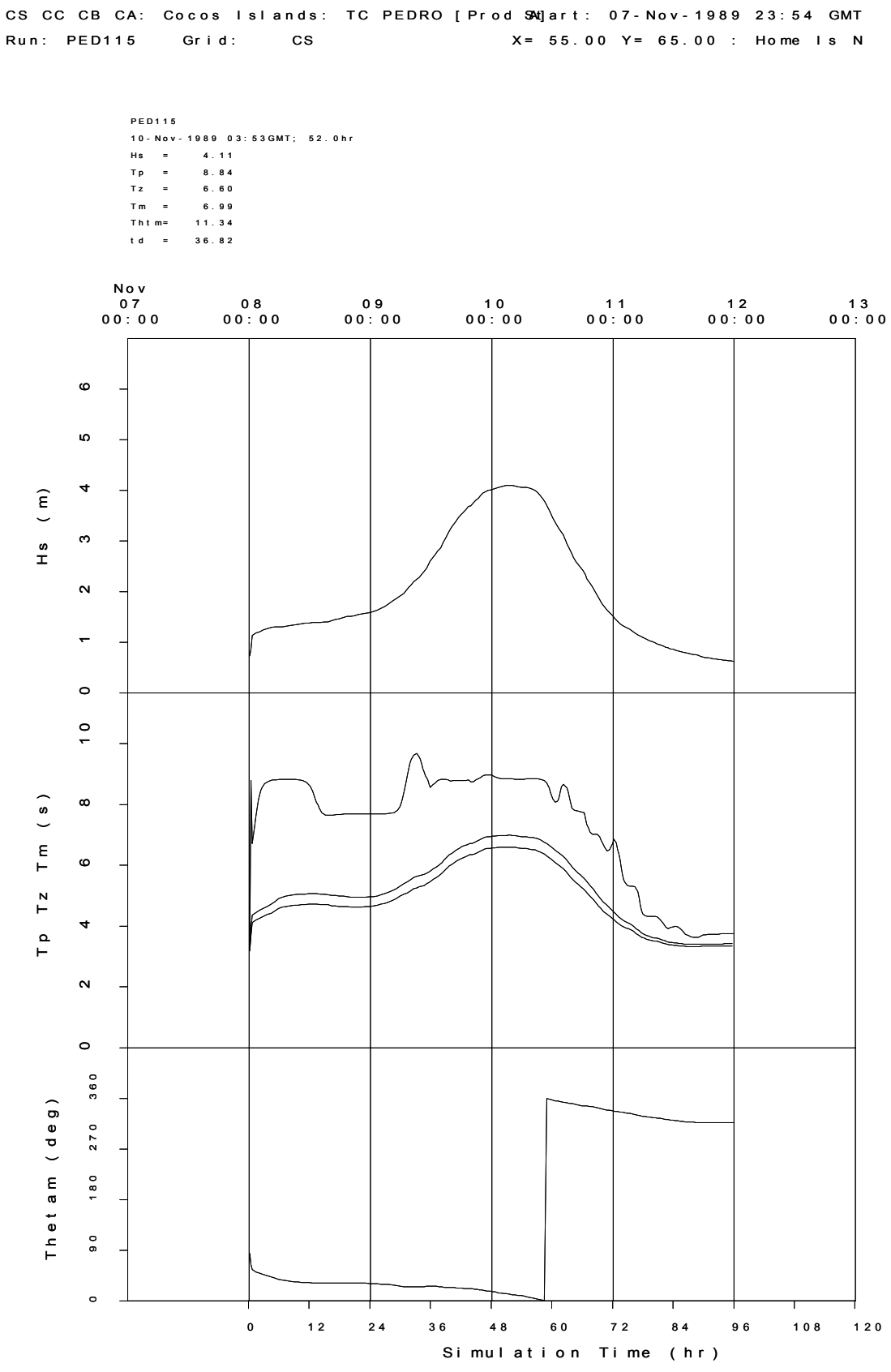
CS CC CB CA: Cocos Islands: TC PEDRO [Prod 3d]
Start: 07-Nov-1989 23:54 GMT
Run: PED115 Grid: CS X= 55.00 Y= 65.00 : Home Is N
PED115
10-Nov-1989 03:53GMT; 52.0hr
Hs = 4.11
Tp = 8.84
Tz = 6.60
Tm = 6.99
Thtm= 11.34
td = 36.82
Nov
07 00:00
08 00:00
09 00:00
10 00:00
11 00:00
12 00:00
13 00:00
Hs (m)
Tp Tz Tm (s)
Thetam (deg)
0 90 180 270 360
0 12 24 36 48 60 72 84 96 108 120
Simulation Time (hr)

CS CC CB CA: Cocos Islands: TC GRAHAM [ProdStart: 02-Dec-1991 23:54 GMT
Run: GRA115 Grid: CS X= 55.00 Y= 65.00 : Home Is N

GRA115
05-Dec-1991 22:23GMT; 70.5hr
Hs = 4.57
Tp = 12.37
Tz = 8.43
Tm = 9.42
Thtm= 20.57
td = 60.83

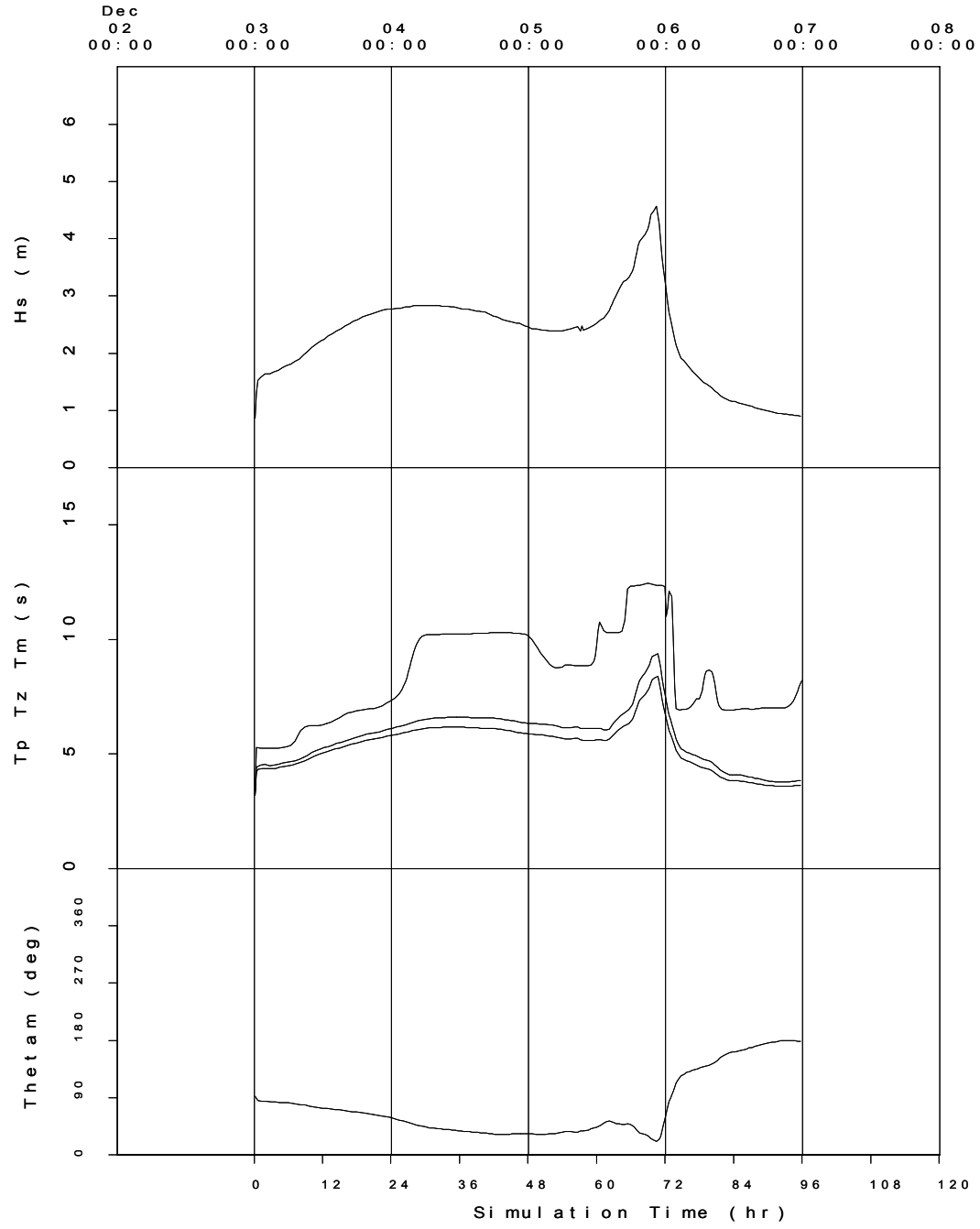

CS CC CB CA: Cocos Islands: TC HARRIET [Prosta] Start: 25-Feb-1992 17:54 GMT
Run: HAR115 Grid: CS X= 55.00 Y= 65.00 : Home Is N

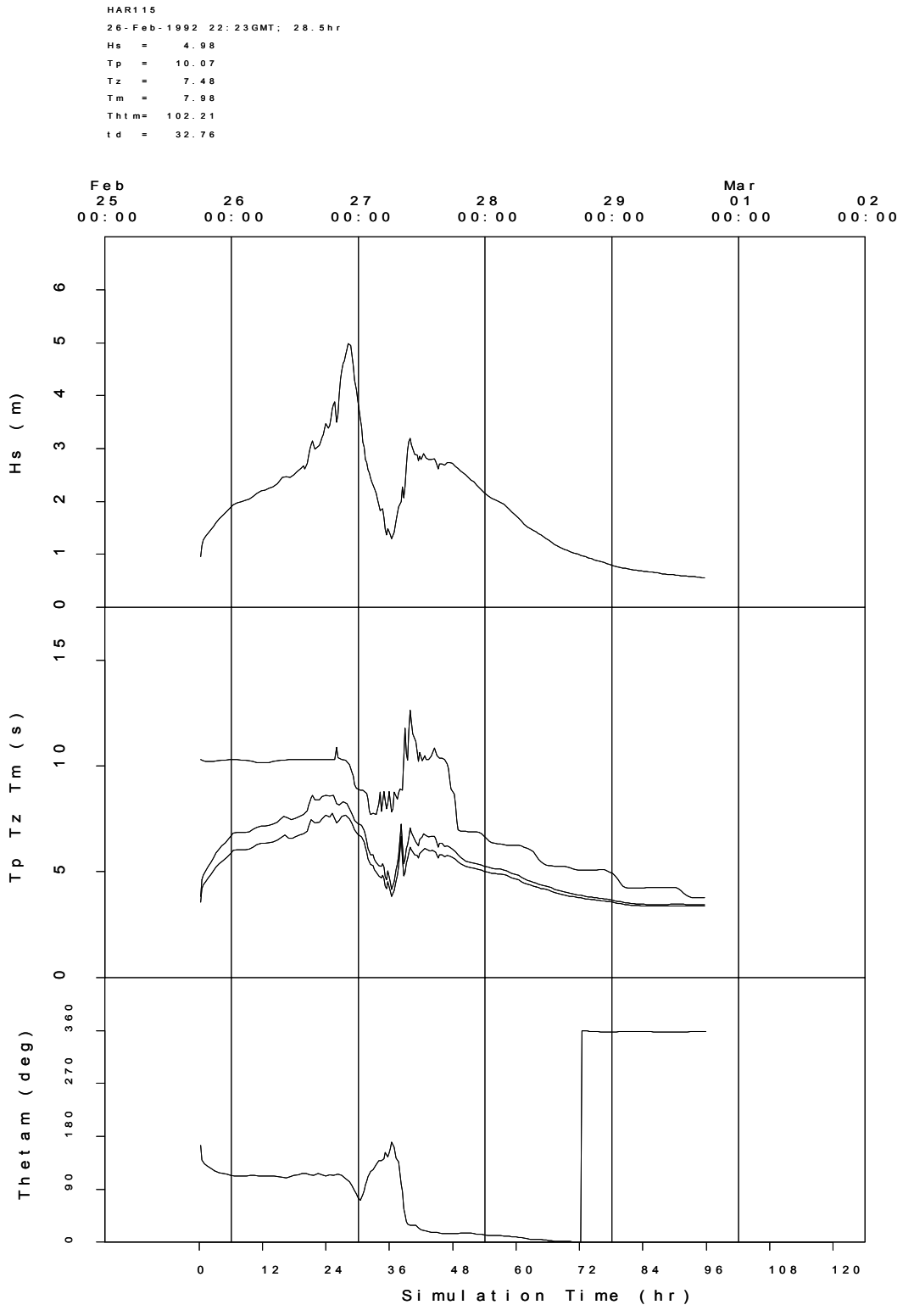

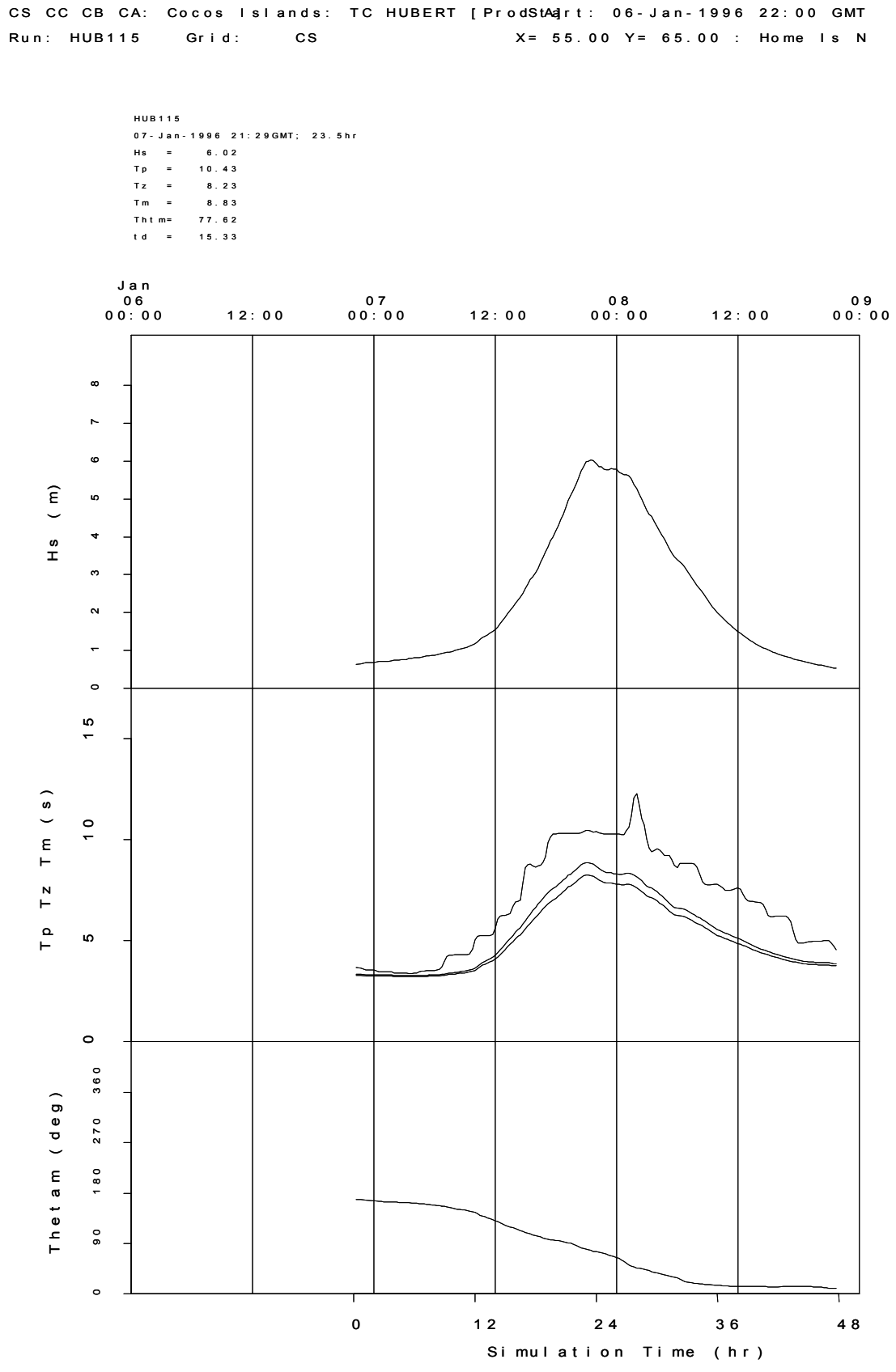
CS CC CB CA: Cocos Islands: TC HUBERT [ProdStart: 06-Jan-1996 22:00 GMT
Run: HUB115 Grid: CS X= 55.00 Y= 65.00 : Home Is N
HUB115
07-Jan-1996 21:29GMT; 23.5hr
Hs = 6.02
Tp = 10.43
Tz = 8.23
Tm = 8.83
Thtm= 77.62
td = 15.33
Jan
06
00:00
12:00
07
00:00
12:00
08
00:00
12:00
09
00:00
Hs (m)
0 1 2 3 4 5 6 7 8
Tp Tz Tm (s)
0 5 10 15
Thetam (deg)
0 90 180 270 360
0 12 24 36 48
Simulation Time (hr)

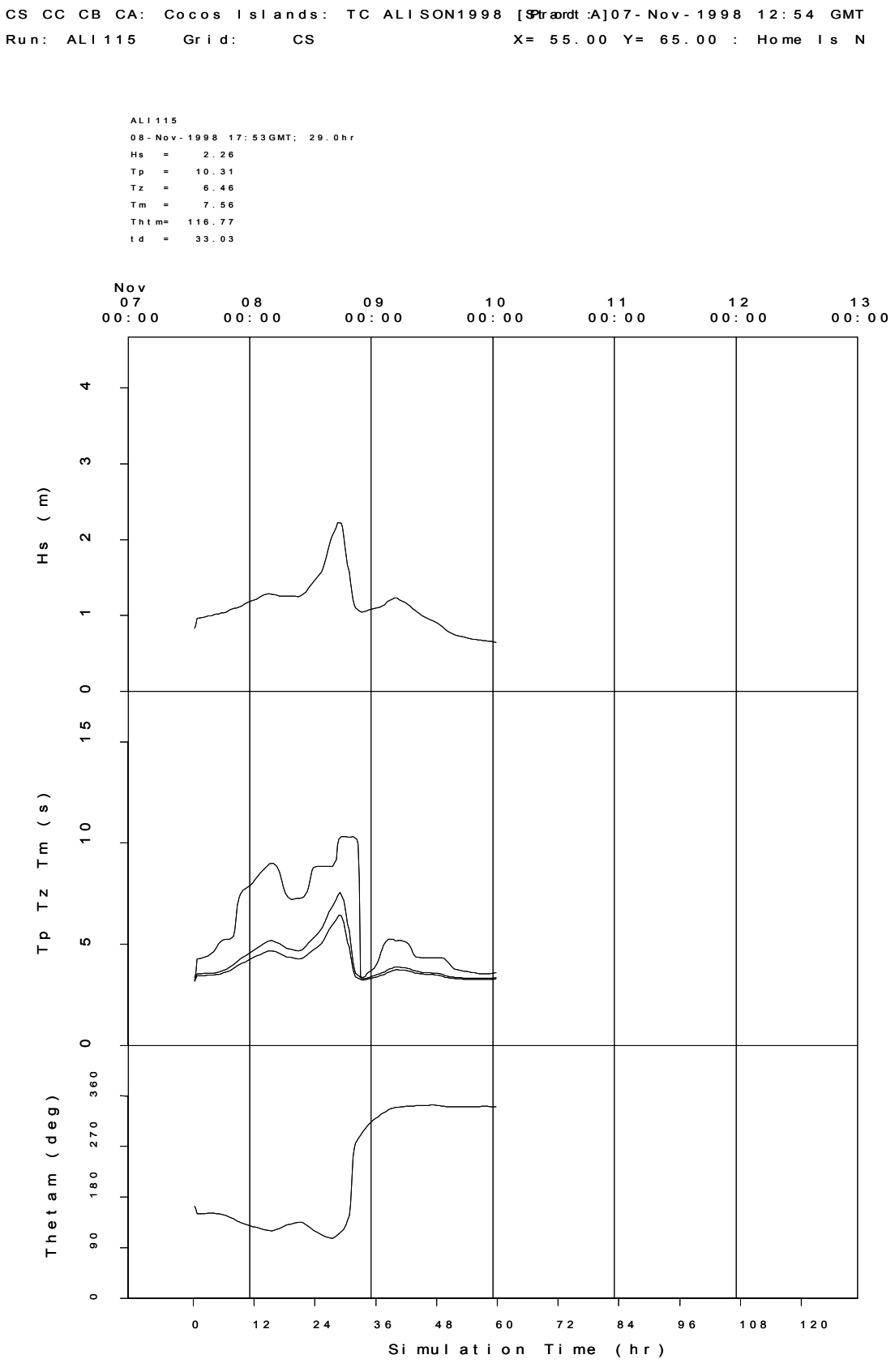
CS CC CB CA: Cocos Islands: TC ALISON1998 [Straordt:A] 07-Nov-1998 12:54 GMT
Run: ALI115 Grid: CS X= 55.00 Y= 65.00 : Home Is N
ALI115
08-Nov-1998 17:53GMT; 29.0hr
Hs = 2.26
Tp = 10.31
Tz = 6.46
Tm = 7.56
Thtm= 116.77
td = 33.03
Nov
07 00:00
08 00:00
09 00:00
10 00:00
11 00:00
12 00:00
13 00:00
Hs (m)
Tp Tz Tm (s)
Thetam (deg)
0 12 24 36 48 60 72 84 96 108 120
Simulation Time (hr)